Illinois U Library

IN TWO SECTIONS—SECTION ONE

Transactions

of the

ASME

Design Criteria for Jet-Propelled Helicopter Rotors . . . . *C. D. Denney* 1

Heat-Transfer Temperature Patterns of a Multicomponent Structure by Comparative Methods . . . . *C. F. Kayan* 9

Test Results of High-Performance Heat-Exchanger Surfaces Used in Aircraft Intercoolers and Their Significance for Gas-Turbine Regenerator Design . . . . *A. L. London and C. K. Ferguson* 17

Heat Transfer and Fluid Friction During Viscous Flow Across Banks of Tubes . . . . *G. A. Omohundro, O. P. Bergelin, and A. P. Colburn* 27

The Gas Turbine as a Stationary Prime Mover . . *L. N. Rowley and B. G. A. Skrotzki* 35

Transmission Systems for Marine Propulsion Gas-Turbine Power Plants . . . . *W. E. Hammond* 43

Gas-Turbine Power Plants for Operation With Low-Cost Fuel . . . *John Goldsbury* 59

Experimental Determination of Velocity of Sound in Superheated Steam by Ultrasonics . . . . *James Woodburn* 65

Jet Mixing of Two Liquids . . . . *R. G. Folsom and C. K. Ferguson* 73

A Remote-Indicating Pressure Gage for Aircraft . . . . *R. G. Jewell* 79

Motion Analysis of Several Intermittent Variable-Speed Mechanisms *G. J. Talbourdet* 83

JANUARY, 1949

VOL. 71, NO. 1

U OF I
LIBRARY

Transactions

of The American Society of Mechanical Engineers

Published on the tenth of every month, except March, June, September, and December

OFFICERS OF THE SOCIETY:

JAMES M. TODD, *President*
K. W. JAPPE, *Treasurer*
C. E. DAVIES, *Secretary*

COMMITTEE ON PUBLICATIONS:

J. M. JURAN, *Chairman*
RONALD B. SMITH
JOHN HAYDOCK
C. B. CAMPBELL
GEORGE A. STETSON, *Editor*
K. W. CLENDINNING, ***Managing Editor***

REGIONAL ADVISORY BOARD OF THE PUBLICATIONS COMMITTEE

KERR ATKINSON—I
OTTO DE LORENZI—II
W. E. REASER—III
F. C. SMITH—IV
TOMLINSON FORT—V
R. E. TURNER—VI
R. G. ROSHONG—VII
M. A. DURLAND—VIII

Published monthly by The American Society of Mechanical Engineers. Publication office at 20th and Northampton Streets, Easton, Pa. The editorial department is located at the headquarters of the Society, 29 West Thirty-Ninth Street, New York 18, N. Y. Cable address, "Dynamic," New York. Price $1.50 a copy, $12.00 a year for Transactions and the *Journal of Applied Mechanics;* to members and affiliates, $1.00 a copy, $6.00 a year. Changes of address must be received at Society headquarters three weeks before they are to be effective on the mailing list. Please send old as well as new address.... By-Law: The Society shall not be responsible for statements or opinions advanced in papers or...printed in its publications (B13, Par. 4)....Entered as second-class matter March 2, 1928, at the Post Office at Easton, Pa., under the Act of August 24, 1912....Copyrighted, 1949, by The American Society of Mechanical Engineers. Reprints from this publication may be made on condition that full credit be given the Transactions of the ASME and the author, and that date of publication be stated.

Illinois U Library

Design Criteria for Jet-Propelled Helicopter Rotors

By C. D. DENNEY,[1] VENICE, CALIF.

Considerable developmental work is progressing on various types of jet rotor systems for helicopters. Among these are the ramjet system, and the pressure system, which are described in some detail in the paper. Application of the gas turbine for driving the compressor used in the pressure system is considered briefly, as well as use of the turbojet engine. A comparison of performance of the two principal jet-rotor systems under consideration with conventional helicopter-rotor drive is given, which indicates advantages for short-haul application over the conventional drive.

Introduction

SINCE the advent of the various types of jet-propulsion engines, a great deal of time and money have been spent in an effort to apply jet propulsion to helicopter rotors. This effort was primarily prompted by the possibility of solving the age-old problem of fuselage torque compensation on the single-rotor type of helicopter. Since the jet-propelled rotor transmits no torque to the fuselage, all devices such as the commonly employed auxiliary tail rotor are eliminated. In addition, an expensive internal-combustion engine supplemented with transmission and clutch assemblies would no longer be required. It was believed that this would yield an aircraft with enhanced performance and greatly reduced mechanical complexity.

To date, the jet-rotor developments have consisted primarily of design studies, and the fabrication and testing of whirl-stand rotors. In a few cases, an effort has been made to construct a complete aircraft and determine the flight characteristics. The outstanding example of this is the German jet-propelled helicopter which was designed and built by Fredrick Dobolhoff. The Dobolhoff machine was brought to this country at the close of hostilities and currently is being flight-tested at Wright Field, Dayton, Ohio. This aircraft has been capable of hovering at low altitudes but the forward flight performance is definitely limited.

At the present time, a surprisingly great number of organizations, large and small, throughout this country are engaged in jet-rotor developments and are seriously considering the practical application of the jet-propelled helicopter. It appears that the jet-propelled helicopter is particularly suited for certain specialized duties and a large potential market is considered by many to exist.

Proposals for jet-propelled helicopters have considered many different types of jet drives; however, only two types will be considered in detail here. One is shown in Fig. 1, and is known as the "ramjet system." The extreme simplicity of a helicopter utilizing this type of power plant is obvious. It is noted that the complete propulsion system consists of a ramjet engine mounted on each rotor-blade tip. For operation of the ramjet engine, only fuel and ignition lines are required and these are integral with the blade structure.

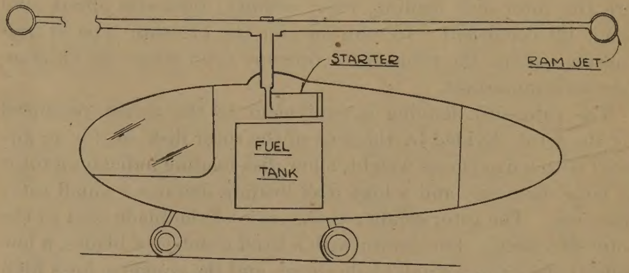

Fig. 1 Ram-Type Jet-Propelled Helicopter

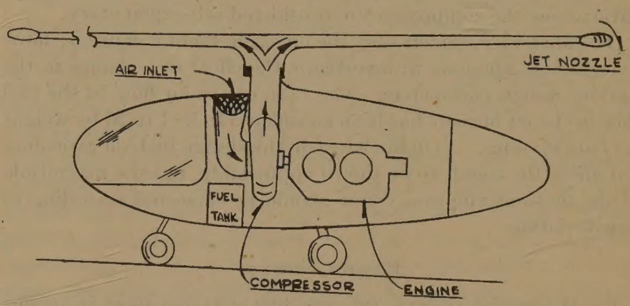

Fig. 2 Pressure-Type Jet-Propelled Helicopter

The ramjet engine is the simplest of power plants, having no moving parts and requiring no lubrication. Consequently, the initial cost is extremely low and essentially no maintenance is required.

The ramjet engine is incapable of producing a useful static thrust; thereby necessitating a rotor-starting device. This can take the form of a small internal-combustion engine or electric starter geared to the rotor shaft, or it is considered possible to start the rotor with small rocket charges located at the blade tips. In either event, the starting problem is considered relatively minor since the power required to accelerate the rotor is quite small at zero lift coefficient.

The second jet system considered is shown in Fig. 2, and is termed the "pressure system." Here, a relatively low-horsepower conventional internal-combustion engine is employed to drive an air compressor in the fuselage. The pressurized air is driven through the hub and along internal blade ducts to a constant-pressure burner mounted at the blade tip. Fuel is introduced into the system either at the compressor or blade tip, forming a combustible mixture. The mixture is ignited in the tip burner and the products of combustion are expanded to atmospheric pressure by an exit nozzle, thus producing the force which propels the rotor. This type of system is that which was employed by Dobolhoff in the German jet helicopter.

It is noted that the inherent simplicity of the ramjet system is not present here. However, as will be shown later, the advantage of this system lies in its reduced fuel consumption.

The inherent properties of jet-powered rotors are largely different from rotors which are gear-driven and a different type of design criteria is required. A design analysis of the ramjet and pressure type of propulsion systems has been made, and the results of this analysis indicate the distinguishing characteristics

---

[1] Chief Helicopter Engineer, Marquardt Aircraft Company.

Presented at the Aviation Meeting of The American Society of Mechanical Engineers, Los Angeles, Calif., May 26–29, 1947.

Note: Statements and opinions advanced in papers are to be understood as individual expressions of their authors and not those of the Society.

43479

of the two types of jet-propelled rotors. It is not possible to present a complete explanation of the method used in the analysis, or the basis for the several assumptions which are necessary. However, the method is quite fundamental and the assumptions are in accordance with experimental data.

In the analysis, an effort has been made to evaluate the effect of a change in the various design parameters upon performance. The major design parameters involved in both propulsion systems are the rotor-disk loading, rotor solidity, blade-tip speed, and blade lift coefficient. In addition, for the pressure type of propulsion system, the value of the pressure ratio across the air compressor is important.

The rotor-disk loading is equivalent to the thrust produced by the rotor, divided by the area of the rotor disk, or, for an aircraft with a fixed gross weight, a low disk loading indicates a rotor of large diameter, and a high disk loading dictates a small rotor diameter. The rotor solidity is the ratio of the blade area to the rotor-disk area. For a rotor with a fixed number of blades, a low solidity indicates a small blade chord, and the converse for a high solidity. The blade-tip speed, blade lift coefficient, and pressure ratio across the compressor are considered self-explanatory.

The analysis considers only the hovering-flight condition; however, this is adequate to investigate the effect of a change in the various design parameters. The ratio of the air flow to the fuel flow in the jet burners has been considered to be 1 to 20 by weight for both systems. A slight change in this design fuel/air ratio does not affect the trends to be shown appreciably, but the magnitude of the fuel-consumption values should be corrected according to any deviation.

RAMJET SYSTEM

For the ramjet system, the principal criterion used in evaluating the effect of a change in design parameters is the fuel consumption per hour of flight. It is convenient to express the fuel consumption as a function of the gross weight of the aircraft. This is termed a weight specific fuel consumption given in pounds of fuel consumed per hour per pound of gross weight or rotor thrust. This permits a determination of the fuel consumption per hour for any size aircraft. In computing the weight specific fuel consumption, the performance properties of the ramjet engine are first determined as a function of velocity. These properties are completely independent of the helicopter rotor. The characteristics of the rotor as a function of the disk loading, solidity, and tip speed are then determined, and these are independent of the propulsion system. By combining the ramjet engine and rotor properties, the fuel consumed as a function of aircraft gross weight is known.

Figs. 3, 4, and 5 show typical ramjet-engine performance characteristics. These characteristics are based upon relatively small engines which would be suitable for powering helicopters with gross weights of 2000 lb or less. The performance of larger ramjet engines capable of powering heavier aircraft is improved materially over that presented here. However, all trends indicated are independent of aircraft size. In the charts, the engine thrust coefficient, specific fuel consumption, and drag coefficient are shown as a function of velocity or blade-tip speed. The thrust coefficient is an indication of the ability of the engine to produce thrust and, as noted, this increases slightly with increasing tip speed.

The thrust coefficients shown in Fig. 3, are gross values and, in order to obtain the net thrust applied to the rotor, it is necessary to substract the drag coefficients shown in Fig. 5.

The engine specific fuel consumption, shown in Fig. 4, is given in pounds of fuel consumed per hour per pound of jet-engine thrust. This is not to be confused with rotor thrust or aircraft gross weight. It is noted that a rapid decrease in specific fuel consumption occurs with increasing tip speed. Increasing the tip speed from 500 fps to 700 fps results in a 40 per cent reduction in specific fuel consumption. This ram-jet characteristic of great saving in fuel consumption at high tip speeds is the most important factor in determining the optimum values for the rotor design parameters. It is indicated here that a designer of a ramjet rotor should use the highest permissible tip speed.

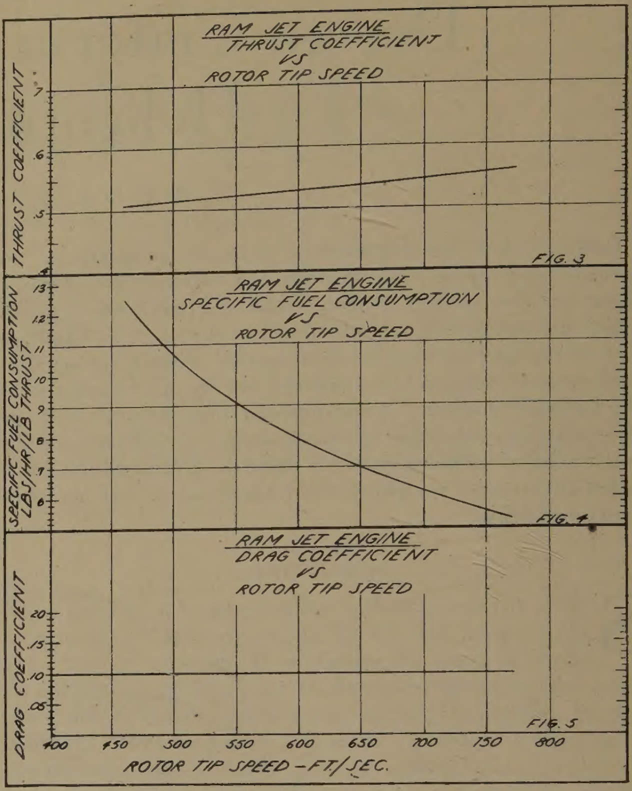

Figs. 3, 4, 5 Ramjet-Engine Performance Data

Fig. 5 shows an assumed jet-engine drag coefficient which has a constant value up to a tip speed of 800 fps. At a tip speed slightly above 800 fps, experimental data indicate that the critical velocity occurs, and the drag coefficient increases rapidly. However, the rotor-tip speed is limited to a value below 800 fps for all flight conditions due to compressibility drag on the rotor blade. Consequently, the exact tip speed at which the drag coefficient of the jet engine increases is not important to this analysis.

The characteristics of the helicopter rotor are not shown since they are common to all helicopters independent of the type of drive used. However, the method was to determine the rotor horsepower required per pound of aircraft gross weight for various disk loadings, solidities, and tip speeds. By combining these data with the ramjet-engine properties, the performance characteristics of the complete ramjet rotor are known.

Fig. 6 is a typical ramjet-rotor design chart showing the effect on fuel consumption of a variation in rotor solidity and rotor-tip speed. These data are based upon a rotor-disk loading of 2.5 psf, but the trends indicated do not change for a variation in this parameter. Each solid line is for a constant rotor solidity, and each dash line represent a constant rotor-tip speed. The ordinate for the plots is the fuel consumed per hour per pound of rotor thrust or gross weight, and the mean rotor lift coefficient is shown as the abscissa. This lift coefficient varies as a result of a variation in the tip speed and solidity.

By following either of the solid lines representing constant rotor solidity, it is noted that the fuel consumption is increasing as the tip speed decreases. As an example, for a rotor solidity of

0.03, an 18 per cent saving in fuel consumption is achieved by increasing the tip speed from 600 to 700 fps. By increasing further the tip speed to 800 fps, an additional 11 per cent reduction in fuel consumption is realized; however, operation in the hovering-flight condition at tip speeds appreciably above 750 fps is prohibited due to compressibility drag on the rotor blade.

The effect on fuel consumption of a change in rotor solidity is shown in this figure by following either of the lines of constant tip speed. It is noticed that, as the solidity is decreased for any given tip speed, the fuel consumption is decreased significantly. Using the plot for a tip speed of 700 fps as an example, a reduction in rotor solidity from 0.04 to 0.03 results in a 17 per cent saving in fuel consumption. By reducing the solidity to 0.02, a further 14 per cent saving is achieved. However, a design solidity below 0.02 is considered impractical from a blade-structure standpoint and also, as is indicated later, the minimum solidity which can be used is affected by the maximum design speed of the aircraft.

It is noted from Fig. 6 that, as the solidity is decreased for a constant tip speed, the mean rotor lift coefficient is increased. This increasing lift coefficient is responsible for the decreased fuel consumption in that the airfoil sections of the rotor blade are operating more efficiently at the higher lift coefficients.

The data in this figure have demonstrated the definite advantage of designing a ramjet rotor with low solidity such that operation at high tip speeds can be accomplished efficiently with a relatively high lift coefficient. Since the proper selection of the rotor solidity is critical in a ramjet-rotor design, it should be chosen carefully considering all factors involved.

Affecting the optimum design solidity are the limits imposed on the blade-tip speed due to compressibility drag on the airfoil sections, and the limits imposed on the mean rotor lift coefficient due to stalling of the retreating blade in forward flight. Both of these limitations are functions of the forward flight velocity of the aircraft. The tip-speed limit decreases with increasing forward flight speed. This is due to the flight speed adding to the rotational speed of the rotor when a blade is in the advancing azimuth position. Consequently, as the forward flight speed increases, the tip-speed limit must decrease, in order to maintain a constant air velocity relative to the blade tip.

The magnitude of the reduction of the tip-speed limit with increasing forward speed is also affected by the rotor lift coefficient. This is due to the fact that the speed at which compressibility drag occurs decreases as the lift coefficient increases.

The limit imposed on the mean rotor lift coefficient is a result of the velocity differential between the advancing and retreating blades in forward flight. This velocity differential necessitates a cyclic-change in lift coefficient in order to maintain a nearly constant lift as the blade travels around the azimuth. Rotors with conventional airfoil sections stall at a mean lift coefficient of approximately 1. Therefore, the lift coefficient must not exceed this value at any azimuth position. The limiting mean rotor lift coefficient decreases with increasing forward speed due to the increased velocity differential as the blade travels around the azimuth.

By considering both of these limitations for several rotor-disk loadings, the solidity design chart, shown in Fig. 7, is obtained. Here, the disk loading is plotted as a function of the solidity for several design maximum forward flight velocities. This chart enables the designer to select the solidity value which yields minimum fuel consumption for a given disk loading and given design maximum forward speed. This solidity value is shown to increase with increasing maximum design speed and with increasing rotor disk loading.

It is noted that with a change in maximum design forward speed, an appreciable change in solidity is required. Therefore, it is important that a designer carefully select a maximum design speed compatible with the use for which the aircraft is intended.

For example, if a disk loading of 2.5 psf is being used and if the design maximum forward speed is 80 mph, the desired rotor solidity is 0.025. If a lower solidity is employed, the rotor is subject to compressibility drag or tip stall at high speeds, and if a higher solidity is chosen, an unnecessary increase in fuel consumption will result.

Selecting the optimum rotor solidity for a given disk loading from Fig. 7, and applying the basic fuel-consumption data, Fig. 8 is obtained. Here, the fuel consumption per hour per pound of gross weight is plotted against rotor-disk loading for several design maximum speeds. It is remembered that all fuel-consumption data presented have been based upon hovering-flight condition and, likewise, the data in this figure give the fuel consumption in the hovering condition but for aircraft designed to attain a specified forward speed. No indication is given of the fuel consumption when the aircraft is operating at its maximum design speed. However, for most designs this usually is not a great deal higher than the fuel consumption in the hovering condition.

The solid lines in Fig. 8, indicate the fuel consumption as a function of the rotor-disk loading for various design maximum speeds; however, the data are based upon the supposition that the pilot is operating the aircraft at the tip speed required at the maximum design speed of the aircraft. As previously indicated, the tip speed can be considerably greater in hovering than in forward flight. Assuming that the pilot increases the tip speed in hovering flight to its maximum allowable value, the fuel consumption is decreased to that indicated by the dash lines. As the pilot, in the hovering condition, increases the tip speed from that represented by the solid lines to that represented by the dash lines, the operating fuel/air ratio of the jet engine must be decreased simultaneously. In computing the dash-line data, it was assumed that the combustion efficiency and friction pressure loss through the ramjet engine did not change for the fuel/air-ratio range considered.

For a given design forward speed, it is noticed that there is an appreciable difference in fuel consumption represented by the two sets of data. This indicates two important characteristics of the ramjet helicopter. The first, as was previously indicated, is that proper piloting of the aircraft is important if maximum fuel economy is to be achieved. It is also shown qualitatively that an aircraft designed to attain a certain specified forward speed automatically provides a great deal of excess power in the hovering and slow-speed flight conditions merely by increasing the operating fuel/air ratio of the jet engine. This serves to give a high-performance aircraft in the hovering and slow-speed flight conditions.

Also, this means that for a given disk loading, the size of jet engine required is determined by the maximum design speed of the aircraft. This is strictly true for the higher design maximum forward speeds; however, for the lower speeds, it may be necessary to increase the jet-engine size slightly in order to achieve the desired vertical-flight performance. This condition has not been investigated quantitatively.

It is also shown in Fig. 8, that for the hovering flight condition, an appreciable sacrifice in fuel consumption must be made as the maximum design forward speed increases. Again, it is pointed out that it is important for a designer to select a design maximum forward speed carefully in accordance with the intended use of the aircraft.

In addition, it is noted from Fig. 8, that for any design maximum speed, there is a slight increase in fuel consumption as the disk loading increases. The fact that fuel consumption increases only slightly with increasing disk loading is a distinguishing characteristic of the ramjet helicopter. This means that it is possible

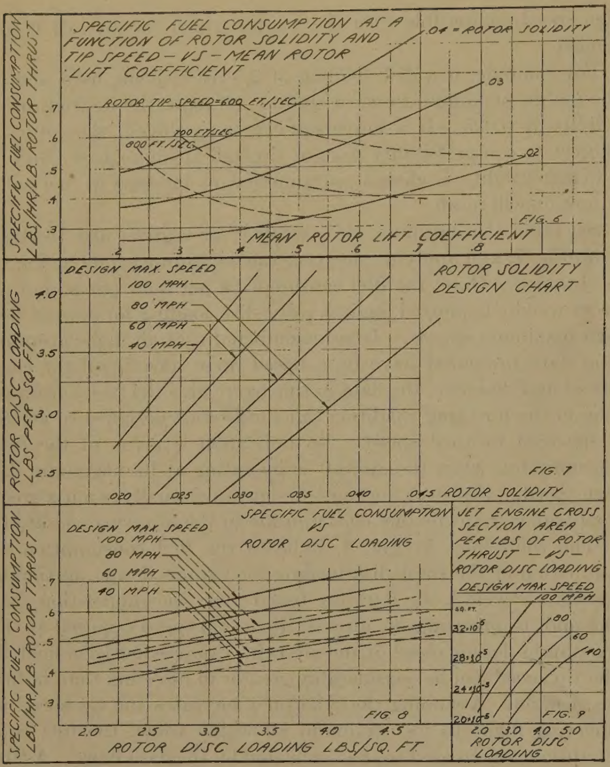

Figs. 6, 7, 8, 9 Ramjet-Rotor Design Charts

to design an aircraft to carry a greater load with a given rotor diameter and only a slight increase in the fuel-consumption results; or, for a given aircraft gross weight, the rotor size can be reduced with a relatively small sacrifice in fuel consumption. This serves to yield a small compact type of aircraft.

However, there is a secondary criterion which possibly may affect the design disk loading; and that is, the size of jet engine required. From Fig. 9, it is shown that the cross-sectional area of the jet engine increases as the disk loading increases for a given design maximum forward speed. This, in turn, means an engine weight increase with increasing disk loading. The jet-engine weight tends to vary approximately in a linear manner with cross-sectional area. Therefore, at a design speed of 100 mph, by increasing the design disk loading from 3 psf to 4 psf, a jet-engine weight increase of approximately 15 per cent results. The effect which the engine-weight increase should have on the design disk loading depends largely upon the type of blade structure used; therefore, it is difficult to make any general comments concerning this parameter.

An important characteristic of the ramjet engine, which has not been considered in this analysis, is the effect that yaw angle has on performance. As the aircraft goes into forward flight, the air flow is no longer perpendicular to the blade-span axis at all blade azimuth positions. The greater the forward speed, the greater the yaw angle at which the jet engine operates. Sufficient data are not available on the effect of yaw angle to consider it in this analysis, with any degree of accuracy.

It is also noticed that the size of the starting engine has not been considered. However, this is not necessary since the starting engine required is essentially independent of the design parameters involved.

In addition, no mention has been made of the desired number of rotor blades. This is likely to be determined by the fact that the optimum design solidities are relatively low, and the fewer blades used the larger the chord per blade; hence a reduction in the blade structural problem. A one-bladed rotor is usually considered undesirable due to its adverse vibrational characteristics. However, the two-bladed rotor has been used quite extensively on the conventional-type helicopter, and it is believed, to be the most desirable configuration for the jet-propelled type.

In summary, the major design points resulting from this ramjet-rotor analysis are as follows:

A slight saving in fuel consumption results with low disk loadings and, if the rotor diameter is not an important factor, considering the intended use of the aircraft, a relatively low design disk loading should be used. Upon selection of the design disk loading, the design maximum forward speed should be chosen carefully, and the solidity required to produce minimum fuel consumption should be used. If a higher solidity is used, an appreciable sacrifice in fuel-consumption results unnecessarily.

The size of jet engine required is determined from the rotor-disk loading and the maximum design speed. If the design maximum forward speed is relatively high, it is probable that sufficient excess power will be available in hovering flight to provide the desired vertical flight performance. If the design maximum speed is quite low, it likely will be necessary to increase the size of the jet engine in order to achieve the desired performance.

Also, proper piloting of the aircraft is important in order to achieve minimum fuel consumption and the maximum performance.

PRESSURE SYSTEM

The pressure type of jet-propulsion system is now considered. In the pressure system it is recalled that an air compressor, driven by an internal-combustion engine, is required to supply air to the jet units through internal blade ducts. Fuel is mixed with the pressurized air, and the combustible mixture is ignited and burned in a blade-tip jet unit.

In the pressure system, it is not possible to separate the performance of the jet unit from the rotor performance, as was possible in the ramjet system. This is because the internal duct area of the rotor blades and concurrently the frictional pressure losses are a function of the rotor solidity and these pressure losses have a significant effect on jet-unit performance.

The method of analysis is similar to that used for the ramjet system in that the rotor horsepower required per pound of gross weight is determined as a function of rotor-disk loading, solidity, and tip speed. Knowing the required rotor power, the fuel consumption of the jet unit required to generate this rotor power is determined. In computing the fuel consumption, standard thermodynamic relationships with factors based upon experimental data are used.

The first design parameter to be investigated is the pressure ratio across the air compressor in the fuselage. In Fig. 10, a typical plot of the fuel consumption of the jet unit in pounds per hour per pound of rotor thrust or gross weight is shown as a function of pressure ratio. It is noted that the fuel consumption decreases very rapidly with increasing pressure ratio. This trend is comparable to the rapid decrease in fuel consumption of the ramjet engine with increasing velocity, since a velocity increase represents a pressure increase. By increasing the pressure ratio from 2:1 to 4:1, a 32 per cent saving in fuel consumption is achieved; however, as the pressure ratio increases, the horsepower required to drive the air compressor increases quite rapidly. Fig. 11 is a plot of the air horsepower on the outlet side of the air compressor per pound of rotor thrust as a function of the pressure ratio. Here it is seen that if the pressure ratio is increased from 2:1 to 4:1, the air horsepower required is increased approximately 34 per cent. These two trends tend to balance each other in that for a given flight duration, the weight saved

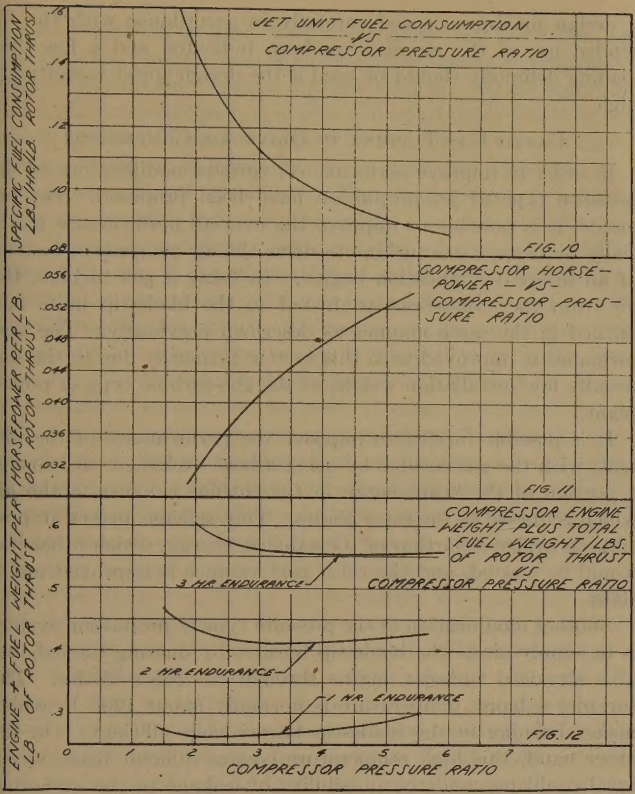

FIGS. 10, 11, 12 DESIGN DATA FOR PRESSURE SYSTEM OF ROTOR DRIVE

at high pressure ratios due to a decreased fuel consumption is counteracted by the weight increase due to the larger compressor and internal-combustion-engine combination.

In order to evaluate this quantitatively, the weight of the fuel consumed by the jet unit plus the weight of the compressor and internal-combustion-engine combination and its final consumption are plotted against pressure ratio in Fig. 12, for three different flight durations. It has been assumed that the air compressor has an efficiency of 75 per cent and that the compressor and engine installation weighs 2.2 lb per engine hp. The fuel consumption of the internal-combustion engine is considered to be 0.6 lb per hp. It is noted that these curves are relatively flat. However, if an aircraft is designed for an endurance of only 1 hr, a slight saving is to be achieved by designing the compressor to operate at a pressure ratio of approximately 2 to 1, and for longer endurances, a pressure ratio of approximately 3 to 1 is desirable.

Secondary criteria, such as the jet-unit size, possibly should be considered in selecting a design pressure ratio. As the pressure ratio increases, the jet-unit size and concurrently the jet-unit weight decrease, thereby tending to decrease the blade structural problem. On the other hand, the blade sealing problems become more difficult as the pressure ratio increases. Also, from these charts, it is indicated that a high pressure ratio has a tendency to increase the initial cost of the aircraft and decrease the operating cost in that a larger internal-combustion engine and air compressor are required, and the fuel consumed by the jet burner is reduced; the converse being true for a low pressure ratio. The importance of this criterion is dependent largely upon the intended use of the aircraft.

The remaining data to be presented on the pressure system are based upon a pressure ratio of 3 to 1; however, the trends to be indicated are applicable to other design pressure ratios.

A typical set of data showing the effect on performance of a variation in rotor solidity and rotor-disk loading are shown in Fig. 13. The data are based upon a constant lift coefficient of 0.6; however, the trends shown do not change appreciably for a variation in this value. As noticed, the fuel consumption of the jet unit per hour per pound of rotor thrust is plotted as a function of the rotor solidity for several disk loadings. The crossing diagonal plots are lines of constant tip speed.

It is noticed that the fuel consumed by the internal-combustion engine, used to power the compressor, is not included in this plot. This is not needed in order to show the effect of a change in the design parameter, since, with a constant pressure ratio across the compressor, the engine fuel consumption varies directly with the jet-unit fuel consumption, and the trends indicated would remain unchanged.

Following either of the constant disk-loading curves, it is noticed that the fuel consumption is reduced appreciably with decreasing solidity. However, there is a sharply characterized lower limit to which the solidity can be reduced. This low limit is determined by the frictional losses in the internal air duct of the rotor blades. The data shown in this figure are based upon a two-bladed rotor, using a monocoque type of blade construction with an internal duct area equal to 70 per cent of the airfoil-contour area. The duct losses for a given solidity are a function of the number of blades and the type of construction employed; therefore, a change in either of these variables will change the low solidity limit. For example, this chart shows the low solidity limit to be 0.02 for a disk loading of 2.5 lb per sq ft, but for a three-bladed rotor, with the same disk loading, the low solidity limit is approximately 0.03. As stated, the solidity limit also is affected materially by the type of blade construction, thereby indicating that in general a two-bladed rotor with monococoque blade construction is the most desirable, if the unsatisfactory use of a one-bladed rotor is precluded. In addition, the solidity limitation is a function of the air-compressor pressure ratio, and the specific data presented in the chart are applicable only for a ratio of 3 to 1.

With a decreasing solidity for any disk loading, it is noticed from the diagonal plots that the tip speed is increasing. This increasing tip speed is primarily responsible for the decreased fuel consumption. As for any constant-pressure thermal-jet engine, the propulsive efficiency of the blade-tip unit is increased materially with increasing velocity.

It is also indicated in this figure that a saving in fuel consumption is achieved by designing with low rotor-disk loading; however, the disk-loading parameter is evaluated more accurately in a later chart. The advantage of designing a "pressure" type jet rotor with relatively low solidity such that it is possible to operate efficiently at high tip speeds has been indicated by these curves. This same conclusion was drawn for the ramjet system and, in the same manner, the tip speed and lift coefficient must be limited as a function of the forward flight velocity.

As a result, the solidity design chart explained for the ramjet system is also applicable to the pressure type of jet rotor and it is repeated here as Fig. 14. After a design disk loading and design maximum forward speed have been selected, the solidity required to achieve maximum fuel economy is determined from this chart. However, the solidity values determined must be in excess of the low solidity limits as established from plots similar to Fig. 13.

Considering all limitations, the fuel consumption of the jet unit in pounds per hour per pound of rotor thrust is plotted as a function of the rotor-disk loading, in Fig. 15. Here, hovering-flight fuel-consumption plots are shown for aircraft designed to attain a maximum speed of 120 mph down to aircraft designed only for hovering flight. It is noted that the curves for relatively low design speeds, 0 to 40 mph, are quite flat; thereby indicating that a relatively high disk loading can be used without a great sacrifice in fuel economy. As the design forward speed increases, it is evident from the curves that a greater sacrifice in fuel consumption is made with increasing disk loading. For example, at a design speed of 40 mph, the disk loading can be increased from 2 lb per sq ft to 4 lb per sq ft with only an 8 per cent increase in fuel consumption. However, a 20 per cent increase in fuel consumption results for the same disk loading increase at a design speed of 100 mph. Therefore, in selecting a design disk loading for a pressure-type jet rotor, particular attention should be given to the maximum design speed of the aircraft. In general, at low design speeds, the advantages of high disk loading and small rotor diameter can be achieved without a great sacrifice in fuel economy. At higher design speeds, it is quite advantageous to design with relatively low disk loadings.

From this same figure, by noting the rapid increase in fuel consumption with increasing design speed for any disk loading, the importance of selecting a design maximum speed carefully is apparent. For example, the fuel economy would be reduced significantly if an aircraft were designed to attain a maximum speed of 120 mph, and the aircrafts application did not require a speed in excess of 80 mph. This same condition exists for the ramjet rotor, and it is an inherent characteristic of any rotor driven by a propulsion system which becomes more efficient as the tip speed increases.

To summarize the data on the pressure type of jet rotor, it has been shown that an air-compressor pressure ratio of approximately 2 to 1 is optimum if it is not necessary for the endurance of the aircraft to exceed 1 hr. For endurances greater than 1 hr, a slight advantage is gained by increasing the pressure ratio to approximately 3 to 1. The advantage of using the proper rotor solidity, as determined by the maximum design speed of the aircraft and affected by the number of rotor blades and the type of blade construction, has been shown. The desirability of selecting a design maximum speed carefully in accordance with the intended use of the aircraft has been indicated and a low disk loading definitely should be used if the design speed is relatively high.

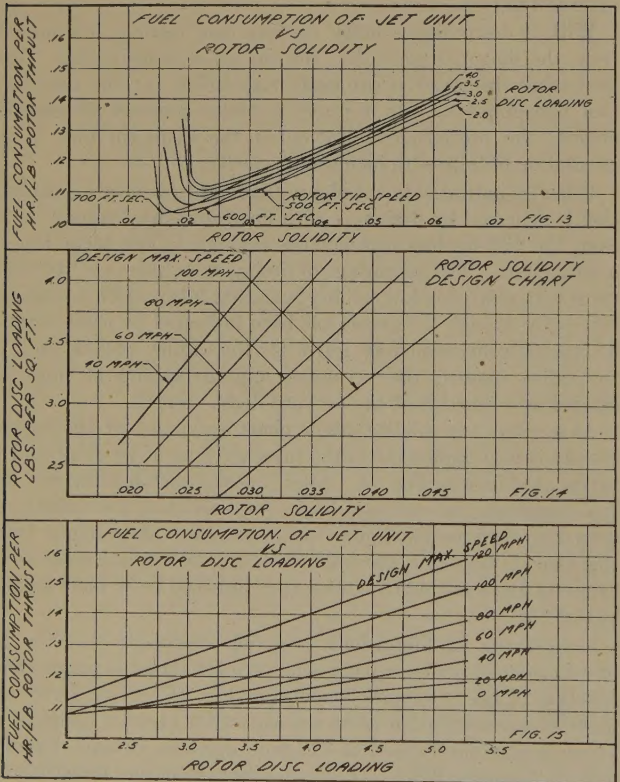

Figs. 13, 14, 15 Performance and Design Data for Pressure Drive System

Use of Gas Turbine to Drive Air Compressor

In order to improve performance, various modifications of the pressure type of jet propulsion have been proposed. For example, it is possible to improve the over-all performance materially by using a gas turbine to drive the air compressor instead of an internal-combustion engine. In using a gas turbine, the air from the compressor is ducted to the blade-tip units and burned in the same manner as described previously. The performance is improved with this system primarily due to the unusually low installation weight of the gas-turbine type of power plant.

It is possible further to improve the performance of the aircraft with the gas turbine by using a heat exchanger to transfer a portion of the heat energy in the turbine exhaust to the air which is ducted to the rotor blades. This scheme makes it possible to utilize a portion of the exhaust energy, which otherwise would be wasted, and the rotor performance is improved materially.

Another modification of the pressure type of propulsion system is to supply air to the blade-tip burners by ducting the exhaust of a standard turbojet engine through the rotor blades. The turbojet exhaust temperature is normally about 1200 F, which makes burning in the blade-tip burner very efficient. On the other hand, this high temperature creates difficult blade structural problems, and the possibility of leakage in the system is greater. These obstacles may not be insurmountable if the recently developed high-temperature alloys are used.

Other Types of Jet Drives

Both of these modified systems for supplying air to a blade-tip burner require the same general type of rotor design as the system using an internal-combustion engine and air-compressor combination. Several other interesting and promising types of jet-propulsion systems have been proposed for helicopter rotors and, in general, these require an entirely different type of rotor design from that indicated for the ramjet or pressure systems. For example, the configuration known as a "cold-air" system, where atmospheric air is pressurized by any of several means in the fuselage and ducted through the rotor with ejection at the blade tip without burning fuel, requires relatively low tip speeds and high solidity for efficient operation. This is primarily because the efficiency of the system depends upon a very low pressure ratio across the air compressor, which permits the movement of a large mass of air at low velocity. Also, in the "cold-air" system without burning at the blade tip, it is highly desirable to design with an unusually low disk loading.

As in the "pressure" system, the standard turbojet engine can be used to modify the "cold-air" system with materially improved performance. Here, the turbojet exhaust is ducted through the rotor and expelled at the blade tip without additional burning. Again, since no fuel is burned at the blade tip, a low tip speed, and, in general, a relatively high solidity are required.

Some attention has been given to the "pulse-jet" type of engine for the propulsion of helicopter rotors; however, the present state of development of this engine prevents its immediate use. On the other hand, when the present performance of the pulsejet engine at speeds of 400 to 500 fps is improved materially, the pulsejet will be a very attractive power plant for the helicopter rotor.

Performance Comparison

It will be recalled from the fuel-consumption data, that the ramjet propulsion system consumes a great deal more fuel per hour than an internal-combustion engine producing an equivalent power. The pressure system also has a higher fuel consumption than an internal-combustion engine, but appreciably less than the ramjet system. The advantage of either propulsion system over a conventional rotor drive lies in the decreased structural and equipment weight of the aircraft. This weight is greatly reduced in the jet-propelled helicopter due to the elimination of the auxiliary torque-compensating rotor and the structure required to support it; due to the elimination of clutch, free wheeling, and transmission assemblies; and due to the elimination of a large internal-combustion engine. Of course, in the pressure system, a relatively low-horsepower engine is required to drive the compressor. The structural and equipment weight saved by using a jet-propulsion system can be used to carry additional fuel or additional pay load, dependent upon the duration of flight. Consequently, for flights of relatively short duration, when it is not necessary to carry a large quantity of fuel, the weight saved in the jet-powered helicopter can be used to transport a greater pay load.

A performance comparison based upon pay load has been made between a helicopter of the conventional type and an equivalent helicopter using each of the jet-propulsion systems which have been described in detail. For the conventional type, data from the Army R-5 helicopter have been used. This aircraft has a gross weight of 4800 lb and uses a 450-hp engine. By removing the equipment and structure of the R-5 which would not be required if a jet-powered rotor were used, and replacing this weight with fuel and pay load, the data shown in Fig. 16 result. In this plot, the increased pay load over that which is normally carried by the Army R-5 helicopter is shown as a function of flight duration for both the ramjet and pressure types of propulsion systems. The data for the pressure system are based upon a compressor pressure ratio of approximately 2:1. It is noted that for a ramjet helicopter, equivalent in size to the Army R-5, a greater pay load can be carried up to an endurance $1^1/_4$ hr. If it is necessary to fly for only $^1/_2$ hr, as much as a 1000 lb additional pay load can be carried by the ramjet helicopter.

For an equivalent helicopter using the pressure type of jet-propulsion system, a greater pay load can be carried up to an endurance of $2^1/_4$ hr. For an endurance of 1 hr, approximately 750 lb additional pay load can be transported.

These characteristics of the jet-propelled helicopter make it particularly suited for specialized applications where only a relatively short endurance is required. However, for endurances of 4 and 5 hr, the two types of jet helicopters which have been considered in detail cannot compete favorably with the conventional type.

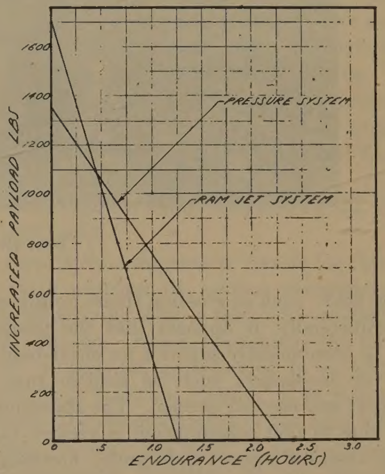

Fig. 16 Increased Pay Load of Jet-Propelled Helicopter Versus Endurance

From a military standpoint, the jet-propelled helicopter could be used to advantage for transporting heavy equipment for a short

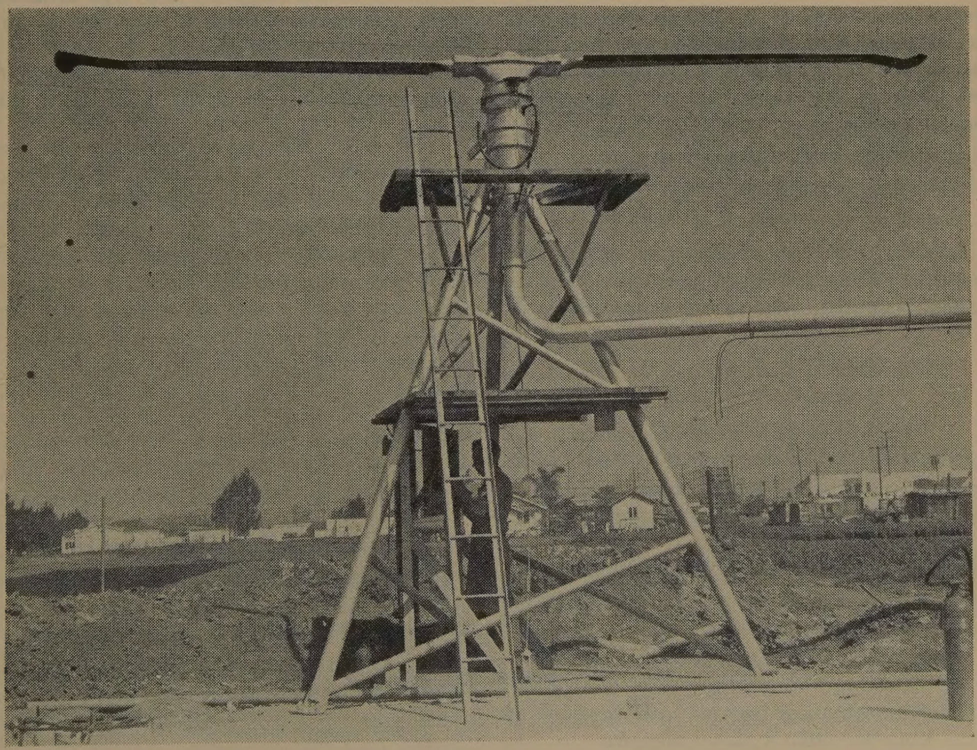

Fig. 17 Whirl-Stand Rotor Using Pressure Type of Propulsion System

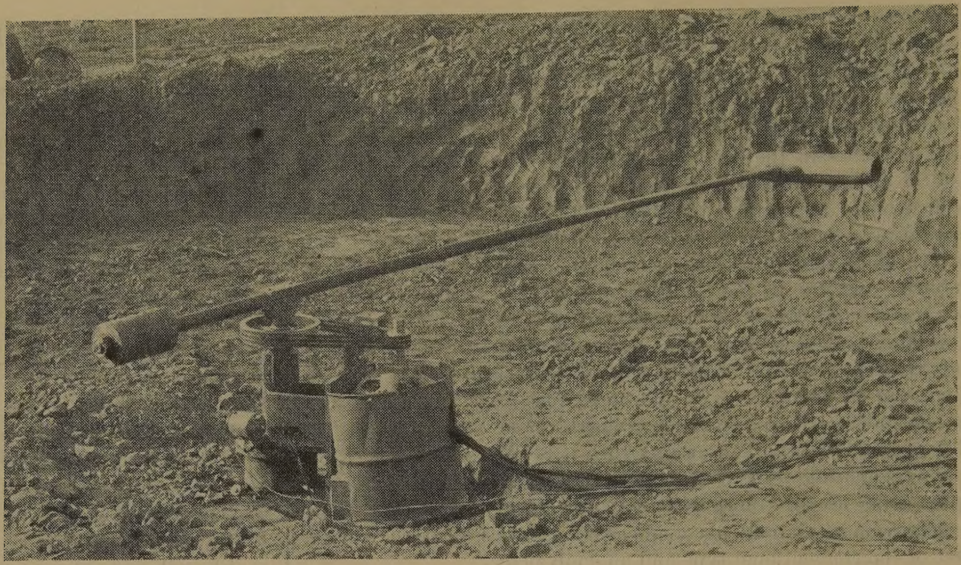

FIG. 18 RAMJET-ENGINE WHIRL-TEST RIG

distance in the field; such as crossing rivers or any other kind of barriers. Commercially, it appears that the jet-powered helicopter would be economically superior for short-haul transportation of cargo or passengers such as shuttle runs between a municipal airport and the city proper. The operating cost of the jet helicopter due to fuel consumption is greater than the conventional type even for a short endurance; however, the return from the increased pay load would make this an insignificant factor.

MARQUARDT AIRCRAFT JET-ROTOR DEVELOPMENTS

Shown in Fig. 17, is a whirl-stand rotor using the pressure type of propulsion system. This rotor has been developed and tested under Army contract. Air is supplied to the rotor through the duct shown and fuel is injected through a manifold just below the rotor hub. The fuel and air mixture is ignited and burned at the blade tip. The test data from this whirl-stand rotor agrees favorably with the analytical data.

Fig. 18 shows a ramjet-engine whirl-test rig. The jet engine is mounted on a counterbalanced steel tube. An electric motor is used to accelerate the engine to the velocity required for starting. Fuel and ignition systems are built in the whirling arm and controlled remotely. The engine shown here is 6.6 in. diam and weighs only 12 lb.

Two such engines mounted on a properly designed rotor would be capable of propelling a helicopter with a gross weight of approximately 1300 lb.

CONCLUSION

In conclusion, it should be mentioned that the jet-propelled helicopter is still a relatively new type of aircraft, and a great deal of development testing is yet to be accomplished before a utility aircraft can be realized. However, development work appears to be progressing quite rapidly, and it is not unreasonble to anticipate a practical aircraft in the relatively near future.

Heat-Transfer Temperature Patterns of a Multicomponent Structure by Comparative Methods

By C. F. KAYAN,[1] NEW YORK, N. Y.

For a thick two-dimensional corner composed of two different materials of unequal thickness, with fluid-boundary conductance on each side, and with a temperature difference established between the two boundary fluids, the isotherms throughout the solid corner are distorted in irregular fashion. Accordingly, calculation is difficult. This problem has been studied by various methods and comparative results have been obtained for the internal temperature distribution. The methods include the experimental "geometrical" and the network electrical analogies, as well as the solution of the equivalent electrical network by the process of arithmetical iteration.

INTRODUCTION

PREDICTION of the temperature patterns for a multicomponent complex wall between two heat-transfer fluids is rendered difficult when the isotherms themselves are distorted in irregular fashion. Orthodox mathematical techniques normally are not sufficient for numerical evaluation, and special techniques, consequently, take on particular significance.

The multicomponent complex structure herewith studied is a thick corner composed of two materials of different thickness and of widely differing conductivity. The fluids on the inside and outside surfaces, representing the high and low temperature levels, respectively, are considered as having different boundary conductances. In this study the wall materials are considered homogeneous and of constant conductivity, i.e., independent of temperature. Joint resistance between adjacent layers is disregarded, and the boundary conductance for each fluid is considered to be uniform over the surface in question.

The cross section of the corner as studied is shown in Fig. 1. As such this represents a two-dimensional heat-transfer problem, with assumed thermal conductivities of 1.00 and 4.00 Btu/(ft^2)(hr)(F/in.) for the inner and outer layers, respectively. The inner layer is uniformly 2 in. thick, and the outer layer 2 in. thick on one side and 3 in. thick on the other. The section studied runs 10 in. in each direction, as measured from the outside corner. A surface conductance, $h_a = 5$ Btu/(ft^2)(hr)(F) has been assumed for the inside-surface conditions, and $h_a = 2$ for the outside, as representative of conditions due to air, for example. The heat flow is presumed to be in steady state from the inner fluid to the outer fluid, on the basis of the prevailing temperature difference. The composite structure is one such as may be found, for example, in refrigeration practice.

Under the circumstances, the isotherms throughout the solid section may be expected to be distorted in complex fashion. The problem therefore is one of establishing just how these are positioned within the section. With the temperature pattern of the structure established, particularly along its surface, the heat-transfer characteristics of the system may be set up.

At the outset it must be emphasized that the results of the present analysis by the different ensuing methods must be recognized as being based solely on the assumed basic data, i.e., thermal conductivities and boundary conductances. It is of course further understood that the values assumed for the analysis have been selected arbitrarily.

This paper reports the comparative results for this two-dimensional steady-state problem by several comparative methods. The philosophy underlying these is that of the so-called resistance concept of heat transfer. Herein specifically the flow of heat in thermal circuits is regarded as behaving in parallel fashion to the flow of current in electrical circuits, as expressed by Ohm's law. Accordingly, the characteristics of the heat flow are established by analogy through the study of an equivalent electrical system. Determination therefore of the isopotential lines through the electrical study permits translation into equivalent isothermal lines, and thereby permits establishment of the temperature distribution in accordance with the impressed over-all temperature difference.

Herein use is to be made of the potential-difference ratio c, defined

$$c = \Delta e_x / \Delta e \ldots\ldots\ldots\ldots\ldots\ldots\ldots [1]$$

where

Δe_x = potential difference between lower (base) potential level and a given point x within the flow field

Δe = electrical potential difference between lower and upper potential level

From the electrical studies which establish the value of c, equivalent temperatures throughout the thermal structure may be established as representative of actual conditions

$$t_x = t_1 + c\Delta t \ldots\ldots\ldots\ldots\ldots\ldots\ldots [2]$$

where

t_x = temperature at given point x, deg F

t_1 = uniform temperature of fluid at lower temperature level

Δt = temperature difference, deg F, between fluid at lower temperature level and fluid at higher temperature level

The following heat-transfer resistance-concept relationships are also of interest

$$R_a = 1/h_a \ldots\ldots\ldots\ldots\ldots\ldots\ldots [3]$$

where

R_a = equivalent thermal resistance at fluid boundary, as, for example, for air, F/[Btu/(ft^2)(hr)]

h_a = fluid boundary-surface conductance, Btu/(ft^2)(hr)(F)

---

[1] Department of Mechanical Engineering, Columbia University. Mem. ASME.

Contributed by the Heat Transfer Division and presented at the Spring Meeting, New Orleans, La., March 1–4, 1948, of THE AMERICAN SOCIETY OF MECHANICAL ENGINEERS.

NOTE: Statements and opinions advanced in papers are to be understood as individual expressions of their authors and not those of the Society. Paper No. 48—S-10.

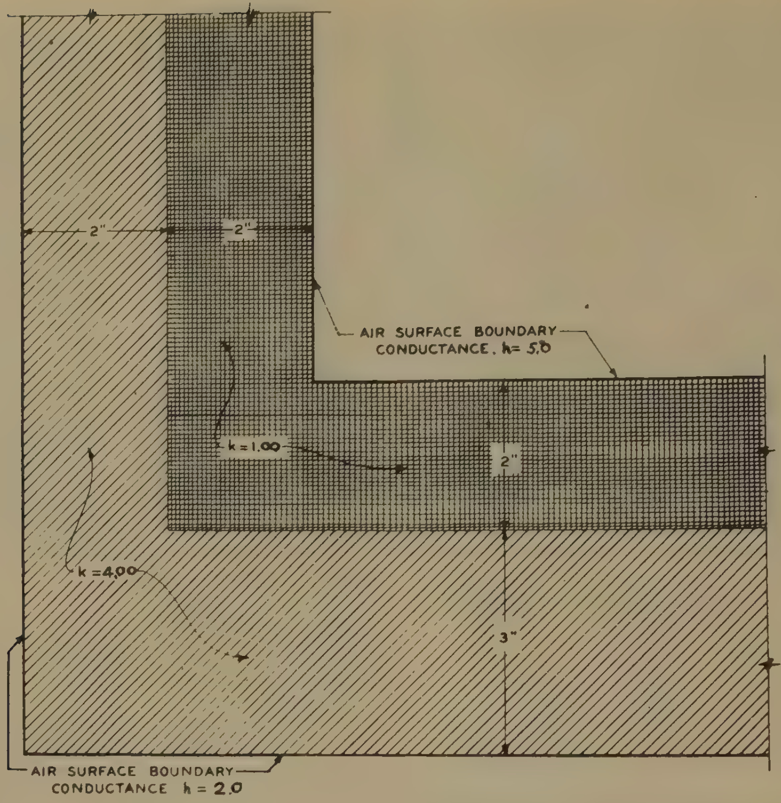
2"
2"
AIR SURFACE BOUNDARY CONDUCTANCE. h= 5.0
k = 1.00
2"
k =4.00
3"
AIR SURFACE BOUNDARY CONDUCTANCE h = 2.0

Fig. 1 Cross Section of Corner Showing Two-Layer Construction

The resistance R_w of wall material of uniform composition

$$R_w = L_w/k_w \qquad [4]$$

where

L_w = thickness of wall material, in.

k_w = thermal conductivity of wall material, Btu/(ft²)(hr)(F/in.). (Shown on the inch basis, as commonly specified; preferred practice for future is foot basis.)

As noted, for a given value of h_a, there is a corresponding value of resistance R_a. Hence for a given conductivity of wall material, there is some equivalent thickness L_e of wall material that would give the same resistance R_e to heat transfer as the fluid boundary

$$R_a = 1/h_a = R_e = L_e/k_w \qquad [5]$$

Hence

$$L_e = k_w/h_a, \text{ in.} \qquad [6]$$

As is to be noted later, this value of L_e is employed in the construction of the "Analogger" model. Furthermore, in the construction of the different electrical arrangements, the electrical-resistance values are to be considered the counterpart of the thermal-resistance values, standing in the same relationship to one another for the different circuits.

Two different experimental electrical-analogy methods have been employed in this study. One deals with the "geometrical" type employing conductive flat sheet, and provides the Analogger method, previously reported on fully so that it need not be detailed extensively here (1, 2).[2] The second method involves an electrical-resistance network or grid of component resistance elements, proportioned so that the assembly represents the heat-transfer-structure conditions. The network, as indicated, is multibranched, and for this a special computational technique has been developed, leading to a numerical solution for the potential values at the different locations within the network.

Results have been obtained showing the value of c (reported in per cent) for different points within the corner structure. The program of investigations covers four separate series of studies. Series I and II represent the Analogger and the network-analogy studies, respectively. Herein merely the fluid temperatures, i.e. potential values, have been defined and impressed upon the system. Series III, however, represents the resistance-network results with end-zone potential distribution specified at both ends, based upon potential values, i.e., temperatures, that would result from one-dimensional flow through the wall sections. Series IV represents, for direct comparison, solution by computational technique of the network under the identical boundary conditions of Series III, i.e., including the one-dimensional end-zone values.

The following summarizes the arrangement of the series for comparative results:

(a) Fluid-boundary values (only) specified:
  Series I Geometrical Analogger.
  Series II Resistance network.
(b) Fluid-boundary values and end-zone values specified:
  Series III Resistance network.
  Series IV Computational technique.

Series I Solution by Geometrical Electrical Analogger

An Analogger model, geometrically equivalent to the cross section of the corner in question, was constructed to scale, using the higher-conductivity material—that of the outer section (k =

---

[2] Numbers in parentheses refer to the Bibliography at the end of the paper.

4.00) as the reference basis for the construction. The model was constructed of electrically conductive flat sheet to present an electrical-resistance path as the counterpart of the heat-flow path represented by the corner cross section, Fig. 1. Across the sheet, current could flow from one electrode system to the other, representative of the heat flow from the fluid at one temperature level to the fluid at the lower temperature level. Under these circumstances potentials throughout the sheet representing the corner structure could be considered the counterpart of the temperatures.

To have the model represent the less conductive inner layer, the electrical properties of the sheet material were modified appropriately by cutting the sheet into a mesh pattern, in the manner described by the author in an earlier paper (1). The effect of the boundary conductance at the surfaces, in turn, was established by offsetting the electrode system by a distance L_e, in scale, representative of the boundary-conductance effect (see Equation [6]). This section of the sheet was slit at regular intervals, perpendicular to the electrodes, to prevent lateral flow in the "boundary" region. The Analogger setup is illustrated in Fig. 2.

The experimental results, as values of c (per cent) at different points within the corner, are shown in Table 1. The different points indicated in the table correspond to junction positions identified in the subsequently shown network system of Fig. 4.

Series II Solution by Electrical-Resistance Network

Use of the perforated mesh pattern in the Analogger model, shown in Fig. 2, obviously suggests the employment here of an electrical-resistance network for determination of the potential distribution. As in the Analogger study, from the potential-distribution results, equivalent values of temperature may be inferred for the heat-transfer circumstances, as provided by Equation [2].

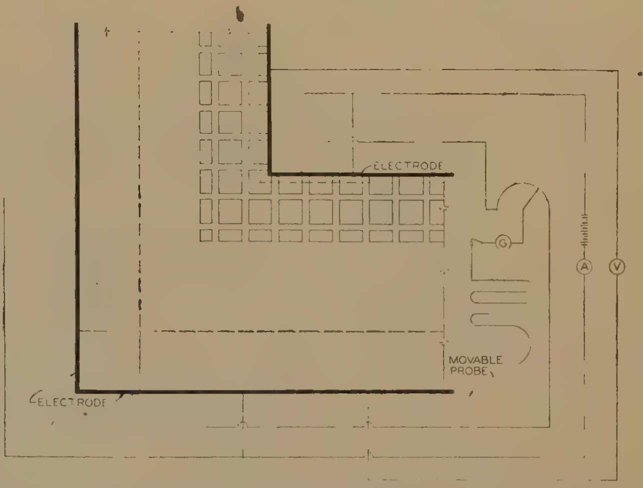

Fig. 2 Experimental Arrangement for Analogger Study

The corner cross section is thought to be divided into a regular pattern of squares, shown in Fig. 3(*a*), each square being regarded as of equal thickness. (If three-dimensional analysis were in question, the material of the corner would be thought of as divided into cubes.) The effect of each square is then considered as concentrated at the center point. In accordance with the electrical-resistance concept, the resistance of the square of material may be set up appropriately as indicated in Fig. 3(*b*). Here the resistance in the X-X-direction is shown as r_x, and in the Y-Y-direction, as r_y. The composite resistance effect is likewise shown, with separate half elements $r_x/2$ and $r_y/2$ representing the X and Y-directions respectively, and totaling r_x and r_y for the entire square.

Based on the material conductivities, $k_w = 4$ for the outer ma-

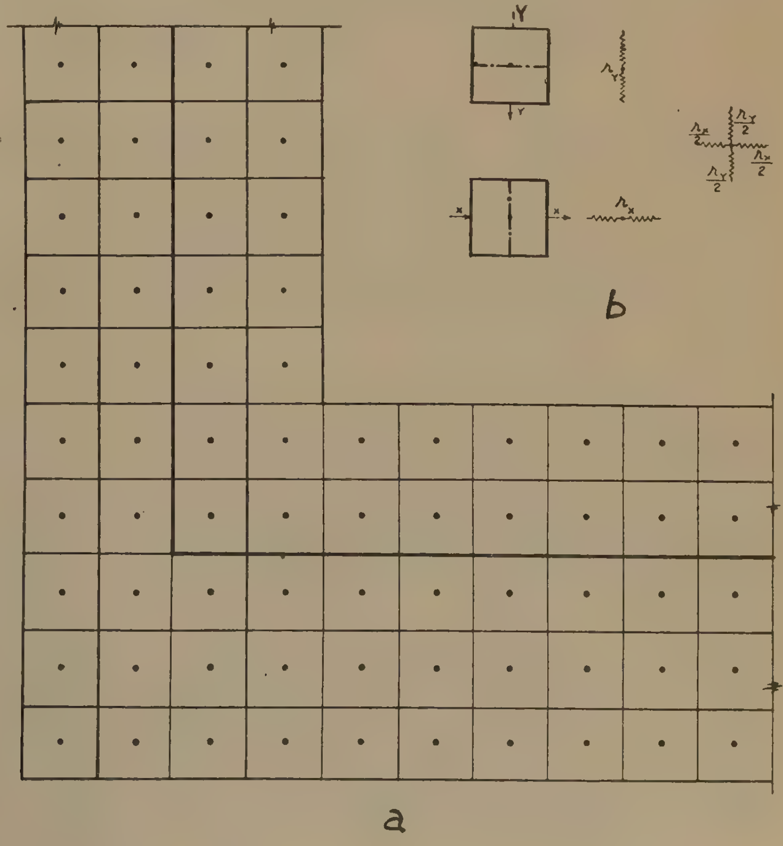

Fig. 3 (*a*) Representation of Corner by Square Elements; (*b*) of Square Elements by Resistance

TABLE 1 RESULTS OF COMPARATIVE STUDIES

		1	2	3	4	5	6	7	8	9	10	11
a	I	0	16.8	24.1	45.9	77.1	100					
	II	0	17.8	25.1	45.0	77.1	100					
	III	0	19.5	27.5	47.0	78.0	100					
	IV	0	19.5	27.5	47.0	78.0	100					
b	I	0	16.8	24.0	45.3	76.9	100					
	II	0	17.4	24.8	44.6	77.0	100					
	III	0	18.6	26.2	45.8	77.5	100					
	IV	0	18.6	26.3	45.9	77.5	100					
c	I	0	16.0	23.0	44.5	76.3	100					
	II	0	16.5	23.9	43.6	76.2	100					
	III	0	17.5	24.9	44.3	76.5	100					
	IV	0	17.5	24.9	44.4	76.6	100					
d	I	0	15.0	21.7	42.6	74.5	100					
	II	0	15.5	22.2	41.5	74.3	100					
	III	0	16.1	22.8	42.0	74.5	100					
	IV	0	16.2	23.0	42.1	74.6	100					
e	I	0	13.4	19.6	38.3	68.4	100	100	100	100	100	100
	II	0	13.8	20.0	37.2	68.5	100	100	100	100	100	100
	III	0	14.1	20.4	37.5	68.6	100	100	100	100	100	100
	IV	0	14.4	20.5	37.6	68.8	100	100	100	100	100	100
f	I	0	11.5	16.3	30.1	50.0	70.1	75.5	77.6	78.2	78.5	79.0
	II	0	11.7	16.5	28.9	49.1	69.3	75.2	77.2	78.2	78.5	78.7
	III	0	12.0	16.9	29.2	49.4	69.4	75.5	77.5	78.6	79.0	79.5
	IV	0	12.3	17.2	29.4	49.6	69.4	75.5	77.7	78.7	79.2	79.5
g	I	0	9.6	13.2	20.1	31.4	40.1	44.5	47.7	48.8	49.3	49.6
	II	0	9.7	13.2	19.9	30.0	38.9	43.6	46.2	47.6	48.3	48.6
	III	0	9.9	13.5	20.0	30.2	39.3	44.1	46.8	48.3	49.4	50.4
	IV	0	10.2	13.9	20.5	30.5	39.5	44.4	47.1	48.6	49.6	50.5
h	I	0	7.8	10.8	14.2	18.4	22.1	24.9	26.9	28.3	29.0	29.4
	II	0	7.8	11.0	14.3	18.5	22.4	25.5	27.5	28.8	29.6	30.0
	III	0	8.0	11.2	14.6	18.9	22.9	26.0	28.3	30.0	31.0	32.0
	IV	0	8.3	11.7	15.0	19.2	23.3	26.4	28.6	30.1	31.2	32.0
i	I	0	6.0	8.6	11.2	14.0	16.4	18.7	20.4	21.4	22.1	22.4
	II	0	6.0	8.5	11.2	14.0	16.8	19.2	20.8	21.8	22.5	22.8
	III	0	6.2	8.8	11.5	14.4	17.3	19.7	21.5	22.8	24.0	24.9
	IV	0	6.6	9.2	11.9	14.8	17.6	20.0	21.8	23.1	24.1	25.0
j	I	0	4.2	6.0	8.1	10.0	11.5	13.0	14.2	15.1	15.6	15.9
	II	0	4.2	6.0	8.0	9.9	11.7	13.2	14.4	15.3	15.8	16.0
	III	0	4.5	6.2	8.2	10.1	12.1	13.7	15.1	16.1	17.0	18.0
	IV	0	4.7	6.6	8.5	10.5	12.4	14.0	15.4	16.4	17.2	18.0
k	I	0	0	0	0	0	0	0	0	0	0	0
	II	0	0	0	0	0	0	0	0	0	0	0
	III	0	0	0	0	0	0	0	0	0	0	0
	IV	0	0	0	0	0	0	0	0	0	0	0

terial and $k_w = 1$ for the inner material, air-boundary conductances $h_a = 5$ for the inner surface, and $h_a = 2$ for the outer surface, an equivalent electrical-resistance network was calculated and set up. This is shown, with appropriate relative resistance, in Fig. 4. Electrical connections, similar to those shown in Fig. 2 for the Analogger, were used.

For each square foot of wall surface, thermal resistances for the vertical section of the wall are as follows: Outer air boundary, $R_a = 1/h_a = 1/2 = 0.50$; for the 2-in. layer of outer structural material with $k_w = 4$, $R_w = L_w/k_w = 2/4 = 0.50$; for the 2-in. layer of insulating material with $k_w = 1$, $R_w = 2/1 = 2$; and for the inner air boundary with $h_a = 5$, $R_a = 1/5 = 0.20$. Thus the total $R = 0.50 + 0.50 + 2.00 + 0.20 = 3.20$. Similarly, for the horizontal section, the total $R = 3.45$. On the basis of 1-in. squares of uniform thickness, the relative resistances of each element of the heat-flow path are 0.50 and 0.20 for the outer and inner air boundaries, respectively, and 0.25 and 1.00 for each inch of outer and inner material path, respectively.

The results for the potential distribution in this Series II study are likewise shown in Table 1, values of c (per cent) being shown for the regularly spaced junction points of the Fig. 4 network. It will be noted that the results are in satisfactory agreement with those of Series I, the Analogger study. It will, however, be recognized that the Analogger represents the wall material as a continuum for a large share of the model, using in effect the lumping technique, via meshing, for only a relatively small part. The network study of course employs the lumping technique throughout the entire simulation setup. It is believed that the small discrepancies which appear between the results of Series I and II may in part be attributed to this factor.

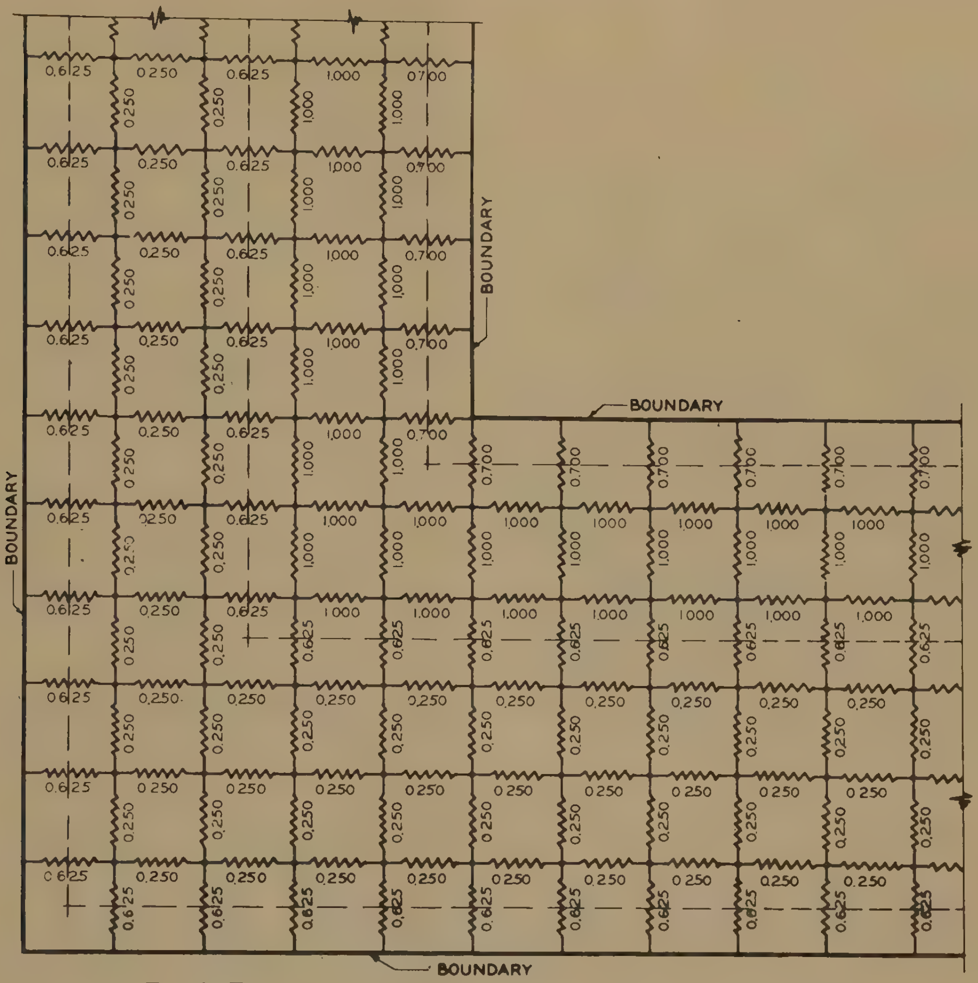

Fig. 4 Equivalent Electrical-Resistance Network for Corner

Both Series I and Series II results are based on specification of fluid-boundary potentials only, and as such are directly comparable.

Series III Solution by Network With End-Zone Values Specified

It will be noted that for both of the previous experimental studies, the potential values at the end-zone junction points were undefined, and as such they were free to vary in an unrestrained manner. The fluid "temperatures" were at 100 and 0, respectively, for the inner and outer locations, by virtue of impressed electrode potential difference. The values in the end-zone locations were free to establish themselves, presumably in accordance with what could be expected with one-dimensional flow, or as indicated through Fig. 6. Study of the end-zone results in Table 1 reveals that the one-dimensional values were not achieved. This may be observed by inspection of the results in row *a*, representing the vertical end zone, and of column 11, for the horizontal end zone.

In Series III, therefore, for comparative purposes, the potential values at the end-zone junctions were adjusted to correspond with the values given in Fig. 6. The results shown in Table 1 indicate that under these circumstances there are marked deviations from the values of the previous comparable set, namely, the values for the Series I and II studies.

Series IV Solution by Computational Technique, End-Zone Values Specified

The numerical solution of the Fig. 4 resistance network, without recourse to the experimental electrical determination, is of specific interest, particularly in view of the many network branches which are involved. The values for the different internal junctions are thus to be determined as for an electric-circuit analysis.

A method for the solution of this type of network has been reported previously by the author (3) and is described here in further detail, it being particularly noted that it requires no experimental setup.

At any junction point, under steady-state electrical-flow conditions, the sum of the currents flowing in must be zero, i.e. there can be no accumulation. Accordingly, considering Fig. 5(*a*), the point *O* is surrounded by points *M*, *N*, *P*, and *Q*. The resistance of the four corresponding branches are r_M, r_N, r_P, and r_Q. Their relative values may be designated by *m*, *n*, *p*, and *q*.

The currents in the four different branches, as dependent upon the difference in potential *e* between the outlying points and the center junction, are next to be considered. The following relationship may be set up

$$\frac{(e_M - e_O)}{r_M} + \frac{(e_N - e_O)}{r_N} + \frac{(e_P - e_O)}{r_P} + \frac{(e_Q - e_O)}{r_Q} = 0 \quad \ldots[7]$$

Thus to satisfy steady-state conditions

$$e_O = \frac{(1/r_M)e_M + (1/r_N)e_N + (1/r_P)e_P + (1/r_Q)e_Q}{1/r_M + 1/r_N + 1/r_P + 1/r_Q} \quad \ldots[8]$$

Similarly, using values of relative resistances

$$\frac{(e_M - e_O)}{m} + \frac{(e_N - e_O)}{n} + \frac{(e_P - e_O)}{p} + \frac{(e_Q - e_O)}{q} = 0 \quad . . [9]$$

To satisfy steady-state conditions

$$e_O = \frac{(1/m)e_M + (1/n)e_N + (1/p)e_P + (1/q)e_Q}{1/m + 1/n + 1/p + 1/q} \quad . . . . [10]$$

The reciprocal values of the relative resistances are of course the relative conductances. In Fig. 5(*b*) the counterpart of the resistance diagram of Fig. 5(*a*) is shown, in terms of relative conductances.

Starting out with initially assumed values for all of the junctions in the conductance network, by carrying out the operation of Equation [10] systematically for the different points in succession, it is possible, after repeated calculation tours, to arrive at final values for the different junction points in the network. These junction points, it will be recalled, represent the center points of the original squares shown in Fig. 3(*a*). The procedure of evaluation may be termed a process of arithmetical iteration, with its own sphere of usefulness in network evaluation.

For simplification of the routine computation, since numerous equations have to be solved successively for each junction, obviously it is desirable first to compute constant coefficients for each potential point. These follow from the division of the individual branch conductances by the sum of the four branch conductances surrounding any one junction. Thus setting

$$1/m + 1/n + 1/p + 1/q = s$$

Equation [10] then becomes

$$e_O = (1/ms)e_M + (1/ns)e_N + (1/ps)e_P + (1/qs)e_Q \quad . . . [11]$$

On the basis of the one-dimensional end-zone values cited under Series III, boundary values of 100 and 0, and estimated values for the remaining junctions, the network was calculated

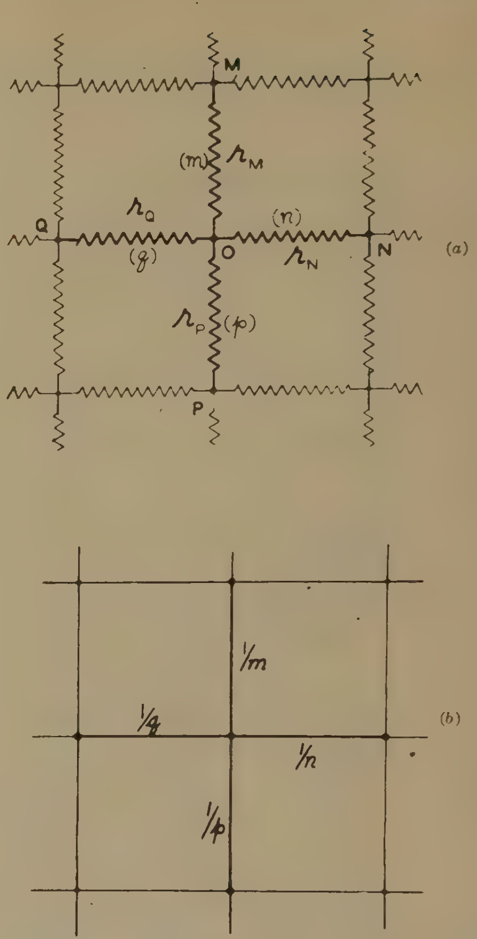

Fig. 5 Network Resistance and Conductance Elements

(*a*, Network resistance elements for a single junction. *b*, Network conductance elements for a single junction.)

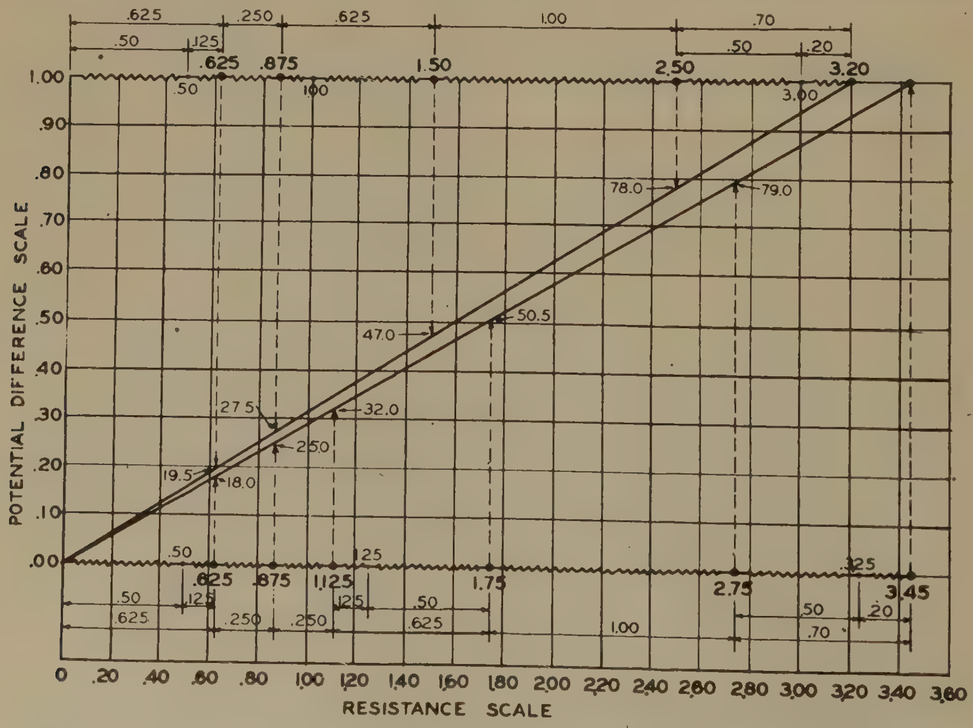

Fig. 6 One-Dimensional Potential Versus Resistance Diagram for End-Zone Conditions

by the foregoing process of arithmetical iteration. Fig. 7 shows a simplified conductance network as the counterpart of the resistance network in Fig. 4. Corresponding reciprocal values for the relative resistances are indicated for each branch; these are conductance values. At each junction the initial estimated value is shown, then the first computed value, and then last, the subsequent value after several systematic and rotative computations. Computations were started at the corner diagonal, and were continued outward, first horizontally, and then vertically. The same sequence was followed on each computing tour.

The calculating procedure involves a routine sequence for operating on each junction on repeated tours, using the previously calculated value at each point on successive tours of the circuit. Computations may be systematized to be carried out expeditiously in routine by slide rule, by calculating machine, or by automatic-sequence computing machines of mechanical or electrical form. It should not, however, be assumed that the iteration technique offers a procedure that may be carried out to an acceptable solution rapidly. However, it does offer an approximate solution fairly readily, of practical use in the absence of the more direct electrical experimental methods.

Obviously, the accuracy of this method is dependent upon the number of elements in the lumping arrangement, and on the extent of the repetitive computational tours. The method, however, points the way toward calculating-machine operations on complex problems of the flow type; it may be pointed out that there are other fields which may be so studied. Included here are problems of diffusion which directly parallel those of heat transfer, as well as others in the general field of applied mechanics and electromechanics. This of course emphasizes the fact that problems of these types are essentially of the same mathematical background, and hence susceptible to the same treatment. Herein is involved the study of potential distribution for various types of circuits—thermal, electrical, diffusional, etc.

Although not identified as an electrical-analogy procedure, particularly to be mentioned here is the heat-flow adaptation of the Southwell relaxation method, originally reported by Emmons in 1943. This was a specialized numerical procedure applied to a single-component case with isothermal boundaries (4). There are also numerous studies in other fields of applied mechanics dealing with the numerical type of approach, and some of these should be mentioned briefly as of particular interest and dealing with the solution of Laplace's equation. Among these are the work of Shortley and Weller (5), and that of Frocht and Leven (6), the former a general mathematical treatment for the numerical solution of equations, and the latter a special study in the field of stress analysis.

The results of the Series IV computational method are also shown in Table 1, and represent the counterpart of the results obtained in Series III, namely, with end-zone values estab-

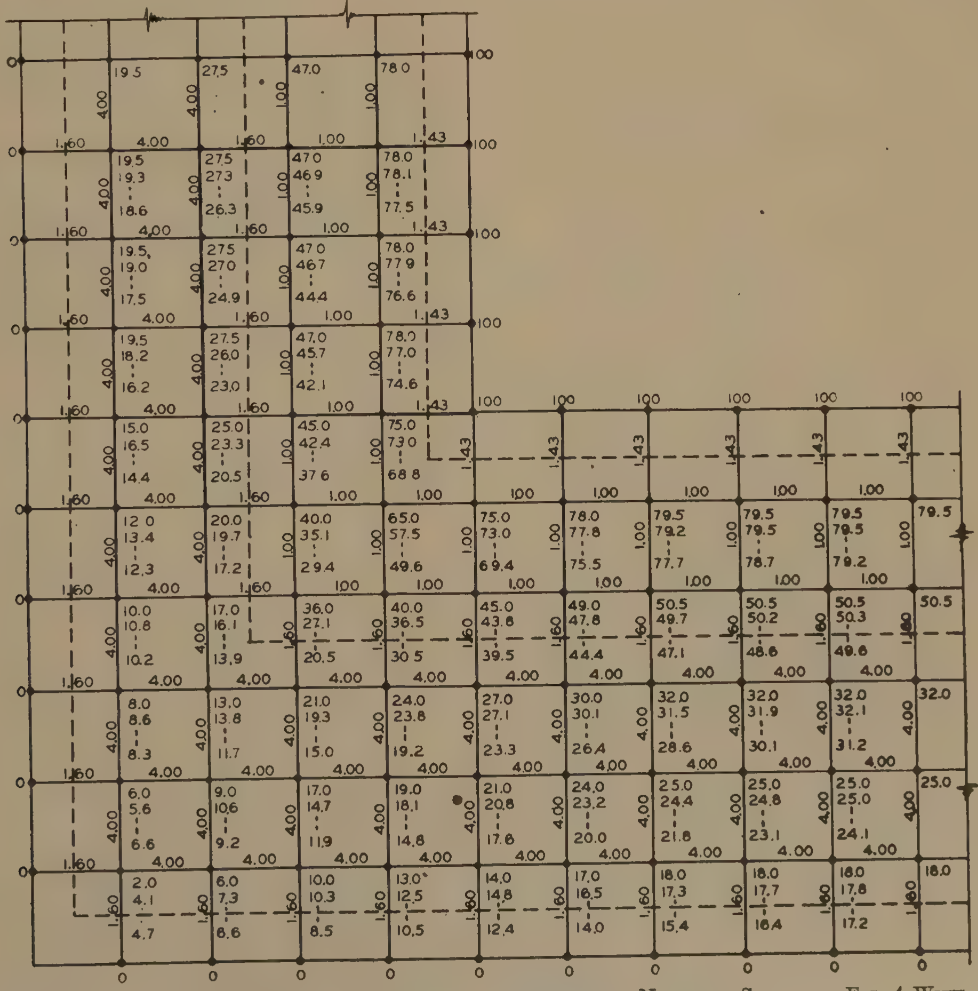

Fig. 7 Conductance-Network Counterpart of Resistance Network Shown in Fig. 4 With Successive Solutions

lished through the one-dimensional flow of Fig. 6. Here again it is to be noted that the agreement in the comparative figures of Series III and Series IV is more than reasonably satisfactory.

CONCLUSION

From the data of Series IV, isopotential lines have been sketched in on the corner cross section and are shown in Fig. 8. Discontinuity at the joint between the two layers of material is of course evident, as is also the irregular pattern of the lines. Based upon Equation [2], translation into temperature values is readily feasible, and likewise, heat-transfer calculations may be made from their values.

It is evident from the study of the data that the extent of the wall section chosen on each side of the corner has not been sufficient for the achievement of one-dimensional flow in the end zones. Thus when the end-zone potentials were not set, as in Series I and II, their values did not of themselves agree with thos of one-dimensional flow, indicating that the area affected by corner may be extensive.

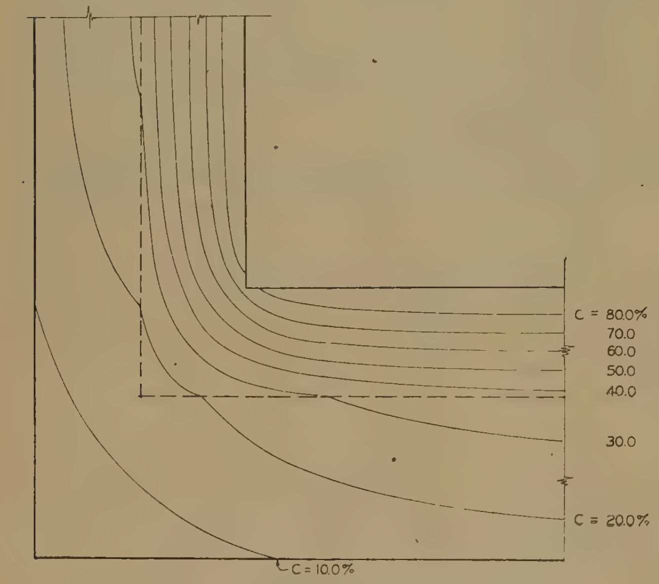

FIG. 8 ISOPOTENTIAL PATTERN FOR CORNER; PERCENTAGE VALUES

It is of course obvious that if an adjustable network board i already available, upon which to set up problems, satisfactory answers may be obtained readily. The work of the computa tional method increases greatly with increase in the number o points studied. Thus if a relatively coarse network is acceptable, calculation time for approximate solution is not apt to be too great. For accuracy, the Analogger gives an excellent account of itself and has the advantage in providing isopotential-pattern detail not readily available by other methods. However, it does require the construction of a special model for each type of program, construction which must be carried through rather carefully.

ACKNOWLEDGMENT

Acknowledgment is hereby made to different associates of the author who have co-operated on various aspects of the investigation, and particularly to Prof. J. Arthur Balmford, of the Electrical Engineering Department at Columbia University, for co-operation on electrical details.

This paper reports the results of another phase of the investigations supported in part by a grant-in-aid to Columbia University from The Refrigeration Research Foundation.

BIBLIOGRAPHY

1 "An Electrical Geometrical Analogue for Complex Heat Flow," by C. F. Kayan, Trans. ASME, vol. 67, 1945, pp. 713–718.

2 "Temperature Patterns and Heat Transfer for a Wall Containing a Submerged Metal Member," by C. F. Kayan, *Refrigerating Engineering*, vol. 46, June, 1946, p. 533.

3 "Heat Flow and Temperature Analysis of Complex Structures Through Application of Electrical Resistance Concept," by C. F. Kayan, Sixth International Congress for Applied Mechanics, Paris, France, September, 1946.

4 "The Numerical Solution of Heat-Conduction Problems," by H. W. Emmons, Trans. ASME, vol. 65, 1943, pp. 607–615.

5 "The Numerical Solution of Laplace's Equation," by G. H. Shortley and R. Weller, *Journal of Applied Physics*, vol. 9, 1938, pp. 334–348.

6 "A Rational Approach to the Numerical Solution of Laplace's Equation," by M. M. Frocht and M. M. Leven, *Journal of Applied Physics*, vol. 12, 1941, pp. 594–604.

Test Results of High-Performance Heat-Exchanger Surfaces Used in Aircraft Intercoolers and Their Significance for Gas-Turbine Regenerator Design

By A. L. LONDON[1] AND C. K. FERGUSON[2]

This paper presents basic heat-transfer and flow-friction esign data for a plate louvered-fin type of extended surace which may be of use in the gas-turbine-plant regeneraor application. Different surfaces are compared on the asis of a heat-transfer coefficient versus friction-horseower plot, and some of the heat-transfer and flow-friction aspects of regenerator design are discussed.

NOMENCLATURE

The following nomenclature is used in the paper:

A = heat transfer and/or friction area, sq ft
A_c = free flow cross-section area, sq ft
a = heat-transfer area (one side) to volume ratio for a particular heat exchange surface, ft^2/ft^3
c_p = air unit heat capacity, Btu/(lb deg F)
E = flow-friction horsepower per unit of area A, hp/ft^2
$_{\text{ref}}$ = E for a fluid having the specified "reference properties," hp/sq ft
f = friction factor defined by Equation [8], dimensionless
$_{\text{iso}}$ = friction factor evaluated from isothermal flow data
G = gas mass velocity, lb/(hr-ft^2 of flow cross section)
h = thermal convection heat transfer "film" coefficient, Btu/(hr deg F ft^2 of A)
$_{\text{ref}}$ = h for a fluid having the specified "reference properties," Btu/(hr deg F ft^2 of A)
$_c$, K_e = flow-contraction and expansion coefficients, respectively, dimensionless
k = gas unit thermal conductivity, Btu/(hr ft^2 deg F/ft)
l = flat plate over-all flow length from leading to trailing edge (corresponding to fin louver spacing), ft
P = gas static pressure, #/ft^2
P = gas static pressure drop, #/ft^2
$_H$ = flow tube hydraulic radius, ft
T = absolute temperature, deg R
u = velocity vector for flow over a flat plate, see Fig. 9
u_0 = undisturbed stream velocity vector for flow over a flat plate, see Fig. 9
v = gas specific volume, ft^3/lb
V = bulk average flow stream velocity, fps
x = flow distance over a flat plate measured from the leading edge, ft
μ = gas viscosity, lb/hr ft
ρ = gas density, lb/ft^3
σ = flow area contraction and expansion ratio, A_c/frontal area
τ_w = wall friction stress, #/ft^2

Dimensionless Groupings:

N_{Pr} = Prandtl number, $\mu c_p/k$, a fluid-properties modulus evaluated for arithmetic-mean bulk air-flow temperature
$\mathbf{R}$ = Reynolds number, $4r_H G/\mu$, based on hydraulic diameter $4r_H$ and μ at bulk mean flow temperature
$\mathbf{R}_f$ = $\mathbf{R}$ with viscosity μ at an average film temperature
$\mathbf{R}_x$ = Reynolds number xG/μ, based on flow distance x, from leading edge of flat plate, with μ at bulk mean temperature
$\mathbf{R}_l$ = Reynolds number, lG/μ, based on flow distance l, from leading to trailing edge of flat plate
N_{St} = Stanton number $h/(Gc_p)$, a heat-transfer modulus

Subscripts:

1 denotes upstream from core
2 denotes downstream from core
avg denotes "average" conditions
iso denotes isothermal conditions
f denotes gas-film conditions
ref denotes evaluation at reference fluid-properties condition

Miscellaneous:

$\cong$ denotes approximate equivalence
# denotes pounds force in distinction to
lb denoting pounds mass

INTRODUCTION

During the present pioneering development of the gas-turbine prime-mover system comparatively little attention has been given to the development of lightweight compact heat-exchanger components, primarily the regenerator.

For a high-efficiency plant with good fuel economy over a wide load range, it is necessary to use a regenerator of high effectiveness and, consequently, of large specific surface area, of the magnitude of 3 to 4 sq ft per shp. This is several times the transfer-area requirement of the boiler plus condenser of a steam power plant. It is therefore evident that for a compact gas-turbine plant, incorporating a high-effectiveness regenerator, it will be necessary to use types of exchanger surfaces having a substantially larger area-to-volume ratio than conventionally used boiler and condenser tube banks. This requirement directs attention to the use of either very small circular tubes, $^1/_4$ in. diam or smaller, or extended surfaces. In the latter case, extended surface on both air and gas sides probably will be desirable in that heat-transfer resistances on both sides are of comparable magnitudes.

---

[1] Professor of Mechanical Engineering, Stanford University, alif. Mem. ASME.

[2] Teaching Assistant in Mechanical Engineering, University of alifornia, Berkeley, Calif. Jun. ASME.

Contributed by the Heat Transfer Division and presented at the nnual Meeting, Atlantic City, N. J., December 1–5, 1947, of THE MERICAN SOCIETY OF MECHANICAL ENGINEERS.

NOTE: Statements and opinions advanced in papers are to be derstood as individual expressions of their authors and not those the Society. Paper No. 47—A-83.

Of possible use in the regenerator application are some of the extended surfaces developed for aircraft intercoolers. However, in order to evaluate the possibilities of these and other developmental types of "high-rating" surfaces, it is necessary that basic heat-transfer and flow-friction design data be obtained and that these data be of accuracy comparable to that available in the literature for flow normal to circular tube bundles and for flow inside tubes. The lack of these data has tended to channel the current regenerator developments toward the use of the shell-and-tube type of surface.

The U. S. Navy Bureau of Ships started a program aimed at this objective in 1945. The Office of Naval Research in conjunction with the Bureaus of Ships and Aeronautics is furthering this work on research contracts. The basic design data summarized in this paper were earlier reported in reference (1)[3] and represent the first results of this program. An additional objective of this paper is to consider some of the heat-transfer and flow-friction aspects of regenerator design.

DESCRIPTION OF APPARATUS AND TESTS

A detailed description and discussion of the test equipment are contained in reference (1); consequently, only a brief description will be given in this paper.

The test system was arranged to provide for heat transfer from steam condensing within the heat-exchanger core to an air-flow stream passing through the core. It consisted of the following essentials:

1 Controllable air-flow duct with a test section of $8^3/_8 \times 9^3/_4$ in. cross section designed to accommodate heat-exchanger cores of standard dimensions. Such a core is shown in Fig. 1.

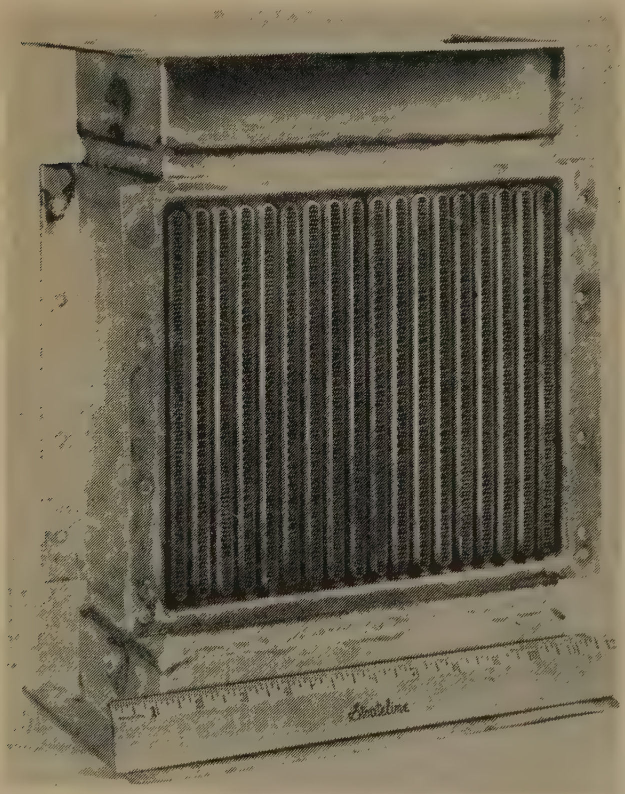

FIG. 1 PLATE-FIN TYPE HEAT-TRANSFER SURFACE MOUNTED IN TEST CORE EQUIPPED WITH HEATING STEAM AND CONDENSATE HEADERS AND FLANGES FOR AIR-FLOW DUCT

2 Steam-heating system for the exchanger core with prov for removing "fixed gases" from the steam side of the heat-t fer surfaces. A large amount of "blow" steam, from 3 to 20 t the condensate rate, was passed through the core to mini condensate flooding of the heat-exchanger surface.

3 Test instrumentation for the measurement of air-flow upstream and downstream air static pressures, temperature velocity distributions, steam-inlet state, blow-steam rate, exit-condensate rate and state.

The seven surfaces tested and their geometry are describe Fig. 2. The plate-fin type of surface incorporated in these cores has had extensive use in aircraft-engine intercoolers. T application is somewhat related to that of the regenerato requirements in common are gas-to-gas transfer, low weight, h compactness, and low friction power.

The surfaces are formed completely from sheet metal 0. in. thick for the plates and 0.006 in. thick for the fin mater Excellent thermal and mechanical joints for the fin and pl junctions are insured by the furnace-brazing method of fabri tion. While all surfaces tested were of aluminum constructi the use of high-temperature materials for the gas-turbine-regen ator application can be visualized.

All of the seven test surfaces of identical plate spacing (0 in.) and fin spacing (11.1 fins per in.) had a varying louver spaci on the air side ranging from $^3/_{16}$ to $^1/_2$ in. and one "plain-fin" s face. All cores had a plain-fin surface on the steam side.

The test data allowed the following calculations:

1 An energy-balance comparison of energy gain by the stream to energy loss by the condensed steam and blow stea The discrepancy in this comparison averaged less than 3 per ce for all the cores tested.

2 Evaluation of the average unit conductance for thermal co vection on the air side. This calculation assumed a relative negligible steam-side resistance. Straight fin theory was use for the prediction of the temperature effectiveness of the extende surface (8). For the aluminum cores used, the temperature e fectiveness of the air-side extended surface was generally in e cess of 95 per cent.

3 Evaluation of flow friction factors for essentially isotherma flow conditions (cold-core runs).

4 Evaluation of flow friction factors for flow through th core with air heating (hot-core runs).

5 Evaluation of the air-flow Reynolds number based on th hydraulic radius of the flow cross-section space between the fin Two Reynolds numbers were evaluated: one for a bulk averag temperature (arithmetic mean of inlet and outlet-air bulk tem peratures), **R**, and the other for a mean film temperature (ave age of bulk average and wall temperature) $\mathbf{R}_f$.

The **R** range for these tests was from 400 to 10,000, correspon ing to mass velocities G of about 2000 to 40,000 lb/(hr ft² fre flow cross section).

SUMMARY OF TEST RESULTS

The test data and calculated results are tabulated in referen (1). Basic heat-transfer and flow-friction design data applicab to the surfaces tested are summarized in Figs. 4 and 3 in dimen sionless form as

$$N_{St}N_{Pr}^{2/3} \text{ versus } \mathbf{R}$$

$$f_{iso} \text{ versus } \mathbf{R}$$

The points for these faired curves, Table 15 of reference (1), a given here in Table 1.

Fig. 5 is included to demonstrate the essential consistency the experimental data. The data points for both f_{iso} and N_S $N_{Pr}^{2/3}$ versus **R** are plotted relative to the faired curves.

---

[3] Numbers in parentheses refer to the Bibliography at the end of the paper.

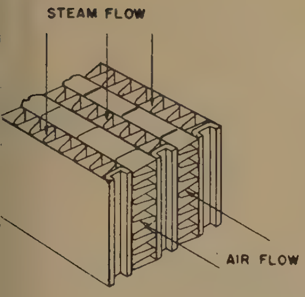

PLATE AND FIN DIMENSIONS

PLATE "FACE SEPARATION" = 0.250 IN.
FIN SPACING = 11.1 FINS/INCH
PLATE METAL THICKNESS = 0.012 IN.
FIN METAL THICKNESS = .0060 IN.
FIN MATERIAL – ALUMINUM
OF THERMAL CONDUCTIVITY
K = 110 BTU/(HR.FT.^{2} °F./FT.)
LOUVER DIMENSIONS ARE AS
SHOWN IN THE FOLLOWING SKETCHES

AIR SIDE

FRONTAL AREA = 0.567 FT.^{2}
FREE FLOW AREA = 0.229 FT.^{2}
FREE FLOW:FRONTAL AREA σ = 0.404
PLATE AREA("DIRECT SURFACE") = 9.89 FT.^{2}
FIN AREA("INDIRECT SURFACE") = 26.78 FT.^{2}
TOTAL AREA, A = 36.67 FT.^{2}
DIRECT:TOTAL SURFACE = 0.270
HYDRAULIC DIA. OF FLOW
$4r_H$ = 0.01012 FT.
AIR FLOW LENGTH = 4.875 IN.

STEAM SIDE

FRONTAL AREA = 0.339 FT.^{2}
FREE FLOW AREA = 0.133 FT.^{2}
PLATE AREA = 8.92 FT.^{2}
FIN AREA = 25.08 FT.^{2}
TOTAL AREA = 34.0 FT.^{2}
HYDRAULIC DIA. OF FLOW
PASSAGES $4r_H$ = 0.01012 FT.

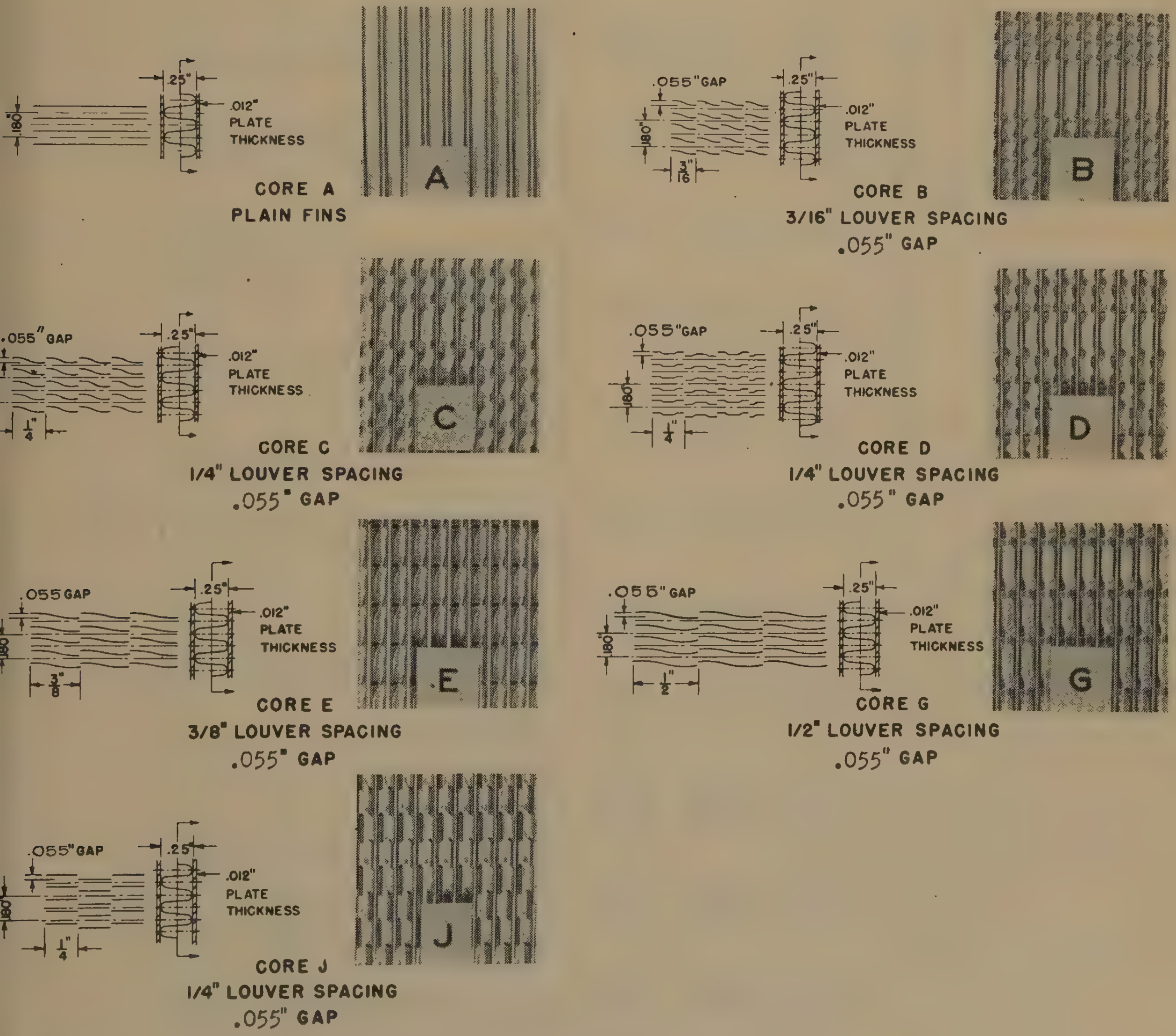

Fig. 2 Description of Cores Tested

TABLE II SUMMARY OF BASIC HEAT-TRANSFER AND FRICTION DATA

$(h/Gc_p)Pr^{2/3}$, f_{iso}, h_{ref}, E_{ref}, vs Re From Smoothed Curves

	Surface A				Surface B				Surface C				Surface D			
Reynolds Rumber Re	$\left[\frac{h}{Gc_p}\right]Pr^{2/3}$	f_{iso}	h_{ref} Btu/(hr°F ft^2)	E_{ref} fhp/ft^2	$\left[\frac{h}{Gc_p}\right]Pr^{2/3}$	f_{iso}	h_{ref} Btu/(hr°F ft^2)	E_{ref} fhp/ft^2	$\left[\frac{h}{Gc_p}\right]Pr^{2/3}$	f_{iso}	h_{ref} Btu/(hr°F ft^2)	E_{ref} fhp/ft^2	$\left[\frac{h}{Gc_p}\right]Pr^{2/3}$	f_{iso}	h_{ref} Btu/(hr°F ft^2)	E_{ref} fhp/ft^2
10,000	.00320	.0098	69.3	1.05	.00525	.0303	114.	3.24	.00565	.0294	122.	3.14	.00615	.0339	133	3.62
8,000	.00338	.0104	58.6	0.569	.00581	.0321	101.	1.76	.00621	.0312	108	1.71	.00660	.0352	114	1.92
6,000	.00362	.0112	47.0	0.258	.00660	.0352	85.8	0.812	.00698	.0338	90.7	0.780	.00720	.0370	93.6	0.854
5,000	.00380	.0117	41.2	0.156	.00715	.0372	77.4	0.497	.00745	.0357	80.7	0.477	.00765	.0382	82.8	0.510
4,000	.00402	.0126	34.8	0.0861	.00782	.0402	67.8	0.275	.00810	.0382	70.2	0.261	.00820	.0400	71.0	0.273
3,000	.00430	.0139	27.9	0.0400	.00878	.0443	57.1	0.128	.00900	.0423	58.5	0.122	.00895	.0427	58.2	0.123
2,500	.00440	.0149	23.8	0.0249	.00940	.0472	50.9	0.0788	.00955	.0450	51.7	0.0751	.00950	.0448	51.4	0.0748
2,000	.00448	.0162	19.4	0.0138	.0102	.0515	44.2	0.0440	.0102	.0485	44.2	0.0414	.0102	.0477	44.2	0.0408
1,500	.00461	.0183	15.0	0.00660	.0113	.0575	36.7	0.0207	.0111	.0540	36.1	0.0195	.0112	.0525	36.4	0.0189
1,200	.00492	.0206	12.8	0.00380	.0122	.0632	31.7	0.0117	.0119	.0590	30.9	0.0109	.0121	.0572	31.4	0.0106
1,000	.00540	.0228	11.7	0.00244	.0132	.0685	27.9	0.00732	.0128	.0635	27.7	0.00678	.0130	.0620	28.2	0.00662
800	.00630	.0258	10.9	0.00141	.0144	.0760	25.0	0.00416	.0139	.0700	24.1	0.00383	.0142	.0685	24.6	0.00339
600	.00775	.0317	10.1	0.000731	.0165	.0875	21.5	0.00202	.0158	.0800	20.5	0.00185	.0161	.0785	20.9	0.00181
500	.00885	.0362	9.6	0.000583	.0181	.0970	19.6	0.00129	.0171	.0880	18.5	0.00117	.0176	.0882	19.1	0.00118
400	.0104	.0430	9.0	0.000294	.0203	.109	17.6	0.000745	.0188	.0990	16.3	0.000677	.0195	.101	16.9	0.000690

	Surface E				Surface G				Surface J			
Reynolds Number Re	$\left[\frac{h}{Gc_p}\right]Pr^{2/3}$	f_{iso}	h_{ref} Btu/(hr°F ft^2)	E_{ref} fhp/ft^2	$\left[\frac{h}{Gc_p}\right]Pr^{2/3}$	f_{iso}	h_{ref} Btu/(hr°F ft^2)	E_{ref} fhp/ft^2	$\left[\frac{h}{Gc_p}\right]Pr^{2/3}$	f_{iso}	h_{ref} Btu/(hr°F ft^2)	E_{ref} fhp/ft^2
10,000	.00545	.0248	118	2.65	.00490	.0217	106	2.32	.00458	.0189	99.2	2.02
8,000	.00587	.0262	102	1.43	.00527	.0225	92.3	1.23	.00501	.0199	86.8	1.09
6,000	.00648	.0279	84.2	0.644	.00580	.0238	75.4	0.549	.00560	.0215	72.8	0.496
5,000	.00688	.0292	74.5	0.390	.00615	.0248	66.6	0.331	.00600	.0227	65.0	0.303
4,000	.00742	.0311	64.3	0.213	.00663	.0261	57.4	0.178	.00655	.0244	56.7	0.167
3,000	.00815	.0338	53.0	0.0975	.00725	.0281	47.1	0.0810	.00733	.0270	47.6	0.0779
2,500	.00864	.0358	46.8	0.0598	.00775	.0297	42.0	0.0496	.00782	.0290	42.3	0.0484
2,000	.00930	.0390	40.3	0.0333	.00830	.0318	36.0	0.0272	.00855	.0320	37.0	0.0273
1,500	.0103	.0437	33.5	0.0158	.00890	.0353	28.9	0.0127	.00950	.0368	30.9	0.0133
1,200	.0112	.0485	29.1	0.00895	.00960	.0390	25.0	0.00720	.0103	.0413	26.8	0.00762
1,000	.0121	.0530	26.2	0.00566	.0106	.0427	23.0	0.00456	.0112	.0454	24.3	0.00485
800	.0134	.0595	23.2	0.00325	.0119	.0487	20.6	0.00266	.0125	.0516	21.7	0.00282
600	.0152	.0700	19.8	0.00161	.0140	.0587	18.2	0.00135	.0142	.0615	18.5	0.00142
500	.0166	.0780	18.0	0.00104	.0154	.0665	16.7	0.000888	.0155	.0690	16.8	0.000921
400	.0183	.0900	15.9	0.000615	.0174	.0780	15.1	0.000533	.0172	.0800	14.9	0.000547

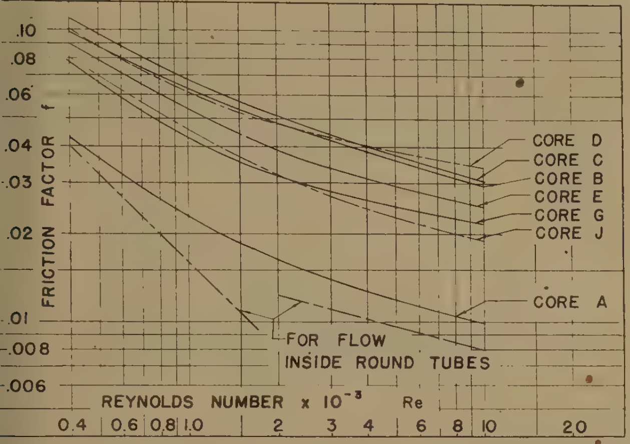

IG. 3 Friction Factor, f_{iso}, Versus Reynolds Number, R, for Seven Surfaces Tested

Iydraulic diameter 0.01012 ft, plate spacing 0.250 in., 11.1 fins per in. Refer to Fig. 2 for geometrical details of surfaces.)

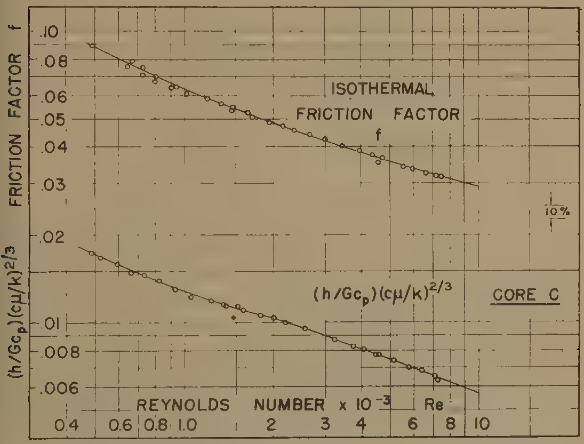

IG. 5 Heat-Transfer Factor, $N_{St}N_{Pr}^{2/3}$, and Friction Factor, so, Versus Reynolds Number, R, for Surface C Showing Deviation of Data Points From Mean Curve

Pressure-drop data taken in conjunction with the heat-ransfer runs, according to the previous calculation of eference (1), yielded an f versus R characteristic which ell 3 to 6 per cent higher than the isothermal f results. he greatest difference existed for low R. This discrepancy esulted from a poor idealization for average air density (or pecific volume) with respect to flow length, namely, an rithmetic-average density. New calculations using a logathmic-average specific volume yielded hot-core friction actors in substantial agreement with the f for the isothermal runs, providing a correlation with R_f is employed. his is demonstrated in Fig. 6 for surface G. Here the ot-core friction factors versus R_f are compared to the isoermal curve from Fig. 3. Reasons for employing the logathmic average specific volume are given in the Appendix.

Fig. 7 is presented for the purpose of comparing the eat-transfer versus friction-power characteristics of the difrent surfaces. The dimensionless correlations of $N_{St}N_{Pr}^{2/3}$ nd f versus R are rearranged after the method of Colburn) to yield a dimensional plot of heat-transfer coefficient $_{ef}$, versus flow-friction horsepower per square foot of trans-r surface, E_{ref}. These coefficients are plotted for the reference gas state (corresponding to air at 500 F), described the caption of Fig. 7. To predict h and E for operation ith any fluid at other than reference properties, the following equations derived in reference (1) may be employed

$$h_{ref} = h\left(\frac{c_{pref}}{c_p}\right)\left(\frac{\mu_{ref}}{\mu}\right)\left[\frac{(N_{Pr})}{(N_{Pr})_{ref}}\right]^{2/3} \quad \ldots\ldots\ldots\ldots [1]$$

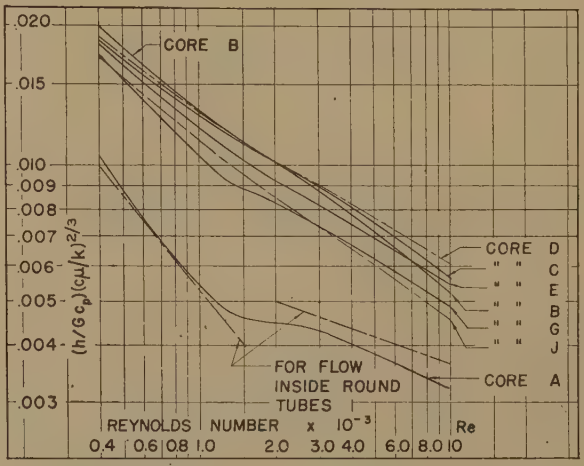

Fig. 4 Heat-Transfer Factor, $N_{St}N_{Pr}^{2/3}$, Versus Reynolds Number, R, for Seven Surfaces Tested

(Hydraulic diameter 0.01012 ft, plate spacing 0.250 in., 11.1 fins per in. Refer to Fig. 2 for details of geometry of surfaces.)

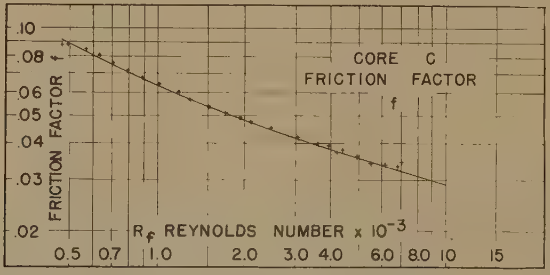

Fig. 6 Friction Factors for Surface C Showing Data Points for Hot-Core Runs Compared to Mean Curve for Isothermal Friction Factors

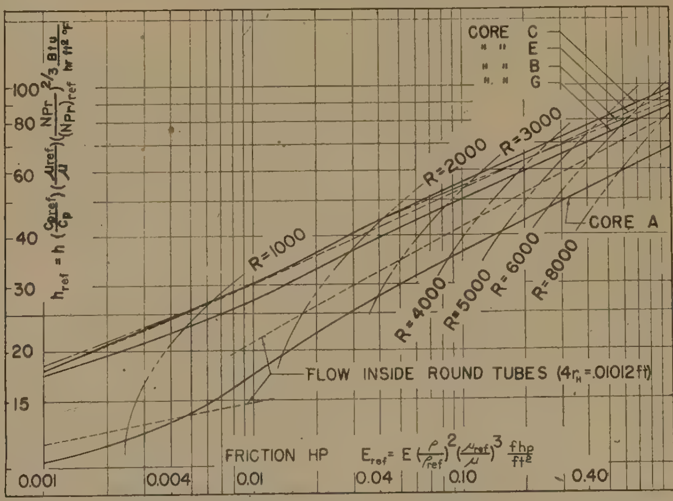

Fig. 7 Heat-Transfer Coefficient Versus Friction-Horsepower Requirement at Reference Conditions for Surfaces A, B, C, E, and G

(Reference conditions are ρ_{ref} = 0.0413 lb/ft³, μ_{ref} = 0.0678 lb/hr ft, c_{pref} = 0.2477 Btu/(lb deg F), $N_{Pr\ ref}$ = 0.671, corresponding to air at 500 F and atmospheric pressure. Surface D and surface J characteristics are omitted for clarity. The D characteristic is close to that of the C surface, and the J characteristic is close to that of the G surface. Reynolds number magnitudes on this plot are approximate only.)

$$E_{\text{ref}} = E\left(\frac{\rho}{\rho_{\text{ref}}}\right)^2\left(\frac{\mu_{\text{ref}}}{\mu}\right)^3 \ldots\ldots\ldots\ldots\ldots [2]$$

Probable accuracies of the basic data are as follows:

R, $\mathbf{R}_l$	±1.5 per cent
f_{iso} core A	±6 per cent for high **R** ±3 per cent for low **R**
f_{iso} other cores	±4 per cent for high **R** ±2 per cent for low **R**
$N_{St} = (h/Gc_p)$	accurate to 5 per cent with a tendency to be smaller than actual
$N_{Pr} = (\mu\, c_p/k)$	±5 per cent

Thermal properties for air were taken from reference (9).

The principal error in f arises from uncertainty of the actual exit and entrance (flow expansion and contraction) loss coefficients used to extract the friction factor from core over-all pressure-drop measurements (see Appendix). There is some possibility that exit and entrance coefficients for "multiple tubes in parallel" differ significantly from the conventionally used "single" contraction and expansion coefficients available in the literature.

The major error in the N_{St} determination evolves from the assumption of a negligible steam-side resistance. Therefore the presented N_{St} magnitudes tend to be lower than actual.

Uncertainty in N_{Pr} is mainly the result of lack of accurate data for air thermal conductivity (9).

Discussion of Test Results

Reference to Fig. 2 will indicate the complexity of the flow path of the air over and between the louvered-fin surfaces. The flow boundary layer is periodically interrupted by the cutout louvers on the fins. The curvature of the fins results in flow accelerations with tendencies toward boundary-layer separation and eddy formations. Wake effects at the trailing edges and flow impingement on the leading edges result in additional turbulence. In the region of contact between the fins and the plate the flow geometry is even more complicated due to the presence of the plate wall and the junction of louver and fin.

As a result of these influences, with the exception of the A surface, the flow is probably characterized by a very high degree of turbulence especially after the first inch or so of the 4.875-in. flow length. In spite of this, however, it is evident from Fig. 4 that there is a tendency toward a viscous-flow characteristic for $\mathbf{R} < 1000$, as revealed by the change of slope and the inflection point of the $N_{St}\,N_{Pr}{}^{2/3}$ versus **R** plot in the region $1000 < \mathbf{R} < 3000$ for all seven surfaces tested. Note that this transition is more marked for the less louvered surfaces.

The theory of boundary-layer formation in flow over a flat plate yields useful qualitative results, Fig. 8. In this consideration, however, it is necessary to make a clear distinction between the laminar sublayer and the Prandtl boundary layer (the "region of influence" of the plate on the main stream flow). The Prandtl boundary layer may be defined arbitrarily as the region contained within the $u/u_0 = 0.99$ velocity contour as indicated in Fig. 8. In contrast, the laminar sublayer will be defined by the $u/u_0 = 0.7$ velocity contour. The laminar sublayer is a few thousandths of an inch thick in average dimensions. It is in this layer that the major resistance to heat transfer resides. Consequently, by reducing its average thickness the heat-transfer conductance for thermal convection h can be increased. The function of the louvers is to provide this effect by periodic interruption and resultant new formation of the laminar sublayer. Accompanying this increase in h will be a corresponding incre in the velocity gradients at the wall and the attendant crease in "skin friction." A further increase in over-all flow fr tion, characterized by the coefficient f, results from impingeme on the leading edges of the louvers, wake formation at the tra ing edges, and flow curvature imposed by the fin shape. Th extraneous friction components may be at least partially effectiv in increasing the heat-transfer coefficient since they tend to pro mote a decreased laminar sublayer thickness.

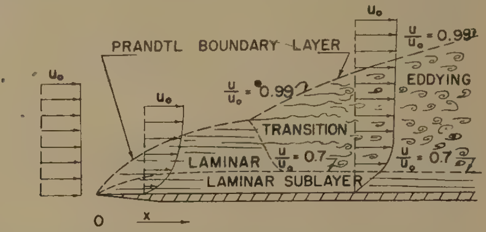

Fig. 8 Schematic Representation of Formation of "Prand Boundary Layer"—Laminar and Eddy Types—and "Lamina Sublayer" for Flow Over a Flat Plate

Rouse (3) gives the following expressions for average ski friction factor (or drag coefficient) for the idealized flow over a smooth flat plate as shown in Fig. 8

$$f = 1.328/(xG/\mu)^{1/2} = 1.328/(\mathbf{R}_x)^{1/2} \ldots\ldots\ldots [3$$

$$f = 0.074/(xG/\mu)^{1/5} = 0.074/(\mathbf{R}_x)^{1/5} \ldots\ldots\ldots [4$$

Equation [3] applies to the classical Blasius solution, which i based on the idealization of purely viscous flow extending fro the plate surface into the main flow stream (2, 3). Equatio [4] is based upon the empiricism that wall shear varies inversely as the Prandtl boundary-layer thickness raised to an exponent $n = 1/4$, (3). It is to be noted that f is an average friction factor for the flow length x measured from the leading-edge position. For the purpose of this discussion, Equation [3] may be considered as representative of conditions for $\mathbf{R}_x < 5 \times 10^5$ when a low degree of turbulence exists in the approach flow; whereas Equation [4] represents conditions for $\mathbf{R}_x > 10^6$ for "low turbulence" approach flow, or for all values of $\mathbf{R}_x$ when a "high turbulence" approach flow exists (2).

If, for the flat plate system with air flow, it is postulated that the temperature and velocity distributions in the boundary layer are identical, it may be shown that

$$N_{St}N_{Pr} = f/2 \ldots\ldots\ldots\ldots\ldots\ldots [5]$$

Then Equations [3] and [4] may be used to evaluate $f/2 = N_{St}N_{Pr}$ versus $\mathbf{R}_x$. This relation is plotted in Fig. 9. The more refined analogies between heat transfer and flow friction will give sensibly the same result, since N_{Pr} for air is close to unity.

Also plotted, Fig. 9, are the experimental values of $f/2$ and $N_{St}N_{Pr}$ versus $\mathbf{R}_l$ for cores C, G, and A. Data for the other cores are omitted to avoid confusion. In this Reynolds number the length dimension l, ranging from $1/4$ in. for core C to 2.44 in. for core A, is taken as the spacing of the louvers on the fins. While the A surface is listed as a plain-fin surface, the fins were fabricated from two corrugated plates 2.44 in. wide; consequently, since perfect matching of the junction did not exist, a set of "louvers" or "boundary-layer interrupters" existed 2.44 in. from the entering section.

The comparison revealed by Fig. 9 indicates remarkably close agreement, within 40 per cent for all surfaces tested, between the flat-plate friction data, extrapolated in accordance with Equation [5] to yield $N_{St}N_{Pr}$, and the test heat-transfer data. How-

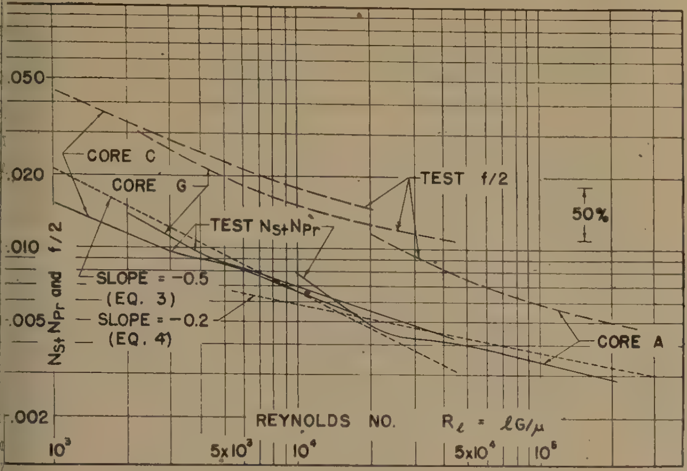

Fig. 9 Heat-Transfer and Friction Characteristics for Surfaces A, C, and G, Compared to Flat-Plate Characteristics Derived From Drag Measurements, Equations [3], [4], [5]

ever, it is also evident that R_l does not specify properly the transition from the Prandtl-laminar to the Prandtl-eddy or turbulent boundary layer as exemplified by Equations [3] and [4], and shown schematically in Fig. 8. Fig. 9 indicates a flow transition for the *A* surface (plain fins) for R_l at about 2×10^4 to 5×10^4 and at about one tenth of this magnitude for the *C* surface ($^1/_4$-in. louvers). Reference to Fig. 4 reveals that these transitions for all surfaces occur in the range of $\mathsf{R} = 4r_H\ G/\mu$ of 1000 to 3000. This better correlation for the flow-transition range indicates that the latter Reynolds number, R, is more descriptive of the average character of the boundary-layer flow than $\mathsf{R}_l = lG/\mu$. However, this must be considered as a tentative conclusion in view of the fact that surfaces tested were of only one hydraulic radius magnitude and that test viscosity was fairly constant.

Considering the comparison of friction factors, the ratio of test $f/2$ to flat plate $f/2$ is of the order of 2 to 3 to 1. The same order of magnitude exists for the comparison of test $f/2$ to test $N_{St}N_{Pr}$. This difference may be construed as indicating that some 50 to 70 per cent of the friction effect is not "useful" in producing a thin laminar sublayer. Since the thickness of the plate material (0.006 in.) is somewhat greater than that of the laminar sublayer, the "loss" or "nonuseful" friction may originate in leading and trailing-edge eddy generation and shock effects, as well as the effective flow restriction introduced by the wall-fin and fin-louver junctions.

Information on the heat transfer from flat plates is reviewed by Jakob and Dow and compared to their test results (4). The data for the case of "no starting section" can be expressed

$$\left.\begin{aligned} N_{St}N_{Pr} &= 0.590\ \mathsf{R}_l^{-0.5} \\ N_{St}N_{Pr} &= 0.028\ \mathsf{R}_l^{-0.2} \end{aligned}\right\} \cdots\cdots\cdots\cdots\cdots [6]$$

or the Prandtl-laminar and Prandtl-eddy layer types of flow, respectively. These results are 13 and 32 per cent lower, respectively, than given by Equations [3], [4], [5] and are in substantial agreement with the heat-transfer data for surfaces *A* to *J* when plotted as in Fig. 9.

Norris and Spofford (5) report both flow-friction and heat-transfer data for interrupted plate-fin surfaces of the same general geometry as the surfaces reported here. Their test sample consisted of a single pair of plates with fins normal to the plate surfaces providing a relatively "clean" rectangular flow-tube cross section. Further, this construction provided a "boundary-layer interrupter" extending the full plate spacing in contrast to the approximately 70 or 80 per cent utilization of the plate spacing by the formed louvers of surfaces *B* to *J*. As a result of this "more ideal" flow geometry it is expected that the Norris and Spofford results should yield about the same heat-transfer characteristic, $N_{St}N_{Pr}$ versus R_l, with a somewhat lower friction characteristic. On a plot such as Fig. 9 this conclusion is confirmed as the data for their surface No. 10 ($l = {}^1/_8$ in. and $^1/_8$ in. fin spacing) agrees substantially with the surface *C* heat-transfer characteristic; and with respect to friction falls some 20 to 30 per cent below that for the *C* surface.

Conclusions which can be drawn from the foregoing comparisons are as follows:

1 Confirming the conclusion of Norris and Spofford (5), flat-plate data can be used to predict the heat-transfer characteristic for plate-fin surfaces within 30 per cent providing the type of Prandtl boundary layer can be specified.

2 Since the friction characteristic for the plate-fin surface depends markedly upon the parasitic shock and eddy-formation losses, in addition to the purely skin-friction effects associated with the laminar sublayer, the *f* versus R characteristic falls substantially higher than that for flat-plate flow, and depends upon the details of construction of the surface. Aerodynamically "cleaner" design may result in a substantial reduction of flow friction.

Applications to Regenerator Design

The primary considerations influencing the design of a regenerator may be summarized as follows:

1 Manufacturing limitations.
2 Cost limitations.
3 Maintenance and cleaning requirements.
4 Mechanical design problems.
5 Weight, space, and shape limitations.
6 Limitations on flow-friction power expenditure.
7 Desired exchanger heat-transfer effectiveness.

Because of space restrictions the following brief discussion will be limited to the heat-transfer and flow-friction aspects as they relate to items 5, 6, and 7.

The usual design procedure consists of a "cut-and-try" method of successive approximations requiring as a preliminary step the specification of the type of surface to be used. The resulting design will not be unique but will depend on the designer's judgment in relation to permissible compromises and "optimum design" criteria with respect to allowable shape of the heat-transfer core, distribution of total friction-power expenditure—gas and air sides—and performance at part load.

Critical judgment is required in the selection of the type of surface to be used and the proportioning of flow areas. In this respect, graphical representation of the heat-transfer coefficient versus the friction-power requirement characteristic is useful for comparing different types of surfaces and for estimating approximate surface-area requirements versus flow-friction expenditure.

Considering the comparison revealed in Fig. 7, it is evident that for the same area requirement (as defined by the *h* magnitude) the *C* surface ($^1/_4$-in. louvers) will require only one fifth of the friction-power expenditure of the *A* surface (plain fins). For the same friction expenditure the *C* surface-area requirement will be only 60 per cent of the *A* surface-area requirement. The conclusion is that the *C* surface will result in the smallest volume and lightest regenerator. However, a caution to be observed in this respect is that volume requirement is only one aspect of the "compactness of the regenerator," and that the shape of the final design is exceedingly important. As a consequence, the surface resulting in the smallest heat-exchanger-surface volume may not result in the best regenerator for a particular machinery arrangement. It may be that the final regenerator design will incorporate two types of surfaces, as, for instance, surface C for the air side and surface A for the gas side with possibly different fin and plate spacings.

Fig. 10 employs the h_{ref} versus E_{ref} plane to compare surface C ($^1/_4$-in. louvers) with the following:

1 Turbulent flow inside round tubes of $^1/_4$ in. diam.

2 Flat plates, $^1/_4$ in. long, with sharp leading edges (corresponding to C surface louver spacing), for two conditions:

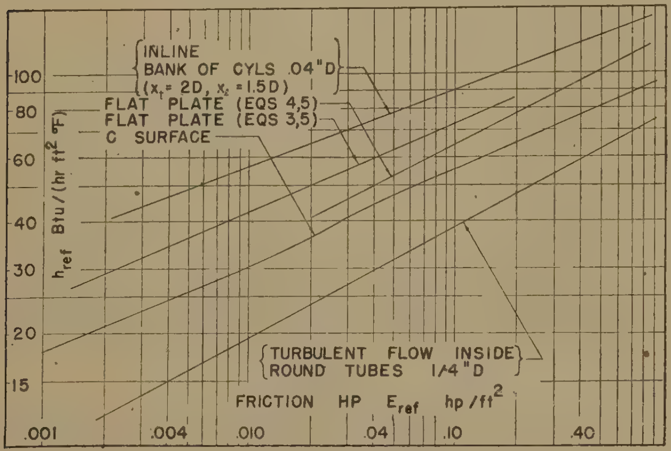

Fig. 10 Comparison for Different Surfaces of Heat-Transfer Coefficient Versus Friction-Horsepower Characteristic

(See Fig. 7 caption for reference conditions. Represented are surface C, flow inside $^1/_4$-in. tubes, flow along a flat plate $^1/_4$ in. long with a sharp leading edge, flow normal to a cylinder bank, 0.04-in-diam cylinders, in-line arrangement, with $2D$ transverse pitch and $1.5D$ longitudinal pitch.)

(a) Prandtl-laminar boundary layer formed at the leading edge and existing over the $^1/_4$-in. flow length, Equations [3], [5].

(b) Prandtl-eddy type or turbulent boundary layer formed at the leading edge and existing over the flow length, Equations [4], [5]. (Note that a laminar sublayer exists adjacent to the plate, Fig. 8.)

3 Turbulent flow normal to a bank of in-line cylinders, D = 0.04 in., with a $2D$ transverse pitch and a $1.5D$ longitudinal pitch using the Grimison correlation (7).

This last surface might be considered as a plate pin-fin surface of the type tested by Norris and Spofford (5), although the Grimison correlation (7), considerably extrapolated, was employed in preference to the data of (5).

The following points may be noted from this comparison:

1 Flow inside of tubes has a poor heat transfer-friction power characteristic.

2 The flat-plate flow with a laminar-type Prandtl boundary layer has a better characteristic than the flow with an eddy-type boundary layer.

3 If the $^1/_4$-in. flat-plate characteristic may be considered as a limit that can be approached by the $^1/_4$-in. louvered-fin surface a substantial improvement of friction performance is possible. This may result from a design which will afford an "aerodynamically cleaner" flow between and over the fins. How this can be accomplished for a surface designed for commercial fabrication is a moot point.

4 The pin-fin type of surface appears to have an excellent heat transfer-friction characteristic. However, the problems of commercial fabrication of such a surface (with 0.04-in. pins) may preclude its use.

From the point of view of the compactness of the final desi it is well to emphasize again that the volume of the heat-trans surfaces, as characterized by the heat transfer-friction charact istic, is only one consideration and that the shape of the exchang core is also of primary importance.

Several other points of interest can be inferred from Fig. 7 10 and from Equations [1] and [2] relating h_{ref} and E_{ref} to h a E at other than reference properties. Since reference properti are taken as corresponding to air at 500 F and 1 atm pressure, h and E_{ref} correspond approximately to hot gas-side cond tions of the regenerator for an open-cycle plant. While h also approximates h on the air side, the friction powe $E \cong E_{\text{ref}}(\rho_{\text{ref}}/\rho_{\text{air}})$,² differs markedly from E_{ref}. This follov since ρ_{air} is from 4 to 7 times ρ_{ref}. Consequently, for compar ble friction-power expenditure, h on the air side may be 2 3 times h on the gas side if the same surface is employe Moreover, due to shape requirements, it may be necessar to use different surfaces for the air and gas sides, as, for i stance, plain fins (A surface) for the gas and $^1/_4$-in. louvere fins (C surface) for the air. Then h air side may be 4 to times that of the gas side, and the gas-side conductanc tends to control the over-all resistance to heat transfer.

Acknowledgments

The experimental program as reported in reference (1 was made possible through the joint efforts of the U. S. Navy Bureau of Ships and the Harrison Radiator Division o General Motors. The tests results reported were obtaine at the U. S. Navy Engineering Experiment Station, Annapolis, Md. Mr. L. P. Saunders and Mr. John W. Godfrey of Harrison Radiator contributed materially to this work by their co-operation and criticism. The Office of Naval Research is currently furthering this program with sponsored research at Stanford University.

BIBLIOGRAPHY

1 "Gas Turbine Plant Regenerator Surfaces," by A. L. London and C. K. Ferguson, Bureau of Ships Research Memorandum No. 2–46, Navships (250-338-3), July, 1946.

2 "Air Flow in a Boundary Layer Near a Plate," by H. L. Dryden, NACA Report No. 562, 1936.

3 "Fluid Mechanics for Hydraulic Engineers," by Hunter Rouse, Engineering Societies Monographs, McGraw-Hill Book Company, Inc., New York, N. Y., 1938.

4 "Heat Transfer From a Cylindrical Surface to Air in Parallel Flow With and Without Unheated Starting Section," by Max Jakob and W. M. Dow, Trans. ASME, vol. 68, 1946, p. 123.

5 "High-Performance Fins for Heat Transfer," by R. H. Norris and W. A. Spofford, Trans. ASME, vol. 64, 1942, p. 489.

6 "Heat Transfer by Natural and Forced Convection," by A. P. Colburn, Engineering Bulletin, Purdue University, Research Series No. 84, January, 1942.

7 "Heat Transmission," by W. H. McAdams, second edition, McGraw-Hill Book Company, Inc., New York, N. Y., 1942.

8 "Efficiency of Extended Surface," by K. A. Gardner, Trans. ASME, vol. 67, 1945, p. 621.

9 "An Investigation of Aircraft Heaters—Part II, Properties of Gases," by M. Tribus and L. M. K. Boelter, NACA Report ARR, October, 1942.

Appendix

The friction factors for the surfaces tested were calculated from over-all core pressure-drop data. This calculation was based upon the following equation for core pressure drop

$$\Delta P = \frac{G^2}{2g} v_1 \Bigg[\underbrace{(K_c + 1 - \sigma^2)}_{\text{entrance effect}} + \underbrace{2\left(\frac{v_2}{v_1} - 1\right)}_{\text{flow acceleration}}$$

$$+ \underbrace{f \frac{A}{A_c} \frac{v_{\text{avg}}}{v_1}}_{\text{core ``skin'' friction}} - \underbrace{(1 - \sigma^2 - K_e) \frac{v_2}{v_1}}_{\text{exit effect}} \Bigg] \ldots\ldots\ldots [7]$$

he terms associated with the flow contraction on entrance into ie core, the flow acceleration within the core, the friction with- the core, and the pressure recovery on flow expansion at the exit e all indicated in Equation [7]. This equation includes the ealization that the density changes at entrance and exit from ie core are negligibly small.

The terms for flow acceleration and friction within the core are erived from a dynamical equation (Bernoulli's equation) in ifferential form incorporating a friction-head-loss term in which ie friction factor f is defined in relation to the wall friction stress $_w$, by

$$\tau_w = f\rho V^2/2g \ldots\ldots\ldots\ldots\ldots\ldots [8]$$

he ratio, friction area to flow area, A/A_c, is equal to the ratio, ow length to hydraulic radius.

The integration of the dynamical equation for pressure drop ithin the core results, for the friction term, in an average speific volume, v_{avg}, defined by

$$v_{\text{avg}} = \frac{1}{A} \int_0^A v dA \ldots\ldots\ldots\ldots\ldots\ldots [9]$$

hat is, v_{avg} is an average specific volume with respect to flow ngth or friction area, A.

For the hot-core test runs, the major variation of specific volme results from the change of temperature rather than pressure. onsequently, since the wall temperature is sensibly constant at aturation steam pressure, and assuming perfect gas behavior for he air flow, it follows that Equation [9] may be written in the pproximate form

$$\frac{v_{\text{avg}}}{v_1} \cong \frac{P_1}{P_{\text{avg}}} \frac{T_{lma}}{T_1}$$

Iere P_{avg} is an arithmetic-average pressure and

$$T_{lma} = T_{\text{steam}} - \Delta T_{lma}$$

ΔT_{lma} being identical to the conventional logarithmic-average emperature difference for heat transfer.

Hot-core friction factors agree substantially with the isothermal riction factors when evaluated on the foregoing basis, Fig. 6.

Discussion

C. F. Bonilla.[4] The use of the proper temperature in computng "hot-core" friction factor and the correlation against R_l are articularly useful and represent significant advances in the corelation of test results on cores.

Undoubtedly both R (based on hydraulic radius) and R_l affect he pressure drop and heat transfer in extended surface with ouvers, but it is reasonable and interesting that data on a series of cores with the same hydraulic radius should correlate better against R_l than against R. In this case, however, it does not hen seem reasonable that the inflection or "critical" region should correlate better against R than R_l. This conclusion should be tested with cores of similar construction but different fin spacing.

Some suitable data for this purpose are becoming available through subsequent work at the U.S.N. Engineering Experiment Station on cores by the same manufacturer with 8.7 and 6.06 fins per in. Careful scrutiny of the plots of f and j against R, however, fails to indicate any appreciable inflection, particularly for 6.06 fins per in. ($^3/_8$ and $^1/_2$-in. louver spacings), that have curves of j versus R which are uniformly convex upward over the full range of R of 600 to 10,000. It is thus strongly indicated that no particular significance can be attached to these points of inflection, considering in particular that besides R and R_l, additional dimensionless ratios involving the thickness and "roughness" of the leading edges of the louvers as well as any deviation from scale of the shape of the louvers must affect the boundary layer and thus f and j.

In considering cores with "standard" louvers, that is, those which are so formed as to tend to push the fluid over toward one side of the core, two questions suggest themselves, which would not come up in "reversed" type louvers. Is there possibility of a variation in the pressure drop and heat-transfer characteristics of the core if the ratio of the length of the fluid path to the width were to be changed from that in the test cores? The possibility exists that a shorter standard core (shorter fluid path) would show up relatively better, and vice versa; also that a standard core would show some advantage near a bend in the fluid line (over one tested in a straight duct), which is the way most of them are probably to be installed.

With standard louvers all aiming to the same side, might the mean temperature difference be appreciably different from that of the reversed louvers when two fluid streams are being handled?

An effort to throw some light on the first question will be made if possible by measuring the temperature and velocity distribution of the air at the outlet plane of a standard core, rather than a distance downstream. The second consideration did not come up in these tests with steam on the other side of the core. However, in case it is an appreciable factor, or if a core is to be tested at a bend in a duct, it would seem desirable to specify to the manufacturer the direction in which the louvers on each side should point. The louvers in adjacent sections of the fluid path in the cores herein tested were subsequently found on inspection to aim either to one side or to the other in a random manner.

H. B. Nottage.[5] It seems desirable to emphasize the authors' statement concerning the way in which the friction factors were calculated by subtracting assumed entrance and exit losses from over-all measurements. As the result of unpublished experience with aircraft installations, and especially under conditions of high passage Mach number, it may be stated that entrance and exit losses for multiple passages differ from those conventionally assumed for single passages. Hence it seems important that the magnitudes of K_c and K_e for Equation [7] be given with this paper rather than in the less accessible reference (1). Persons using the friction data should be advised to employ these same magnitudes of K_c and K_e and not to perform unwarranted extrapolations beyond the test conditions.

It is understood from the authors that continuing research is providing data on K_c and K_e directly. It would be interesting to have an advance indication regarding the nature of these results, for it is believed that both the flow rate and the flow-system geometry will influence appreciably these loss coefficients.

As a further caution, in flows with high Mach number, it may no longer be acceptable to postulate constant density for the entrance contraction and the exit expansion. Experience and analysis indicate that at a Mach number of roughly 0.25, and from there on up, density changes exert a more and more appreciable influence.

The logarithmic-mean density may be useful where the approximation is justified, but this, too, needs to be judged in relation to the Mach number, and the actual rate of heat transfer along the flow-passage length. Gas-turbine regenerators do not commonly employ a condensing fluid with the consequent approximate uniformity of exchanger-surface temperature.

---

[4] Professor of Chemical Engineering, The Johns Hopkins University, Baltimore, Md.; and Consultant, Gas Turbine Project, U.S.N. Engineering Experiment Station, Annapolis, Md.

[5] American Society of Heating and Ventilating Engineers, Research Laboratory, Cleveland, Ohio. Jun. ASME.

AUTHOR'S CLOSURE

Professor Bonilla comments that $\mathbf{R}_l$ should provide a better correlation for the transition flow region than **R**. He quotes some recently obtained U.S.N. Engineering Experiment Station data to indicate that when r_H was varied, by changing fin spacing, the transition effect disappeared and the $N_{St}N_{Pr}{}^{2/3}$ versus Reynolds number characteristic was uniformly convex up over the range of $\mathbf{R} = 600\text{–}10{,}000$. The data quoted,[6] was for nonsimilar louver shapes, however, and later data taken at both EES and Stanford University, on cores of varying fin spacing and the same louver design, do continue to show a transition in the range $\mathbf{R} = 1000$ to 3000 for the heat-transfer results. These data (Stanford University results), shown in Fig. 11 of this closure, reveal even a more marked transition effect for the larger r_H magnitudes.

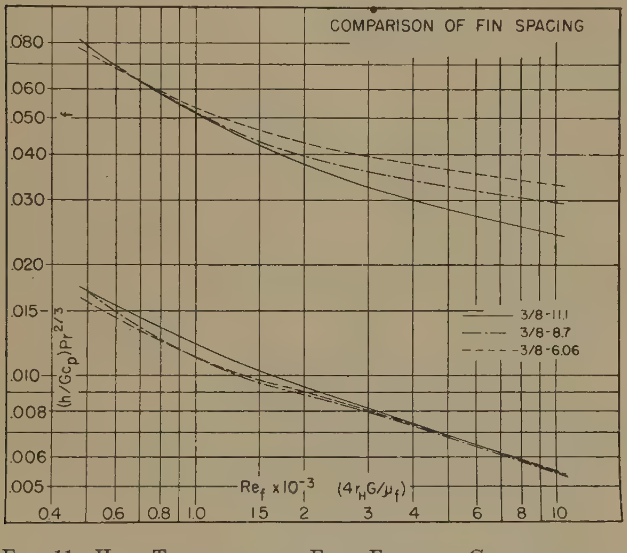

FIG. 11 HEAT-TRANSFER AND FLOW-FRICTION CHARACTERISTICS FOR THREE PLATE-FIN SURFACES

(3/8 in. louver spacing, 0.055 in. louver gap, and $r_h = 0.00253$ ft. 0.00299 ft, 0.00365 ft, for the 11.1, 8.7, and 6.06 fins/in. surfaces, respectively.)

The comments regarding the effect of louver design on diverting the flow are of interest. Downstream velocity traverses on the *E* core show no marked trend in this respect for this surface. For other surfaces this condition may not obtain, however, and downstream-velocity-traverse data on each surface tested is highly desirable.

Mr. Nottage discusses the importance of K_c and K_e data for the friction-factor analysis of test results. Work at Stanford[7] inc cates both theoretically and experimentally that for essential incompressible flow K_c increases with decreasing **R** below 500 10,000 and K_e decreases. At high **R**, the conventionally us coefficients for single-tube flow provide a good first approxim tion for multitube flow, and, since the low Reynolds number effect mentioned tends to cancel the K_c effect, the net result on t f data reported in this paper is minor.

Mr. Nottage raises the point of what is the correct avera density to be employed in estimating pressure drops for hig velocity flow with heat transfer. Recent work at the NAC provides a partial answer to this question. Also Equations [and the following reduced form of Equation [7] for pressure dro within the tube

$$\Delta P = \frac{G^2}{2g}v_1\left[2\left(\frac{v}{v_1}-1\right)+f\,\frac{Av_{\text{avg}}}{A_c v_1}\right]\ldots\ldots\ldots [7$$

may be used, employing a method of successive approximation as follows:

1 The gas temperature as a function of transfer area must b known from $A = 0$ to $A = A_{\text{total}}$.

2 Assume as a first approximation a linear variation of P wit A.

3 With steps (1) and (2) use Equation [9] (numerical o graphical integration) to get v_{avg} from 0 to A as a function of A Also get v as a function of A.

4 Substitute back into Equation [7a] to get P as a functio of A from $A = 0$ to $A = A_{\text{total}}$. This will serve as a second ap proximation for P and steps (3) and (4) can be repeated. Generally, for Mach number less than 0.15, it is sufficiently accurat for step (4) to substitute into Equation [7a] on an over-all basi for the over-all evaluation of ΔP, as further approximation fo P as a function of A will not change the answer appreciably.

With respect to Mr. Nottage's final comments regarding the use of the log-mean density: Equation [9] defines the correct "specific volume" to be employed. Where the percentage pressure change is small, i.e., less than 10 per cent, with good approximation Equation [9] reduces to

$$\frac{v_{\text{avg}}}{v_1} = \frac{P_1}{T_1 P_{\text{avg}}}\left[\frac{1}{A}\int_0^A T\,dA\right]\ldots\ldots\ldots\ldots [9a]$$

That is, an average T "with respect to transfer area" is required. For the gas-turbine regenerator, because of sensibly equal flow-stream-capacity rates (mass-flow rate times specific heat), the temperature is sensibly linear with transfer area, and an arithmetic average of the terminal temperatures, in degrees R, equals the bracketed correct average temperature of Equation [9a].

---

[6] "Basic Heat Transfer and Flow Friction Data for Gas Turbine Regenerator Surfaces," by J. J. Dinan, U.S.N. Engineering Experiment Station Report No. C-2171-D, Aug. 26, 1947.

[7] "An Investigation of Losses of Flow Stream Mechanical Energy at Abrupt Changes in Flow Cross-Section," by W. M. Kays, Technical Report No. 1, Navy Contract n-ONR-251, Task VI (NR-035-104), Sept. 15, 1948.

[8] "Generalized Charts for Determination of Pressure Drop of a High Speed Compressible Fluid in Heat-Exchanger Passages," by M. F. Valerino; paper presented at the Institute on Heat Transfer and Fluid Mechanics, Los Angeles, Calif., June 21–23, 1948.

Heat Transfer and Fluid Friction During Viscous Flow Across Banks of Tubes[1]

By G. A. OMOHUNDRO,[2] O. P. BERGELIN,[3] and A. P. COLBURN[4]

A co-operative program is in progress for the study of fluid friction and heat transfer in idealized models and in commercial tubular heat exchangers over a wide range of variables and under standardized conditions of equipment and technique. Suitable equipment for rapid and accurate testing of the models is described. Heat-transfer coefficients during cooling, and pressure-drop data during both isothermal and cooling runs are reported for low velocities chiefly in the region of viscous flow over an unbaffled tube bank. The data are plotted in ways previously used in the literature with fair agreement in most cases. It is expected, however, that when data for widely different conditions have been obtained, other methods of correlation may prove more suitable.

Nomenclature

The following nomenclature is used in the paper:

A = surface area, sq ft

b = longitudinal pitch, distance between center lines of adjoining transverse rows

c = heat capacity, Btu/(lb) (deg F)

D_e = equivalent diameter = $\dfrac{4 \times \text{free volume}}{\text{exposed area of tubes}}$, ft

D_p = outside tube diameter, ft

f = friction factor defined by $\dfrac{f}{2} = \dfrac{g\,\Delta p \rho D_e}{4G^2L}$, dimensionless

f' = friction factor defined by $\dfrac{f'}{2} = \left(\dfrac{g\,\Delta p\rho D_e}{G^2L}\right)\left(\dfrac{\mu}{\mu_s}\right)^{0.14}\left(\dfrac{D_e}{S_T}\right)^{-0.4}\left(\dfrac{S_L}{S_T}\right)^{-0.6}$

f'' = friction factor defined by $\dfrac{f''}{2} = \left(\dfrac{g\,\Delta p\rho D_e}{4G^2L}\right)\left(\dfrac{\mu}{\mu_s}\right)^n$, dimensionless

$G_{\max}$ = weight velocity through minimum cross section, lb/(hr) (sq ft)

g_c = conversion factor, 4.18×10^8 (mass lb) (ft)/(force lb) (hr)^2

h = surface coefficient of heat transfer based on outside surface area of tubes, Btu/(hr) (sq ft) (deg F)

j = heat-transfer factor, $j = \left(\dfrac{h}{cG}\right)(N_{Pr})^{2/3}\left(\dfrac{\mu_s}{\mu}\right)^{0.14}$, dimensionless

k = thermal conductivity, Btu/(hr) (sq ft) (deg F/ft)

p = pressure, psf

q = rate of heat transfer, Btu per hr

L = length of flow, $L = Nb$, ft

N = number of rows of tubes in direction of flow

N_{Pr} = Prandtl number. $\dfrac{c\mu}{k}$, dimensionless

N_{Re} = Reynolds number, $\dfrac{DG}{\mu}$, dimensionless

n = a constant

S_L = longitudinal pitch, center-to-center distance from tube in one row to nearest tube in adjoining transverse row, ft

S_T = transverse pitch, center-to-center distance between tubes in a transverse row, ft

t = temperature, deg F

t_f = $t_m - 0.32\,\Delta t_m$

t_m = arithmetic average of inlet and outlet bulk temperatures deg F

U = over-all coefficient of heat transfer based on outside surface of tubes, Btu/(hr) (sq ft) (deg F)

$V_{\max}$ = velocity through minimum cross section, fps

Δt_{am} = arithmetic mean of terminal temperature differences between water stream and oil stream

Δt_m = logarithmic-mean temperature difference between oil stream and outer tube surface, as defined by Chilton and Genereaux (2),[5] deg F

μ = absolute viscosity of fluid at average-bulk temperature, lb/(hr) (ft)

μ_s = absolute viscosity at tube-surface temperature, lb/(hr) (ft)

μ_f = absolute viscosity at oil-film temperature, lb/(hr) (ft)

ρ = Density, lb per cu ft

Subscripts:

f = refers to film

o = refers to oil

s = refers to outer surface of tubes

w = refers to water

Introduction

Notwithstanding the widespread use of heat exchangers of the shell-and-tube type, the status of the information on heat-transfer coefficients and pressure drops on the shell side is such that considerable uncertainties exist both in design and in the utilization of existing equipment for new services. The available data are either the results for flow across single banks of tubes taken by many investigators in different types of apparatus in a relatively narrow region of Reynolds number so that systematic trends are difficult or impossible to evaluate, or are spot results on complete heat exchangers but without enough information on all the dimensions and clearances to permit the determination of

---

[1] This is the first contribution from the ASME sponsored Heat Exchanger Research Project which is being conducted by the University of Delaware in co-operation with manufacturers and users of heat exchangers.

[2] Research Fellow in Chemical Engineering, University of Delaware, Newark, Del. Present address, The Koppers Company, Pittsburgh, Pa.

[3] Associate Professor of Chemical Engineering, University of Delaware.

[4] Assistant to the President and Professor of Chemical Engineering, University of Delaware. Mem. ASME.

Contributed by the Heat Transfer Division and presented at the Annual Meeting, Atlantic City, N. J., December 1–5, 1947, of The American Society of Mechanical Engineers.

Note: Statements and opinions advanced in papers are to be understood as individual expressions of their authors and not those of the Society. Paper No. 47—A-102.

[5] Numbers in parentheses refer to the Bibliography at the end of the paper.

leakage and the effects of nonuniform velocities. A two-front attack on this problem appeared to be called for: (*a*) an extensive study of "ideal" models under comparable conditions of uniform flow and no leakage; (*b*) a program of testing full-scale heat exchangers, where all critical dimensions are available, so that eventually it would be possible to correlate the "ideal" flow results with those from the commercial units. The initial step in this program has been under way for some time and the first results are now being reported; the next step, that of testing full-scale heat exchangers, is in course of development.

The present study of ideal models was undertaken with the plan of investigating as wide a range of variables as possible at one location, using the same techniques and in so far as possible the same auxiliary equipment and operating personnel, so that all the data would be on a common basis for comparison. The general program calls for variation of Reynolds numbers from 1 to values greater than 100,000, for variation in fluid viscosity from that of air to that of a heavy oil, and for a wide variation of tube arrangements and spacings in both straight flow and baffled tube banks. The present paper provides a description of the apparatus being used and presents data for one oil flowing across a typical tube bank. A rather viscous oil was chosen so as to include the region of viscous flow, for which few data are available.

EQUIPMENT AND PROCEDURES

The test equipment consists of the heat-exchanger model, an oil-circulating system, a water-circulating system, temperature-measuring equipment, and pressure-measuring equipment. A schematic diagram of the flow system is shown in Fig. 1, and the insulated test exchanger with connecting headers is shown in Fig. 2.

Heat-Exchanger Model. The model is shown in Fig. 3, with the essential dimensions given in Table 1. It consists of a rectangular steel shell containing seventy $^3/_8$-in-OD copper tubes rolled into two fixed forged-steel tube sheets. The rectangular tube bundle is arranged in a staggered equilateral pattern on a pitch of $^{15}/_{32}$ in. (1.25 tube diameters). The tube sheets and the walls of the shell adjoining the tube bundle are lined with sheets of $^1/_2$-in. laminated phenolite plastic to serve as thermal insulation. The outer row of tubes on each side of the tube bundle is half embedded in the plastic. Bronze core rods placed inside the tubes permit high linear velocities without using extremely large quantities of water. These are held in place by $^1/_{16}$-in. bronze pins extending across the ends of the tubes and are centered by pins soldered to the rods about 1 in. from each end. The exchanger is installed with the tubes vertical so that water can be passed upward through the tubes and oil can be passed horizontally across the tube bank.

Circulation Systems. These systems were designed to keep the amount of fluid small, so that equilibrium would be reached quickly after a change of test conditions. The water-circulation system is made of $1^1/_2$-in. brass pipe, insulated with magnesia lagging. Connections to the test exchanger are made through rectangular brass headers. The water is circulated by means of a centrifugal pump. The rate of flow is manually controlled with a "flocontrol" valve and measured with a 3-in. guided-float rotameter. For calibration of the rotameter a storage tank is connected to the suction side of the pump, and an auxiliary weigh tank and scales are used. During cooling runs the temperature of the water system is regulated by the addition of cold water to the suction side of the pump from a constant-head tank connected to the city water mains. The addition of cold make-up water is controlled by a needle valve and a small rotameter. Water forced out of the system by the make-up water is removed through a small surge tank located at the highest point in the system, and this also serves to remove entrained air.

The oil-circulation system is made of standard 2-in. iron pi insulated with magnesia pipe lagging. The headers and test exchanger are covered with 1 in. of corrugated asbestos bo and then wrapped with 2-in. blankets of glass wool, as shown Fig. 2. The oil passes from the storage tank through a bas strainer and then to a suction manifold for three gear pum having capacities of 2, 15, and 48 gpm, respectively. For ea test run a pump of approximately the desired capacity is used order to minimize by-passing and improve control. The oil th passes through a steam-jacketed preheater, after which the fl rate of the heated oil is measured by one of four "ultra-stab vis" type rotameters with capacities of 0.2–1.0, 0.8–5.0, 4. 21.0, and 20–66 gpm, respectively. The rotameters were ca brated in position using the test oil at four temperatures rangi from 80 to 210 F. Check calibration runs were made until r producibility within ±1 per cent was obtained.

The rate of oil flow is controlled manually with "flocontro valves located between the rotameters, and the inlet header the test exchanger and a by-pass line between the pump suctio and discharge manifolds. The oil-inlet header is 42 in. long ar has the same cross section as the tube bundle in the exchange The entrance end of the header is packed with copper tubes e tending for 26 in. to act as velocity diffusers and flow straighte ers. Following the test exchanger is a reducing header and a oil mixer which is used for oil rates up to 20 gpm. The mixe consists of a 1-ft section of 2-in. pipe containing four disks abou 2 in. apart. There are six $^1/_{16}$-in. holes in each disk, and th disks are placed with the holes in a staggered arrangement t give the oil stream a twisting motion as it passes through th mixer.

Temperature Measurements. These are made with coppe constantan thermocouples placed at the control points indicate in Fig. 1. These couples are connected through a selector switc to a direct-reading electronic-type potentiometer, and also to ten-point temperature recorder. The potentiometers are checke against a standard potentiometer each week. The thermocouple are calibrated at the melting and boiling points of water.

The temperature changes across the exchanger are measure with five-junction series-connected thermocouples made fro 24-BWG copper and constantan wires. These multiple-junctio couples are located in each stream on either side of the test ex changer, and the ten couples for each stream are connected dif ferentially. The leads are brought out through a double selecto switch to an electronic-type potentiometer which has a specia scale of 500 divisions for a 5-mv range. Based upon an instrument sensitivity of $^1/_3$ scale division and a precision of $\pm ^1/_3$ scale division, the multiple-junction couples are capable of a sensitivity and precision of ±0.03 deg F. The calibration of each assembly of couples is checked by placing both sets of junctions in a constant-temperature bath to obtain the zero point. Then one set of junctions is placed in another bath at a higher temperature. The lower-temperature bath is held at constant value, and the higher-temperature bath is raised about 4 deg F, as measured by a Beckman thermometer, to determine the change in potential with change in temperature. This procedure is repeated at three temperature levels in the working range of 100–200 F.

In every case the calibration of the multiple couples has been the same as the value calculated from the four-decimal place calibration data obtained from the manufacturer. The differential couples are arranged to obtain an average value in case there are variations in temperature within the stream. The multiple couple for the entering oil is mounted in a grid across the 3-in. × 6-in. entrance header and is located 3 in. beyond the end of the straightening vanes and 15 in. from the front of the tube bank. Calibrated mercury thermometers are installed near the thermocouple grids to provide a check on the differential

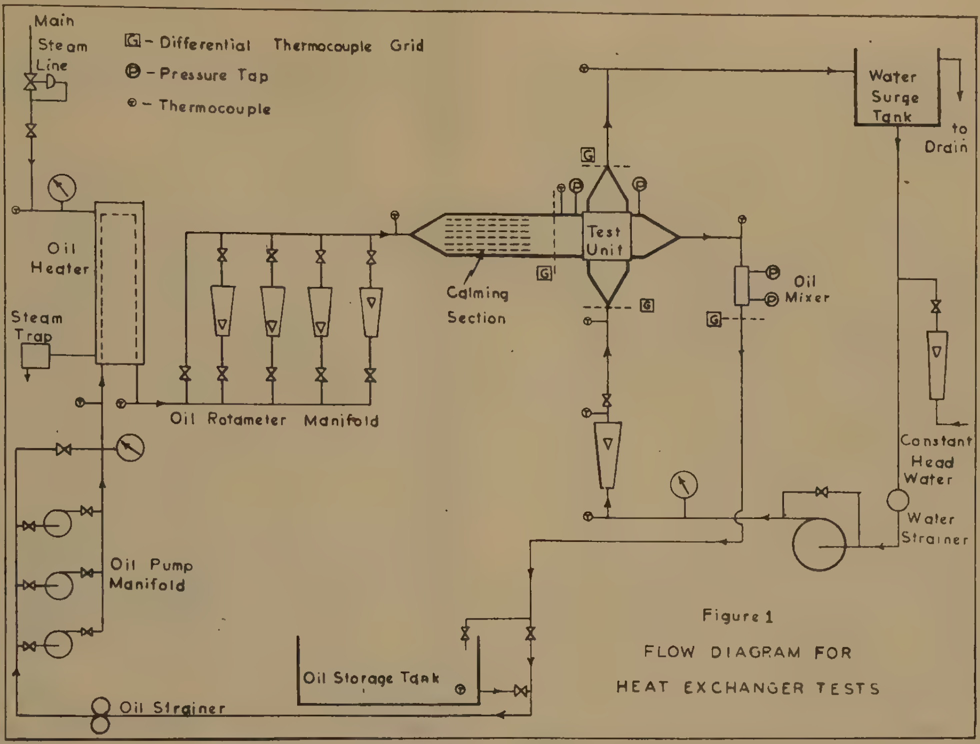

Fig. 1 Flow Diagram for Heat-Exchanger Tests

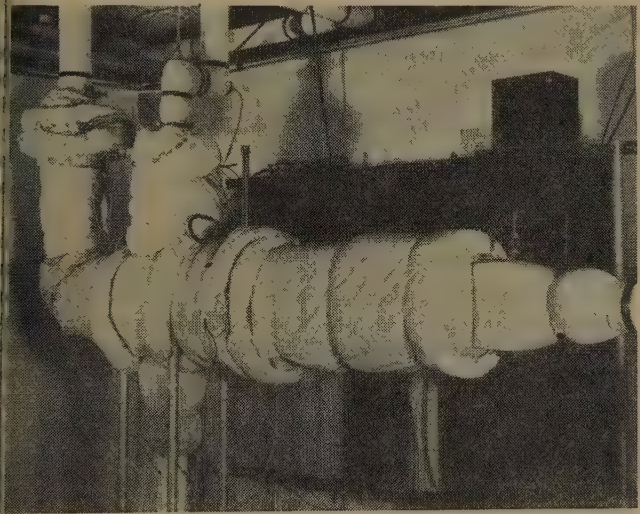

Fig. 2 Insulated Header and Unit Assembly

TABLE 1 TEST-EXCHANGER CONSTANTS

Model number		I
Outside tube diameter	0.375 in.	0.0313 ft
Inside tube diameter	0.277 in.	0.0231 ft
Tube arrangement	...	Equilateral triangle
Tube pitch	0.46875 in.	0.0391 ft
Pitch/outside diameter ratio	...	1.25
Clearance between tubes	0.09375 in.	0.00781 ft
Exposed tube length	6.0 in.	0.5 ft
Number exposed tubes per row	...	6.5
Number tube rows	...	10
Total exposed tubes	...	65
Total tubes	...	70
Tube material	...	Copper
Minimum shell-side area for flow	3.66 sq in.	0.0254 sq ft
Shell-side heat-transfer surface area	460 sq in.	3.19 sq ft
Shell-side equivalent hydraulic diameter	0.27 in.	0.0225 ft
Tube-wall thickness(18 BWG)	0.049 in.	0.00408 ft
Tube-core diameter	0.1875 in.	0.01562 ft
Annulus clearance	0.0448 in.	0.00373 ft
Annulus ratio	...	1.48
Total annulus for flow	2.275 sq in.	0.0158 sq ft
Longitudinal distance between rows of tubes	0.406 in.	
Thermal conductivity of plastic liner	...	0.17 Btu/(hr.) (sq ft)(deg F/ft)

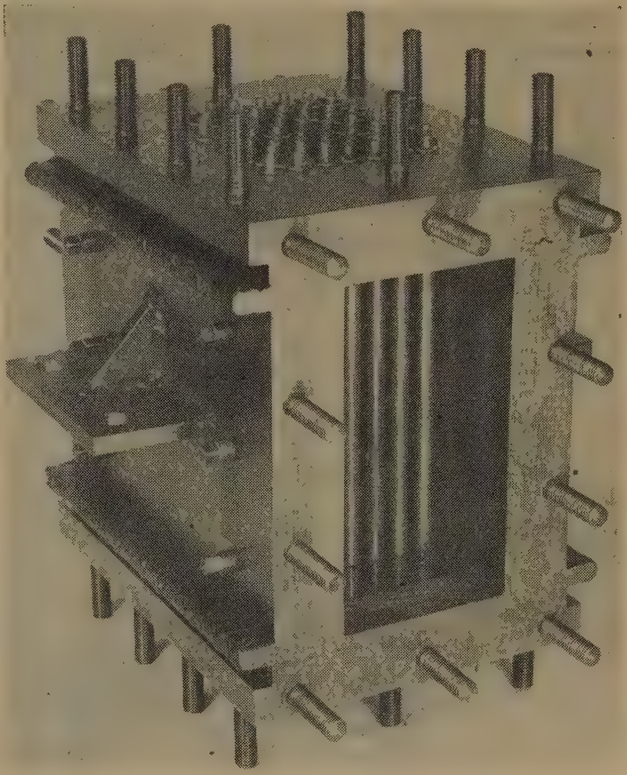

Fig. 3 Test Model

couples. The thermometers are graduated in units of 0.1 deg C over a range of 25 deg C.

Pressure Drop. The shell-side pressure drop of the exchanger is measured with an inverted differential air-over-oil manometer, using oil from the system as the indicating fluid. Pressure taps,

$^1/_8$ in. diam, are located in the top of the headers 6 in. upstream from the first row of tubes and $7^1/_2$ in. downstream from the last row of tubes. An air separator is located over each tap, from which the leads are carried horizontally to the manometer board. The leads are not insulated and are soldered together for a distance of 12 in. so that the oil in both leads will be at room temperature at the manometer. For large pressure drops, an oil-over-mercury manometer is used with the same pressure taps.

Materials. A highly refined turbine oil, Gulfcrest "E", is being used for these tests. Accelerated oxidation tests performed by maintaining a sample of oil at 200 F and bubbling air through it for 30 days showed no change in the physical properties of the oil. The viscosity of the oil was determined by means of a Saybolt viscosimeter at temperatures over the test range. The values of the viscosity corresponded exactly with those given by the supplier. The density of the oil was determined with standard hydrometers at temperatures over the test range. The physical properties of this oil over the temperature range of interest are given in Table 2.

Water from the city mains is used as a cooling medium. Previous tests in this laboratory have shown the physical properties of the city water to be the same as those of distilled water in so far as heat-transfer experiments are concerned. A small amount of Calgon and copper sulphate is added to the water system during the periods when the equipment is standing idle to retard scale and algae growths.

Operation. For the isothermal pressure-drop tests, the water system is drained completely and valves in the lines are closed to prevent air circulation. The oil is circulated until all piping and insulation have reached thermal equilibrium with the oil temperature at or near 150 F. Some difficulties were encountered in maintaining equilibrium at oil velocities less than 0.1 fps. About $1^1/_2$ hr at any given oil flow rate are sufficient to complete a test run. The oil rate is varied over the entire operating range of pump capacity to obtain maximum variation of pressure-drop data. Isothermal tests were made to determine heat losses from the test exchanger, and no measurable temperature change in either the oil or water streams was found at the working temperatures.

For cooling tests, water is circulated at 45 gpm and at about 100 F for all runs, while the oil is circulated at varying velocities and at an average bulk temperature of 150 ± 10 deg F. Equilibrium is considered established at each oil-flow rate when three successive readings at 15-min intervals show little or no change in conditions, and when a heat balance is obtained with less than 5 per cent error.

The exchanger was thoroughly cleaned at the start of the tests and the entire water system was cleaned with a dilute solution of hydrochloric acid. Inspection at the beginning of the tests revealed no scale or dirt on either side of the exchanger, an experiments were made within 3 weeks after this inspection. the end of the tests one of the first points was rerun, yieldi check value slightly higher but within 3 per cent of the orig value.

Experimental and Calculated Results

The experimental results are presented in Table 3, and culated heat-transfer and friction values are given in Tables 4 5. During these tests the temperature change across the changer was much larger for the oil than for the water; theref for greater accuracy, all possible calculations are based on heat load calculated from the temperature change of the oil stre The entering-oil and water temperatures, together with changes in temperature as measured by the multiple-junct thermocouples, are used to calculate the arithmetic-mean t perature differences. An average error in heat balances of 2 per cent was found in the cooling runs. All of the data seem be consistent, except the isothermal pressure drop for run num E-1-26 which therefore is not considered in the discussion.

The water-film coefficient of heat transfer is calculated by tre ing the cored tubes as annuli and using the data of Carpenter al (1). The water-film coefficient, which was practically c stant at about 1480 for all runs, is 6.2 times the maximum coefficient and 38.4 times the minimum oil coefficient. The film coefficients of heat transfer are calculated by subtracting t resistance of the water film from the over-all values, the resista of the metal wall being negligible (h_{metal} = 46,700). The changer is considered clean in this series of experiments so allowance is made for dirt or scale.

While the heat-transfer coefficients are all computed using t arithmetic-mean temperature difference, even though some the runs were in the early turbulent region, the temperatu changes are so small for these latter runs that the arithme and logarithmic means are essentially equal. The correcti factor for temperature difference for crossflow was found to b negligible in all runs.

Discussion of Results

In Fig. 4 the experimental pressure-drop data are plotted ve sus the linear velocity through the minimum cross-sectional ar for flow. The marked increases in the slope of the pressure-dr curves at a velocity of about 1 fps may be attributed to turbule forces becoming predominant above this point. The displaceme of the cooling curve from the isothermal curve is thought to b due to increased frictional resistance caused by the cold surfa of the tubes. The considerable divergence of the cooling line u ward from the isothermal line at velocities below about 0.2 fps noteworthy. There is reason to believe that it may be attribute

TABLE 2 PHYSICAL PROPERTIES OF GULFCREST "E" OIL

t deg F	c_p[a] Btu/(lb) (deg F)	μ[b] lb/(hr) (ft)	k[c] Btu/(lb) (sq ft) (deg F/ft)	$\frac{c\mu}{k}$	$\left(\frac{c\mu}{k}\right)^{2/3}$	ρ[b] lb per cu ft
90	0.461	321	0.0757	1955	156	54.06
110	0.473	177	0.0753	1110	107	53.62
130	0.484	106	0.0748	685	77.5	53.18
150	0.495	68	0.0743	453	58.5	52.76
170	0.507	46	0.0739	316	46.0	52.34
190	0.518	32	0.0734	226	37.0	51.94
210	0.530	23	0.0730	167	30.2	51.57

[a] Calculated using equation of Watson and Nelson (8)

$$c_p = 0.6811 - 0.308s + t(0.000815 - 0.000306s)\,(0.055\,K + 0.35)$$

where s = specific gravity at 60 F
t = temperature, deg F
K = characterization factor = 12.6

[b] Experimentally determined values.

[c] Calculated using equation of C. S. Cragoe (9)

$$k = \frac{1}{12}\,\frac{0.813}{s}\,[1 - 0.0003\,(t - 32)]$$

s = specific gravity at 60 deg F (0.877)
t = temperature, deg F

TABLE 3 EXPERIMENTAL RESULTS

Run number	Oil rate lb per hr	Oil temp in, deg F	Oil temp out, deg F	Oil Δp lb per sq ft	Oil temp drop, deg F[a]	Water rate, lb per hr	Water temp, in, deg F	Water temp, out, deg F	Water temp, rise, deg F[a]
				Cooling Data					
E-1-16	225	162.9	117.8	2.47	45.1	23050	98.3	98.4	0.22
E-1-15	340	162.9	126.0	3.15	38.4	23050	99.6	99.8	0.26
E-1-14	488	165	134.4	3.80	31.0	23050	101.5	101.7	0.34
E-1-13	709	161.6	137.4	5.20	24.2	23050	100.2	100.5	0.37
E-1-12	1030	158.0	139.6	7.22	18.6	23050	100.2	100.7	0.42
E-1-11	1515	156.8	143.8	9.90	14.3	23050	102.1	102.5	0.45
E-1-10	2240	155.7	144.2	14.6	11.1	23050	100.9	101.1	0.52
E-1-7	2820	162.3	150.3	16.3	10.5	23050	100.5	101.1	0.66
E-1-6	4470	164.2	156.7	24.9	7.60	23050	104.5	105.0	0.78
E-1-8	6070	162.4	155.2	36.6	6.40	23050	100.5	101.1	0.83
E-1-36	12300	152.0	148.6	98.8	3.50	23050	100.2	101.1	0.96
E-1-38	18600	152.0	149.4	173.	2.85	23050	100.0	101.1	1.14
E-1-35	26250	151.8	149.5	287.	2.54	23050	99.0	100.2	1.47
				Isothermal Data					
E-1-26	204	147.4		0.72					
E-1-50	270	148.9		1.22					
E-1-25	346	149.0		1.71					
E-1-24	463	150.2		2.29					
E-1-22	710	149.3		3.43					
E-1-21	1040	149.2		5.14					
E-1-23	1510	149.3		7.45					
E-1-20	2290	150.9		10.9					
E-1-19	2930	151.3		14.0					
E-1-18	4370	150.4		23.1					
E-1-17	6180	151.2		33.1					
E-1-49	9275	149.2		59.5					
E-1-46	14050	149.2		103.					
E-1-47	19500	150.0		164.					
E-1-48	26300	150.1		261.					

[a] Measured with differential thermocouples.

TABLE 4 CALCULATED HEAT-TRANSFER RESULTS

Run mber	q_o Btu per hr	q_w Btu per hr	$\frac{q_o - q_w}{q_o}$	Δt_{am} deg F	U	h_w	h_o	Oil V_{max} fps	Oil G_{max} lb/(hr)(sq ft)	t_s deg F	Oil t_m deg F	$\left(\frac{\mu_s}{\mu}\right)^{0.14}$	j	$\frac{D_p G_{max}}{\mu}$
1-16	4980	5045	−1.30%	42.0	37.3	1460	38.0	0.047	8850	99.6	140.4	1.16	0.677	3.33
1-15	6420	6100	+4.98	44.0	45.8	1470	47.3	0.070	13350	102.0	144.5	1.16	0.524	5.48
1-14	7500	7830	−4.40	47.8	49.2	1490	51.0	0.101	19200	103.6	149.7	1.18	0.371	8.81
1-13	8500	8520	—0.24	49.1	54.2	1480	56.4	0.147	27850	102.2	149.5	1.18	0.284	12.8
1-12	9480	9670	—2.01	48.3	61.5	1480	64.3	0.213	40500	102.6	148.8	1.18	0.223	18.3
1-11	10720	10370	+3.26	47.3	71.0	1500	74.5	0.313	59500	104.4	150.3	1.17	0.169	27.7
1-10	12300	11990	+2.52	49.0	78.7	1480	83.3	0.464	88100	103.7	150.0	1.17	0.131	40.4
1-7	14780	15200	—2.85	56.2	82.5	1480	87.5	0.585	111000	103.3	156.3	1.20	0.102	57.7
1-6	17050	17900	—5.00	55.5	96.1	1520	103	0.929	175800	108.7	160.4	1.18	0.0706	99.6
1-8	19400	19100	+1.55	58.3	104.3	1480	112	1.26	238500	104.8	158.8	1.20	0.0585	130
1-36	21350	22150	—3.75	49.6	135	1480	149	2.53	484000	105.4	150.3	1.16	0.0419	222
1-38	26300	26300	0.00	50.0	165	1480	186	3.85	731000	106.5	150.7	1.16	0.0347	341
1-35	33100	33850	—2.27	50.8	204	1470	238	5.43	1032000	106.7	150.6	1.16	0.0314	474

TABLE 5 CALCULATED PRESSURE-DROP RESULTS

Run mber	Oil t_m deg F	Oil t_f deg F	Oil G_{max} lb/(hr)(sq ft)	Oil V_{max} fps	$\frac{f}{2}$	$\frac{D_e G_{max}}{\mu_f}$	$\left(\frac{\mu}{\mu_s}\right)$	$\left(\frac{\mu}{\mu_s}\right)^{0.14}$	$\left(\frac{\mu}{\mu_s}\right)^{0.25}$	$\frac{f'}{2}$	$\frac{f''}{2}$ (n = 0.14)	$\frac{f''}{2}$ (n = 0.25)	$\frac{D_e G_{max}}{\mu}$
-1-16	140.4	128.8	8850	0.047	11.7	1.81	0.349	0.863	0.768	50.0	10.05	8.94	2.40
-1-15	144.5	131.8	13350	0.070	6.52	2.92	0.338	0.859	0.762	27.8	5.57	4.94	3.96
-1-14	149.7	134.4	19200	0.101	3.78	4.60	0.318	0.852	0.751	15.9	3.20	2.81	6.35
-1-13	149.5	133.6	27850	0.147	2.46	6.40	0.303	0.846	0.741	10.3	2.07	1.81	9.22
-1-12	148.8	134.0	40500	0.213	1.62	9.30	0.316	0.851	0.750	6.82	1.37	1.20	13.2
-1-11	150.3	136.0	59500	0.313	1.03	14.3	0.323	0.854	0.754	4.34	0.871	0.772	20.0
-1-10	150.0	135.2	88100	0.464	0.690	21.1	0.318	0.852	0.751	2.91	0.585	0.517	29.2
-1-7	156.3	139.4	111000	0.585	0.497	29.4	0.279	0.836	0.726	2.06	0.414	0.360	41.6
-1-6	160.4	143.7	175800	0.929	0.294	52.1	0.303	0.846	0.741	1.24	0.248	0.218	71.9
-1-8	158.8	141.8	238500	1.26	0.236	65.5	0.281	0.837	0.727	1.00	0.202	0.175	92.7
-1-36	150.3	136.2	484000	2.53	0.155	120.	0.341	0.860	0.764	0.660	0.132	0.118	160.
-1-38	150.7	136.4	731000	3.85	0.119	181.	0.336	0.858	0.761	0.505	0.102	0.0899	246.
-1-35	150.6	136.6	1032000	5.43	0.099	256.	0.347	0.862	0.767	0.423	0.085	0.0757	347.
						Isothermal Data							
-1-26	147.4		8020	0.0422	4.10	2.54				20.4	4.10	4.10	2.54
-1-50	148.9		10630	0.0559	3.94	3.52				19.6	3.94	3.94	3.52
-1-25	149.0		13600	0.0717	3.39	4.43				16.9	3.39	3.39	4.43
-1-24	150.2		18200	0.0960	2.54	6.07				12.7	2.54	2.54	6.07
-1-22	149.3		28000	0.147	1.61	9.11				8.03	1.61	1.61	9.11
-1-21	149.2		40900	0.216	1.13	13.3				5.61	1.13	1.13	13.3
-1-23	149.3		59300	0.313	0.773	19.4				3.85	0.773	0.773	19.4
-1-20	150.9		90100	0.474	0.505	30.2				2.52	0.505	0.505	30.2
-1-19	151.3		115000	0.607	0.388	38.7				1.94	0.388	0.388	38.7
-1-18	150.4		172000	0.905	0.286	57.7				1.42	0.286	0.286	57.7
-1-17	151.2		243000	1.28	0.205	81.6				1.02	0.205	0.205	81.6
-1-49	149.2		365000	1.92	0.164	119.				0.816	0.164	0.164	119.
-1-46	149.2		553000	2.92	0.123	180.				0.612	0.123	0.123	180.
-1-47	150.0		767000	4.03	0.102	254.				0.508	0.102	0.102	254.
-1-48	150.1		1035000	5.45	0.0895	344.				0.446	0.0895	0.0895	344.

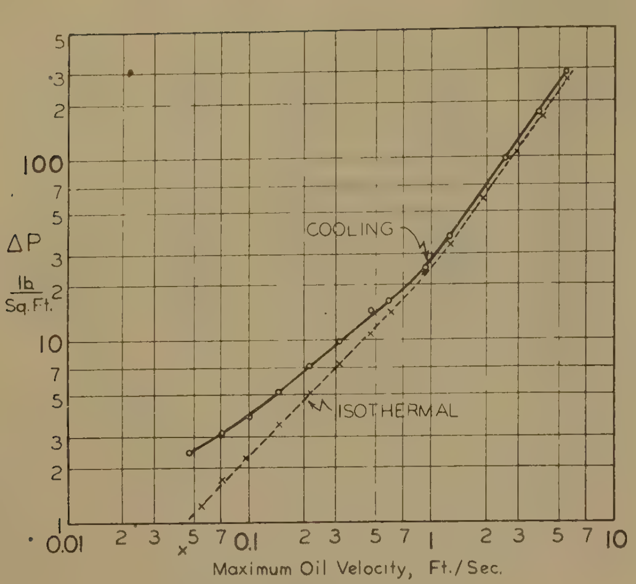

FIG. 4 PRESSURE DROP, ΔP

(Flow normal to $^3/_8$-in-OD tubes, $^{15}/_{32}$ in. equilateral pitch. Bulk-oil temperature range for cooling runs, 140–160 F; surface-oil temperature range for cooling runs, 100–110 F; bulk-oil temperature range for isothermal runs, 147–152 F. Gulfcrest "E" oil, 525 SSU at 100 deg F, 98 centipoises.)

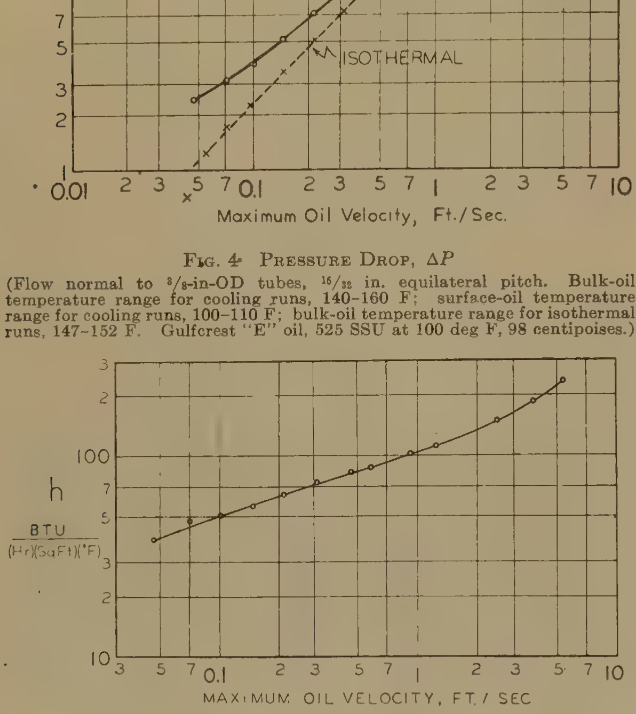

FIG. 5 OIL-FILM COEFFICIENT OF HEAT TRANSFER, h_0

(Flow normal to $^3/_8$-in-OD tubes, $^{15}/_{32}$ in. equilateral pitch. Bulk-oil temperature range, 140–160 F; surface-temperature range 100–110 F. Gulfcrest "E" oil, 525 SSU at 100 deg F, 98 centipoises.)

to the uneven distribution of flow which tends to occur during cooling of viscous liquids. This condition often results when cooling viscous streams in parallel because of the instability arising when greater cooling of one stream causes higher viscosity, and therefore lower velocity, at a given over-all pressure drop. This in turn means a greater temperature decrease of the slow stream, etc. Because of mixing between streams, this effect might not be appreciable during flow across banks of staggered tubes. Additional data in the low-velocity range, together with velocity and temperature traverses across the tube bundle, are needed to obtain a better understanding of this effect.

The friction data for isothermal and cooling tests, calculated as friction factors, are presented in Fig. 6 by the Chilton and Genereaux (2) method of correlation. This correlation uses both the isothermal and nonisothermal data of Sieder and Scott (3), to obtain a relation between the friction factor and Reynolds number, with the physical properties based on a film temperature, and the equivalent hydraulic diameter used in calculating the Reynolds number. The curve of Chilton and Genereaux falls parallel to and about 12 per cent below a straight line through the present isothermal data over the range of Reynolds numbers from 5 to 40. Above a Reynolds number of 40, the isothermal

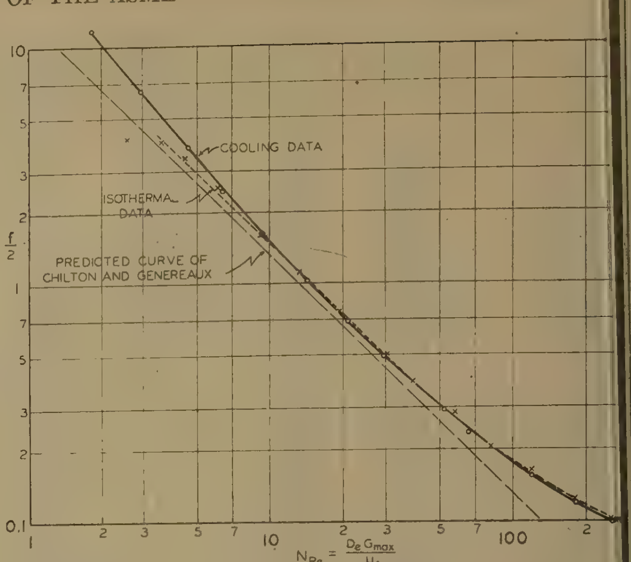

FIG. 6 FRICTION-FACTOR CORRELATION METHOD OF CHILTON A GENEREAUX

$$\frac{f}{2} = \left(\frac{g\Delta p\rho D_e}{4G^2L}\right)$$

(Flow normal to $^3/_8$-in-OD tubes, $^{15}/_{32}$ in. equilateral pitch. Bulk-oil te perature range for cooling runs, 140–160 F; surface-temperature range isothermal runs, 100–110 F; bulk-oil temperature range for isothermal ru 147–152 F. Gulfcrest "E" oil, 525 SSU at 100 deg F, 98 centipois Predicted curve $f/2 = 13.25\ N_{Re}^{-2}$; $t_f = t_m - 0.32\ \Delta t_m$.)

data depart from a straight line. This tendency was also tr of the data of Sieder and Scott as reported by Chilton a Genereaux and indicates the beginning of turbulence. The co ing data practically coincide with the isothermal data throug out the region of partial turbulence and into viscous flow down a Reynolds number of 10. Below this point the friction fact increases rapidly and the film-temperature correction is no long adequate to bring the cooling data in line with the isotherm points, again showing the possibility of nonuniform distributi of flow at low velocities.

In Fig. 7 the friction data are plotted according to the metho of Gunter and Shaw (4), in which $f'/2$ is plotted against N_{Re} wi the average bulk temperature used in evaluating all physical pro erties. By this method the cooling data fall close to the propose curve down to a N_{Re} of about 10, but at lower values they devia in the same manner as in the Chilton and Genereaux method correlation. The Gunter and Shaw curve falls parallel to th isothermal data but about 17 per cent above them for Reynol numbers from 5 to 50. Both the isothermal and cooling dat fall on or near the curve of Gunter and Shaw above a Reynol number of 100.

It must be kept in mind that both of the procedures mentione for correlation in the region of viscous flow were based upo Sieder and Scott's investigation which covered only one tub size, one tube arrangement, and two tube spacings. As pointe out by Boucher and Lapple (5) these data are exceedingly limite in scope to serve as the basis for a general correlation. Moreove since the tube size and pitch of the present unit are one half those used by Sieder and Scott, further data are necessary t determine the quantitative effects of these variables.

Fig. 8 shows the effect of applying the Sieder and Tate viscosit correction to the data on pressure drop during cooling in an ef fort to correlate them with the isothermal data. The viscosit ratio μ/μ_s is shown raised to the 0.25 power as recommended fo viscous flow by Sieder and Tate (6), and the 0.14 power as recom mended by Gunter and Shaw. From Fig. 8 it is evident that single viscosity-ratio correction is not adequate for the correla tion of these data and that the μ/μ_s ratio should be some functio

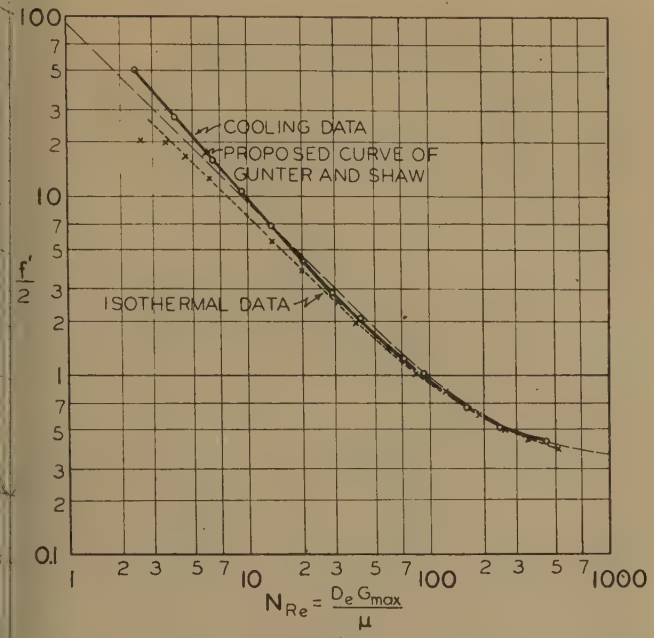

IG. 7 FRICTION-FACTOR CORRELATION BY METHOD OF GUNTHER AND SHAW

$$\frac{f'}{2} = \left(\frac{g\,\Delta p\rho D_e}{G^2L}\right)\left(\frac{\mu}{\mu_s}\right)^{0.14}\left(\frac{D_e}{S_T}\right)^{-0.4}\left(\frac{S_L}{S_T}\right)^{-0.6}$$

Flow normal to $^3/_8$-in-OD tubes, $^{15}/_{32}$ in. equilateral pitch. Bulk-oil tem-erature range for cooling runs, 140–160 F; surface-temperature range for ooling runs, 100–110 F; bulk-oil temperature range for isothermal runs, 47–152 F. Gulfcrest "E" oil, 525 SSU at 100 deg F, 98 centipoises.)

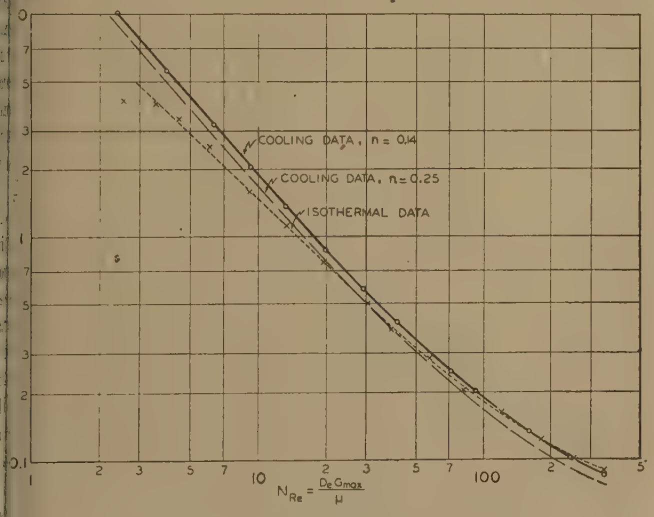

FIG. 8 FRICTION-FACTOR CORRELATION

$$\frac{f''}{2} = \left(\frac{g\,\Delta p\rho D_e}{4G^2L}\right)\left(\frac{\mu}{\mu_s}\right)^n$$

Flow normal to $^3/_8$-in-OD tubes, $^{15}/_{32}$ in. equilateral pitch. Bulk-oil emperature range for cooling runs, 140–160 F; surface temperature range or cooling runs, 100–110 F; bulk-oil temperature range for isothermal runs, 47–152 F. Gulfcrest "E" oil, 525 SSU at 100 deg F, 98 centipoises.)

f the rate of flow. When additional data have been obtained a orrelation will be attempted upon this basis.

The heat-transfer data have been calculated as j-factors and lotted on Fig. 9 versus the Reynolds number based on tube iameter. The j-factor here utilizes the Sieder and Tate viscos-ty-ratio correction. While the curve through the experimental ata has a steeper slope than that predicted by Colburn (7) arallel to a plot for single tubes, it is of interest that the data all so close to the predicted curve, since the proposed correlation was made at a time when no data on tube banks were available. Although the simple group of variables included in the j-factor is at best a rough approximation for the exact factors of importance, further data for other conditions are necessary before a general correlation can be attempted.

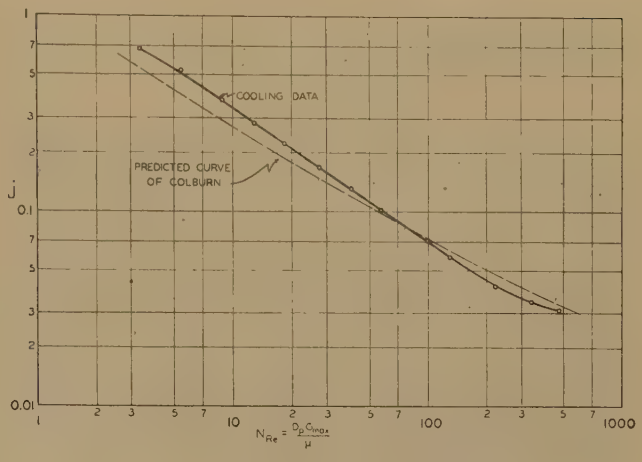

FIG. 9 j-FACTOR FOR HEAT TRANSFER

$$j = \frac{h}{cG}\,(N_{Pr})^{2/3}\left(\frac{\mu_s}{\mu}\right)^{0.14}$$

(Flow normal to $^3/_8$-in-OD tubes, $^{15}/_{32}$ in. equilateral pitch. Bulk-oil temperature range for cooling runs, 140–160 F; surface-temperature range for cooling runs, 100–110 F. Gulfcrest "E" oil, 525 SSU at 100 deg F, 98 centipoises.)

At the lowest velocities, free convection may have had some effect; this was probably very small because of the high viscosity and close tube spacing. This factor will be explored in future work.

CONCLUSIONS

1 The equipment and technique are satisfactory as shown by the uniformity of the friction and heat-transfer data, and the agreement of the friction data with average values of previous investigators.

2 Neither the proposed correlation of Chilton and Genereaux, which is approximately 12 per cent low, nor that of Gunter and Shaw, which is approximately 17 per cent high, adequately correlate the isothermal friction data, indicating a possible effect of tube size or pitch not exactly covered by those correlations.

3 A viscosity correction which is a function of the flow rate seems to be indicated for the correlation of cooling data with isothermal friction data.

4 The heat-transfer data appear to fall near the curve previously drawn parallel to data obtained with single cylinders.

ACKNOWLEDGMENT

The authors acknowledge the suggestions on design of the apparatus and on the program of study by the Special Advisory Committee of the Heat Transfer Division, which is sponsoring this co-operative research project. The committee at the time of the work, was composed of W. H. McAdams, chairman, A. Y. Gunter, A. C. Mueller, B. E. Short, W. H. Thompson, T. Tinker, and P. R. Trumpler. The help of A. Wurster in the design and construction of the test unit was invaluable. Assistance in the experimental work was given by Research Fellows, Edward S. Davis and Harold L. Hull. Funds and equipment were kindly furnished by the Tubular Exchanger Manufacturers' Association, Andale Company, Davis Engineering Company, Downingtown Iron Works, du Pont Company, Standard Oil Development

Company, and York Ice Machine Company. The oil was provided by the Gulf Oil Corporation.

BIBLIOGRAPHY

1 "Heat Transfer and Friction of Water in an Annular Space," by F. G. Carpenter, A. P. Colburn, E. M. Schoenborn, and A. Wurster, Transactions of the American Institute of Chemical Engineers, vol. 42, 1946, pp. 165–187.

2 "Pressure Drop Across Tube Banks," by T. H. Chilton and R. P. Genereaux, Transactions of the American Institute of Chemical Engineers, vol. 29, 1933, pp. 161–173.

3 "Fluid Friction at Parallel and Right Angles to Tubes and Tube Bundles," by E. N. Sieder and N. A. Scott, Jr., ASME unpublished papers, No. 83, 1932.

4 "A General Correlation of Friction Factors for Various Types of Surfaces in Crossflow," by A. Y. Gunter and W. A. Shaw, Trans. ASME, vol. 67, 1945, pp. 643–660.

5 "Pressure Drop Across Tube Banks," by D. F. Boucher and C. E. Lapple, *Chemical Engineering Progress*, vol. 44, 1948, p. 117.

6 "Heat Transfer and Pressure Drop of Liquids in Pipes," by E. N. Sieder and G. E. Tate, *Industrial and Engineering Chemistry*, vol. 28, 1936, pp. 1429–1435.

7 "A Method of Correlating Forced-Convection Heat-Transfer Data and a Comparison With Fluid Friction," by A. P. Colburn, Transactions of the American Institute of Chemical Engineers, vol. 29, 1933, pp. 195–199.

8 "Improved Methods of Approximating Critical and Thermal Properties of Petroleum Fractions," by K. M. Watson and E. F. Nelson, *Industrial and Engineering Chemistry*, vol. 25, 1933, pp. 880–887.

9 "Thermal Properties of Petroleum Products," by C. S. Cragoe, National Bureau of Standards, Miscellaneous Publication No. 97, 1929, pp. 24.

Discussion

T. Tinker.[6] The data reported in this paper constitute a
finite contribution to heat-transfer literature. These carefu
run data disclose certain peculiarities in fluid flow and h
transfer in the N_{Re} regions which should be investigated furt
for a variety of tube sizes and arrangements.

The downward divergence of the heat-transfer characteris
from the theoretical at low flow rates attributed to uneven d
tribution of flow is similar to that observed and reported by t
writer for commercial heat exchangers. In most commerc
heat exchangers, these effects are much more drastic because
addition to the flow routes through the tube nest, there are ot
parallel flow routes of low hydraulic resistance through the
changer.

The authors suggest that the viscosity-ratio correction μ
should possibly be some function of the rate of flow in order
bring friction factors for oil-cooling in line with the isotherm
data. It may be possible that part of the irregularity in the lo
velocity region may be due to uneven distribution of flow a
only partly due to an improper exponent applied to the viscosi
ratio. Should this be the case, the portion of the irregularity d
to uneven flow distribution might be quite different for a bank
tubes 6 rows wide from that of a bank 15 rows wide or for banks
different tube lengths. In consideration of this possibility
might be advisable to investigate the variations in flow distrib
tion for tube banks of different proportions before assigning
specific function to the viscosity ratio correction.

---

[6] Chief Engineer, Ross Heater & Manufacturing Company, In
Buffalo, N. Y.

The Gas Turbine as a Stationary Prime Mover

By L. N. ROWLEY[1] AND B. G. A. SKROTZKI,[2] NEW YORK, N. Y.

To date more than a score of stationary gas turbines, ggregating well over 100,000 kw, have been built or are nder construction. About three quarters of these might roperly be classed as commercial units. All the plants n this category operate at modest inlet temperatures nd utilize alloy materials on which extensive experience as been obtained. This indicates definite places in the tationary power field for gas turbines such as can be built oday under essentially commercial conditions. It seems vident that if the gas turbine is to move ahead as fast as s proponents desire, engineering effort and ingenuity omparable to that now going into technical development ust be expanded on defining and evaluating the gas urbine's economic possibilities so they may be fully exloited. This paper presents some preliminary thinking long these lines. For the case where power generation is he sole requirement, the authors analyze several specific ituations. It must be clearly understood that such nalyses are instructive only if their limitations are recogized; nothing is more dangerous than economic generaliation. For cases where process heat as well as power must e supplied, the economic problem is even more complex. he authors have, of necessity, approached this question rom a qualitative viewpoint, and merely indicate the eneral position of the gas turbine in this field and some f the modifications that might enhance its usefulness.

GAS-TURBINE CHARACTERISTICS

THE performance and physical characteristics of gas turbines have been thoroughly discussed in many papers. It would be well, however, to review briefly those characteristics at have a bearing on economic decisions.

Present commercial capacity range for gas turbines operating t 1100 F varies from 1000 to 25,000 kw. When inlet temperaures can be raised, the range will increase. Gas turbines now urn fuel oil and gas. In the light of present aggressive research rograms it is likely they will be able to burn coal in the not-oo-distant future.

Gas-turbine plants require only small building volumes, on the rder of one third that needed by steam plants of equal capacity. his feature, coupled with the relatively few plant components, eans that operating labor can be reduced considerably. Furhermore, gas turbines can be started from cold in 6 to 10 min, iminating banking losses and minimizing starting losses. On he basis of necessarily limited experience, reliability and mainenance cost seem closely comparable to steam-turbine figures.

Small physical size and low weight are advantageous in reducing foundation requirements and hence investment costs. For plants of 6000-kw capacity and less, no water is needed, which means the plant can be located anywhere. Plants above 6000-kw capacity have proved more economical when compression is divided into two or more stages and intercooling utilized. This reduces compressor dimensions and raises over-all cycle efficiency and capacity. Water for intercooling is only a small fraction of that used by a steam plant of equal size. Again, this gives greater latitude of plant location for the gas turbine.

Typical performances at full load with 1100-F inlet gas for 10,000-kw gas turbines are as follows: Simple cycle, no intercooling, 19,000 Btu per kwhr; simple cycle with one intercooler, 16,000 Btu per kwhr; 2-turbine arrangement with intercooler, 15,000 Btu per kwhr; regenerative cycle with intercooling and reheating, 13,000 Btu per kwhr.

Because gas turbines are flexible in design, increasing investments produce a more efficient plant. For example, plants built for 30 per cent thermal efficiency cost about 50 per cent more than plants to operate at 20 per cent thermal efficiency. Any plant built for intermediate efficiency would be roughly prorated in investment cost between these limits.

ISOLATED-PLANT COMPARISON

Having seen how the gas turbine shapes up in general terms, let us attempt to make some economic comparisons in situations where the gas turbine might be considered as a possible prime mover. For the first case, assume that an isolated plant, solely for power generation, is to be built.

Economic conditions being extremely variable, depending on geographical situation and local conditions, it becomes pointless to assume just one set of costs and expect to draw any conclusions of general value. However, original investment and unit fuel costs are the primary determinants for evaluating the economic desirability of alternate schemes, and Figs. 2 to 5 indicate how a gas-turbine plant of definite heat-rate characteristic compares with alternate steam and Diesel installations as these two principal costs are varied. The heat-rate characteristics for the three plants are given in Fig. 1. Other pertinent data for this elementary economic comparison are given in Table 1.

TABLE 1 COMPARATIVE DATA FOR POWER SYSTEMS

	Plant	Steam turbine	Diesel engine	Gas turbine
1	Capacity, kw	10000	10000	10000
2	Operating crew, men	12	7	7
3	Annual labor cost	$36000	$21000	$21000
4	Average cost of maintenance, repairs, supplies, lubricating oil, miscellaneous, mills per kwhr	1.0	1.8	0.8
5	Annual investment—charge rate, per cent	12	12	12

Fig. 2 shows the justifiable investment in a gas turbine (in per cent of steam-turbine investment) for various combinations of original cost, unit fuel cost and plant capacity factors of 30, 50, and 70 per cent. For any steam-plant investment and capacity factor, the justifiable gas-turbine investment increases with lower unit fuel costs. Unit fuel costs are assumed equal for gas-turbine and steam-turbine plants. At one value of unit fuel cost, the gas-turbine justifiable investment equals steam-plant investment.

---

[1] Managing Editor, *Power*, McGraw-Hill Publishing Company, nc. Mem. ASME.

[2] Associate Editor, *Power*, McGraw-Hill Publishing Company, nc. Mem. ASME.

Contributed by the Gas-Turbine Power Division and presented at he Spring Meeting, New Orleans, La., March 1-4, 1948, of THE MERICAN SOCIETY OF MECHANICAL ENGINEERS.

NOTE: Statements and opinions advanced in papers are to be nderstood as individual expressions of their authors and not those f the Society. Paper No. 48—S-5.

To draw conclusions from these curves, relative costs of gas-turbine and steam-turbine plants must be known. As yet, we have no experience in this country, but a clue to this relation may be taken from Swiss experience which reports that, for equal capacities, a gas-turbine plant costs about 85 per cent of a steam-turbine plant. Using this value as a criterion, we can then conclude that at, say, 50 per cent capacity factor, the gas-turbine plant economically equals the steam-turbine plant at investments for the latter of $58 per kw with 30 cents per million Btu fuel, $121 per kw with 40 cent fuel, or $184 per kw with 50-cent fuel. If actual fuel costs are less than these at the given investments then the gas-turbine plant is economically superior and vice versa.

The families of curves for the three capacity factors show that gas-turbine desirability increases with greater utilization at given investments and fuel costs.

There may be cases where the steam plant can burn coal and the gas turbine must burn relatively expensive oil. To show the effect of this condition, Fig. 3 indicates the shift in the curves for a 10 per cent increase in unit fuel cost for the gas turbine. Such a condition of course adds an economic burden on the gas-turbine plant.

Similar relations are established between the gas turbine and Diesel engine in Fig. 4, for 30, 50, and 70 per cent capacity factor. Since the gas turbine may burn cheaper oil than the Diesel, Fig. 5 shows the effect of gas-turbine unit fuel cost being 90 per cent of Diesel unit fuel cost.

According to reported Swiss experience, the differential capital cost between Diesels and gas turbines is much greater than that between steam and gas turbines. Assuming, for the purpose our example, that gas-turbine-plant investments are 75 per cent Diesel-plant investments and that fuel costs are equal, some of t break-even points in terms of Diesel investments for 50 per ce capacity factor are $54 per kw with 30 cent fuel; $119 per k with 40-cent fuel; $189 per kw with 50-cent fuel.

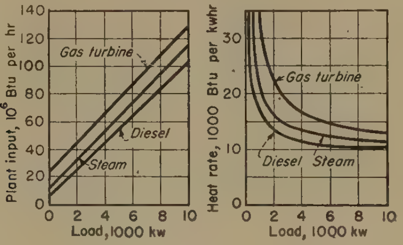

Fig. 1

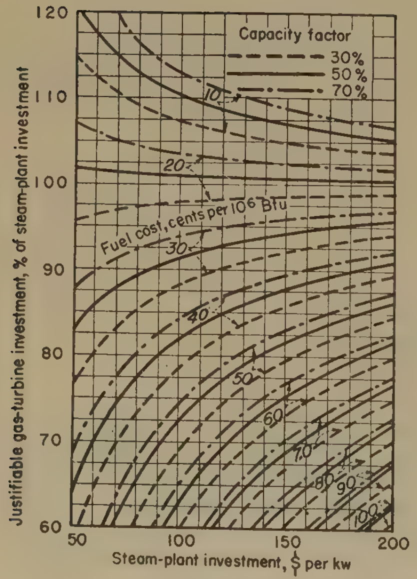

Fig. 2

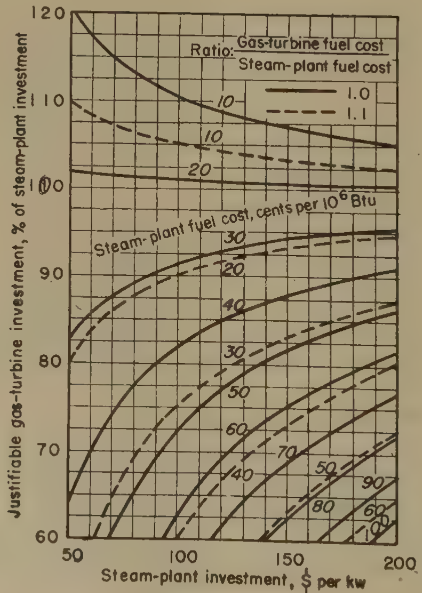

Fig. 3

EXTENDING AN EXISTING SYSTEM

A somewhat different problem is involved when we consid an addition to an existing system, since it will be seen that t

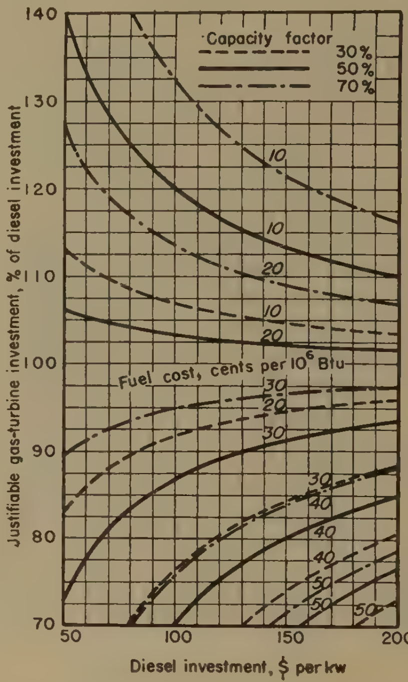

Fig. 4

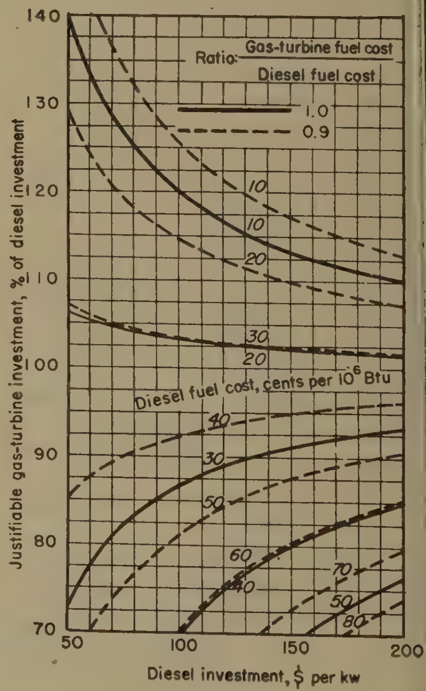

Fig. 5

state of efficiency development of the system exercises a substantial influence on the results. Assume that 10,000-kw capacity is to be added to a system with a 100,000-kw peak load and a load-duration curve as in Fig. 6. The existing system has 100,000-kw capacity and the new unit is needed to re-establish a one-unit reserve.

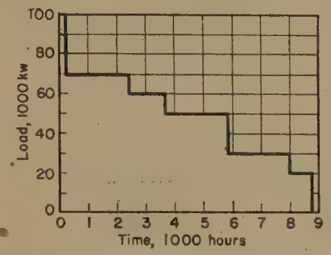

FIG. 6

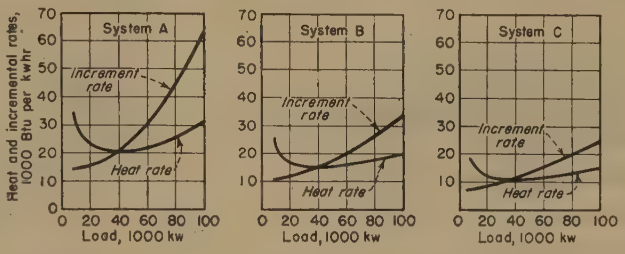

FIG. 7

To illustrate the influence of system development, assume that three systems A, B, and C, are involved, each having a different heat-rate and incremental-rate curve, as shown in Fig. 7. To bring the problem within reasonable limits, and to simulate conditions encountered in an actual case, fuel cost and investment are not handled as variables, as in the isolated-plant case, but are assumed. For further simplification, other operating costs are taken as a percentage of fuel cost. While ordinarily no definite physical relationship exists between these two cost groups, experience indicates that under limited conditions such as maintain here there tends to be a correlation for plants of equal capacity.

It should be clearly understood that the necessity for making assumptions as outlined definitely limits the conclusions drawn from this case to situations where the assumed figures are roughly applicable. The results of the comparison do show, however, certain relationships which are interesting and that will appear, altered in magnitude, in other generally similar comparisons.

In studying the addition of a base-load steam plant, the first objective is to determine the reduction in operating cost of the existing system caused by the new unit taking over its share of the load. Here the new unit is assumed to be fully loaded and available and on the line 90 per cent of the time, thus fixing its annual output in item 1, Table 2. The system average decrement rate comes from (1) integrating the load-duration curve, Fig. 6, with the system heat-rate curve, Fig. 7, and (2) subtracting from this the integration of the load curve minus 10,000 kw at all loads with the same heat-rate curves. Dividing the difference of these two integrations by 8760 hr × 10,000 kw gives the values in item 2.

Decrement fuel cost is the product of items 1 and 2. Decrement operating costs of item 3 are taken as 30 per cent of the decrement fuel instead of 50 per cent since experience shows that incremental values are usually less than the ratio of total values on a system consisting of several units. Total reduction on costs of operating existing units appears as item 5. Total generating cost of the new base-load steam plant (including carrying charges) is then subtracted from the existing system decrement costs to find the savings resulting from installation of the new unit. For system A the considerable saving indicates the obsolescence of the existing equipment and shows that the new unit should be installed to improve over-all operating economy even if the additional capacity were not needed. For systems B and C the negative savings indicate the cost of providing the reserve capacity by means of adding an efficient base-load plant.

Next considered is the installation of a simple cycle 1100 F gas-turbine plant to act purely as a peak-load and stand-by plant. This requires only a few hours' operation a year during the peak when it will generate 1752 megawatt-hours. The existing system drops an equivalent amount of generation at a high incremental heat rate, obtained from the system increment-rate curve, Fig. 7, corresponding to the averages for the 90 and 100-mw loads. Annual operating costs will then decrease as shown in item 17. These will be replaced by the new operating costs incurred by operating the gas-turbine peak load plant. The difference of these costs, item 21, is the annual savings realized, excluding the gas-turbine carrying charges. Then, comparing the peak-load plant to the base-load steam plant, the difference of their annual savings, item 21 — item 11, gives the amount of money available for carrying charges on the peak-load gas-turbine plant.

For system A this works out to give —$50 per kw justifiable investment for the gas turbine. This means that besides being given the gas-turbine plant, the system would also have to be given $50 per kw of capacity to end up in the initial financial position.

System B, however, could afford to pay $73 per kw for the gas turbine or about 56 per cent of the steam-plant cost, which rules out the gas-turbine peak-load application. In system C, which is highly developed with very efficient generating units, $140 per kw can be paid for the gas-turbine plant compared to $130 for the steam plant. In this system the gas-turbine peak-load plant is much better than a base-load steam plant. This brings out the point that peak-load plants can be applied profitably only to systems already operating at high levels of efficiency.

Finally, in Table 2, the application of a regenerative gas turbine is studied as a base-load plant. This is essentially the same problem as that worked out for the isolated plant, except here the plant is operated mostly at full capacity. In other words, the steam plant and gas turbine are directly compared to produce the same annual output. This comparison holds regardless of the remaining system characteristics, that is, whether they are applied to systems A, B, or C. An additional influence is studied here by assuming different levels of operating cost. These are computed with total gas-turbine operating cost equaling 1.4 and 1.3 times the fuel cost.

These two ratios make the gas-turbine labor, repair, and supplies cost 90 and 68 per cent, respectively, of the comparable figures for the steam plant. Again, both of these ratios are conservative reductions in favor of the gas turbine. The comparable justified gas-turbine investments are then $119 and $135 per kw, or 92 and 103 per cent of the steam-plant investment. Compared with 85 per cent from Swiss experience, the gas turbine seems favorable compared with steam in these conditions.

TRANSMISSION-LINE BOOSTER

Instances will be found throughout the United States where

TABLE 2 INSTALLATION OF ADDITIONAL 10,000-Kw UNIT ON EXISTING SYSTEM

Comparison of peak-load and base-load gas turbine with base-load steam plant, system annual load factors = 50 per cent

	System A		System B		System C	
1. New base-load unit, annual output mwhr	78,840		78,840		78,840	
2. Existing system average decrement heat rate	24,800		17,000		12,670	
3. Decrement annual fuel cost at 20¢ per 10⁶ Btu	$391,000		$268,000		$200,000	
4. Decrement repairs, labor, supplies at 30% of fuel	117,000		80,000		60,000	
5. Total annual decrement cost		$508,000		$348,000		$260,000
New 800-psi 950-F Steam Plant, Base Loaded						
6. New station average heat rate, Btu per kwhr	11,600					
7. New station annual fuel cost at 20¢ per 10⁶ Btu	$183,000					
8. New station repairs, labor, supplies at 50% of fuel	91,000					
9. Annual investment charges at 12%	156,000					
10. Total new-station annual generating cost		$430,000		$430,000		$430,000
11. Net annual over-all savings		$ 78,000		−$ 82,000		−$170,000
New 1100-F Peak-Load Gas-Turbine Plant						
12. New station average heat rate, Btu per kwhr	19,000		19,000		19,000	
13. Existing system decrement heat rate, Btu per kwhr	60,000		32,000		24,000	
14. New unit annual output, mwhr	1,752		1,752		1,752	
15. Decrement annual fuel cost at 20¢ per 10⁶ Btu	$21,000		$11,000		$8,400	
16. Decrement repairs, labor, supplies at 30% of fuel	6,000		3,000		2,600	
17. Total annual decrement cost		$27,000		$14,000		$11,000
18. New station annual fuel cost at 20¢ per 10⁶ Btu	$6,700					
19. New station repairs, labor, supplies at 30% of fuel	2,000					
20. New station annual operating cost		$ 8,700		$ 8,700		$ 8,700
21. Net annual savings, excluding new investment charges		$18,300		$ 5,300		$ 2,300
22. Money available for gas-turbine investment charges, referred to steam plant (Item 21)—(Item 11)		−$59,700		$87,300		$172,300
23. Justifiable gas-turbine investment compared to base-load steam plant at 12%, per kw capacity	−$50		$73		$144	
New 1100-F Regenerative Gas-Turbine Plant, Base Loaded						
24. New station average heat rate, Btu per kwhr	13,000					
25. New station annual fuel cost at 20¢ per 10⁶ Btu	$205,000					
26. New station repairs, labor, supplies at 40% of fuel	82,000					
27. Total new plant operating cost (1.4 × fuel cost)		$287,000		$287,000		$287,000
28. Total new plant operating cost (1.3 × fuel cost)		$268,000		$268,000		$268,000
29. Money available for gas-turbine investment charges referred to steam plant (Item 10)—(Item 27)		$143,000				
30. Money available for gas-turbine investment charges referred to steam plant (Item 10)—(Item 28)		$162,000				
31. Justifiable investment based on (29), per kw capacity	$119		$119		$119	
32. Justifiable investment based on (30) per kw capacity	$135		$135		$135	

local load centers at the present time can be fed only through long transmission lines because of lack of local water. Gas turbines serve such a situation admirably since they can do without water and are quick-starting. Generating capacity at the end of the lines aids in bettering voltage regulation and can serve as back-up capacity during transmission-line failure. Such capacity will also be available to the remainder of the system if it suffers a forced outage at some other time than when the local peak load occurs.

Table 3 gives a quick idea of the financial advantages of installing a 10,000-kw transmission line, plus a local peak-load 10,000-kw gas-turbine plant to serve a 20,000-kw peak-load demand having a 50 per cent load factor, as compared to providing a 20,000-kw transmission line. The more costly the transmission line the greater the advantage that accrues to the gas-turbine scheme. Here 30 to 45 per cent more can be spent for a gas turbine than a steam plant whereas gas turbines probably will cost less.

Admittedly, the figures that are given in Tables 2 and 3 are speculative and rough, but they are of an order that is practical. Many related questions which must be answered for any actual system have not been touched. However, power-system designers should give serious consideration to gas turbines. If they do not, many good bets to achieve minimum-cost power will be overlooked.

Industrial Applications

In industrial-power applications, the plant must usually supply process heat as well as mechanical or electrical energy. In selecting the plant the usual economic factors apply, but the effect of the relationship between the two kinds of loads—heat and power—overrides to the extent that it largely determines the nature of the plant selected.

Any comparison of plants for industrial-power supply usually resolves into an examination of their ability to meet a variety of heat and power conditions. This test can be summed up in the answers to three questions: (1) Can the plant's ratio of heat to power be altered readily by design, and to what extent?

TABLE 3 COMPARISON OF 20-Mw TIE-LINE SUPPLY WITH 10-Mw TIE-LINE SUPPLEMENTED BY 10-Mw-PEAK-LOAD GAS TURBINE AT LOCAL LOAD CENTER

1. Local annual energy requirements, 50% load factor, kwhr		87,600,000
2. Local annual peak load, kw		20,000
3. Transmission-line energy losses, percent		10
Supply From Central-Station High-Pressure Steam Over 20-Mw Tieline		
4. Transmission-line investment, dollars per kw	40	60
5. Allocated plant capacity, kw	22,000	22,000
6. Allocated plant investment at $130 per kw	$2,860,000	$2,860,000
7. Tieline investment	$ 800,000	$1,200,000
8. Total investment	$3,660,000	$4,060,000
9. Allocated heat rate, Btu per kwhr	12,800	12,800
10. Annual fuel cost at 20¢ per 10^6 Btu*	$246,000	$246,000
11. Annual total operating cost at 1.5 × fuel cost	$369,000	$369,000
12. Total investment carrying charges at 12%	$439,000	$487,000
13. Total generation cost including transmission	$808,000	$856,000
Supply From 10-Mw Tieline Supplemented by 10-Mw Gas-Turbine Peak Plant		
14. Allocated steam-plant capacity, kw	11,000	11,000
15. Allocated steam-plant investment at $130 per kw	$1,430,000	$1,430,000
16. Tieline investment	$ 400,000	$600,000
17. Total investment excluding gas-turbine plant	$1,830,000	$2,030,000
18. Supply from tieline, kwhr	74,600,000	74,600,000
19. Supply from gas-turbine peak plant, kwhr	13,000,000	13,000,000
20. Allocated steam-plant heat rate, Btu per kwhr	12,800	12,800
21. Gas-turbine plant heat-rate, Btu per kwhr	19,000	19,000
22. Annual steam-plant fuel cost at 20¢ per 10^6 Btu*	$210,000	$210,000
23. Annual gas-turbine plant fuel cost at 20¢ per 10^6 Btu	$ 50,000	$ 50,000
Annual total operating costs:		
24. Steam plant at 1.5 × fuel cost	$315,000	$315,000
25. Gas turbine at 1.4 × fuel cost	$ 70,000	$ 70,000
26. Steam-plant and tieline investment carrying charges	$220,000	$244,000
27. Generation cost excluding gas-turbine carrying charges	$605,000	$629,000
28. Money available for gas-turbine carrying charges	$203,000	$227,000
29. Justified gas-turbine investment, dollars per kw	169	189

* Includes additional generation for 10% tieline energy loss

(2) In an operating plant can the heat-power ratio be regulated readily to meet load fluctuations? (3) At what temperature level or levels is process heat available?

Let us see how two currently popular types of plants measure up to these questions and how the answers have influenced their application. By appropriate combinations of extraction and back-pressure turbines a wide range of heat-power ratios can be obtained with steam plants, and suitable controls are available for readily adjusting the balance between heat and power. Heat in the form of steam can be provided at any level up to boiler conditions of, say, about 1000 F as an upper limit. The steam-turbine plant represents about the maximum in industrial-power versatility, but shows up best where the ratio of heat to power is high.

The Diesel plant produces shaft power at the highest efficiency, but its heat-producing possibilities are limited. Of the fuel input to a conventional engine, not more than 50 to 60 per cent is recoverable as heat even in theory, while in practice the maximum recovery is much less. The heat-power ratio is more or less constant and cannot be altered readily in operation. Furthermore, heat is available at relatively low levels. Jacket-water temperatures rarely exceed 180 F; exhaust temperature runs about 400 to 550 F for 2-cycle engines and 650 to 800 F for 4-cycle engines. Hence Diesel plants find widest use where power requirements are high in relation to heat requirements; in other words, where heat-power ratio is low.

Comparatively little has been done to explore the possibilities of the gas turbine for industrial-power applications, but it seems likely to occupy a place somewhat between the steam-turbine and the Diesel-engine plant. Let us see in a qualitative way why this is so.

EXHAUST-HEAT RECOVERY

The arrangement commonly visualized for industrial power has a waste-heat boiler in place of the regenerator or in parallel with it. A series arrangement has also been suggested. Taking the simpler hookup first, Fig. 8, it can be seen that with a single-shaft plant, output control will be by temperature variation, with gas-flow rate essentially constant. As temperature varies with load, heat available in the exhaust will also vary with load. To this extent the situation closely parallels that encountered in Diesel plants, but with the exception that gas flow per kilowatt-hour is much higher, about 100 lb per kwhr for gas turbines against about 13 lb for Diesels. According to Pfenninger of Brown Boveri, about 12 lb of steam per kwhr can be produced by an arrangement similar to Fig. 8.

The ratio of heat to power of this hookup cannot be altered to any appreciable extent by design, nor is it possible to meet demand variations readily in operation. When power loads are high and steam loads low, the boiler can be by-passed, but little can be done to meet the reverse condition. It might be thought that the turbine could be by-passed or gas extracted from it after partial expansion, as in steam-turbine plants. But the high cost of compression work done on the gas before heating makes this undesirable. The only other solution, equally applicable in Diesel plants, lies in fitting the boiler with auxiliary oil burners to operate when power loads are light and steam loads heavy. Since gas turbines employ very high excess-air ratios, sufficient oxygen will be available in the exhaust to support combustion.

If the waste-heat boiler is in parallel with a regenerator, operation at high power loads and low steam loads is more efficient, Fig. 9. A suitable valve setup divides gas flow between boiler and regenerator in accordance with steam-load variations so the plant always operates under the most favorable conditions. Choice between this hookup and Fig. 8 would depend on the value of the added efficiency at low heat-power ratios compared with the cost of the added equipment.

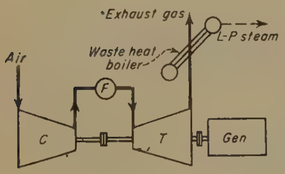

Fig. 8

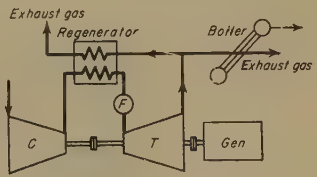

Fig. 9

To improve part-load efficiency on small gas-turbine plants and to permit building plants of large total output without exceeding economical and mechanical limitations in size of rotating parts, 2-shaft designs are used, Fig. 10. This practice allows control by gas-flow variation, with the temperature held essentially constant over a substantial part of the load range. For waste-heat recovery this plant offers the advantage that gas temperature at the waste-heat boiler is at a high level over a great part of the load range. Although not shown, the hookup using a regenerator in parallel applies equally well to 2-shaft designs.

Industrial suitability of gas-turbine plants fitted for exhaust-heat recovery may be summarized as follows: (1) They are less flexible in design and operation than steam-turbine plants and not so well-suited for high heat-power ratios. (2) They are somewhat more flexible than the Diesel plant on both counts. In fact, they seem best suited for intermediate heat-power ratios. According to an analysis by Pfenninger, Brown Boveri, a gas-turbine plant with waste-heat boiler compares with a back-pressure steam-turbine plant producing steam at 85 psig, as shown in Table 4.

TABLE 4 COMPARISON OF GAS-TURBINE AND STEAM-TURBINE PLANT PERFORMANCE

Steam consumption for heating, lb per kwhr........	0	4	8	12
Total thermal efficiency of plant, %:				
a. Gas turbine with waste-heat boiler.........	25	56	63	70
b. Backpressure steam-turbine plant...........	25	50	62	74

HIGH-PRESSURE STEAM

Most thinking about industrial-power gas turbines has dea with heat recovery at the low end of the cycle. What are perha more interesting possibilities lie at the high end. Fig. 11 show production of high-pressure steam at the combustion chambe With forced-circulation "series" design, superheated steam virtually any pressure and temperature could be generate It then becomes possible to obtain any desired heat-power rati from almost all power and no heat (the conventional gas-turbi plant) to all heat and little or no power (the Velox boiler Absorption of heat at the combustion chamber reduces ga temperature at the turbine inlet, an operation normally done b excess air. To protect heat-transfer surfaces, steam generatio could not be allowed to drop below a certain minimum flow.

The principal problem in this arrangement lies in controllin steam output to meet variations in demand for power and steam While it is possible to visualize by-pass arrangements that woul either alter the effective heating surface or the gas flow over fixed amount of surface, such schemes appear unnecessarily complex. For simplicity, it might be better to generate steam in accordance with whatever gas flow is required for shaft power, and find some way to utilize excess steam in the cycle itself.

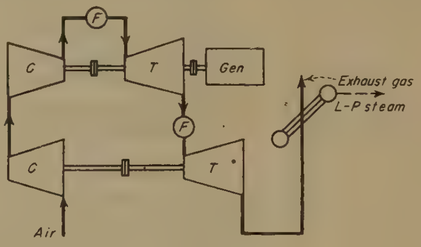

Fig. 10

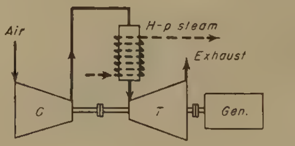

Fig. 11

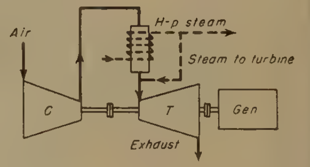

Fig. 12

In Fig. 12 part of the steam produced is diverted back into the gas circuit and the turbine becomes a combined gas-vapor machine. With normal expansion ratios this should involve no moisture problem at the exhaust; the added working fluid increases the shaft output. If steam is generated at a pressure above turbine throttle pressure, as is likely, an arrangement like that in Fig. 13 could be used. Here the excess steam expands first through a steam turbine, say, an impulse wheel, which exhausts to the gas-vapor turbine at its normal inlet pressure. Governing should be no more complex than that of the extraction-condensing and back-pressure steam turbines now widely used.

Generation of steam at the high end of the cycle might well be combined with recovery of heat at the low end, leading to hookups like that in Fig. 14 in which an economizer heats feedwater for the steam-generating surface at the combustion chamber.

COMBINED AIR-STEAM PLANT

Another interesting steam- and gas-turbine combination has been suggested by W. Karrer, Oerlikon Works, Zurich. He points out that steam boiler plants designed for exclusive supply of heat can be converted to highly economical plants for heat and power by raising boiler pressure and temperature, and expanding he steam in a back-pressure turbine. He then shows that the haft power can be about doubled by addition of an air turbine nd its compressor, and that the increased fuel input required is avorably utilized.

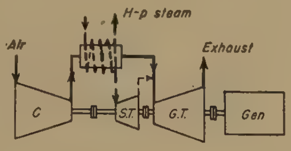

FIG. 13

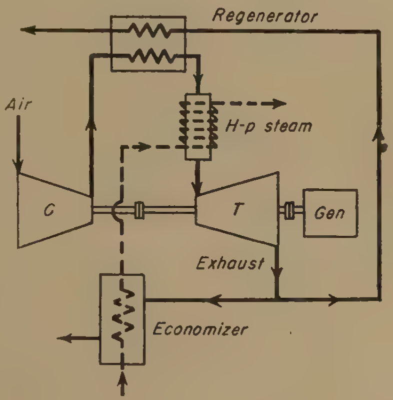

FIG. 14

As shown in Fig. 15, a fuel-fired boiler supplies steam to a back-pressure turbine. Flue gas from the boiler first heats air or the turbine and then feedwater for the boiler. The air-urbine circuit starts with a compressor taking in fresh air. After ir pressure has been raised, air flows through a regenerator, picking up heat from the turbine exhaust, and then flows through he flue-gas air heater. Heated pressure air then expands through he turbine, and flows through the regenerator to the boiler where it serves as combustion air. Turbine output is sufficient to drive the compressor and produce electrical energy to add to that generated by the back-pressure turbine.

It is realized that these various gas-turbine industrial-plant hookups have been put forward without the exhaustive analysis required to establish fully their practical and economic feasibility. It is believed, however, that they indicate worth-while possibilities for the gas turbine in this field, and that they should be the subject of further study by gas-turbine engineers and power-plant designers.

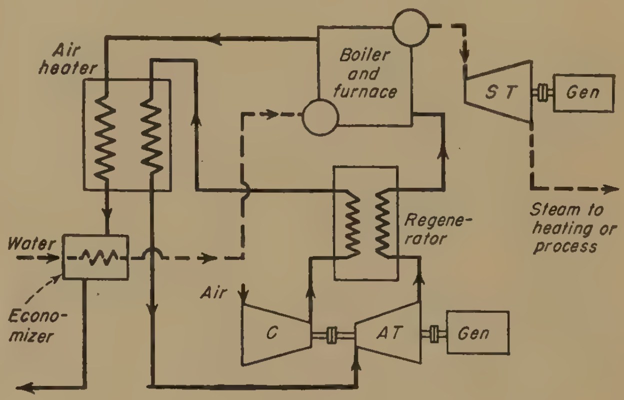

FIG. 15

SPECIAL APPLICATIONS

No discussion of the use of gas turbines in industry can afford to overlook a number of specialized applications such as the Houdry process and blast-furnace blowing. These have been well-covered in the literature, however, and it would be superfluous to consider them in any detail here. In view of the tendency to speed reaction time of chemical processes by devices such as supercharging, it is likely that many other attractive possibilities for the gas turbine as a compressor will develop.

CONCLUSION

The foregoing makes it clear that in the gas turbine we have a prime mover of outstanding versatility that is already demonstrated by applications in virtually all fields, but not yet fully explored in many. It seems reasonable to conclude that within the field of stationary power there are many applications to which the gas turbine is inherently suited if its many interesting characteristics are fully exploited. Furthermore, many of these possibilities can be realized with gas turbines of such conservative design that their production today on a fully commercial basis seems entirely justified. As technological advances remove present limitations on efficiency and fuel range, the field of application will widen.

We should remember, however, that, historically, no prime mover ever succeeds in fully supplanting others. Each tends to find its special place in a world that finds ever larger and more far-reaching needs for stationary and propulsive power.

Transmission Systems for Marine Propulsion Gas-Turbine Power Plants

By W. E. HAMMOND,[1] WELLSVILLE, N. Y.

The author discusses various transmission systems now available which might be used in connecting a gas-turbine power plant to the propeller of a merchant ship. The major problems to be met by any transmission system are those relating to reversibility and maneuverability. It is concluded that alternating-current electric drive, mechanical reversing gears, and mechanical reduction gear with the controllable and reversible pitch propeller offer acceptable solutions to the problems.

SINCE the characteristics of turbine-type machinery provide optimum efficiency at high rotative speeds while the characteristics of marine propellers require low rotative speeds for optimum efficiency, it is necessary to utilize a transmission system which permits both objectives to be realized for a successful marine application. Various types of transmission systems have been developed in connection with the application of the steam turbine to marine propulsion that are now commonplace. These systems have experienced long periods of development and have encountered many difficulties in attaining their present position.

In the case of the gas-turbine power plant it would appear desirable to review the present state of the art before outlining possible solutions to the particular problems introduced by the gas turbine. The gas-turbine power plant today is in an analogous position to the steam turbine before the start of the first world war. The particular problem to be faced in applying this prime mover to a ship lies with reversibility and maneuverability. The path followed in the solution of this problem for the steam turbine is well known. Therefore it is well to consider now the various possibilities that are available as a general solution to the problem. In considering this question, it is essential that the ultimate benefit be evaluated in selecting a course of action rather than an immediate advantage. For the real advantages accruing from the introduction of the gas-turbine power plant can be completely canceled by an unfortunate choice of transmission system.

It is the purpose of this paper to discuss briefly the various transmission systems available today in order to determine which might offer the most attractive prospects in connecting the gas turbine to the marine propeller for merchant vessels. It is not intended that a solution be established for every gas-turbine power-plant application but rather that a general solution be sought which has the widest application. It is recognized that certain special applications will involve special circumstances thus establishing a new evaluation problem. It is believed that these cases can be handled only on an individual basis.

REQUIREMENTS OF A MARINE TRANSMISSION SYSTEM

A marine transmission system must be capable of reducing the revolutions from those required by the prime mover to those required by the propeller. It must be reliable and simple in operation within the capabilities of the crews that are available. The transmission losses should be a minimum. The first cost and maintenance cost should be commensurate with those of the prime mover so that the advantages of the prime mover will not be nullified by the transmission system. The weight and space required should also be commensurate with that required of the prime movers for the reason just given. If the torque characteristics of the prime mover do not coincide with the requirements of the propeller for all conditions of operation, then the transmission system must be capable of adjustment to meet these requirements. If the prime mover is not reversible, then the transmission must provide this feature. Should it be possible accidentally to disconnect the propeller from the prime mover while under load, it must be possible to re-establish the connection immediately. If this cannot be accomplished, the consequences can be extremely serious and result in totally wrecked machinery. It is preferable that the transmission system selected for merchant ships have a wide application to reduce development cost, simplify manning problems, and reduce maintenance.

There are available today many arrangements of marine transmission systems in successful operation with steam turbines which may be applied to the gas turbine. However, there is one important difference in the two prime movers, i.e., the steam turbine as it is known today is reversible and the gas turbine is not. True, many suggestions and proposals have been made to provide a reversible gas turbine, but to date such a machine has not been developed. In evaluating this factor, it should be apparent from the development of the reversible steam turbine that a number of difficult problems must be solved and that possibly many of these will not be foreseen adequately.

In any event, the following transmission systems at present available might be considered as possible solutions to the problem:

1 Electric drive, direct current.
2 Electric drive, alternating current.
3 Mechanical geared drive with controllable-pitch propeller.
4 Mechanical geared drive containing reversing features.
5 Mechanical geared drive with reversing gas turbine.

The foregoing list is not intended to be all-inclusive.

It would be well to consider the various aspects of each transmission system as they are now known in order to evaluate the possibilities of each for use with the gas-turbine power plant.

ELECTRIC DRIVE—DIRECT CURRENT

The direct-current drive consists of one or more direct-current generators connected through control gear to a direct-current motor. The generator is generally of the separately excited type to provide variable-voltage control of the motor from standstill to rated speed. The motor commonly is of the compound type to provide high torque for stopping and reversing the vessel. The control gear consists of a lever for operating the forward, reverse, and dynamic braking contactors and to operate the field application and generator excitation; another lever is provided to operate the prime-mover governor; and a third lever for emergency stop. The control for the direct-current drive provides two means of propeller-speed control: (*a*) generator excitation providing

---

[1] Research Department, The Air Preheater Corporation.

Contributed by the Gas Turbine Power Division and presented at the Annual Meeting, Atlantic City, N. J., December 1–5, 1947, of THE AMERICAN SOCIETY OF MECHANICAL ENGINEERS.

NOTE: Statements and opinions advanced in papers are to be understood as individual expressions of their authors and not those of the Society. Paper No. 47—A-69.

variable voltage to the propulsion motor when the prime mover is operating without speed change; and (*b*) governor control of the prime mover which controls the system voltage by speed without a change of generator excitation. Another means of speed control may also be provided by motor field weakening. The control also provides an indication of motor horsepower, voltage, current, and motor and generator speed and temperature, Fig. 1.

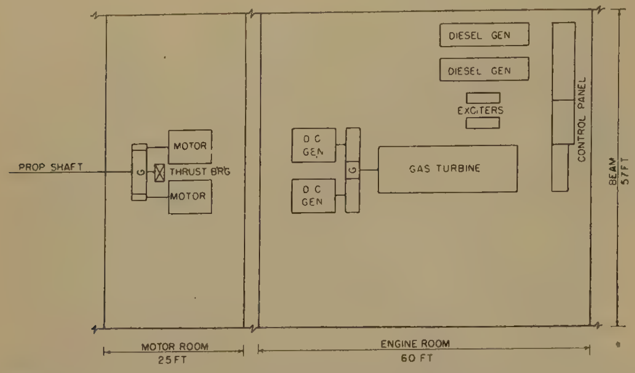

Fig. 1 Block Machinery Arrangement of Engine Space and Motor Space for a Geared Direct-Current System to Approximate Scale for Midship Installation in a Vessel Similar to a C2, Victory, or Liberty Ship

This particular transmission system is in successful use in moderate numbers at the present time. It has been utilized principally with Diesel engines to provide rapid reversals (approximately 15 sec from full ahead revolutions to $^2/_3$ rated revolutions astern) and also to permit adjustments in propeller speed so that the torque requirements are within the capabilities of the engine.

The application of this drive to the gas-turbine power plant does not introduce any new problems of a serious nature provided the turbine is geared to the generator. If this is not done then either the turbine speed must be reduced or else development must be undertaken to permit direct-current generation to operate at 4000 rpm. While there may be some engineers who are optimistic about the possibilities of so designing a generator, there are some serious problems connected with this development. In any event, there is scant background at present on which to base a decision in favor of this development.

In regard to power range, the present design of this equipment is adequate for the range in shaft horsepower presently being considered for the gas-turbine power plant. However, there appears to be some reason to question the application of this transmission system to large horsepowers for single units. Since a single unit is restricted to low-voltage design owing to commutation difficulties, its application to large powers results in large costly equipment.

This system is extremely flexible and will lend itself to either series or parallel connection of multiple units so that relatively large horsepowers might be accommodated by existing gas-turbine designs. However, the series connection is preferable, since it permits relatively high voltage to be used and avoids the complication of paralleling. Furthermore, it will function equally as well with any of the gas-turbine arrangements whether a separate power turbine is used or not since the torque requirement of the propeller may be adjusted to be within that of the prime mover.

In regard to the installation of this transmission system, it will be noted from Table 1 that it does not compare very favorably with other systems in regard to weight and space, and, in fact, it reduces the advantages of the gas turbine with respect to these items. Further, the efficiency of this drive is about the lowest of all systems considered, as will be noted from Table 1.

The first cost of this system is considerably higher than that o other drives which, coupled with its low efficiency, further handicaps the gains to be realized from the gas turbine. In addition the maintenance of direct-current machinery will exceed that fo the mechanical drives or the alternating-current systems.

The operational features of this transmission system are acceptable in that the controls are relatively simple and reversing is direct and positive. While there is always the possibility of disconnecting the driven unit from the prime mover, it is not serious since contact may be re-established readily if done immediately Infinite speed control is readily obtained, and it is possible to adjust the torque requirements of the propeller to remain within the capabilities of the prime mover. Further, this system can be used with pilothouse control if desired.

Electric Drive—Alternating Current

Inasmuch as the induction alternating-current drive has been supplanted by synchronous alternating-current drive, the discussion will be limited to this latter type.

The synchronous electric drive is essentially a constant-ratio speed-reducing transmission as the output speed for continuous operation is always a constant ratio of the input speed. Consequently, the synchronous electric drive in itself does not provide speed or power control and is dependent upon the speed control of the prime mover to vary the speed of the propeller. The synchronous electric drive does provide means of coupling, reversing, and vibration isolation independent of the direction of rotation of the prime mover. An additional feature of the synchronous drive is its ability to provide electric power for auxiliary and port applications.

The synchronous electric drive consists of one or more synchronous alternating-current generators connected through control gear to a synchronous alternating-current motor. The generator is provided with special field coils and exciter to permit field forcing of the generator at subnormal frequency during induction operation of the synchronous motor while starting and reversing the propeller. The salient-pole-type synchronous motor is provided with heavy copper squirrel-cage windings in the pole faces to permit short-time operation as an induction motor during propeller-shaft starting, stopping, and reversing. The control gear consists of a starting lever, governor-control lever, and emergency-stop lever. The starting lever operates the forward and reverse electrical phase contactors, the generator field-forcing contacts, and dynamic braking when provided. The governor control lever controls the speed of the propeller through the governor in the prime mover and operates the generator and motor field rheostat for power-factor control. The emergency-stop lever operates to reduce quickly the speed of the prime mover. Supplementary control equipment to indicate motor horsepower, speed, frequency, current, voltage, and to determine the temperature of the generator and motor is provided, Fig. 2.

This transmission system has experienced wide service in the marine field. Many merchant and naval vessels at present in service are so equipped. Disregarding applications made during the war for production reasons, this transmission is generally applied for the purpose of obtaining high economy at low power operation and/or for application in which it is desired to utilize the main machinery for an auxiliary purpose such as operating pumps on a tanker or dredge.

The application of this type of transmission to the gas-turbine power plant should not prove difficult for those gas-turbine arrangements whose torque characteristics approximate the steam turbine. However, for some arrangements of gas-turbine power plants, the range of torque with revolutions is rather narrow and as a result, some difficulty might be experienced in matching the two characteristics. Accordingly, the application of this trans-

TABLE 1 COMPARISON OF EFFICIENCY, FIRST COST, SPACE, AND WEIGHT REQUIREMENTS FOR VARIOUS TRANSMISSION SYSTEMS

	Economic Cost	Shafting & Propeller	Total Cost	Fixed Charges/yr. 10%	F. P. #/SHP/Hr.	F. O. Cost/Yr.	Total Yearly Cost
(1) 3000 SHP							
AC, Mfgr A	153,400	13,700	167,100	16,710	.498	75,650	92,360
AC, " B	137,000	13,700	150,700	15,070	.504	76,500	91,570
DC, " A	195,000	13,700	208,900	20,890	.532	80,900	101,790
DC, " B	267,500	13,700	281,200	28,120	.531	80,800	108,900
Rev. Gear Air Flex (K = 175)							
(K = 125)	126,000	13,700	139,700	13,970	.469	71,300	85,270
Red. Gear C.P.P. (K = 75)	116,000	86,000	202,000	20,200	.459	69,800	90,000
Red. Gear only (K = 75) (for reversing turbine)	116,000	13,700	129,700	12,970	.459	69,800	82,770
Red. Gear C.P.P. (K = 175)							
(K = 125)	73,500	86,000	159,500	15,950	.459	69,800	85,700
(2) 6000 SHP							
AC, Mfgr. A	223,500	17,400	240,900	24,090	.486	147,800	171,890
AC, " B	213,000	17,400	230,400	23,040	.495	150,500	173,540
DC, " A	319,600	17,400	337,000	33,700	.531	161,500	195,200
DC, " B	395,500	17,400	415,900	41,690	.528	160,600	202,190
Air Flex.	225,000	17,400	242,400	24,240	.469	142,800	167,040
Red. Gear C.P.P. (K = 75)	192,000	117,000	309,000	30,900	.459	139,600	170,500
Red. Gear (K = 75) (for reversing turbine)	192,000	17,400	209,400	20,940	.459	139,600	160,540
Red. Gear - C.P.P. (K = 175)							
(K = 125)	124,000	117,000	241,000	24,100	.459	139,600	163,700
(3) 9000 SHP							
AC, Mfgr. A	293,000	21,300	314,300	31,430	.478	218,000	249,430
AC, " B	272,500	21,300	293,800	29,380	.484	221,000	250,380
DC, " A	449,100	21,300	470,400	47,040	.529	242,000	290,040
DC, " B	557,500	21,300	528,800	57,880	.526	240,000	297,880
Air Flex	—	—	—	—	—	—	—
Red. Gear C.P.P.	240,000	159,000	399,000	39,900	.459	209,500	249,400
Reduction Gear Only (for reversing turbine)	240,000	21,300	261,300	26,160	.459	209,500	235,630
Red. Gear - C.P.P.	167,000	159,000	316,000	31,600	.459	209,500	241,100

NOTE: All drives include propellers, shafting, thrust bearings, and gears where necessary. The direct-current drive proposed by manufacturer (A) consists of geared generators, and geared motors connected in a series loop using variable-voltage means of speed control. For the 3000-shp proposal, there are two generators rated at 600 volts each and 750 rpm, connected to the turbine through gears; the two motors, also rated at 600 volts each and 750 rpm, are geared to the 90-rpm propeller shaft. The 6000 and 9000-shp installations differ by having four 600-rpm generators and four 600-rpm motors. The direct-current drive proposed by manufacturer (B) consists of a geared double-armature generator and direct-connected double-armature motor, connected in a series loop, using variable-voltage speed control. All armatures are rated at 600 volts each. The 3000-shp installation utilizes 900-rpm generators, whereas the 6000 and 9000-shp systems use 600-rpm generators. All motors operate at 90 rpm.

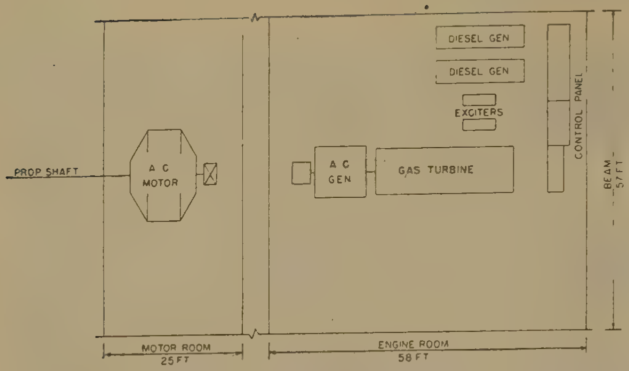

Fig. 2 Block-Machinery Arrangement of a Direct-Connected Alternating-Current System

(This system has the generator direct-connected to the prime mover and the propulsion motor direct-connected to the propeller.)

mission must depend upon the type of gas-turbine power plant under consideration.

Regarding the power range of this equipment, nothing need be feared, since the present practice includes units well in excess of any size likely to be considered for the gas-turbine power plant. Furthermore, this transmission adequately lends itself to the use of multidrive units. In other words, several small units may be coupled electrically to a given motor in order to achieve the desired output. However, it must be remembered that multidrive units require parallel operation, which adds to control complications. In this respect it is not as simple as a series-connected multidrive direct-current system. The alternating-current system, when used with multiple generators, does not permit the full power of the connected generators to be used when one or more generators are taken off the line.

There may be a limitation in the use of this transmission system with some arrangements of gas-turbine power plants. In particular, for those arrangements not containing a separate turbine for power output, it is practically impossible to meet the minimum speed and torque requirement (approximately 150 per cent torque at 25 per cent speed) for maneuvering, and difficulty may be experienced further in meeting the torque requirements of the propeller, particularly under foul bottom conditions with high inlet temperatures, Fig. 3.

In so far as arrangement is concerned, this transmission does not impose any special difficulties. However, the control equipment required is generally rather large and occupies considerable space. The weight of this transmission is appreciably less than direct-current equipment and compares favorably with the mechanical drives, Table 1.

Considering efficiency, this transmission system has an advantage over the direct-current system, but it is still below that obtained with mechanical drive, Table 1. This loss of efficiency in the transmission system obviously reduces the advantages of the gas-turbine application.

The first cost of this system is lower than the mechanical drive with a controllable-pitch propeller, but, when coupled with a lower operating efficiency, its operating cost, including fixed charges, is about the same as the mechanical drive.

The operational features of the alternating-current transmission system involving synchronous motors need to be considered carefully. This type is rather slow in maneuvering (60 to 90 sec from full ahead revolutions to $^2/_3$ rated astern revolutions), and particular care must be taken in determining the torque characteristics of the propeller for the particular ship under consideration. Figs. 4 and 5 indicate the variation between the predicted value and the measured value of the torque required to reverse two particular vessels. Comparison of these curves also gives some idea of the variation in characteristics between vess Further, speed control below 20 per cent is generally not possi with this system. Another consideration which must be evalu ted is the possibility of accidentally disconnecting the motor fr the generator while under load. Of course the governor shou provide for this eventuality but experience has demonstrated th such things do happen in spite of the automatic safeguards. It then impossible to reconnect the motor to the line under the circumstances so that the power plant would be destroyed. Th condition occurred a number of times during the recent war, a while the source of the difficulties was located, it is too serious possibility to be ignored. Another factor which must be evalu ted in considering this system is the maintenance of the contr It is extremely difficult to obtain ship crews which are qualified i the operation and maintenance of this equipment so that rath high control maintenance may be expected.

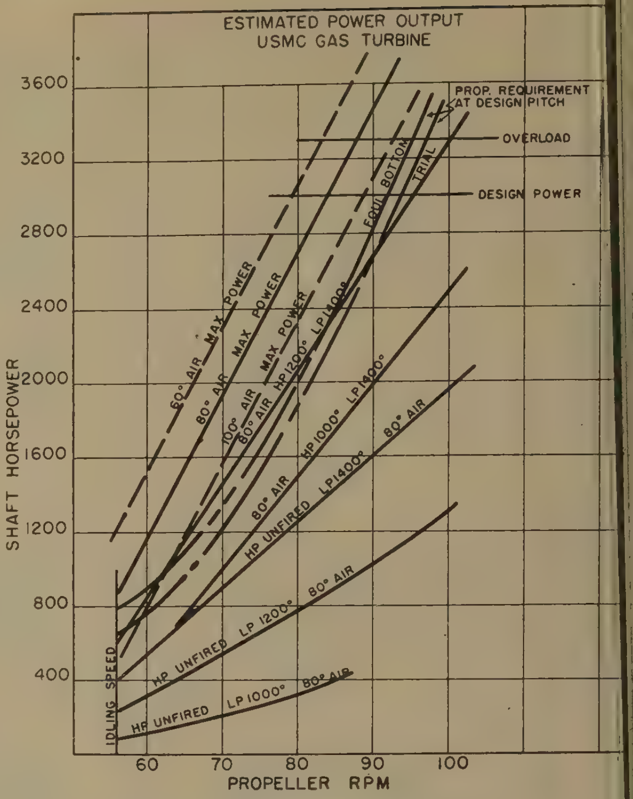

Fig. 3 Horsepower-Speed Relationship of Gas-Turbine O put Versus Propeller Requirements

Mechanical Gears With a Controllable and Reversib Pitch Propeller

This transmission system consists of the usual marine mechan cal reduction gear, at present used with steam turbines, couple with a controllable and reversible pitch propeller. The primar function of the propeller is to reverse the vessel although the co trollable-pitch feature will also provide infinite speed variatio from zero to maximum revolutions ahead and astern. This pe mits adjustment of the torque requirements of the propeller t match the characteristic provided by the machinery for any an all conditions that are encountered in service.

One type of controllable and reversible pitch propeller rotate the blades through a crank arrangement in the hub. The crank are operated through a piston rod and crosshead by a servomotor lo cated in the line shaft. Pressure is supplied to the servomoto through a distributor valve by a pressure tank which is charge

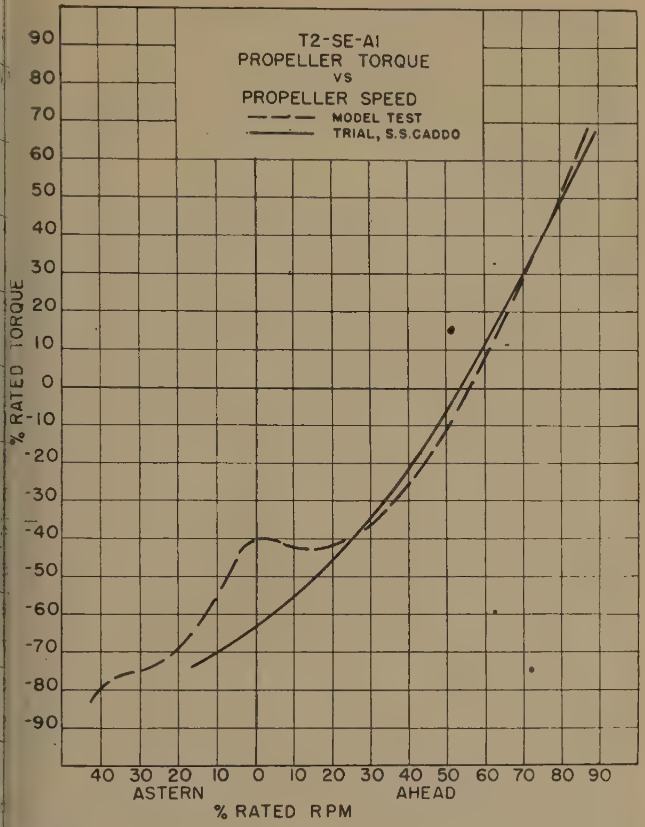

IG. 4 TORQUE-RPM CURVES DURING REVERSING FOR T2 SINGLE CREW TANKERS HAVING TURBINE-ELECTRIC ALTERNATING-CURRENT DRIVE

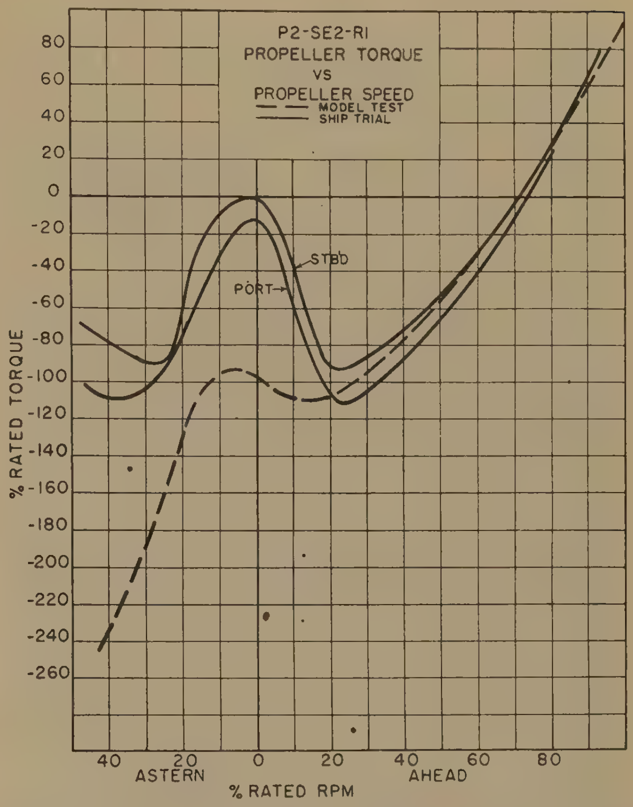

FIG. 5 TORQUE-RPM CURVES DURING REVERSING FOR P2 TWIN-SCREW PASSENGER VESSELS HAVING TURBINE-ELECTRIC ALTERNATING-CURRENT DRIVE

y pumps automatically controlled. The pumps are capable of perating the system if the pressure tank is empty. Fig. 6 shows n installation on the motorship *Single Hitch.*

This system is operated by a combination of pneumatic, hyraulic, and direct acting forces. From the engine room the conrol lever operates an oil control valve by means of compressed ir. This valve determines the position of a servomotor piston ocated within a section of hollow line shafting by directing lowressure oil to one or the other of its sides. The piston is conected to the propeller blades, so that any movement of the piston s transmitted to the blades, changing their pitch angle. In this ay the propeller pitch is regulated quickly and accurately from the control station in the engine room The pneumatic control system is operated by compressed air of 100 psi furnished by the ship's service compressor. If a breakdown should occur, the servomotor piston can be actuated by using a manual control valve.

The hydraulic operating mechanism is entirely in the shaft alley. The aft section of line shafting is hollow, and includes a servomotor built into its forward end. It is coupled to a hollow tail shaft, which is connected to the propeller hub. Within these hollow shafts, and extending the whole length, is a piston rod which is free to move longitudinally. The rod is connected at the forward end to the servomotor piston, and at the aft end to a crosshead in the propeller hub.

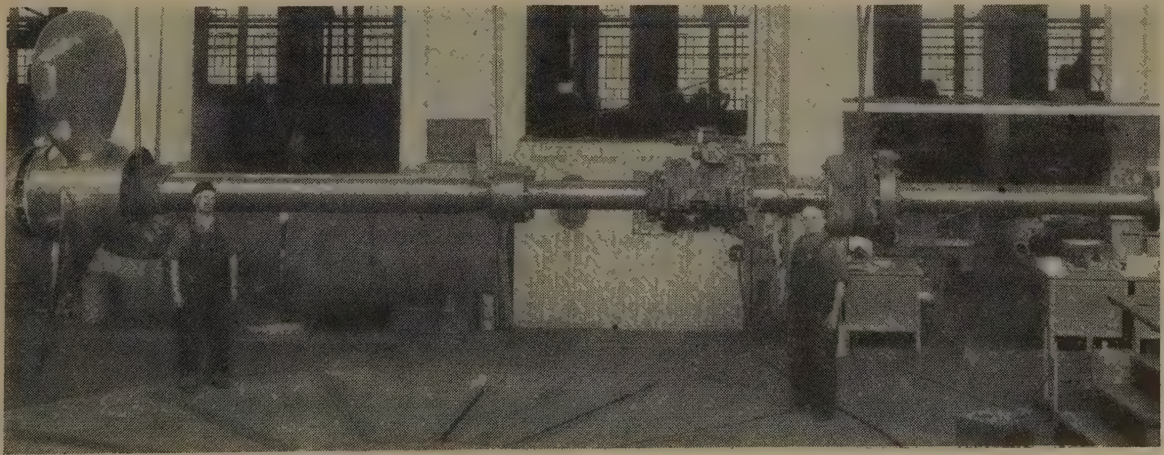

FIG. 6 SHAFTING ARRANGEMENT ON THE MOTORSHIP "SINGLE HITCH"

Low-pressure oil is supplied by a system consisting of a pressure tank and two motor-driven oil pumps. Oil from the tank is piped to a distributor fitted around the hollow line shaft. From there it passes through passages in the shaft to either side of the servomotor piston. Oil pressure in the tank is maintained between 300 to 330 psi by automatic loading valves. This insures sufficient pressure available at the servomotor to meet all demands of the propeller. If failure should develop in the hydraulic pressure system, the servomotor piston can be moved by a hand pump, and then mechanically locked into position.

The propeller consists of three detachable blades keyed to cranks which are linked to the crosshead in the hub. Sealing rings are used to prevent in-leakage of sea water. To further insure water from entering the hub, and to provide lubrication for the blade spindle bearings, the hub is kept full of lubricating oil. The oil is led from a gravity tank to the oil distributor, through ports in the shaft to the space between the shaft bore and the piston rod. The oil head is always greater than the water head.

While the controllable and reversible pitch propeller is a comparative newcomer to the marine field in this country, there is ample background upon which its performance and reliability may be judged. A number of installations have been made in Europe of which Escher Wyss has made approximately 35 and Kamewa about 70. Further, a large number of Kaplan type water turbines, which for all practical purposes duplicate the function of the controllable-pitch propeller, have been used both in this country and abroad. In fact, 156 units have been installed here with wheel diameters ranging up to 24 ft 4 in. diam for 55,000 shp. In addition, there have been 6 large marine propeller installations made in this country in addition to about 1100 landing-boat applications.

One of the marine installations in this country was made by the U. S. Maritime Commission in the motorship *Single Hitch.* The primary purpose of this installation was to obtain firsthand experience to guide the application of this propeller to the gas-turbine power-plant installations that the Commission was considering. The results were very satisfactory and confirmed the expectations that the application of this propeller was feasible. It might be well to mention that the motorship *Single Hitch* is a C1-M-AV1 design powered by a 1700-shp Diesel engine operating at 180 rpm. The propeller is three-bladed with a diameter of 11 ft. The pitch is variable from 7.9 ft astern to 8.8 ft ahead with normal ahead pitch at 6.75 feet.

While the largest marine propeller of the controllable and reversible design that has been built to date is 14 ft 9 in. diam and 3500 hp, there is every reason to believe that in so far as merchant-ship designs are concerned, the limitation on diameter and power will be the same as are experienced with fixed-pitch propellers. The basis for this statement lies in the fact that the Kaplan turbines have been in successful operation in much larger sizes than would be encountered in marine propeller design. In addition, Kamewa has a 17-ft-diam controllable and reversible-pitch propeller for 7500 shp under construction, and S. Morgan Smith has a 17-ft-diam controllable and reversible-pitch propeller for 3000 shp also under construction.

However, there is one precaution that should be observed in the application of the controllable and reversible propeller. In view of the fact that a major component of the total force acting on the blades is centrifugal force, it is important to weigh carefully the revolutions when large diameters are considered.

Examination of the design and installation of the controllable and reversible pitch propeller in the *Single Hitch* will indicate that there were no design problems excepting those immediately associated with the propeller and its mechanisms. Further, it will be observed that there was considerable design precedent for all aspects of the propeller design. If the shaft gland in the distri tor which seals against the pressure of the servomotor system considered it will be found that this gland has been used in Kaplan turbine practice for a number of years with satisfact results. The application of this gland to the installation abo the vessel introduces nothing basically different from its appli tion to the Kaplan turbine.

Consider the servomotor and its supply system. The syst consists of a pressure tank charged by a continuously runni pump with the appropriate valves responding to tank pressure direct the pump discharge to the tank or the sump as the occasi requires. This system is standard for a number of applicatio used on board ship or ashore. Its application to the controlla and reversible pitch propeller did not involve any particul problems. All of the foregoing has been demonstrated in the i stallation aboard the *Single Hitch.* Of course it is expected any initial installation that certain difficulties will be experience Further, it is almost a certainty that the difficulties encou ered will concern that portion of the design which is consider commonplace. In this respect, the motorship *Single Hit* was no exception, and certain minor difficulties were experience when the system was first put into service.

The first mishap concerned the setting of the tank pressu valve. The valve permitted the tank pressure to reach too low value before recharging. This was easily remedied. The ne difficulty resulted from a failure of the intercooling coil on th ship air compressor (which was not a part of the propeller installa tion). This flooded the pneumatic control system and interfere with the propeller response. It also was easily detected and remedied. The final incident that occurred concerned operatio with the propeller mechanically locked in position. The firs operator of the vessel ordered the propeller to be locked in a fixe position and in so doing did not provide adequate lubricatio While this resulted in damage to the distributor packing, no fu ther packing difficulties have been experienced.

All these mishaps occurred shortly after the vessel was place in service, and all were easily remedied. There have been n further difficulties with this installation which has now had 1 months of service. During a routine dry-docking period the propeller has been inspected and found to be in excellent condition Furthermore, there is every assurance from the present performance that the propeller will give satisfactory service and tha the maintenance will be minor. It might be well at this point to discuss the criticism which is made concerning the unattractiveness of this propeller due to the "complicated mechanism" in the hub which cannot be inspected or maintained without dry-docking the vessel.

Actually, the hub mechanism can hardly be classed as complicated since it consists of nothing more than a crank arrangement for rotating the blades. Further, the importance of ready inspection rests with the necessity for the inspection. To date there has not been any cause in the installation of the *Single Hitch* to require inspection of the hub. In fact, early Swedish experience indicates that in severe ice conditions when damage occurs to the hub gear, the blades, propeller shaft, and hull were also badly deformed. On a more recent Swedish design the propeller grounded at full speed resulting in serious blade and shaft damage but with no damage to the hub gear.

While the use of this transmission system involving mechanical gears and a controllable and reversible propeller does not lend itself to the use of large numbers of multiple-drive units, it can be used with multiple-drive units not exceeding four in number for each shaft. Furthermore, this system of transmission is suitable for any gas-turbine arrangement proposed so far, i.e., whether a separate power turbine is provided or whether the power turbine also furnishes the compressor power.

In regard to arrangement, this system is practically identical with the mechanical geared system used with the steam turbine. The controllable and reversible propeller and its shafting are heavier, however, than a fixed-pitch propeller and its shafting so that in the higher horsepower ranges an increase in weight must be accepted.

In considering the efficiency of this system, there is no need to review the efficiency of mechanical reduction gears which are well established. Therefore the only element about which any controversy might originate is the controllable and reversible pitch propeller. Considerable comment has already been made indicating that the controllable and reversible pitch propeller would have an efficiency appreciably below that of a conventional fixed-pitch propeller. In fact, some writers have indicated that this reduction in efficiency might approach 6 per cent. It is possible that those making these claims were considering the open water efficiency only which does decrease with increase in hub size. However, the propulsive coefficient, which, after all, is the only important factor, does not decrease with increases in hub size within reasonable limits on single-screw vessels. It cannot yet be determined whether this will also apply to twin-screw installations. However, there is reason to believe that the large hub might reduce the efficiency on twin-screw applications but not to a serious extent. Of course it is important that adequate fairing of the stern, propeller hub, fairwater, and rudder be provided. A propeller was designed and tested by the Maritime Commission in 1942, with two different hubs, one being 3.97 ft (hub ratio 0.183) and the other 5.67 ft in diameter (hub ratio 0.261). The propulsive efficiency was ostensibly the same in both cases, although the large hub showed slightly greater efficiency (see Fig. 7). Further, the controllable and reversible pitch propeller on the *Single Hitch* had a hub diameter of 3 ft (hub ratio 0.273), as compared to a diameter 2.17 ft (hub ratio 0.197) for the fixed-pitch propellers used in the other vessels of this design. Model tests of this vessel indicated that the controllable and reversible pitch propeller was slightly more efficient at the design condition than the fixed-pitch

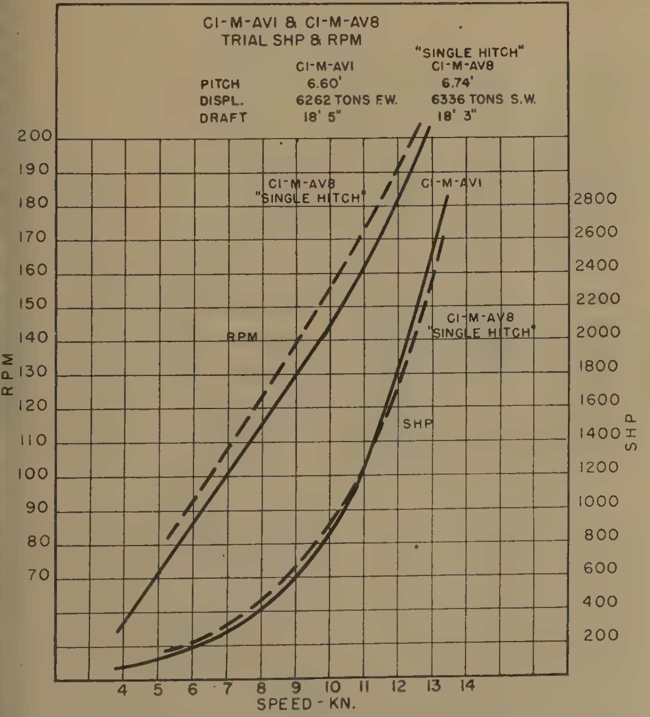

Fig. 8 Comparison of Controllable-Pitch Propeller and Fixed-Pitch Propeller Installed on Similar Ships

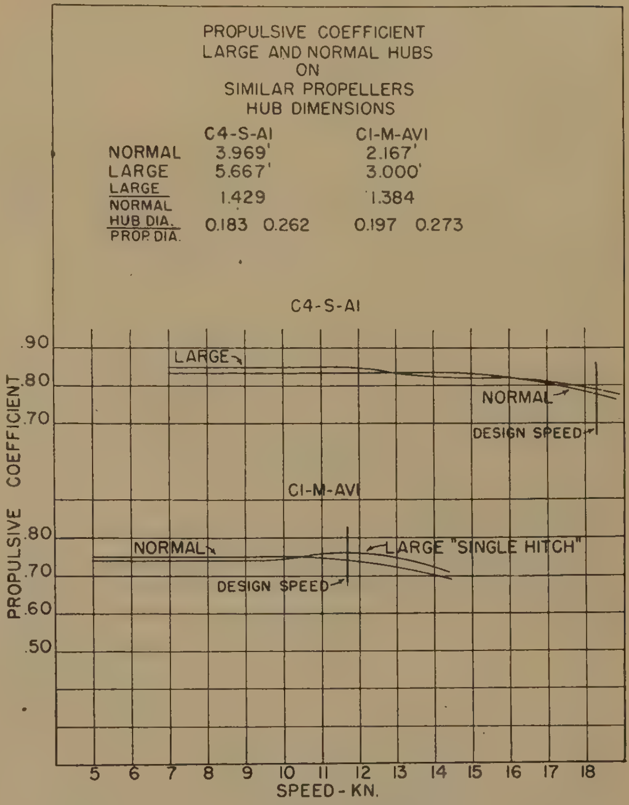

Fig. 7 Some Results of Self-Propelled Model Tests Illustrating Effect of Hub Size on Propulsive Efficiency

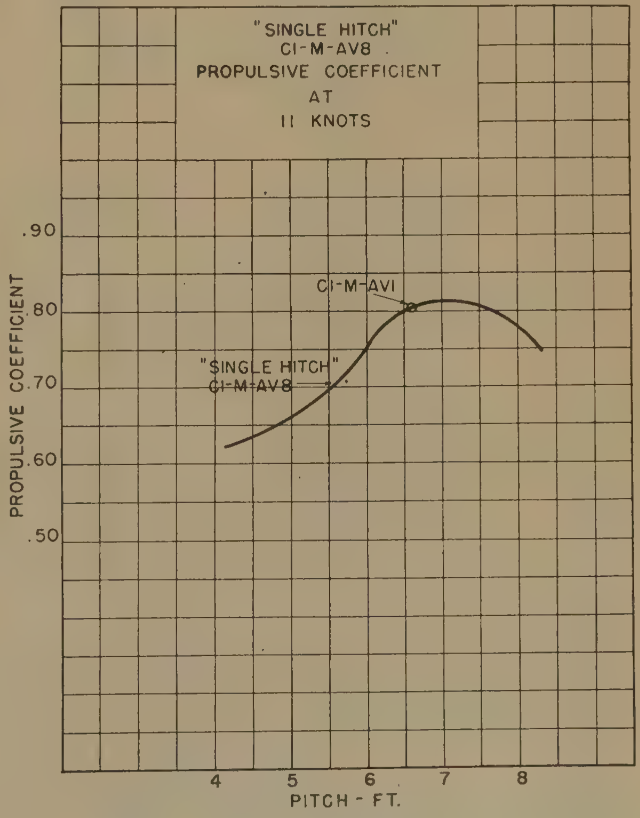

Fig. 9 Variation in Propulsive Efficiency of Controllable-Pitch Propeller on the Motorship "Single Hitch" for Design Sea Speed at Various Pitch Settings

propeller (see Fig. 7). On trials it will be noted that it was possible to make a greater speed for the same shaft horsepower with the controllable and reversible-pitch propeller than with the fixed-pitch propeller (see Figs. 8 and 9).

Another question that has been raised concerns the ability of the controllable and reversible pitch propeller to stop and reverse the vessel. The test and trials of the *Single Hitch* demonstrated that this propeller provides the fastest maneuvering time yet to be achieved on a marine drive; less than 8 sec from full ahead pitch at design revolutions to full astern pitch. This has been substantiated by the operator of the vessel during the 18 months the vessel has been in service.

It has been claimed that the efficiency of a controllable pitch propeller will rapidly fall off as the blade is twisted owing to unfavorable pitch distribution. However, results of full-scale trials indicate that pitch reductions of 30 per cent below design pitch gave efficiencies comparable to calculated efficiencies for fixed-pitch propellers. In addition, dead-pull astern tests with the pitch reversed showed equal or better pull than with a comparable constant-pitch propeller.

Furthermore, the controllable pitch propeller permits the torque characteristics to be adjusted to meet the capabilities of the prime mover for any and all conditions of service operation. This is particularly advantageous with the gas turbine should it become necessary to reduce the operating temperature in servi (see Fig. 3), or it may be used to compensate for reduction power due to increases in inlet temperature. In this respect, it comparable in flexibility to the direct-current electric-transmi sion system.

While the first cost of this transmission system is higher tha that of alternating-current electric drive due to higher propell cost, its higher efficiency offsets this, so that the operating co per year is one of the lowest of all drives considered (see Table 2 Further, the cost of the controllable and reversible pitch propelle is based upon rather limited production and application. Ther is every reason to expect a reduction in the cost of this ite as its use increases which will further improve its competitiv position.

The control offered by this transmission system is probably th simplest of all the systems considered. All maneuvering is con trolled by a single lever operating the pitch of the propeller blades This provides both directional control as well as speed control However, operation at reduced powers for long periods should b obtained by changing the prime-mover speed with the propelle at designed pitch for best efficiency. Those installations that ca benefit by pilot-house control can readily be accomodated by this system. A block arrangement of this system is shown in Fig 10.

TABLE 2 ECONOMIC EVALUATION FROM VARIOUS MODES, OF TRANSMISSION
Factors Considered in Evaluation

	Eff.	Approx. Vol. Cu. Ft.	Total Wt. Lbs.	Wt/HP Lbs.	Total Cost	Cost/HP
(1) 3000 SHP						
AC Drive (mfg A)	90.3	2370	158,800	53.0	$167,100	$55.7
AC Drive (mfg B)	89.4	2370	158,700	53.0	150,700	50.2
DC Drive (mfg A)	84.6	2500	192,300	64.0	208,900	69.3
DC Drive (mfg B)	84.8	2500	271,300	90.5	281,200	93.7
Cont. Pitch Prop. (K = 75)	98	1000	161,000	53.7	202,000	67.4
Cont. Pitch Prop. (K = 175)	98	700	133,000	44.4	159,500	53.2
Reduct. Gear (K = 75)	98	800	115,000	38.4	129,700	43.2
Reversing Gear (K = 175)	96	1000	122,000	40.8	139,700	46.6
(2) 6000 SHP						
AC Drive (mfg A)	92.6	3360	233,200	38.8	$240,900	$40.2
AC Drive (mfg B)	90.9	3360	226,700	37.8	230,400	38.4
DC Drive (mfg A)	84.7	3640	320,700	53.5	337,000	56.0
DC Drive (mfg B)	85.3	3640	448,700	74.7	415,900	69.2
Cont. Pitch Prop. (K = 75)	98	1600	235,000	39.2	309,000	51.5
Cont. Pitch Prop. (K = 175)	98	1100	182,000	30.4	241,000	40.2
Reduct. Gear (K = 75)	98	1400	184,000	30.8	209,400	34.8
Reversing Gear (K = 175)	96	1600	135,000	22.5	242,400	40.3
(3) 9000 SHP						
AC Drive (mfg A)	94.1	5345	305,000	33.8	$314,300	$34.8
AC Drive (mfg B)	92.9	5345	294,500	32.8	293,800	32.6
DC Drive (mfg A)	85.0	6180	450,500	50.0	470,400	52.2
DC Drive (mfg B)	85.5	6180	633,500	70.6	578,800	64.2
Cont. Pitch Prop. (K = 75)	98	2300	320,000	35.5	399,000	44.4
Cont. Pitch Prop. (K = 175)	98	1900	247,000	27.4	316,000	33.2
Reduct. Gear (K = 75)	98	2100	241,500	26.8	261,300	29.0
Reversing Gear (K = 175)	No information available					

---

1 K factor for reversing reduction gear is 175 in first reduction and 125 in second reduction.
2 Foundation costs of respective drives have not been considered.
3 Fixed charges figured on basis of 4 per cent interest; 6 per cent insurance; 5 per cent amortization.
4 Gas-turbine fuel rate held constant at 0.45 lb per shp-hr for all power ranges.
5 Diesel fuel oil at $3.04 per bbl (New York) used.
6 Total yearly cost does not include fixed charges on turbine, so that difference is due to transmission.
7 In computing fuel cost, the vessel was considered to be at sea 60 per cent of the time.
8 The costs in the first column include the cost of thrust bearing.

Notes:

(*a*) The alternating-current drive has direct-connected generator at 3600 rpm and motor at 90 rpm.

(*b*) The direct-current drive, manufacturer (A) has geared generators of 750 rpm and 600 volts; the motors are 750 rpm and 600 volts, geared to propeller at 90 rpm. System uses series loop and variable-voltage control.

(*c*) The direct-current drive, manufacturer (B) has 750 or 900-rpm generators at 600 volts per armature, connected in tandem arrangement. Motors are 600-volt direct-connected to propeller; two armatures are in tandem at 600 volts each. System is series loop and can be provided with variable-voltage control.

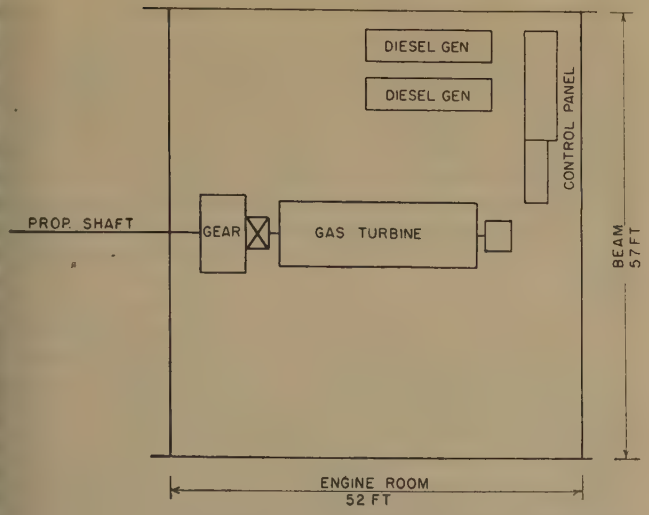

FIG. 10 BLOCK MACHINERY ARRANGEMENT USING A DIRECT-CONNECTED REDUCTION-GEAR SYSTEM

MECHANICAL REVERSING GEARS

This type of transmission was first used on the towboat *Bull Calf* in 1939. It was also used by the U. S. Navy during the war in connection with nonreversing Diesel engines. Approximately 3000 units were installed ranging from 750 to 1600 shp per unit. It is understood that the operation has been very satisfactory and no particular difficulties have been encountered.

This transmission consists of a combination of gears and clutches which can effect the transfer of power with rotation in either direction to a propeller from a prime mover which is not reversible.

The airflex clutch used in this arrangement can be described briefly as comprising two concentric rotating elements, one the driven member and the other the driving member. Disposed radially between the two members is an inflatable element attached to the driving member which serves functionally to engage the driven member when inflated.

Reduction in speed from the turbine to the propeller is accomplished by a double-reduction-gear assembly. In its simplest form the turbine pinion drives one of two first gears arranged and meshed to form a gear train wherein the first or driven gear rotates in one direction and the second rotates in a direction counter to that of the first. Each of the first gears is coupled to one of two second-pinion gears by means of an airflex coupling. All second pinions are in mesh with the periphery of a bull gear direct-connected to the propeller shaft. It is the provision of couplings which makes possible the selection of direction in which the propeller shall rotate and it is accomplished by inflation of one or the other of the couplings (see Fig. 11).

A specific application of this drive to a power plant delivering 3000 hp will require a modified form of the system. Because of the limitations in power which can be handled by couplings of the airflex type, four should be used, two for forward and two for reverse. Also, instead of two first gears there should be four, and also four of the second-pinion gears. To reduce the space requirements for such a gear assembly the four couplings would probably be arranged on one side of the bull gear and the first gears on the opposite side. The second-pinion gears would be direct-connected to the outer portion of the airflex clutch by means of a hollow shaft and the first gears connected to the inner member of the clutch by means of a shaft extending through the hollow shaft of the second pinion. With the four first gears in a train, the first and third would operate in the same direction, whereas the second and fourth would rotate counter to the first and third. To propel the ship forward it is necessary to inflate the airflex clutches corresponding to first and third gears only, and for reverse the clutches for second and fourth gears must be inflated, with the other two deflated.

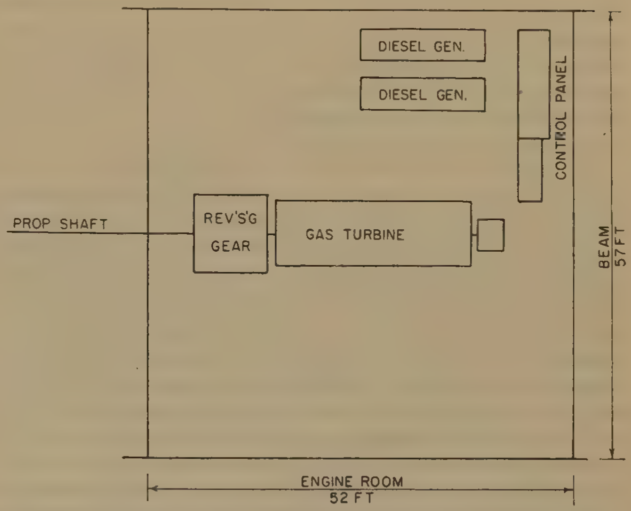

FIG. 11 BLOCK MACHINERY ARRANGEMENT UTILIZING AN AIR-CLUTCH REVERSING-GEAR SYSTEM

The present experience with this transmission concerns relatively low-speed application so that some design modification may be necessary to adapt this transmission to the higher speed required by a gas-turbine application. The reason for this development lies with the effect of centrifugal force on the airflex-gland contact. Previous designs in which a constricting gland was used, i.e., the gland gripped the shaft externally, was subject to reduced contact pressure due to the centrifugal force at high rotative speed. Another arrangement involves the use of an expanding gland so that centrifugal force will assist the contact; however, there are some questions as to the ability of this type to declutch without reducing speed. Another method concerns the adoption of a radial contact so that the gland contact will not be affected by centrifugal force.

A 3000-hp unit represents the highest horsepower and revolutions for which this type of transmission has been considered. However, the manufacturer advises that several studies have been made for possible application at 6000 shp, which indicate that no unusual difficulties need be expected. Accordingly, it would appear that the upper range of this transmission system cannot be established for the present.

If we accept the maneuverability of the present steam-turbine propulsion plants as a minimum standard, then the application of this transmission system should be restricted to those gas-turbine arrangements in which the compressors are driven independently from the power turbine. It will be noted from Fig. 3 that for those gas-turbine arrangements in which the power turbines also drive a compressor, the vessel will have a minimum speed in excess of 50 per cent of full speed. Further, since the torque available with this last turbine arrangement diminishes sharply with revolutions, the accelerations ahead and astern will be less than is possible with the present steam-turbine drives.

In so far as the arrangement weight and space requirements are concerned, this transmission system is the lightest considered, although it is based upon a K factor of 175 for the first reduction and 125 for the second reduction. Further, the gear was based upon a turbine speed of 4000 rpm.

Where this transmission system is used with a separate power turbine, the characteristics of the drive will be the same as the prime mover. The reversing time should be rapid and can prob-

U OF I
LIBRARY

ably be made at full revolutions if a suitable interlock is provided to reduce the fuel during the interval when one gland is emptying and the other gland is filling. With this interlock a single control lever may be used for reversing operations. Speed changes of course are made by changing turbine speed.

Reversing-Gas-Turbine Power Plant

The possibility of achieving a satisfactory reversing-gas-turbine power plant appears very improbable at this time. Furthermore, there is considerable doubt that development in this direction would be warranted. Normal development of the gas turbine for use ashore will be restricted to a unidirectional gas turbine. Therefore it is apparent that all development on a reversing gas turbine must be supported by the marine application. Consequently, it does not appear sound economically to add further cost to a product which today cannot be economically justified. Further, any application of a reversing gas turbine can be made only on an arrangement containing a separate power turbine, since those arrangements in which the power turbine also drives a compressor cannot produce the torque-revolution relationships necessary to reverse a ship. This further restricts the application of the reversing gas turbine so that the development cost cannot be spread over all the possible marine applications.

In evaluating the possibilities of developing a reversing-gas-turbine power plant, there is practically no experience upon which to plan other than that of the steam turbine, and several aspects of the gas turbine indicate that this experience would not be of major assistance. The fact that the windage losses in the ahead sections or elements when going astern are so much higher than those experienced in the steam turbine due to a twentyfold increase in density, will require a new cooling concept. In addition, thermal shock of the astern turbine would have to be considered carefully in determining the rapidity at which it could be brought to power. This last item, coupled with the heating of the astern elements when going ahead, would indicate that the astern element would have to be maintained at operating temperature at all times either by heating or cooling as the operating conditions required. Cooling of the astern element when going ahead could be obviated by a declutching arrangement.

A novel method of reversing the gas-turbine power plant has been outlined by R. Tom Sawyer,[2] Gas Turbine Construction, Prentice Hall, Inc., 1947. This system consists of a compressor turbine and a power turbine. The arrangement provides for the power turbine and compressor turbine to be in line and connected by an electric coupling which is not energized when going ahead. Further, the rotation of the compressor turbine is the reverse of the power turbine. To reverse this machine the power turbine is by-passed and the electric coupling is energized, thus permitting the compressor turbine to drive the propeller in the reverse direction through the power turbine (see Fig. 12).

This arrangement appears to solve the question of thermal shock since the compressor turbine is at operating speed and temperature. However, careful study will indicate that the excess of power developed by the compressor turbine due to the lower back pressure will not be sufficient to provide adequate astern power or torque, so that it will be necessary to design the compressor turbine with excess capacity over the compressor load if acceptable maneuvering characteristics are to be obtained. Thus in normal operation this compressor turbine, operating at partial load, will have a lower efficiency than could normally be obtained. Further, this lower efficiency applies to the largest power component of the plant which will affect seriously the normal fuel rate of this arrangement. In addition, it will be necessary to raise the operating temperature of this turbine suddenly when reversing so th
thermal shock will still be a consideration.

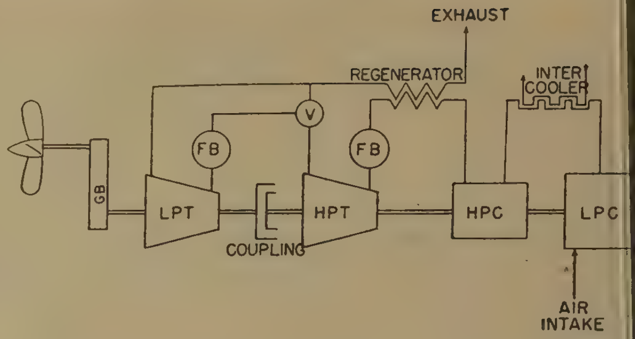

Fig. 12 Arrangement for Reversing a Gas-Turbine Pow
Plant Using Compressor Turbine for Astern Operati

Another aspect of this problem lies with the construction of
electric coupling suitable for the high rotative speeds required
the gas-turbine application. Present experience on these cou
lings has been obtained in Diesel-engine application at low rot
tive speeds. To apply this coupling to high rotative speeds wi
require new designs based upon induction-generator practic
using small diameters and long rotors. This will add materiall
to the cost of the coupling and complicate the arrangement pro
lem by lengthening the unit.

Electric couplings that have been used in marine service to dat
have required that the engine be brought to minimum speed whe
the coupling is excited during reversals and then accelerated at
moderate rate. This was necessary in order to avoid damage du
to coupling heating at high slips. Obviously, such a procedur
could not be followed in this gas-turbine application since in thi
case the turbine furnishing the power also drives the compressors
Accordingly, it would be necessary that the coupling be designe
to withstand the heat generated and that a variable-voltage sys
tem of excitation be used to maintain the heating effects at
minimum. This will add further to the cost and complexity o
this arrangement.

The use of an electric coupling in this arrangement will ad
appreciably to the complexity of the vibration aspects of the system. Contrary to popular belief, the coupling has a definite spring constant so that when it is excited it couples a high inertia system to the propulsion arrangement through a comparatively weak spring. This increases the possible modes of vibration during a period when the propeller exciting force is very large.

Economic Considerations

Having reviewed briefly the essential characteristics of the principal transmission system, it is now desired to consider the economic aspects of this problem. Some may question economic analysis of a component of the gas-turbine system on the grounds that the gas turbine to date does not hold an economic position in the marine field. However, it is believed to be apparent that the situation would be compounded in difficulty only if a component such as the transmission system were not planned on a sound economic basis.

In considering the economic side of this situation, it is desirable to establish a criterion for judging the economic merits of the various systems. To date, numerous economic studies have appeared in which the criterion of "return on capital investment" has been used in evaluating relative merits. In this comparison, it is preferred to establish the "minimum operating cost per year" as the criterion of comparison. The reason for this preference lies with the fact that return of capital investment concerns the banker's or investor's viewpoint and ignores the viewpoint of an perator whose returns accrue not because of investment but ecause he is rendering a service for which those served are willing o pay. There he is primarily interested in rendering the best ervice at the lowest possible cost. Further, careful study will ndicate that the maximum return on investment is associated ith minimum first cost and depreciates the importance of operating cost which is of utmost significance in judging the efficiency f operation. It is obvious that the design of a vessel or its components can affect only operating cost. Availability of cargo is etermined by many circumstances over which the designer has o control. Consequently, to use a criterion involving revenue in udging the merits of a design component is misleading.

---

[2] "The Modern Gas Turbine," by R. Tom Sawyer, second edition, Prentice Hall, Inc., New York, N. Y., 1947.

Another consideration entering this discussion concerns the bility to render a service competitively. In evaluating the nerits of a vessel or a component economically, it is apparent that he vessel or component which performs the service at the lowest perating cost offers the best competitive position and that this is articularly significant in a poor market.

Table 2 is a summary of an economic study recently made and ased upon current prices. In order to compare the various ransmissions, the turbine speed was established at 3600 rpm and he propeller speed at 90 rpm. This turbine speed was selected ince it was felt that this machine had the widest application and ccordingly would be of the most immediate interest in this comparison. However, the only information available on the mechanical reversing gears is based upon a turbine speed of 4000 rpm, ith a K factor of 175 on the first and 125 on the second reduction.

Many miscellaneous items such as foundations, duct work, iring, and piping, have not been included since their inclusion ould complicate the study appreciably. The fixed charges have een based upon 4 per cent interest, 6 per cent insurance, and 5 er cent amortization. Allowance has been made for reduction n interest and insurance due to amortization so that an even 10 er cent per year is charged. The fuel rate for the turbine was elected at 0.45 lb per shp-hr for purposes of comparison, and this ate was held constant for the power range of the study. A fuel rice of $3.04 a barrel is used, based upon the current rate for Diesel oil in the New York area. It might also be mentioned that he total yearly cost obviously does not include the gas-turbine ower-plant fixed charges which were not a factor in this comparison.

Strictly speaking, annual operating cost should also include rews' wages and subsistence, and equipment maintenance. It is elt that the omission of the crews' wages and subsistence does not ffect the result appreciably. While the omission of maintenance does decrease the value of the study, its inclusion could be undertaken only with considerable misgivings. Information regarding maintenance is not plentiful and is subject to considerable interpretation. Accordingly, maintenance is omitted and its addition left to the reader in accordance with his own opinion as to its magnitude.

It will be noted that for the 3000-shp condition, the mechanical reversing gear possesses the lowest operating cost. However, this comparison is not equitable since the mechanical-reversing-gear cost is based upon a design utilizing higher K factors than have been generally accepted.

Direct comparison was not possible between these two transmissions since price information was not available for the mechanical reversing gear based upon conventional design practice. However, indirect comparison can be obtained by increasing the K factor of the mechanical reduction gears, combined with the controllable-pitch propeller. It will be noted from Table 2 that when this is done the yearly costs of the two drives are very close for the 3000-shp condition, and that the mechanical reduction gear combined with the controllable-pitch propeller is lower for the 6000-shp vessel.

The alternating-current drive while higher in annual operating cost than the mechanical drives is close enough to be a real factor since this difference in operating costs might in many instances be more than offset by other considerations.

In so far as the direct-current drive is concerned, this evaluation indicates it would be quite difficult to justify its application in the power range considered and particularly for the higher powers.

It is of interest to note the relationship between annual fixed charges and annual fuel cost to the total annual operating cost. It is significant that the bulk of the cost is for fuel so that the study is quite sensitive to fuel price. Lower-price fuels would tend to favor the transmission with the lower first cost. However, for the present at least, bunker C fuel is not a factor so that the evaluation must be made upon the basis of Diesel fuel oil.

The transmission system, as such, for a reversing gas-turbine power plant, if available, is obviously the most economical. However, it is not possible to evaluate such an arrangement properly, since many of the factors are dependent upon the type, arrangement, and cost of the reversing gas-turbine power plant which as yet has not been developed and therefore cannot be evaluated.

SUMMARY

Having reviewed the various phases of this problem, it might be well to summarize briefly the findings for each system.

Electric Drive—Direct Current. It is believed apparent that the direct-current electric drive has little to offer when considered for gas-turbine power-plant application. Its first cost is quite high and its efficiency low, resulting in high operating cost. Further, the weight and space required are appreciably above those of other transmissions. Its one advantage of adjustable propeller speed, independent of prime-mover speed, can be obtained in another drive without sacrificing efficiency, weight, space, and annual operating cost. Further, it probably has the highest maintenance cost of all the drives considered. Of course there may be special applications where this transmission system may be attractive, but in the general application its advantages are limited.

Electric Drive—Alternating Current. For gas-turbine power-plant arrangements using a separate power turbine, this transmission system appears well-suited. Its economic position is among the lowest when conventional designs are considered. The space required by this drive is appreciably greater than the mechanical drives, which might handicap its use for some applications. In regard to weight, it compares favorably with the mechanical drives, being surpassed only by mechanical gears with unconventional K factors. In regard to maneuvering time, it appears deficient for those applications requiring rapid reversals. Further, as presently constituted, it is not the easiest plant to maneuver and is more susceptible to overspeeding than other transmissions. However, it has experienced long and successful service at sea and is regarded very favorably by certain operators.

Mechanical Gears Combined With Controllable-Pitch Propeller. This system is suitable for use with all gas-turbine power-plant arrangements. Its flexibility is the equal of direct-current electric drive, while its cost, weight, and efficiency are considerably superior. It compares favorably with the alternating-current drive in regard to annual operating cost and weight, and requires less volume. When compared on the same design basis with the mechanical reversing gear, it appears that the annual operating costs are about equal at 3000 shp but at 6000 shp the controllable-pitch propeller has some advantage. Its maneuvering and reversing characteristics are superior to the other drives considered and its control quite simple since all operations are performed by a single lever. It is believed that the existing background on the controllable-pitch propeller and Kaplan turbine establishes the reliability of this transmission system as being equal to any of the other types.

Mechanical Reversing Gear. This system appears to offer attractive possibilities for application to gas-turbine power-plant arrangements having a separate power turbine. Its economic position is excellent for powers up to 6000 shp. Its maneuvering and reversing characteristics are good, and all operations are performed through simple controls. Further, its weight, space, and arrangement factors are very suitable. However, its general application may be questioned due to the high K factors used in the design evaluated herein. It would appear that if designed with conventional factors its position might be altered so that final judgment as to its merits must be deferred. If the question of K factor can be reconciled satisfactorily, then this system should provide a very acceptable solution to the problem.

Reversing Gas-Turbine Power Plant With Mechanical Reduction Gears. At the present time this system cannot be evaluated intelligently. While the transmission system proper does not present any problems, the design and development of the reversing gas turbine appears quite remote. In fact, it is felt that effort in this direction is not warranted since other acceptable solutions are available.

CONCLUSIONS

In selecting a transmission system most suitable for general marine application, it is helpful to compare the two basic gas-turbine power-plant arrangements with existing marine-propulsion power plants in regard to their power and torque capabilities. A reasonably close comparison exists between the Diesel engine and the gas turbine, in which the power turbine also drives a compressor. Both of these prime movers produce rated power at rated revolutions if the brake mean effective pressure for the Diesel and the temperature for the gas turbine are maintained at designed values. However, the comparison is not so close when torque is considered, for, as the revolutions of the gas turbine, with attached compressors, are reduced, the torque likewise is reduced, whereas the Diesel engine under similar circumstances maintains constant torque with constant mean effective pressure.

A similar comparison may be made between the steam turbine and the gas-turbine arrangement which includes a separate power turbine. Each of these power plants can produce rated power at less than rated revolutions, and each can produce approximately 200 per cent torque at standstill.

Therefore, since the simple gas turbine has a revolution-power characteristic equal to the Diesel engine and a revolution-torque characteristic inferior to the Diesel engine, we may establish that those transmission systems successfully applied to the Diesel engine represent a minimum requirement for this gas-turbine arrangement. These systems are as follows:

1 Direct-reversing Diesel engine.
2 Direct-current electric drive.
3 Mechanical-reversing-gear drive
4 Controllable and reversible pitch propeller.

The reversing gas-turbine power plant should not be considered for the reasons previously outlined. The direct-current electric drive will function equally as well for the gas turbine as it does for the Diesel engine. Due to minimum speed limitations and inadequate accelerating forces the mechanical reversing gear is not suitable for this type of gas turbine. The controllable and reversible propeller offers the same operating advantages as the direct-current electric drive.

By similar reasoning it is equitable to establish the transmission systems used with steam turbines as a minimum requirement for the gas-turbine power-plant arrangement in which a sepa power turbine is provided. These systems are as follows:

1 Reversing turbine.
2 Alternating-current electric drive.

As in the case of the Diesel analogy, the reversing-turb power plant should not be considered. Since this gas-turbine rangement has approximately the same torque characteris as the steam turbine, the alternating-current electric drive wil acceptable.

In addition to the two systems mentioned, it is logical, in c junction with the separate power-turbine arrangement, to c sider the other modes of transmission used with Diesels. W these are not used with steam turbines because the revers turbine provides a more economical solution, the direct-curr electric and the controllable-pitch propeller apply equally well this arrangement as to the turbine with attached compress Moreover, due to the better torque-revolutions characteris of the separate power turbine, the mechanical reversing gear also a practical form of transmission.

Thus for the power turbine with attached compressor, there a two satisfactory modes of transmission, reduction gear with c trollable-pitch propeller and direct-current-motor drive. F the separate power-turbine arrangement there is, in addition the two mentioned, the reversing-gear drive and the alternatin current-motor drive.

Now in establishing a general solution to the over-all proble the transmission systems having the widest application offer t greatest possibilities and therefore their development is mo logical. Assuming equal economic position the mechanical r duction gear with a controllable and reversible propeller and t direct-current electric drive should receive first consideratio While the choice of the direct-current electric drive appears qui logical from existing experience, in that it meets all the requir ments for a marine-transmission system, its economic standing one of the poorest of the drives considered (see Table 2). Fu ther, its weight, space, efficiency, and maintenance factors furth add to its unattractiveness and tend to offset the advantages the gas turbine. Therefore it would appear that the mechanic reduction-gear transmission with a controllable and reversib pitch propeller represents the best solution to the problem co sidering the extent of application, i.e., it is suitable with any gas turbine power-plant arrangement, and its economic standing simplicity of control, efficiency, maintenance, and reliability ar satisfactory.

For limited application, the alternating-current electric driv and the mechanical reversing gears both offer acceptable solu tions, in addition to the mechanical reduction gear with control lable-pitch propeller. Considering conventional design practice the choice must lie between the electric drive and the controllable pitch propeller. Each of these drives possesses certain advantage which must be taken into account for the particular applicatio under consideration. Inasmuch as there is little differenc economically between them, other factors such as weight, space arrangement, maintenance, reversing time, and manning prob lems, etc., must be evaluated.

In so far as weight is concerned, neither drive offers any advantage. The space required by the mechanical drive is sufficiently below that of the electric drive to be a factor in favor o the mechanical drive. Arrangement of the two transmissions appears about equal with a possible advantage accruing to the electric drive for certain applications. It is believed that the maintenance of the electric drive will run higher than the mechanical and that manning of an electric-drive vessel with qualified and capable personnel will be more difficult. For those applications where reversing time is a factor, the mechanical drive offers n advantage. Upon the whole, the choice between these two rives can be made only for a specific application.

If the high design factor offered in the mechanical reversing ear be acceptable, then the selection must be made between the wo mechanical transmissions, i.e., the reversing gear and the ontrollable-pitch propeller, since on this basis they both possess onsiderable economic advantage over the electric drive.

For the 3000-shp range, these two drives compare favorably on ll points, although the mechanical reversing gear has a small dvantage in weight. In the 6000-shp range, the mechanical ear with the controllable-pitch propeller shows some economic dvantage although its weight is almost 30 per cent greater. In he 9000-shp range, it appears that the controllable-pitch propeller is the only choice.

The evaluation of the gears based on high K factor indicates he gains that might be made by departing from conventional practice. While it is recognized that some increase in K factor may be warranted, it is not considered feasible to increase this actor so far beyond present-day practice until more experience s obtained at some intermediate value. It is further recognized hat, while in certain applications, high K factors have been used uccessfully, it does not constitute sufficient background for general application.

In considering the possibilities of gas-turbine power-plant application, it should be remembered that for the power range presently considered, the competition is with the Diesel engine having a thermal efficiency of 34 per cent. The Diesel has long established its economic supremacy in the low horsepower range. Consequently, the gas turbine cannot afford to support economic parasites in the form of expensive low-efficiency systems if it is to compete with the Diesel engine.

ACKNOWLEDGMENTS

It is desired to express the author's appreciation to the following for their assistance in furnishing the various estimates of cost, weight, etc., that were used in this discussion: General Electric Company, Westinghouse Electric Manufacturing Company, Falk Company, S. Morgan Smith Company, and Allis-Chalmers Manufacturing Company. The author is also indebted to the following for their assistance in assembling the data and figures: C. G. Kurz, A. G. Lundquist, and E. K. Sullivan.

Discussion

M. L. IRELAND.[3] The author has presented a thoroughgoing economic study of various proposed gas-turbine transmission systems and has gone into considerable detail regarding their operating features.

Much of the author's material on the controllable-pitch propeller installation on the *Single Hitch* is presented here for the first time and is extremely interesting. The 3500-hp foreign installation referred to is of course the Swedish twin-screw motor vessel *Suecia* which was completed early in 1945. Perhaps the author has heard some reports on the service experience of this vessel which would be of interest. It would also be desirable to have some particulars of the other five large marine propeller installations in this country mentioned by the author.

One feature of the application of the controllable-pitch propeller to gas-turbine drive which appears to deserve careful study is the transient condition while reversing. For a brief interval the propeller blades operate at negative angles of attack and are receiving energy to drive the shaft. Normally this condition is of such short duration that the resulting shaft acceleration is probably negligible. However, one wonders what would happen if the pitch control should become jammed in the critical position. In this connection it would be interesting to know what position the propeller blades take up when the oil pressure is suddenly lost.

With regard to the economic study, the writer agrees that minimum operating cost is a satisfactory criterion. However, he suggests that caution should be used in the interpretation of such results for a single component of the power plant. For instance, the author draws attention to the disparity between annual fuel costs and fixed charges, but this may be misleading because the annual fuel costs are for the entire plant, whereas the fixed charges apply only to the transmission component. It is believed that a clearer conception is obtained by selecting the design with lowest annual cost as a basis and comparing incremental fixed charges and fuel costs. When this is done it is found that the increased fuel cost is in some cases less than one half the total increase. Therefore it would appear that these particular items are less sensitive to increases in fuel price than the author's Table 1 would indicate.

J. S. NEWTON.[4] The writer is pleased to see that the controllable reversible pitch propeller rates well economically, for he has stated on several occasions that this type of propeller, to furnish variable thrust in both directions with reasonable speed variation, appeared to provide the solution to the transmission problem for a practical marine gas-turbine propulsion system. The writer is heartily in accord with the plans for the development of this type of propeller, sponsored by the U. S. Maritime Commission and others.

It is a safe prediction that all five of the transmission systems enumerated and, no doubt, others will be attempted with a gas-turbine prime mover. However, as with the steam turbine, certain combinations will be found best suited to specific applications. For marine service, the reversible gas turbine and the large-capacity direct-connected direct-current generator are in the same category. Both border on the impossible. Four thousand revolutions per minute is a low speed for a gas turbine, but an impractical, if not impossible, speed for a direct-current generator of more than a few hundred kilowatts' rating. Similarly, while a reversing turbine is a possible solution for backing power, the complications encountered in making one practical are in large measure responsible for the interest evidenced in other means of accomplishing the desired result.

The writer cannot agree with the author's statement that "all development on a reversing gas turbine must be supported by the marine application." The need for reverse power in land-transportation work is well known and, except for the fact that the direct-current transmission is better adapted economically and has a favorable torque characteristic for locomotive applications, the necessity for reverse turbine marine and locomotive drives is comparable. For gas-turbine locomotives, substitution of gear-type transmissions for the costly electric-transmission equipment does appear possible. From future development work in this as well as in the marine field, a reversing gas turbine may evolve. Thermal shock to the astern turbine may not be as serious as expected. Our 2000-hp experimental gas turbine has been subjected to several thousand temperature shocks (700 to 1350 F) without apparent damage or distortion. At this time there is no evidence to indicate that, because of thermal shock, there is a limiting rate of increase of temperature for gas turbines. Future use of course may disclose limits, which the tests made thus far have not shown.

---

[3] Engineering Department, Technical Division, Newport News Shipbuilding and Dry Dock Company, Newport News, Va. Mem. ASME.

[4] Assistant Manager of Engineering, Steam Division, Westinghouse Electric Corporation, South Philadelphia Works, Philadelphia, Pa. Mem. ASME.

With respect to fuel cost, it is noted that a price of 7.25 cents per gal and a basic fuel rate of 0.45 lb per hp-hr have been used in making the economic analysis. These are favorable choices. While bunker C is now cheaper, it appears that in the future there will be a smaller differential in price between residual and refined fuels. Also, a fuel rate as good as 0.45 lb per hphr may not be economic for the gas turbine itself. These would indicate that higher percentage cost for the transmission, shafting, and propeller may be economically justifiable.

R. E. B. Sharp.[5] With the permission of the Maritime Commission, the writer would like to show (Fig. 13 of this discussion), the results of the open water test of the model of the controllable-pitch propeller which will be installed in the Liberty collier EC2-G-A-W2. The prototype propeller will be driven by a 3000-hp gas turbine at a speed of 90 rpm. It has four blades with a tip diameter of 17 ft 6 in., and was designed under the direction of Dr. J. Kreitner. The efficiency of 74 per cent is of interest in view of the ratio of hub to tip diameter being 0.286. Under this open water test, as the author points out, a propeller with large hub ratio is at a disadvantage. Unfortunately, no self-propelled test date and therefore no value of the propulsive coefficient is available. The latter value of course reflects the effect of the hull and sudden fairing on the propeller performance.

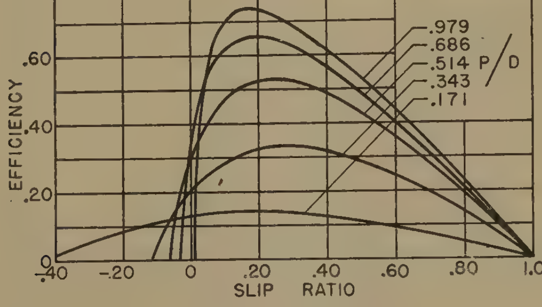

Fig. 13 Open Water Tests: Model 2869 S. Morgan Smith Controllable-Pitch Propeller Submitted by U. S. Maritime Commission and Tested at D. W. Taylor Model Basin July 29–31 and August 1, 1946

In connection with the flexible torque characteristics with controllable-pitch propellers, as mentioned by the author, relative tests made on two Navy tugs showed an increase in dead pull of 30 per cent with a controllable pitch propeller for the same engine torque over that obtained with fixed pitch. With gas-turbine drive, this will permit more effective utilization at zero and low ship speeds of the power available by operation at a higher rpm than would otherwise be possible. Reference is made to the author's Fig. 3.

Wilhelm Spannhake.[6] This discussion reminds me of about 40 years ago when the introduction of the steam turbine for marine propulsion brought up the same problem as is faced today with gas turbines. At that time Dr. Foettinger, the inventor of the hydrodynamic torque converter, proposed its use between the turbine and the propeller. The Vulcan Werke of Hamburg and Stettin undertook the design and manufacture of the converter and, after satisfactory performance of several units installed in merchant ships, obtained an order from the German Navy to install two units of 20,000 hp each in the light cru *Wiesbaden*. The two steam turbines operated at 1200 rpm the propellers at 350 rpm. Reversing was effected by arrang within the same casing two flow circuits, one for ahead and other for astern. The efficiency of the converter itself was per cent, but by recovering the heat generated by warming boiler feedwater, the over-all efficiency was increased to 91.5 cent. As a result of this success the German Navy ordered converters of 30,000 hp each to be installed in three bat cruisers, but when they were ready for shop test, World Wa ended and so nothing more was done.

There appears to be no reasonable limit to the power tra mitted per unit because of the similarity to hydraulic turbin which may be readily designed for 100,000 hp in a single runn Although hydraulic torque converters are limited to a transm sion ratio of not greater than 1 : 5, they can be successfully co bined with mechanical gear transmission, such as would custo arily be installed on a steam turbine. The mechanical gear ca thus be greatly reduced in size and cost. The ship's speed ca best be controlled by varying the speed of the gas turbine sin torque converters for variable ratios are rather complicate even though it is possible to design them with good averag efficiency. There are, however, other means of obtaining hig efficiency at low speeds. Small turbines for cruising speed can b arranged so that the power can be transmitted to the main pro peller shafts by means of the Foettinger hydrodynamic clutc and a mechanical gear.

Hydrodynamic transmission has, in the writer's opinion, grea advantages for ship propulsion. It is very reliable and there is n wear on the blades of the converter. Cavitation may easily b avoided. The maneuvering characteristics are excellent. Inas much as it is impossible to have an astern gas turbine, the revers ing of the propeller must be accomplished by the torque con verter. On the *Wiesbaden* the propeller shaft could be started i the reverse direction 6 sec after the order "full speed astern."

In regard to space and weight the hydrodynamic transmission is generally more advantageous than any other system even though for larger ratios it may be necessary to use mechanical geared transmission as well.

Consequently, it is obvious that as with steam turbines the hydrodynamic transmission should be considered in connection with gas turbines as well.

H. J. Chase.[7] Mr. Hammond's paper covers this interesting subject so fully that it is a great temptation to discuss the several possibilities at great length.

A few notes on some features of the a-c transmission may be in order as supplementing the author's statements, particularly on the maneuvering characteristics of these systems. The statement that 60 to 90 sec are required to go from full ahead rpm to $^2/_3$ rated rpm astern is quite true for some classes of vessels and a design specification that does not require extreme rapidity for this maneuver.

Some data are available which cast doubt on the advantage of quickly attaining high-astern propeller speed for the purpose of stopping a ship during a full-speed crashback. However, when this is a matter of design specification, the a-c transmission can be given characteristics that will substantially reduce the 60 to 90 sec quoted.

As far as normal dockside maneuvering is concerned, the a-c transmission is not handicapped at all in producing rapid maneuvering in response to signals.

The problem of maneuvering, both as to reversing and speed control, may be attacked in another way which produces an a-c ystem that may allow the gas-turbine characteristic to be ex-loited more fully. Reference is made to the possible use of igni-on-type rectifiers. As presently designed for commercial use, hese are not wholly seaworthy, but there appear good prospects hat tubes can be designed and built which can be used at sea.

---

[5] Consulting Engineer, S. Morgan Smith Company, York, Pa. Mem. ASME.

[6] Technische Hochschule Karlsruhe, Baden, American Zone. Contractee U.S. Navy.

[7] Federal and Marine Engineering Division, General Electric Company, Schenectady, N. Y.

With such tubes developed, the a-c transmission then permits election of generator speed to suit the gas turbine and the use of n a-c propulsion motor with very flexible speed control and re-ersing characteristics.

The author mentions the difficulty of obtaining crews qualified r operation and maintenance of a-c equipment, particularly om the standpoint of a-c control maintenance. The present pe of propulsion control is very similar to the a-c distribution nd generation equipment control for ship's service which, in gen-ral, has a good reputation and is widely used on shipboard. Per-aps the difficulty has been in obtaining trained crews during artime conditions. It would seem that more difficulty would ise in obtaining experienced operating and maintenance crews r the gas-turbine plant itself.

AUTHOR'S CLOSURE

The author would like to express his appreciation to the arious discussers for the interest they have shown in participat-ng in the presentation of this paper, and for the additions they ave made.

In connection with Mr. Ireland's request for particulars con-erning the other five large marine propeller installations in this ountry, it is regretted that the author is not in a position to upply the propeller particulars. However, the names of these ther vessels are as follows: Steamship *Albatross III*; motor essel *Commercial Clipper*; U. S. S. *Dahlgren*[3] U. S. S. *Apoholar;* . S. S. *Chononaga.*

With regard to Mr. Ireland's query, concerning the possibility f negative angle of attack adversely affecting the operation of ne propeller, it might be said that to date no adverse experience as been obtained from the aspect. It is known that the crash est of the Navy tug *Apohola* indicated that the momentary orque drop reached a minimum of 20 per cent of the free-running orque for an instant and then increased rapidly. The change n rpm during this 2-sec interval was from 100 to 102. Theoretical nalysis of this question indicates that the torque will never each zero, even if all blade sections were to reach their worst osition simultaneously. In fact, there is considerable doubt whether this condition could ever be reached, since generally the negative angle is approached at each blade section at a different time.

As to the position which the propeller blade will assume with loss of oil pressure, it is not possible to generalize this factor, since it depends upon the algebraic sum of all the moments acting upon the blades. These moments of course will vary from design to design, and a certain amount of control can be exercised so that the blade will assume a selected position in the event of oil failure. In the case of the *Single Hitch*, the forces were such as always to cause the propeller blades to assume maximum negative pitch in the event of a failure.

Analyzing the economic factors of Table 1, Mr. Ireland's point is well taken. However, in interpreting this table, it is intended that the total yearly cost for the various transmission systems be compared to the base "reduction gears only." This then gives a comparison of the increases which must be assessed to each of the various systems.

Mr. Newton's assurance regarding thermal shocking of the gas turbines is welcomed, and it is gratifying to learn that shocks of the magnitude indicated can be applied to the equipment without apparent damage or distortion.

In connection with the possibilities of land-transportation groups supporting the development of a reversing gas turbine, it is felt that this is quite remote in view of the wide acceptance of the transmission characteristics obtained from the Diesel-electric drive. Since these characteristics are apparently so well-suited to the requirements of railway locomotives, the development of a reversing gas turbine would have to be of a type which could offer a similar characteristic before very much interest could be aroused.

Mr. R.E.B. Sharp's addition of the open-water characteristics for the control-pitch propeller to be installed in the *Liberty Collier* EC-2A-W2 is welcomed. The addition by Mr. Wilhelm Spannhake of the information concerning Dr. Foettinger's hydrodynamic torque converter is appreciated.

Mr. H. J. Chase's comments regarding electric-drive characteristics are interesting. Of course to evaluate the electric-transmission system with improved reversing characteristics would require that cost data be available. The possibility of using ignitron-type rectifiers with the alternating-current transmission system is quite interesting. Future development of this system may prove that it is a valuable adjunct to the existing transmission systems.

Gas-Turbine Power Plants for Operation With Low-Cost Fuel

By JOHN GOLDSBURY,[1] LYNN, MASS.

**This paper presents a discussion of the economics and
neral design requirements of gas-turbine power plants
be operated with low-cost fuel, such as natural gas and
ude oil in the oil fields, refinery by-products, and by-
oduct gases from industrial processes. It is pointed out
at factors affecting first cost become relatively more im-
ırtant than those affecting efficiency as fuel cost de-
eases. When fuel cost is very low, water injection may
ıll be considered if a suitable supply of water is availa-
e. Brief mention is made of the flow-type turbine
ıwer plant with preheated gas, which is a special case
the combustion-gas-turbine power plant. Approxi-
ate costs of these flow-type turbine power plants are given.**

Introduction

N planning a gas-turbine power plant for operation with low-
cost fuel, the basic considerations will be low first cost, re-
liability, convenience of operation, and, when the power
ınt may be moved from one site to another, compactness and
ight. Fuel economy in itself will be of lesser importance. It is
e purpose of this paper to present the results to date of certain
ıdies which are being made to determine how a stationary gas-
rbine power plant of moderate size can best be designed to meet
ese requirements.

The term "low cost" is of course relative, since a low cost for
el in one region might be relatively high in another. This
per has been prepared with such fuels as natural gas and com-
ıstible by-product gas particularly in mind. However, some of
e data given will permit economic comparisons over a wide
nge of fuel costs. Natural gas has been reported as available in
rge quantities in certain oil-field regions at a price of approxi-
ately 7 cents a thousand standard cubic feet for 1000-Btu gas,
7 cents per million Btu gross heating value. For calculations
volving the properties of the fuel, natural gas with an assumed
mposition of 65 per cent methane and 35 per cent propane by
ight has been used.

The paper has been prepared with the requirements for power
ants of 2000 kw and less particularly in mind.

Devices for interstage cooling of compressors, interstage heat-
g of turbines, and preheating of combustion air by the turbine-
haust gas can contribute greatly to power-plant efficiency, but
e cost of such a device per unit of rating tends to increase with
crease in plant rating, while the fuel saving from a given in-
ease in plant efficiency is a constant percentage regardless of
ting. For this reason it will be more difficult to justify the use
such devices for the smaller ratings when the fuel price is low.
s fuel price increases, the advantage of higher thermal efficiency
creases until a point is reached where a heat exchanger is justified by the reduced over-all fuel cost. Because of the heat exchangers involved, it seems unlikely, also, that closed-cycle plants will be economical for use with low-cost fuels, except possibly in very large ratings. In this paper, therefore, only the simple open-cycle power plant, consisting of a compressor, one or more combustion chambers, a turbine, a generator, or other machine to absorb the useful output, and the necessary accessories will be considered. The accessories will include a starter, and if a generator is to absorb the load, an exciter. They may also include one or more gears to permit each rotating element to run at optimum speed if the effects on first cost are favorable. Such a simple open-cycle gas-turbine power plant is shown diagrammatically in Fig. 1.

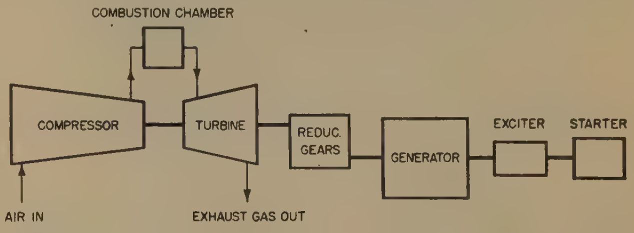

Fig. 1 Diagram of the Simple Open-Cycle Gas-Turbine Power Plant

Fuel Costs

Before proceeding with an examination of the design factors involved, it will be well to consider some actual effects of fuel costs on justifiable power-plant prices. In Table 1 are given prices per million Btu net heating value of several fuels. The figures for coal, bunker C oil, and fuel oil are based upon recent prices of fuel delivered at Lynn, Mass. Prices at points where shipping charges are lower should of course be less. The natural gas figure is based upon an assumed composition of 65 per cent methane and 35 per cent propane by weight and a price of 7 cents a thousand standard cubic feet in the gas fields for 1000 Btu gross heating value gas.

TABLE 1 FUEL PRICE

	Price per million Btu net heating value
Natural gas	$0.077
Process by-product gas	0.0825
Bunker C oil	0.504
Coal	0.458
No. 2 fuel oil	0.718

Savings in fuel cost are normally the only justification for paying any premium for increase in plant efficiency. However, in making cost comparisons between different fuels, price is not the only consideration. Relative costs of storing, pumping, handling, and feeding must be taken into account. Such costs normally will be low for natural gas, particularly if it is received at the point of use under pressure high enough to avoid the need of a fuel pump.

In Fig. 2 are shown fuel costs per year per 1000 kw rating plotted against plant thermal efficiency for different values of fuel price per million Btu lower heating value. Since 1 hp equals 0.746 kw the costs per 1000 hp are approximately three quarters as great. For other values of load factors and hours operated

---

[1] Turbine Engineering Division, General Electric Company. Mem.
SME.

Contributed by the Gas Turbine Power Division and presented
the Spring Meeting, New Orleans, La., March 1–4, 1948, and at
ıe Semi-Annual Meeting, Milwaukee, Wis., May 30–June 5, 1948,
The American Society of Mechanical Engineers.

Note: Statements and opinions advanced in papers are to be
nderstood as individual expressions of their authors, and not those
the Society. Paper No. 48—S-6.

per year than those used in the curves, the costs will vary in direct proportion.

Curves like those in Fig. 2 are useful for making comparisons between power-plant designs of different thermal efficiencies. For the rapidly changing conditions common in the oil fields, we may assume that the annual saving in fuel cost for the more efficient plant can be capitalized at 30 per cent, that is, that the extra cost of the more efficient plant should be written off in less than 4 years. As an example, let us assume that two 1000-kw power-plant designs, A and B, are to be compared using fuel costing \$0.077 per million Btu in both cases. If the plant efficiency of A is 10 per cent and that of B is $12^1/_2$ per cent, then, from Fig. 2

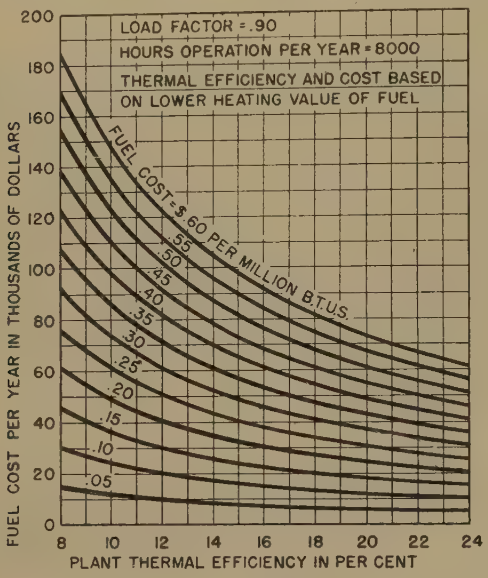

Fig. 2 Yearly Fuel Costs Per 1000 Kw Power-Plant Rating

Fuel cost per year for A......................	\$18930
Fuel cost per year for B......................	15150
Saving per year..........................	\$ 3780

The value of this saving, capitalized at 30 per cent is 3780/.30 = \$12,600. If the cost of design B is less than that of design A plus \$12,600, then purchase of a plant to design B is justified. Otherwise, design A should be used.

We shall now consider individually the most important factors which affect first cost and efficiency.

Element Efficiencies

Fig. 3 shows how the over-all efficiency of the power plant is affected by the turbine and compressor efficiencies. It is evident from the curves in Fig. 3 that the gain in plant efficiency from an increase in turbine efficiency is greater than that from a corresponding increase in compressor efficiency. Conversely, less harm is done by decreasing compressor efficiency than by a corresponding decrease in turbine efficiency.

The efficiency of a turbine or compressor is determined: (*a*) by the design; and (*b*) by the accuracy and quality of manufacture. The increased cost involved in holding to high standards of accuracy and quality of manufacture is usually a relatively inexpensive way of improving efficiency, and such standards tend also to contribute to the reliability of operation.

Some design features yield relatively large returns in efficiency for the cost involved. In general, however, careful comparative studies must be made to determine the optimum design. As an example, the axial-flow type of compressor is more efficient t the centrifugal type, but, for a particular application, compara studies might indicate a net economic advantage for the centr gal type. The advantage may lie with the latter type when rating is small and fuel costs are very low. A standardized des using an axial-flow type of compressor, appears to be attrac for a wide variety of applications for the larger ratings.

Pressure Drop Through Passages

Any pressure drop which cannot be utilized by the turbine c stitutes a loss in potential plant output. The pressure drop fr the compressor discharge through the combustion chambers the turbine inlet probably can be kept down to 5 or 6 per cen the absolute compression pressure without excessive cost. exception to this statement may be the case of a gas turbine a compressor which are integral parts of a catalytic petroleu refining plant in which the compressor is used to supply air catalyst regeneration, and the combustion gas from the regene tion process is sent to the gas turbine. In this case the proc requirements are of paramount importance and the net pov output of secondary importance. It then may be necessary accept a large pressure drop between the compressor and t turbine.

The compressor-inlet size and turbine-exhaust size should generous, and the installation should be so arranged that the a inlet and gas-discharge pipes will be short. A vertical stack f the exhaust gas will help to cut down the exhaust loss.

Compression Pressure

Fig. 4 is shown as an illustration of the net electrical outpu obtainable from a flow of 1,000,000 standard cu ft per day natural gas burned in gas-turbine power plants, designed f various combinations of compression pressure ratio and turbin inlet temperature. A compressor-inlet temperature of 80 F h been assumed. The full-line curves show outputs for desig using single-stage centrifugal compressors, while the dashed lin are for designs using axial-flow compressors. The axial-flow com pressors are assumed to have numbers of stages best suited to th

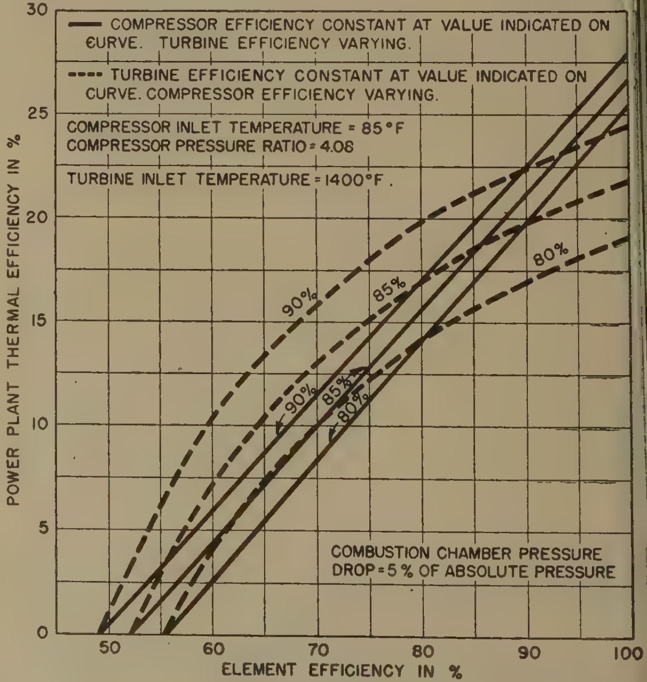

Fig. 3 Effect of Turbine and Compressor Efficiencies on Power-Plant Thermal Efficiency

esign pressure ratios. Multistage centrifugal compressors ight also be considered, but it seems to the author that the ormal choice will be between the high efficiency of the axial-flow ompressor and the extreme compactness and simplicity of the ngle-stage centrifugal compressor, and that effort should not be issipated over too many variations.

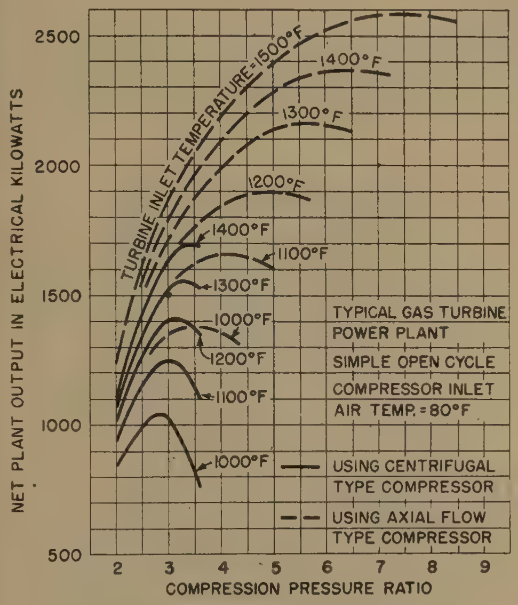

IG. 4 ELECTRICAL OUTPUT FROM 1,000,000 SCFD OF NATURAL GAS

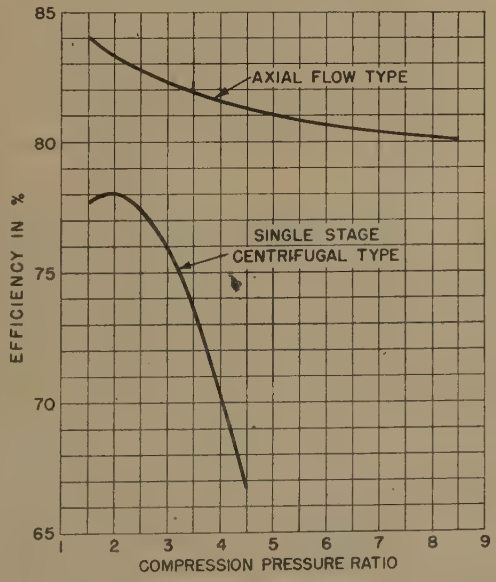

FIG. 5 ASSUMED COMPRESSOR-EFFICIENCY CHARACTERISTICS

Typical curves of compressor efficiency plotted against comression pressure ratio are shown in Fig. 5. These were used n the calculations for Figs. 4, 6, and 7. Higher efficiencies of ourse have been obtained, but the values given in these curves ppear to be conservative for normal continuous performance. The turbine efficiency used was 0.833 in all cases.

Fig. 6 shows the corresponding thermal efficiencies. These urves show that the compression pressure ratio for maximum lant output for a given fuel flow and for maximum thermal fficiency is a function of the turbine-inlet temperature. High turbine-inlet temperatures require relatively high compression pressure ratios and vice versa. Therefore the turbine-inlet temperature must be taken into account in selecting the compression pressure.

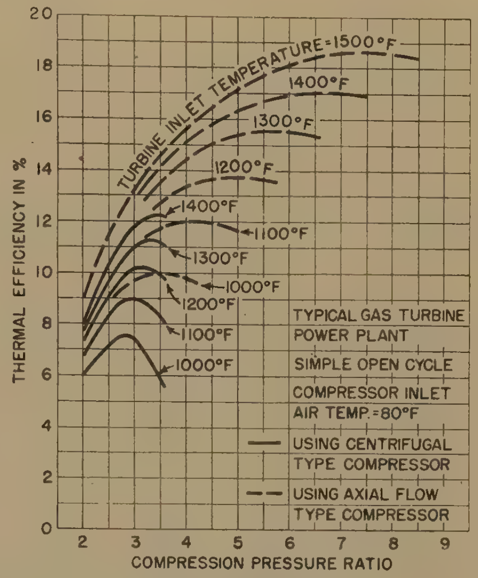

FIG. 6 PLANT THERMAL EFFICIENCY BASED UPON LOWER HEATING VALUE OF FUEL

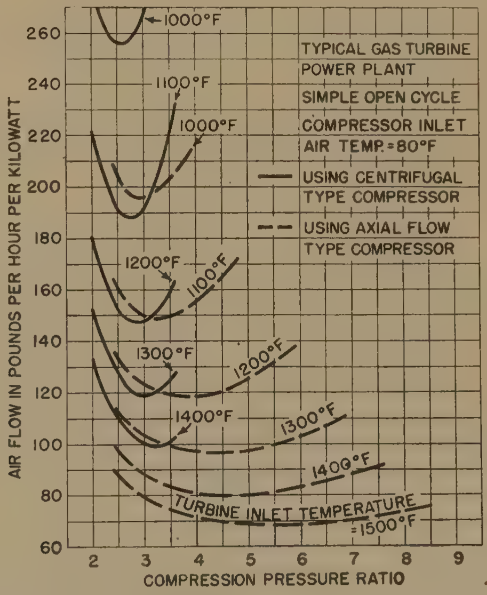

FIG. 7 AIR FLOW PER ELECTRICAL KILOWATT NET PLANT OUTPUT

Fig. 7 shows the relationship between air flow per kilowatt of electrical output, plotted against compression pressure ratio for various turbine-inlet temperatures and for the two types of compressors. It should be noted that the compression pressure ratio for maximum air flow at a given turbine-inlet temperature is lower than that for maximum output or maximum thermal efficiency. This is because the fuel/air ratio increases with decrease in compression pressure ratio. The air flow affects the sizes of the passages through the compressor, the combustion chamber, and the turbine. The compression pressure affects such items as rotor diameter, operating speed (rpm) and numbers of compression and expansion stages required. It also affects the wall thicknesses required for casings and pipe. Both these factors therefore affect first cost. For the designs involving axial-flow compressors, air flows are smaller and compression pressure ratios are greater at maximum thermal efficiency than for the centrifugal-compressor designs at the same turbine-inlet temperature. These factors must be taken into account in making comparative studies as to net economic merit.

In making such studies for small ratings, the possibility of using a small relatively high-speed centrifugal compressor should not be overlooked. The cost of a possible additional gear and the effect of the gear losses must of course be taken into account.

Compressor-Inlet Temperature

Figs. 4, 6, and 7 show performance at design conditions with 80 F compressor-inlet temperature. At a lower compressor-inlet temperature, the thermal efficiency would be greater and the air flow per kilowatt would be lower. Conversely, at higher air temperature, the thermal efficiency would decrease, and the air flow per kilowatt would increase. This is not only true for gas-turbine power plants, designed for different air-inlet temperatures, but it is, in general, true that the power output per pound of fuel for any gas turbine will increase with decrease in air-inlet temperature and vice versa when other operating conditions are constant. At inlet temperatures very much lower than the design value, a point may be reached where the compressor-inlet Mach number is too high for good efficiency, so that further decrease in inlet temperature will cause decrease in output and perhaps pulsation. The designer should make sure that this will not occur at expected winter temperatures.

Increase in output in winter is sometimes a desirable characteristic for a gas-turbine power plant. In selecting the size and design of the power plant, care must be taken to insure adequate capacity under hot-weather conditions.

Turbine-Inlet Temperature

As shown in Fig. 6, increase in turbine-inlet temperature yields a marked increase in plant efficiency, other things being equal. For the higher temperatures shown, however, the materials necessary for long life are very costly and expensive to work with. When fuel cost is low, the materials needed for the highest temperatures may increase first cost to a value unjustified by the increase in plant efficiency. The optimum turbine-inlet temperature for a given fuel price and power-plant rating, at this stage of gas-turbine experience, will be largely a matter of the judgment of the designer.

As compression pressure ratio increases, greater flexibility of design makes it possible to obtain relatively low turbine-blade temperatures without serious sacrifice in efficiency. It is probably impractical with presently known materials to consider designs for temperatures above 1400 F for the pressure ratios suited to the single-stage centrifugal compressor.

Water Injection

If, in addition to low-cost fuel, an adequate supply of water is available at the plant site, water injection should be considered. Before making a decision to use water injection, the nature of any impurities in the water should be determined to see whether it should be pretreated to prevent depositing of solids on the interior surfaces of the gas turbine. The cost of pretreatment should be taken into account in estimating the economics of water injection.

Fig. 8 shows curves of the ratio of water flow to fuel flow, plotted against fuel flow per kilowatt for different temperatures and for different values of excess air. The curves are plotted for a power plant using a single-stage centrifugal compressor with 80 F air-inlet temperature and 3.2 compression pressure ratio. The term "excess air" is used to describe the air in excess of that required for complete combustion of the fuel. This excess air c tributes to the cooling of the combustion gas to the desired t bine-inlet temperature. The remainder of the cooling is suppl by the injection water which here is assumed to be injected i the combustion chamber. The highest ratios of water flow fuel flow shown are beyond the range known to the author having been tried out successfully, and the problem of startin power plant designed for so much water injection would prese some special problems. However, the curves in Fig. 8 show th for the conditions and element efficiencies assumed, fuel rates maximum values of water injection compare favorably with tho for zero water injection at the lower values of turbine-inlet ter perature.

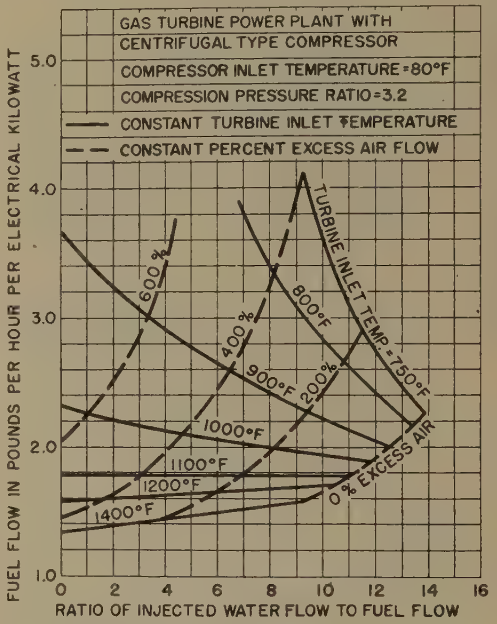

Fig. 8 Fuel Flow in Pounds Per Hour Per Electrical Kilowatt Versus Injected Water Flow

The cost of a turbine or compressor is affected materially by the passage areas required to pass the working fluid, particularly the passage areas through the blading. The passage areas required for a given power plant rating at given pressure and temperature conditions are reduced by water injection. This is shown in Fig. 9 in which are given curves of the approximate ratio of the passage area with water injection to that for turbine-inlet temperature of 1400 F, with no water injection, plotted against the ratio of injected water flow to fuel flow for different values of turbine-inlet temperature. The curves show that in every case the passage-area function decreases rapidly with increase in injected water flow, and that at large values of injected water flow the sizes of the 750 F turbine and its compressor are only a little greater than those for the higher turbine-temperature designs. Since the allowable turbine-blade stresses will decrease rapidly with increase in turbine-inlet temperature, the advantage for the low-temperature turbine in the materials that can be used is very great in so far as first cost is concerned.

Fig. 10 shows curves of available energy per pound of turbine gas plotted against the ratio of water-injection flow to fuel flow for various turbine-inlet temperatures. In order to maintain high turbine efficiency, the blade speed of the turbine design must be related directly to the available energy, as indicated in the following formula

$$E \doteq CN^2 \Sigma (D^2)$$

here

E = available energy per pound of turbine gas, Btu
C = const
N = rotating speed, rpm
D = mean blade diameter of turbine stage
Σ = symbol of summation

If the number of turbine stages and the mean blade diameters re kept constant, an increase in available energy requires an inrease in the operating rpm with accompanying increase in the lade stresses. The curves in Fig. 10 show that the available nergy per pound of turbine gas increases with increase in waterjection rate at constant turbine-inlet temperature, so that there will be some offset to the cost saving from reduced turbine and compressor-passage areas. However, there should be a substantial net reduction in first cost from the use of water injection.

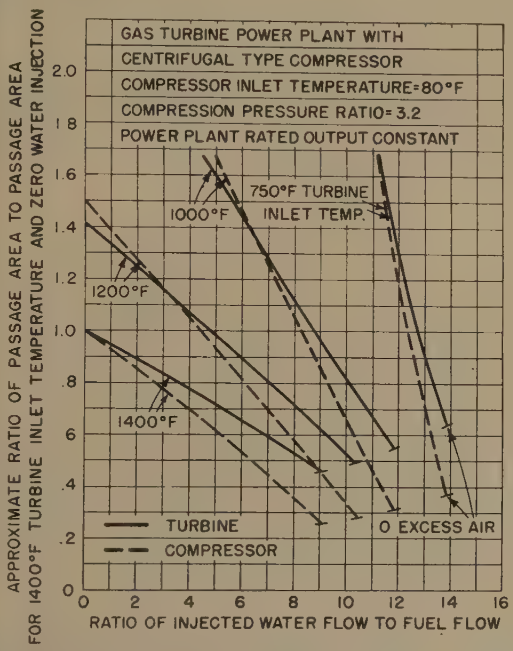

FIG. 9 PASSAGE-AREA RATIO VERSUS INJECTED WATER FLOW

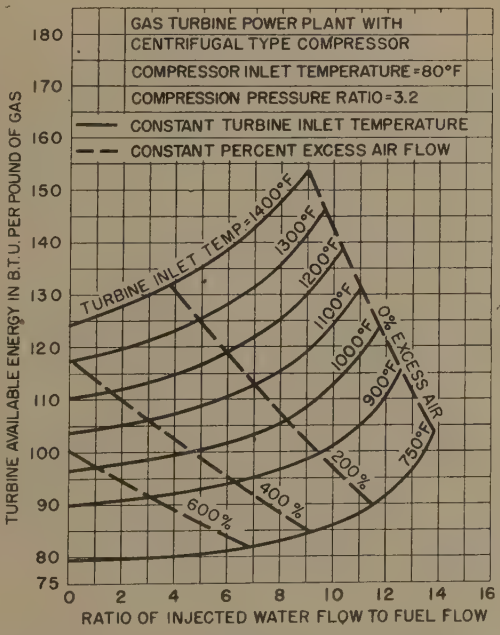

FIG. 10 TURBINE AVAILABLE ENERGY VERSUS INJECTED WATER FLOW

The power required for pumping the water will be less than 1 per cent of the net plant output.

FLOW-TYPE-TURBINE POWER PLANT

The flow-type-turbine power plant obtains its power from the expansion of a gas which has been compressed by natural means or by compression incidental to an industrial process. The basic cycle involved is the same as that previously described for the combustion-gas-turbine power plant. Since the compression power is not chargeable to the power plant, some net power output can be obtained regardless of the temperature of the gas as received, and whether or not it is heated at the power plant. However, the power available can be increased very greatly in many cases by heating the gas to a relatively moderate temperature, so such heating should be considered seriously.

When the gas involved is a fuel, such as most natural gases, the total gas flow can be passed through a heater before going to the turbine. A small portion of the gas flow coming from the turbine exhaust can be used as fuel for the heater. The remainder can be sent to a low-pressure fuel line for distribution and use as needed.

Since natural gas often comes from the ground at about 100 F, and since for the same initial and final turbine pressures the theoretical power obtainable from a given flow of gas is approximately proportional to the absolute initial temperature, heating the gas to approximately 660 F would double the available power. Actually, the power would probably be more than doubled because of improvement in turbine efficiency and avoidance of condensation and freezing of water vapor, carbon dioxide, etc., at very low turbine-exhaust temperatures.

If the gas is noncorrosive, the turbine can often be practically a standard noncondensing steam turbine designed for the same pressure, temperature, and rating. The chief difference from a steam turbine will be the special precautions to avoid explosion hazard. Any electrical equipment used in such a plant should be designed and arranged to avoid danger from explosion. It should be noted that steam turbines are usually sold for temperatures up to 750 F with no temperature premium. For temperatures from 750 F to 1000 F, temperature premiums are added because of the special materials and design features required.

The flow of natural gas required for a flow-type-turbine power plant will be many times greater than that for a combustion-gas-turbine power plant of the same rating, but the first cost will be less. Fig. 11 shows the approximate power output obtained from a flow of 20,000,000 standard cu ft of gas per day plotted against initial pressure available for different initial temperatures. A 5 per cent pressure drop is allowed through the heater and an overall turbine and generator efficiency of 70 per cent is used. A turbine-exhaust pressure of 22 psia is used to allow for low-pressure fuel-line requirements. The composition of the natural gas is assumed to be 65 per cent methane and 35 per cent propane by weight.

The flow-type gas-turbine power plant will consist of a turbine with a cost normally approximating that of a steam turbine for the same pressures, temperature, and rating, a generator or other driven unit with cost little, if any, affected by its association with a gas turbine, and usually a heater. Our investigations seem to indicate that a suitable heater can be obtained for from 60 to 75 per cent of the cost of the turbine-generator set with which it might be used. The heater price would include burners, automatic combustion control, and a stack. In many localities an outdoor installation is possible, so that the total cost of the power plant will be little more than the cost of the apparatus mentioned, plus suitable allowance for foundations, piping, and electrical or

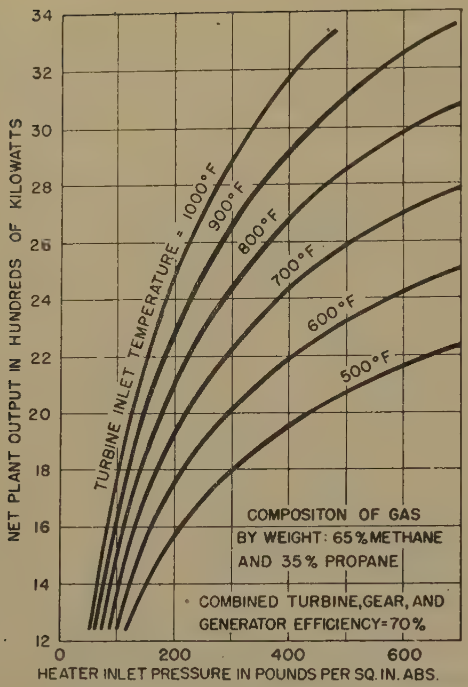

Fig. 11 Power Obtainable From 20,000,000 Standard Cu Ft per Day of Natural Gas in Flow-Type Gas-Turbine Power Plant

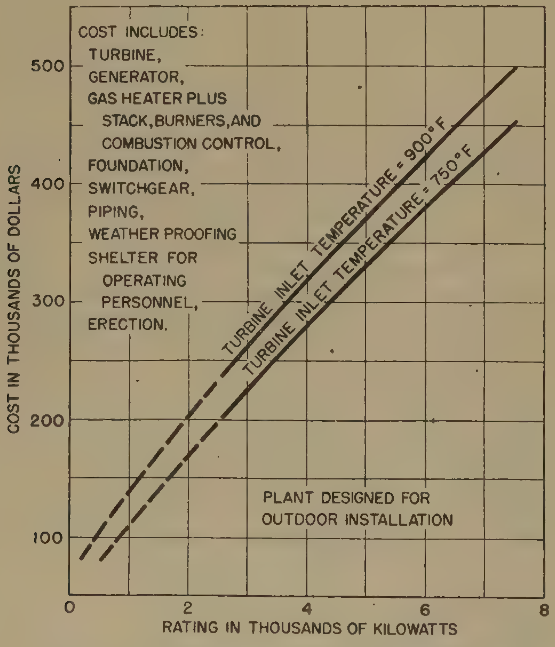

Fig. 12 Estimated Costs of Flow-Type-Turbine Power Plants for Operation With Noncorrosive Natural Gas

other control and transfer equipment. Fig. 12 shows curves of estimated cost plotted against rating for flow-type gas-turbine power plants designed for 750 F and for 900 F turbine-inlet-gas temperatures.

Conclusions

1 First cost rather than efficiency should be the primary c sideration when a power plant is to be operated with very lo cost fuel.

2 Compressor efficiency is less important than turbine e ciency, so that for the smaller ratings, at least, the centrifug type compressor should be considered.

3 The efficiency characteristic of the compressor used has dominant effect on the selection of compressor-discharge pr sure.

4 The determination of optimum turbine-inlet temperatu must await further studies.

5 Water injection has an important favorable effect on powe plant first cost, but pure or treated water must be used to avo injurious deposits on interior turbine surfaces.

6 The flow-type-turbine power plant may well be considere when natural or process gas is available at suitable pressure. T output obtainable from a given flow of gas varies approximatel with the absolute turbine-inlet temperature, so that preheatin of the gas may often be desirable.

Discussion

J. R. Haskin, Jr.[2] This discussion is limited to those gas turbine installations burning a fuel which also can be used in steam-turbine or Diesel-engine plant.

The greatest single factor in the cost of power generation is th fuel cost per kilowatthour. A breakdown of the cost of powe production will usually show that between 75 and 85 per cent o this cost is the cost of fuel. Because of this, when the fuel cos per million Btu is the same for two or more types of plants, high-efficiency steam-turbine or Diesel-engine plant may be mor advantageous economically than a low-efficiency gas-turbin plant, even though the high-efficiency plant has a greater first cost The author has not given any comparison for this case. Sinc management is vitally interested in the cost of its product, an since the gas turbine must compete with the steam turbine an the Diesel engine in power production, such a comparison woul be of great interest.

Author's Closure

The gas-turbine power plant must compete with other types of power plants as Mr. Haskin points out. The curves in Fig. 2 can be used for comparisons between power plants of any types. The first costs and thermal efficiencies of the power plants to be compared must be known or assumed, and the fuel cost for the comparison must be selected. The thermal efficiencies must, of course, include allowance for all auxiliary power and all losses which are chargeable to a power plant.

Certain other factors, also, will or may be of importance. Such factors are relative water requirements, relative attendance and maintenance requirements, relative weight, size, portability, etc.

At the present stage of development, no general data on the prices of combustion gas-turbine power plants can be given From experience to date, however, it seems certain that such power plants will be selected for many applications as preferable to other types.

---

[2] St. Louis, Mo. Mem. ASME.

Experimental Determination of Velocity of Sound in Superheated Steam by Ultrasonics[1]

By JAMES WOODBURN,[2] HOUSTON, TEX.

This paper describes apparatus which has been contructed for determining the velocity of sound in supereated steam. A quartz crystal, vibrated electrically at ts natural frequency, is used as a sound source to set up a eries of standing waves in a vertical cylinder filled with team. The frequency of the sound source and the length f the standing waves are measured with high accuracy y simple and convenient methods. Experimental results re presented which show close agreement with data calulated from the steam tables of Keenan and Keyes.

INTRODUCTION

SOUND may be considered to be a sudden compression at a given point in a medium which possesses both elasticity and inertia. The medium most commonly encountered is tmospheric air, and the point in question is the ear of the listener. Vith the introduction of electrical and mechanical methods for etecting pressure waves, the definition of sound must be broadned.

A sudden compression in a gaseous medium is always followed y a rarefaction, as the particles which are initially compressed end to resume their original position, due to the elasticity of the edium, and thereby react on the neighboring particles. These articles, in turn, are compressed, and the sudden compression r disturbance travels away from a point source in the form of wave. Due to inertia, the particles overshoot their positions f rest, and a rarefaction succeeds the compression, to be folowed in turn by a weaker compression as the vibrations of the articles about their original positions are rapidly damped out. . single wave of compression may be partially realized by a ort sharp tap or pulse. If, by mechanical means, a series of ompressions is caused to emanate from the source, there results train of compressions and rarefactions which produces the ensation of noise in the ear of the auditor.

The human ear is limited in its ability to detect sound vibraons, the upper limit being about 20,000 vibrations per sec. 'he term "ultrasonic" is used to describe sound waves which are igher in frequency than 20,000 cycles per sec, and hence are audible. Electrical methods are available, however, which an detect waves of much higher frequency, and the apparatus escribed in this paper can cover the range from 50,000 to ,000,000 cycles per sec.

If a sudden compression is produced at a point in a gas, the ompression will travel with a velocity C which depends upon e physical properties of the gas and also upon the nature of the ompression. The compression can be conceived to be either isothermal or adiabatic. It was Sir Isaac Newton who first derived an expression for calculating the velocity of sound in a gas. He assumed that the compression was isothermal, and his calculated value was about 16 per cent below the experimental value, indicating an error in his theory.

Laplace, in 1816, concluded that the compressions and rarefactions of the sound wave took place so rapidly that there was no time to share with the surrounding air the heat developed by a compression, or the "cold" developed by a rarefaction. Thus the process must be adiabatic, and not isothermal, as Newton had assumed. Laplace derived an equation, employing the adiabatic elasticity instead of the isothermal elasticity of a gas, and his calculated values agreed very well with experimental values. His equation was

$$C = \sqrt{kg\,PV} \qquad [1]$$

where

C = velocity of sound, fps
g = universal gravity constant, 32.17 fps per sec
k = ratio of specific heats
P = absolute pressure, psf
V = specific volume, cu ft per lb

It is of interest to note that Equation [1] also appears in deriving the equation for the velocity of a gas passing through the minimum section or throat of a nozzle when the back pressure is less than the "critical" pressure.

Experiments carried out in 1846 by Graham on air flowing from a high-pressure chamber through a nozzle into a vessel at lower pressure showed that the flow rate increased with diminishing back pressure until a certain pressure ratio, about 0.53, was reached. Further reductions in the back pressure did not increase the rate of flow through the nozzle. R. D. Napier (1)[3] performed similar experiments with steam in 1867, and he observed the same phenomenon, except that the critical-pressure ratio for steam was found to be about 0.55. This curious effect was also observed by Wilde, Zeuner, Fliegner and many others. An observation which complicated the explanation of this phenomenon was the failure of a sharp-edged orifice to behave in the same manner as a rounded nozzle.

In 1886, Osborne Reynolds (1) showed that the velocity of the gas at the minimum section or throat of the nozzle was that given by Equation [1], where P and V were the pressure and specific volume at the throat. In other words, when critical flow was established, the throat velocity was the same as the velocity with which sound waves passed through the gas, and changes in the pressure beyond the nozzle could no longer be "telegraphed" back to the inlet of the nozzle. With a sharp-edged orifice, the continuously increasing flow with decreasing back pressure is explained by the continuous change in the area of the minimum section or vena contracta.

The derivation of Equation [1], as established by Osborne Reynolds, can be found in any standard thermodynamics text, but no experimental value for the velocity of sound in superheated steam has been published. Therefore it is hoped that the

---

[1] This paper is an abstract of a thesis having the same title and subitted to Johns Hopkins University, June, 1947, in partial fulfillent for a doctoral degree in Mechanical Engineering.

[2] Associate Professor in Mechanical Engineering, Rice Institute; rmerly Assistant Professor in Mechanical Engineering, The Johns opkins University, Baltimore, Md. Jun. ASME.

Contributed by the Power Division and presented at the Annual leeting, Atlantic City, N. J., December 1–5, 1947, of THE AMERICAN OCIETY OF MECHANICAL ENGINEERS.

NOTE: Statements and opinions advanced in papers are to be nderstood as individual expressions of their authors and not those of e Society. Paper No. 47—A-119.

[3] Numbers in parentheses refer to the Bibliography at the end of the paper.

present work will help to supply the need for such data. Obviously, from Equation [1], if the pressure and specific volume of a gas are known, and the velocity of sound can be measured accurately, it becomes possible to calculate the value of k, the ratio of specific heats at the existing conditions.

Methods for Determining Velocity of Sound in Steam

In 1812 Benzenberg (2) determined the velocity of sound in steam at atmospheric pressure by comparing the frequencies of a reed when blown with steam and with other gases. Lucchi (3), in 1887, used the well-known dust-figure method for steam at atmospheric pressure and a few degrees of superheat. The results are quite good considering the experimental difficulties encountered, but they are only of historical importance.

Many other methods of producing a sound wave in a gas are given in Partington (4), but the quartz-crystal method, developed by Pierce (5), possesses distinct advantages, and is used present work.

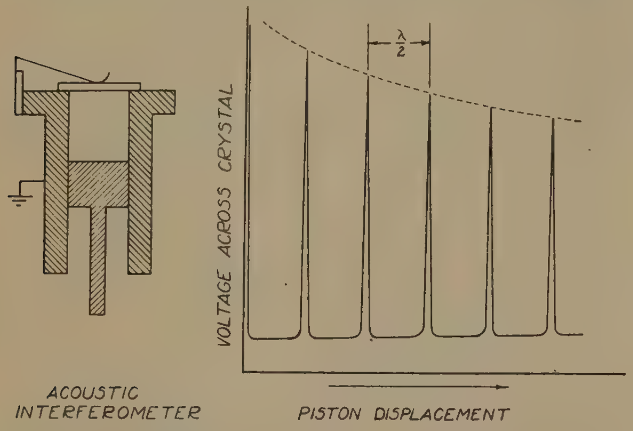

(a) (b)

Fig. 1 Diagrammatic Sketch of Acoustic Interferometer and Sound Peaks

The acoustic interferometer is a device for measuri length of a standing sound wave, and the general principles instrument used in this work are shown in Fig. 1. Fig. 5 s more detailed diagram of the apparatus. The quartz cry caused to vibrate at its natural frequency by an electroni lator or driver, thereby setting up a series of standing wav vertical cylinder, the lower end of which is closed with a m piston. The top of the piston is exactly parallel to the low face of the quartz plate, which is approximately 1 in. squa $^3/_8$ in. thick. When the piston is moved to a position suc the distance between the piston and the quartz crystal integral number of half wave lengths, a sharp peak is pro in the voltage across the crystal. Fig. 1(b) represents a of the voltage across the crystal, plotted in terms of the displacement. The decrease in the voltage peaks is due t absorption of the sound in the steam as the piston is m away from the quartz plate.

The fundamental equation for the velocity of sound ir medium is

$$C = f \times \lambda \ldots\ldots\ldots\ldots\ldots\ldots$$

where

C = velocity of sound, fps
f = frequency of sound, cycles per sec
λ = wave length, ft

If the frequency can be measured accurately by electrical me and the movement of the piston can be measured accura the velocity can be calculated readily.

Description of Apparatus

Because the interferometer is a highly sensitive instrum the results obtained with it are reliable only if great care is ta in its construction and operation. A description of the appara

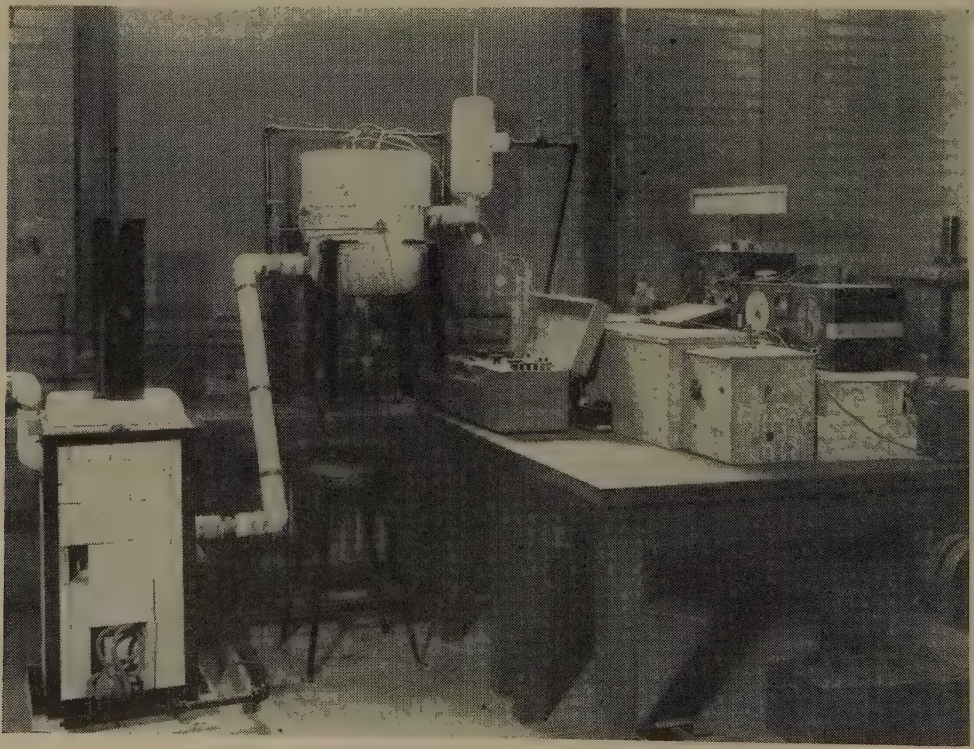

Fig. 2 General View of Apparatus

sed in the work at Johns Hopkins University will indicate the recautions which were taken to eliminate errors due to the con- amination of the steam or other causes. Fig. 2 shows a general iew of the apparatus. Steam from the university power plant as supplied through a gas-fired superheater. A steam jacket as also used to house the interferometer, to prevent tempera- ure variations. The piston rod extends through the bottom f the jacket and is connected rigidly to the index head and the and wheel by which the piston is moved.

The pressure and temperature of the steam were controlled by alves in the superheated-steam line and in the gas line, while a lose regulation of the steam pressure was maintained by regu- ting the rate at which it was allowed to escape through the eating jacket to the atmosphere.

The electrical apparatus, shown on the right in Fig. 2, con- sted of a shielded driving oscillator, used to cause the vibra- on of the quartz crystal, a crystal-controlled frequency meter, radio receiver, and a galvanometer.

Fig. 3 shows the assembled interferometer before it is placed the steam jacket. It is approximately 4 in. diam and 10 in. ng. Steam enters through the curved pipe at the top and is ischarged through the horizontal pipe at the right side of the ody. The connection to the upper surface of the quartz crystal made through an electrode, consisting of a model aircraft- ngine spark plug.

The component parts of the interferometer are shown in Fig. 4. They were machined from stainless steel to prevent oxidation. The inside of the cap was machined out to form a recess for the quartz crystal. A small splash plate, mounted on the lower side of the cap, prevented the steam from impinging directly on the quartz plate.

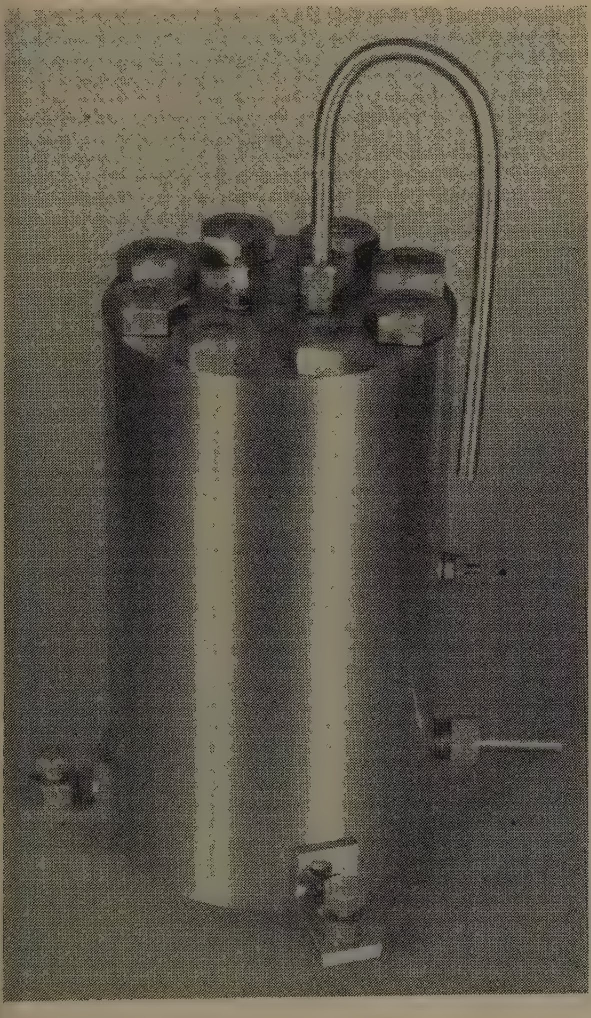

Fig. 3 Acoustic Interferometer

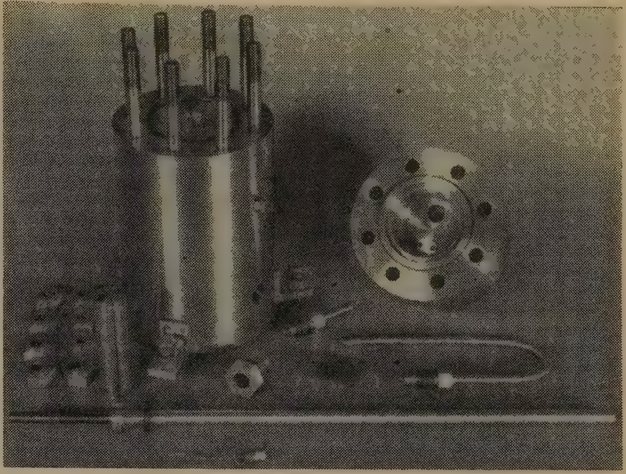

Fig. 4 Component Parts of Acoustic Interferometer

The piston, which was $^3/_4$ in. diam, was machined and lapped into the body of the interferometer. Great care was taken in this operation to keep the face of the piston parallel to the quartz plate. A $^1/_{16}$-in. slot was milled into each side of the piston, to provide a keyway to prevent the piston from turning when the spindle was rotated, and to give a passage through which the steam could escape from the bottom of the acoustic chamber to the atmosphere. The spindle and the interferometer piston were machined for a standard micrometer screw thread.

The location of the quartz plate in the interferometer is shown in Fig. 5. A slight recess, milled across the face of the chamber, provided a passage for the steam to flow under the quartz plate and into the acoustic chamber. The quartz pegs, shown in Fig. 5, were used to keep the plate in a central position. The faces of the plate were covered with thin gold films, which were sputtered on in the usual manner. The upper face of the plate, upon which the spring electrode rested, was the high-potential side, the opposite side serving as the ground electrode.

After the interferometer had been assembled, it was placed inside the steam jacket, and leveled on a horizontal platform within the jacket by means of three screws. It was then clamped rigidly to the platform. The spindle which projected through the bottom of the jacket was then connected by a rigid coupling to the index head and the hand wheel by which the piston could be moved to any desired position. The steam outlet on the side of the interferometer was connected to a pipe coil, which passed through the rear wall of the jacket to a valve, by which the flow of steam through the interferometer was controlled during starting periods.

Since the interferometer screw was subjected to high temperatures, the expansion of the thread could cause a serious error because the half-wave-length intervals of the sound wave were only a few thousandths of an inch in length. In order to prevent such an error, the interferometer screw was calibrated in position at three different temperatures by the following method: The cap of the interferometer and the quartz crystal were removed, and a long thin quartz rod was passed through a small hole in the flanged lid of the jacket and rested directly upon the surface of the piston. The opposite end of the quartz rod was connected to a dial gage which had previously been checked with a set of standard precision gage blocks. By rotating the

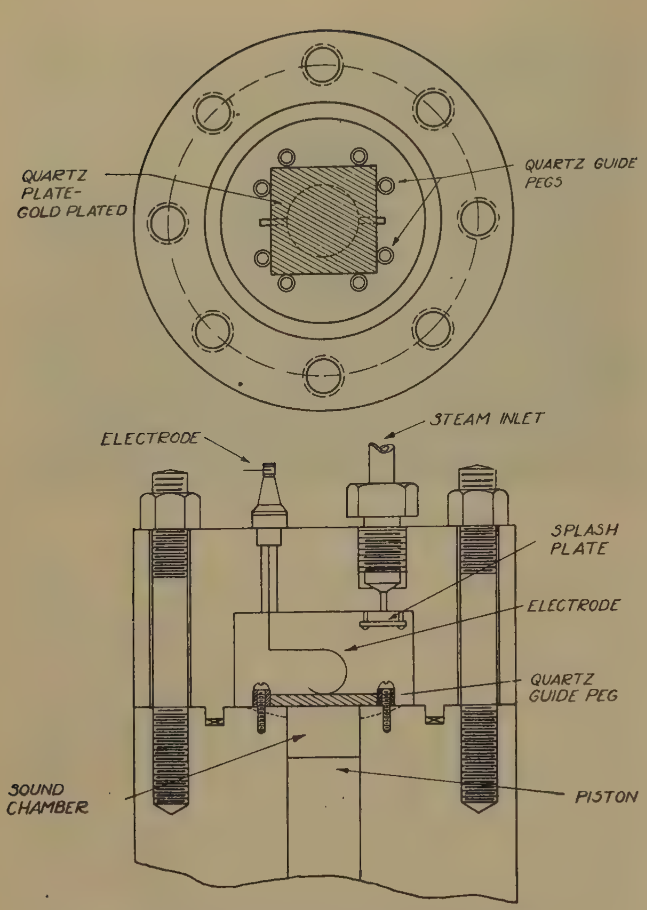

Fig. 5 Quartz Crystal Mounted in Interferometer

handwheel slowly, the index head which was mounted directly above it could be checked against the dial gage. A series of measurements were taken at room temperature and then with superheated steam at 400 F and at 700 F. The expansion of the screw thread was then plotted against temperature from the three calibrated points and was used in correcting all wave-length measurements.

The temperature of the steam entering the interferometer was measured by means of three thermocouples placed 120 deg apart and at different depths inside the steam jacket around the interferometer. The thermocouples were calibrated previously against the ice point, the boiling point of water, and the sulphur point. The steam pressure gages were calibrated with a conventional dead-weight test apparatus before being used.

Method of Operation

Steam was admitted to the apparatus for a period of approximately 8 hr to bring all parts up to the desired temperature at a uniform rate. Any sudden increase in temperature caused the interferometer piston to bind in the acoustic chamber. During the warming-up period, the exhaust valve to the interferometer was opened to allow steam condensate to escape. When the desired temperature was reached, all drain lines to the jacket were closed and the exhaust valve to the interferometer was left slightly open to indicate that the acoustic chamber was always filled with steam.

The electrical oscillator was then turned on and as it was slowly tuned to the natural frequency of the quartz crystal, the voltage across the crystal suddenly decreased to a minimum value which indicated that the crystal was vibrating at its maximum amplitude, thereby sending out a series of sound waves the steam. The face of the piston in the acoustic chamber flected the sound waves back to the crystal, thus setting up standing waves.

By rotating the handwheel slowly, the piston was moved the acoustic chamber, and, as it passed each half-wave-leng point, the voltage in the crystal circuit increased to a sharp a well-defined maximum. A vacuum-tube voltmeter-and-ga vanometer arrangement was used to detect the voltage peaks.

Because of the nature of the quartz crystal, a slight change steam pressure or temperature would alter its natural frequenc However, this change was detected readily by a change in t pitch of the beat note between the driving oscillator a the calibrated crystal-controlled frequency meter attached to t broadcast receiver. The variation in steam conditions cou also be detected by a slow drift in the galvanometer reading. T galvanometer reading, as a matter of fact, would vary appr ciably before the temperature change was large enough to b observed from thermocouple readings. The beat note and th galvanometer were used to indicate equilibrium conditions place of the thermocouple because of their sensitivity and quic response.

When a test run was completed, and the steam was turne off, the piston would soon bind in the acoustic chamber, due t the different rates of cooling of the interferometer body and th piston. About 20 hr later, however, all parts of the interfe ometer would cool down to room temperature and the piston wa free to move. The piston, screw, and body were made fro three slightly different grades of steel to prevent galling or bind ing. No trouble has been encountered from galling of the closel fitting parts.

The range of frequencies ordinarily used in ultrasonic wor is from 50,000 to 3,000,000 cycles per sec. At the lower limi acoustical correction factors must be employed because the soun wave is not plane. At the upper limit, the length of the wav is so short there is difficulty in measuring it accurately. In th present work, a crystal was used which had a natural frequenc of 575,000 cycles per sec in air at room temperature.

The frequency of the sound source was measured with an ac curacy of one part in 200,000, while the length of the soun wave was measured to one part in 2000. Since the acousti velocity is the product of these two factors, as given in Equatio [2], the actual velocity of sound in steam was measured wit high accuracy.

The measurement of the steam temperature was accurate t 0.5 per cent, while the steam pressure was measured with an accuracy of 1 per cent. The effect of pressure upon the velocity of sound in a gas is very small.

In taking the data, 24 to 36 individual measurements of half wave-length intervals were noted and recorded. During each test a continuous check was made of the frequency of the soun source. If for any reason there was a change in temperature, the results were discarded.

TABLE 1 COMPARISON OF EXPERIMENTAL VELOCITY OF SOUND IN SUPERHEATED STEAM WITH CALCULATED VALUES FROM KEENAN AND KEYES[a]

Steam conditions		Keenan and Keyes, calculated, fps	Experimental "acoustic method," fps
Pressure, psia	Temperature deg F		
24.69	300	1650.19	1649.68
24.69	400	1756.50	1758.06
24.69	500	1854.36	1848.83
24.69	600	1945.12	1939.64
24.69	700	2031.07	2027.35
24.69	800	2115.65	2107.35
99.69	400	1727.89	1720.28
99.69	500	1835.42	1823.09
99.69	600	1932.23	1923.45
99.69	700	2020.64	2019.45

[a] "Thermodynamic Properties of Steam," by J. H. Keenan and F. G. Keyes, John Wiley & Sons, Inc., New York, N. Y., 1936.

Experimental Results

able 1 presents experimental values for the velocity of sound steam at an absolute pressure of 24.69 psi, and at temperaes ranging from 300 to 800 F. A second set of data is given an absolute pressure of 99.69 psi, at temperatures from 400 to F. For the same conditions, values are given for the velocity ound as calculated from the specific-volume data given in the nan and Keyes steam tables. The agreement is quite good, maximum deviation being about 12 parts in 1800, at 99.69 and 500 F.

ig. 6 shows the data plotted with steam pressure as the paeter.

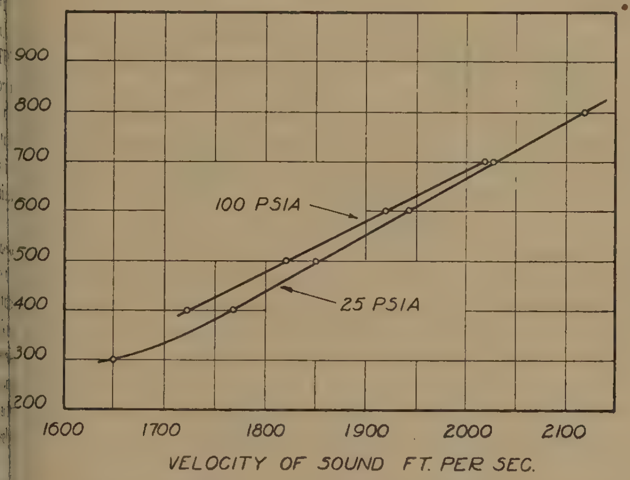

6 Velocity of Sound Versus Temperature and Pressure in Superheated Steam

able 2 gives the values of the ratio of specific heats, as calted from Equation [1], and as given by Keenan and Keyes. agreement is again remarkably good. Data for the 99.69- 700 F run are given in Table 3, and it can be seen that the e-length readings are consistent to within the limits of accy of the screw thread.

ork which was conducted subsequent to the tests reported is paper has shown that there is no measurable change in the city of sound with frequencies as high as 2,000,000 cycles sec.

he theory of gases indicates that the velocity of sound should dependent only upon absolute temperature for a perfect gas. 6 indicates that the dependence upon pressure becomes much ller as the temperature of the steam increases, and its beior approaches that of a perfect gas more closely.

o summarize the advantages of the acoustic interferometer, possible to measure the sound velocity with high accuracy out employing large quantities of gas. A new interferometer, . 7 and 8, similar in principle to that of Fig. 1, has been concted which uses an acoustic chamber only $^3/_8$ in. diam and in. long. The quartz crystal is $^1/_2$ in. diam, and has a natural uency of 1,000,000 cycles per sec.

general, even a slight trace of any impurity in a gas will r materially the velocity of sound. By using this fact, ultracs may be developed as a means of detecting traces of air in m, for example.

xperimental data can be obtained for mixtures of gases, and use of the sensitivity of the equipment changes in composican be detected readily. The electrical equipment required ot complicated, and only 0.3 volt was needed to keep the tal vibrating in superheated steam. The crystal responds h more quickly in superheated steam than in air, and, under certain circumstances the crystal would not vibrate at all in the atmosphere, yet no trouble was encountered when superheated steam was used.

TABLE 2 COMPARISON OF RATIO OF SPECIFIC HEATS BY ACOUSTIC METHOD WITH TABULAR VALUES FROM KEENAN AND KEYES[a]

Steam conditions: Pressure, psia	Steam conditions: Temperature, deg F	Keenan and Keyes, k	Experimental acoustic method, k
24.69	300	1.316	1.316
24.69	400	1.310	1.312
24.69	500	1.304	1.303
24.69	600	1.297	1.294
24.69	700	1.290	1.290
24.69	800	1.284	1.281
99.69	400	1.303	1.294
99.69	500	1.301	1.287
99.69	600	1.295	1.290
99.69	700	1.289	1.289

[a] "Thermodynamic Properties of Steam," by J. H. Keenan and F. G. Keyes, John Wiley & Sons, Inc., New York, N. Y., 1936.

TABLE 3 SERIES OF ACTUAL MEASUREMENTS OF SUCCESSIVE SOUND PEAKS OR HALF-WAVE-LENGTH INTERVALS

Screw reading, in.	$^1/_2$ λ, in.[a]	Screw reading, in.	$^1/_2$ λ, in.[a]	Screw reading, in.	$^1/_2$ λ, in.[a]
0.28182	...	0.28123	...	0.27995	...
0.26038	0.02144	0.25971	0.02152	0.25853	0.02142
0.23866	0.02172	0.23812	0.02159	0.23694	0.02159
0.21672	0.02194	0.21665	0.02147	0.21550	0.02144
0.19500	0.02172	0.19487	0.02178	0.19387	0.02163
0.17356	0.02144	0.17350	0.02137	0.17229	0.02158
0.15184	0.02172	0.15186	0.02164	0.15100	0.02129
0.12997	0.02187	0.13019	0.02167	0.12923	0.02177
0.10893	0.02104	0.10877	0.02142	0.10754	0.02169
0.08694	0.02199	0.08680	0.02197	0.08564	0.02190
0.06527	0.02167	0.06561	0.02119	0.06437	0.02127
0.04335	0.02192	0.04374	0.02187	0.04267	0.02170
0.02142	0.02193	0.02184	0.02190	0.02130	0.02137
0	0.02142	0	0.02184	0	0.02130

[a] Half wave lengths in inches.

Note: Steam conditions: 99.69 psia, 700 F.
Frequency 560,703 cycles per sec.
Readings corrected for expansion of interferometer screw thread.

Work has already been performed on certain of the freons, and the data on Freon-12 are particularly interesting. The velocity of sound in Freon-12 is only about one third as great as that in superheated steam.

Conclusions

The agreement of the experimental data presented in Tables 1 and 2 indicates that the simple acoustic interferometer can give accurate values of the velocity of sound in superheated steam. The method can be developed readily to such an extent that a laboratory technician could operate the necessary apparatus without difficulty.

Future work is planned with steam at higher pressures and temperatures than those reported in this paper. It was the intention of the author in presenting this paper to acquaint engineers with this particular application of ultrasonic sound waves, and to present for the first time actual measurements of the velocity of sound in superheated steam.

Acknowledgments

The author is grateful for the advice and assistance of Prof. J. C. Hubbard of The Johns Hopkins University, Department of Physics. Also for the many constructive comments and suggestions offered by Prof. A. G. Christie of the Department of Mechanical Engineering, in which department the work was done. The encouragement and comments offered by Prof. J. H. Keenan of the Massachusetts Institute of Technology during the initial phases of this work is appreciated by the author. Grateful acknowledgment is also made to Mr. Bernard Baker for machining the acoustic interferometers.

BIBLIOGRAPHY

1 "Collected Works," by Prof. Osborne Reynolds, Cambridge University Press, London, England, vol. 2, 1901, p. 321.

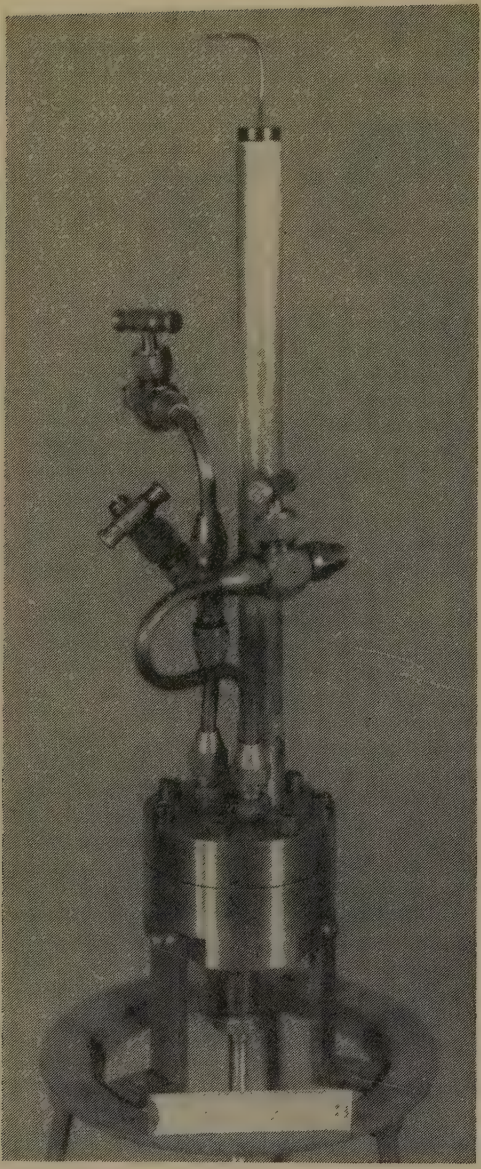

Fig. 7 Acoustic Interferometer for Freon Gases

2 "Velocity of Sound in Steam and Other Gases," by J. F. enberg, *Annalen der Physik*, vol. 42, 1812, pp. 12–36.

3 "Velocity of Sound in Steam, Carbon Dioxide and Phosp Vapor," by Lucchi, Atti del Reale Instituto Veneto di Scienze 7, 1887, p. 15.

4 "The Specific Heats of Gases," by J. R. Partington and Shilling, E. Benn, Ltd., London, England, 1924.

5 "Piezoelectric Crystal Resonators and Crystal Oscil Applied to the Precision Calibration of Wavemeters," by G Pierce, Proceedings of the American Academy of Arts and Scie vol. 59, 1923, pp. 81–106.

6 "Handbook der Experimental Physik," by A. Eucken, *A mische verlags Gesellschaft*, Leipzig, vol. 8, 1929, p. 421.

Discussion

A. G. Christie.[4] The author undertook the developmer a method to determine the velocity of sound in superheated st by ultrasonic methods. It was the intention to develop method in order to determine certain of the thermal prope of other fluids that may be used by engineers such, for insta as refrigerants. However, superheated steam was selected the first experiments as reliable data are at hand in Keenan Keyes "Steam Tables" against which the author's results c be checked.

This study required the development of satisfactory eq ment and new techniques. The results, given in Tables 1 an show close conformity with values derived from the steam tab Improvements resulting from experiences with the equipm described in this paper have led to a greater degree of accu on later work by others. This method has been applied sinc a new fluid with hitherto unknown properties.

G. H. Van Hengel.[5] This very useful paper fully conf by experiment that the old formula of $C = \sqrt{gkPV}$, as used perfect gases, can now be applied safely to the sound-velo calculation for steam.

As this sound velocity is used in the calculation for maxim flow through nozzles, it is therefore appropriate to publish graphs for the full region of superheated steam as calculated fr the Keenan and Keyes Steam Tables. Fig. 9 of this cussion gives this value as represented by the author as funct of temperature. Fig. 10 gives a clearer picture in which sound velocity is a function of the pressure.

---

[4] Professor of Mechanical Engineering, The Johns Hopkins U versity, Baltimore, Md. Fellow and former president ASME.

[5] Engineer, Production-Mechanical, The Detroit Edison C pany, Detroit, Mich. Mem. ASME.

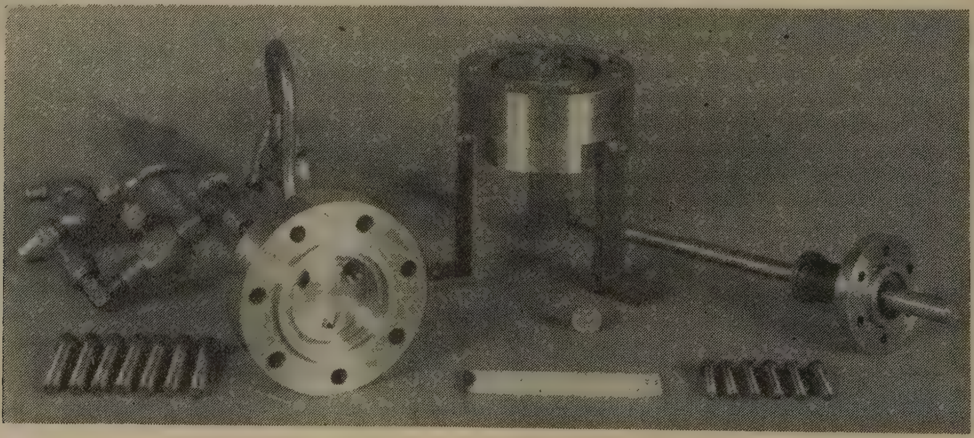

Fig. 8 Component Parts of Acoustic Interferometer for Freon Gases

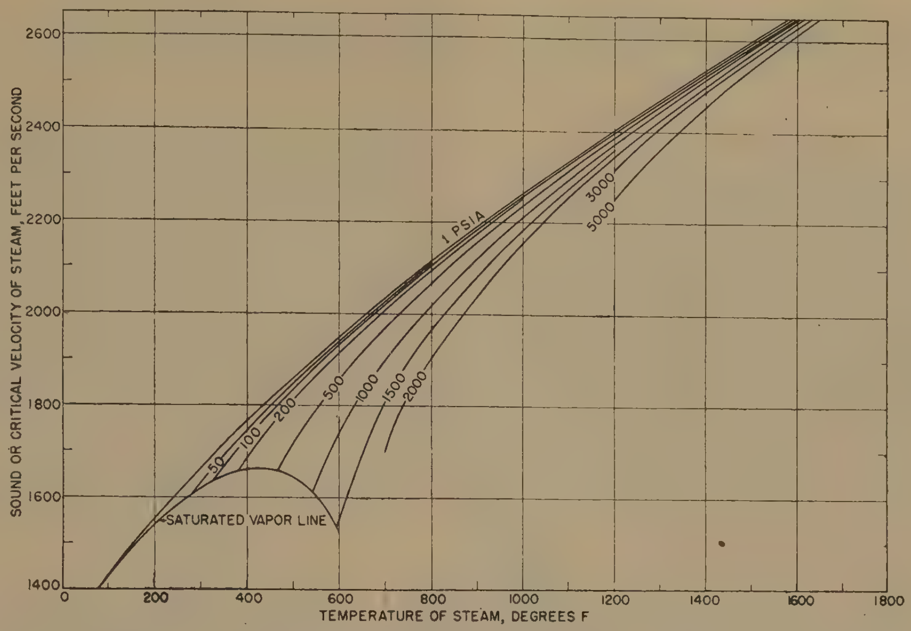

Fig. 9 Sound Velocity of Steam in Feet per Second Given as Function of Temperature in Degrees F for Different Pressures in Pounds per Square Inch Absolute

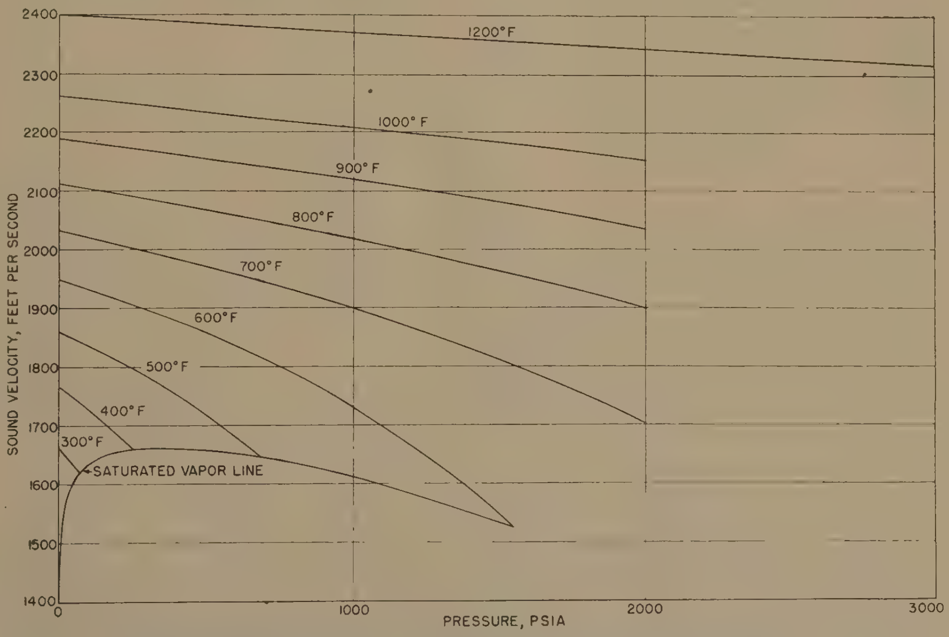

Fig. 10 Sound or Critical Velocity of Steam in Feet per Second Given as Function of Pressure in Pounds per Square Inch Absolute for Different Temperatures in Degrees F

Furthermore, a very handy graph is the value of the sound-velocity energy as represented in Fig. 11. This graph can very well be used to follow the expansion on the enthalpy-entropy diagram.

Author's Closure

The author appreciates the remarks of Mr. Van Hengel in regard to this work and also the graphs as shown in Figs. 9, 10, and 11. Since the completion of the present work the acoustic velocity has been determined for the same steam conditions using different frequencies; however, no change was observed in the acoustic velocity as a function of frequency of the sound source. Further work is being done at Rice Institute both at high steam pressures and temperatures in order to complete Mr. Van Hengel's statement regarding the use of the perfect-gas equation. For practical purposes the perfect-gas equation can be used but accurate work particularly at high pressures simple correct factors will have to be used.

Professor Christie's remarks are rather interesting; howe it should be pointed out that the author realized the degree accuracy of the experiments which were consistent with accuracy of existing PVT data. Therefore increased accur over the present method would be of little value. It is v simple to increase the accuracy of the experiments by us optical methods such as Haidinger fringes to measure the h wave-length interval which the author originally considered did not use for the foregoing reason.

The author has completed a series of experiments on the use Freon 12 in regard to the acoustic velocity with the appara as shown in Figs. 7 and 8 which will be published at a later da

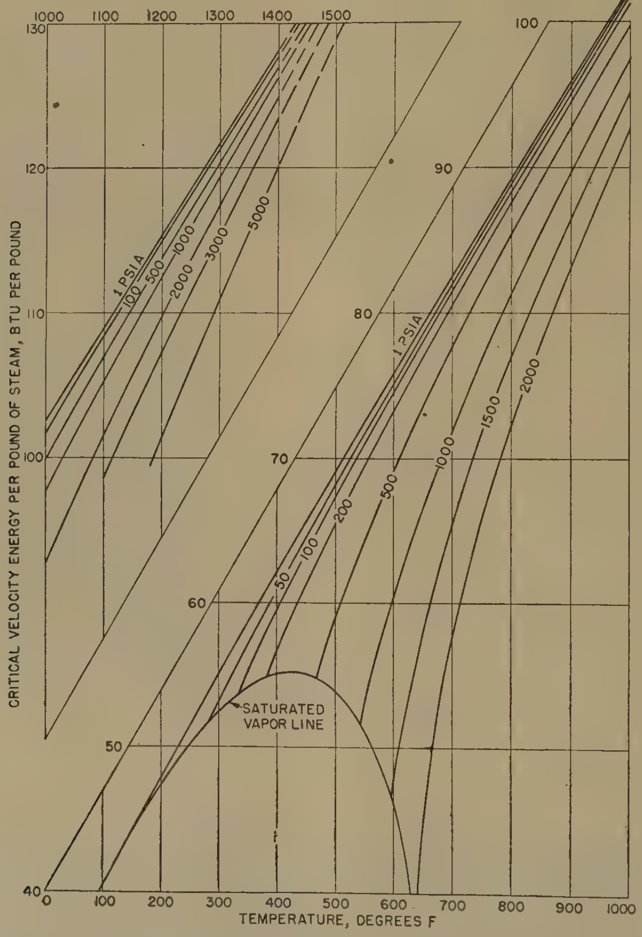

Fig. 11 Sound or Critical-Velocity Energy of Steam in Btu per Pound as Function of Temperature in Degrees F for Different Pressures in Pounds per Square Inch Absolute

Jet Mixing of Two Liquids[1]

By R. G. FOLSOM[2] AND C. K. FERGUSON,[3] BERKELEY, CALIF.

The problem of mixing or blending in a tank of two or ›re liquids of low viscosity and the same density has been ›estigated in terms of available information on turbu- ›t fluid jets discharging into a very large volume. Under ›e assumption that all fluid inducted into the jet is ›xed completely, the effectiveness of any arrangement ›s been expressed in terms of a performance parameter ›ich is defined as the gallons per minute of fluid inducted ›· horsepower supplied. The calculated results for a ›ge gasoline-blending tank demonstrate the superiority performance of the propeller-type mixer over typical ›s produced with transfer-pump and pipe-line equip- ›nt. The economics of the installation and operation of ›ipment were not included.

NOMENCLATURE

›he following nomenclature is used in the paper:

= factor of proportionality between velocity and dimension ratio, dimensionless
= width of jet in radial direction, ft
= factor of proportionality between jet axial distance x, and jet width b, dimensionless
= diameter, ft
= hydraulic head, ft-lb/lb
= power, hp (prime indicates ft-lb/sec)
= flow rate, gpm (prime indicates cfps)
= radius, ft
= axial velocity, fps
= radial velocity component, fps
= specific weight, lb per cu ft
= axial distance from plane of jet orifice, ft (prime indicates distance from theoretical jet origin, ft)
= $(r_0 - r)/r_0$, dimensionless
= unit shear force, lb per sq ft
= density, slugs per cu ft
= kinematic viscosity, sq ft per sec
= stability parameter, dimensionless
= hydraulic efficiency, dimensionless

scripts:

= center line
= average as specified
ı = total input to system
= jet orifice condition
= induced flow property
= critical flow value
= in plane perpendicular to jet axis at distance x
1 = suction line to transfer pump
2 = discharge line from transfer pump

INTRODUCTION

Mixing of two or more liquids in a large tank may be accomplished with a variety of devices and by several procedures. If the liquids are miscible, they are frequently mixed by the turbulent action of a relatively high-speed jet of liquid, discharging into a region of slowly moving or stationary liquid. Because of the several different methods of producing a high-speed jet, designers and engineers who select and specify mixing equipment require a knowledge of the fundamentals of jet operation. A method of estimating jet-mixing performance is developed in this paper.

Propeller-type agitators are common in laboratory and field installations. These agitators produce a large-diameter jet of liquid which is carried by propeller-supplied momentum into regions of fluid having little motion. A similar effect may be achieved by a high-speed jet of liquid discharging from a nozzle, a system which appears particularly attractive where existing pumps and pipe lines offer a working arrangement for a minimum capital expenditure.

The method of analysis presented in this paper was developed from existing theory and experimental data on fluid jets for the purpose of evaluating comparative economies of the different mixing procedures. The analytical developments lack direct experimental confirmation, but they are believed to be of sufficient value to warrant the presentation of a summary treatment. An experimental program is to be undertaken.

CONDITIONS

The general problem, with allowable simplifications necessary for an analytical analysis, will be formulated on the basis of avialable experimental information and qualitative observations of water jets and dye in a transparent container. The maximum rate of mixing takes place in the highly turbulent jet. It will be assumed that the fluids to be mixed are of approximately the same specific gravity, and that all fluid inducted into the turbulent jet in a distance specified by tank geometry will be mixed uniformly with the driving fluid. Observations indicate that the mixing of fluid accomplished in regions outside the turbulent-jet boundaries is negligible. Circulation currents aid in efficient mixing, but their direct contribution to mixing is small in comparison with that caused by the violent agitation in the turbulent jet. The circulation results from pressure gradients in the flow system, but since the circulation velocities are small compared to the jet velocities, the pressure gradients will be negligible.

Many data are available regarding the mixing process for a jet of gas discharging into a stationary gas infinite in extent with no appreciable pressure or temperature gradients (1, 2).[4] In this case the gas acts as an incompressible fluid, and the results are dynamically similar to those for corresponding flow of liquids at the same Reynolds number. Since the Reynolds numbers concerned are large, no appreciable differences are expected over the range of values considered. The data and methods for gases will be applied directly to the liquid-mixing problem.

The total amount of fluid picked up by the jet and mixed with the jet fluid through the action of turbulence increases as the

---

This paper under the title, "Mixing of Fluids by Inductors," › presented in preliminary form by the Process Industries and ›lraulic Divisions at a meeting of the Los Angeles Local Section, ›. 4, 1947, of THE AMERICAN SOCIETY OF MECHANICAL ENGI- ›RS.

Professor of Mechanical Engineering, University of California, ›n. ASME.

Research Fellow in Fluid Mechanics, University of California. ›. ASME. Present address: California Research Corporation, ›Habra, Calif.

›OTE: Statements and opinions advanced in papers are to be ›erstood as individual expressions of their authors and not those of ›Society.

[4] Numbers in parentheses refer to the Bibliography at the end of the paper.

distance from the jet source increases. It seems desirable to formulate a parameter (stability) which will indicate the distance over which appreciable turbulent mixing action takes place. For a free turbulent jet, all types of usual stability parameters tend to remain constant with distance from the jet source, thus providing no useful information regarding the mixing process. The limit of effective turbulent mixing will be specified in terms of the geometry of the tank and the jet.

As a measure of the effectiveness of the mixing process, the performance parameter for mixing is defined as the quantity rate flow of the induced liquid per horsepower input into the liquid jet, Q_s/P_{in}. In order to give an over-all performance parameter, the horsepower input is taken as the input to the device producing the jet.

THE FREE JET

The ideal symmetrical free jet is one that issues from a point source into an infinite fluid of identical properties at rest. The actual approximation to this condition is shown in Fig. 1 in which the jet issues from an orifice of finite diameter. Kuethe (3) has shown that velocity distributions in the real jet correspond to those of the ideal jet for distances from the source greater than about 8 diam. Beyond this location the axial velocity is inversely proportional to the distance from the origin, x'. In the region less than 8 diam from the orifice, the jet of uniform velocity fluid gradually approaches the free symmetrical jet-velocity distribution shown in Fig. 2. The region between the origin and a distance of 8 diam contains a central core of uniform velo for some 5 diam, as shown in Fig. 1. For usual mixing arra ments, the initial length of 8 jet diameters is a small propor of the total stream length. Consequently, solutions develope Tollmien (4) for the ideal free jet may be applied for dista greater than 8 jet diameters downstream, when modified num cally to agree with averaged experimental values. Tolln based his calculations upon the Prandtl mixing-length theory with the added assumption that the mixing length is dire proportional to the width of the jet; thus

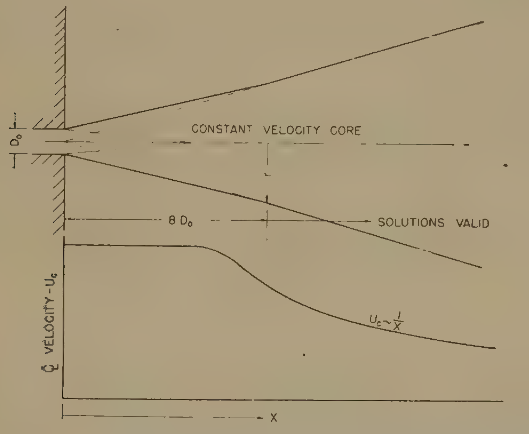

FIG. 1 SPREAD OF SYMMETRICAL TURBULENT JET AND CENTER-LINE VELOCITY DISTRIBUTION

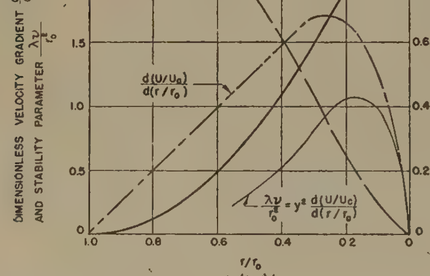

FIG. 2 VELOCITY, DISTRIBUTION, RADIAL VELOCITY GRADIENT, AND PER CENT FLOW VERSUS RADIUS
(From Tollmien's solution for the symmetrical free jet.)

$$l = cx$$

since the jet of incompressible fluid expands at a uniform ra With application of the principle of conservation of moment and the condition that viscous forces are negligible, the Navi Stokes equation for symmetrical flow becomes

$$U\frac{\partial U}{\partial x} + v\frac{\partial U}{\partial r} = c^2x^2\frac{1}{r}\frac{\partial}{\partial r}\left(r\left|\frac{\partial U}{\partial r}\right|\frac{\partial U}{\partial r}\right)\ldots\ldots$$

and the equation of continuity is

$$\frac{\partial}{\partial x}(Ur) + \frac{\partial}{\partial r}(vr) = 0\ldots\ldots\ldots\ldots$$

Tollmien's solution is given in Fig. 2.

The experimental data of several authors for air jets provi adequate demonstration that the theory closely checks actuali The constant c, in Equation [2] appears to be in the nature o universal constant. The extrapolation to liquids appears val although lacking in experimental verification.

In order to provide working equations describing the geome and flow conditions of the jet, the experimental results have be combined with the theoretical solutions to provide numeri equations. The radius of the expanding jet at any axial d tance x, is thus approximated by

$$r_x = 0.232x\ldots\ldots\ldots\ldots\ldots\ldots$$

Thus the free-jet origin seems to coincide with the plane of t jet orifice, a coincidence not predicted by theory. From theo the center-line velocity is expressed as

$$U_c = C_1(D_o/x)U_o\ldots\ldots\ldots\ldots\ldots\ldots [$$

where C_1 is a constant to be evaluated from experimental dat Using the experimental results of several investigators, as r ported by Cleeves and Boelter (1) the center-line velocity di tribution for values of x/D_o greater than 8 is

$$U_c = 5.13\,(D_o/x)\,U_o\ldots\ldots\ldots\ldots\ldots\ldots [6$$

The values in Equation [6] are equivalent to adopting an averag velocity of 0.422 U_c, compared to an average velocity compute from the Tollmien velocity distribution of 0.328 U_c. Equatio [4] and [6] represent to ±8 per cent the available experiment data.

The solution may be employed to predict the rate of inductio of fluid into the turbulent jet from the surrounding quiet fluid In terms of the volume rate of flow in the jet Q_o', the induce flow is

$$Q_s' = [0.234(x/D_o) - 1]\,Q_o'\ldots\ldots\ldots\ldots [7$$

The power in the jet is

$$P_o' = Q_o'\,w\,\frac{V_o^2}{2g}$$

re the continuity relationship is

$$Q_o' = \frac{\pi D_o^2 V_o}{4}$$

bining the last three equations

$$Q_s' = (0.795\, x\, D_o^{1/3} - 3.40\, D_o^{4/3})\,(P_o'/w)^{1/3} \ldots\ldots [8]$$

character of the curves of Equation [8] is illustrated in Fig.

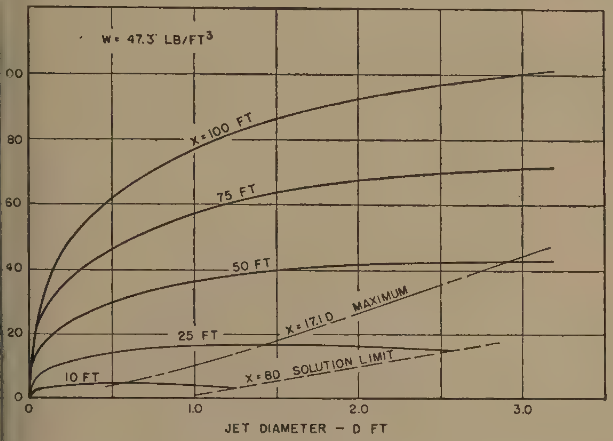

3 Q_s GPM/$(P_o\text{HP})^{1/3}$ Versus Jet Diameter, D_o ft, Calculated for Gasoline of Specific Weight 47.3 pcf

The maximum performance parameter for mixing may be vn to occur at $x = 17.1\, D_o$.

Limits of Turbulence

s the jet flows away from the origin, the fluctuating velocity ponents become gradually smaller. According to data of sin (2), maximum longitudinal fluctuating velocities remain bout 25 per cent of the center-line velocity for distances ter than $8D_o$ to the limit of experimental data (about 40 ı). Therefore the turbulence intensity decreases in a hyper- relationship as does the center-line velocity. hat the turbulence will remain a constant proportion of the enter-line velocity may be predicted from a consideration of a ility parameter. A suitable stability parameter (5) is defined

$$\lambda = \frac{(r_x - r)^2\, dU/dr}{\nu} \ldots\ldots [9]$$

nich $(r_x - r)$ represents the distance from the jet boundaries; velocity gradient, dU/dr, is proportional to the shearing s; and the kinematic viscosity is ν. This parameter repre- a ratio of unstable and stable forces. For a jet, in which the nsionless velocity profiles at any distance x, are similar, orm of the stability parameter may be plotted in dimensionless as in Fig. 2. The dimensionless location of the maximum lity parameter at a given value of x, and the magnitude of dimensionless velocity gradient at that point may be sub- ted into Equation [9] to obtain,

$$\lambda_{\max} = 1.305\, \frac{D_o U_o}{\nu} \ldots\ldots [10]$$

he stability parameter, similar to the Reynolds number, has a ition value above which the flow will be fully turbulent. critical value has been evaluated from pipe-flow conditions $_{\text{rit}} \cong 600$, corresponding to a Reynolds number of 2100 in a pipe. The approximate magnitude of this critical stability parameter has been checked by calculating λ corresponding to locations in the jet for which Corrsin (2) has given oscillograms. The agreement is satisfactory, as bursts of turbulence occur at a Reynolds number of 2640, and no turbulence but occasional fluctuations are still visible at Reynolds number of 428. Near the outer edges of the jet, where the stability parameter $\lambda < 600$, it appears that a region of induction of fluid by viscous flow surrounds the central turbulent core. Investigation of the flow through the annular viscous ring indicates that, for cases in large tanks, less than 5 per cent of the total fluid flowing is in the viscous envelope. As a result, satisfactory calculations may be carried out on the basis of Equation [4] for the mixing process, assuming that all induced fluid is mixed by turbulence.

Equation [10] shows the maximum magnitude of the stability parameter to be independent of x. This result is based upon the solutions for completely turbulent jets in which viscous forces are neglected as being of low order of magnitude. The decay of the expanding turbulence is not predicted but physical considerations indicate that a maximum distance must exist beyond which the mixing through turbulence mechanisms is no longer predominant. Experimental data for air extend over 40 diam from the jet nozzle. In that distance appreciable viscous effects are unobserved. For fluids such as gasoline and water, where the kinematic viscosity is $^1/_{10}$ that of air, the applicability of the results should extend to greater downstream distances.

Experimental and theoretical information presently available provides no means of estimating the length of jet in which effective turbulent mixing is accomplished. In an enclosed tank with a jet issuing perpendicularly from the wall, the jet mixing is considered to proceed across the tank to the point where recirculation currents predominate. For a full circular tank of about 1 radius depth, the effective jet-mixing length is estimated to be about 75 per cent the tank diameter. At this distance, the recirculation currents begin to reduce the fluid-induction process to a negligible amount.

Making use of the analogy between momentum, heat, and mass transfer, it is possible to state that the form of the concentration distribution in the jet-mixing core will be similar to the velocity distributions. From Equation [6] the center-line velocity at 100 jet diameters will be 0.051 U_o, and the corresponding average velocity at that distance will be 0.021 U_o. The concentrations at this section will possess a similar distribution. This consideration justifies the assumption previously stated that all fluid inducted into the jet would be completely mixed in the effective mixing distance.

Typical Mixing Problem

The specific problem of mixing hydrocarbons such as gasolines in large tanks will be investigated. Two possible methods of mixing will be considered. The first example will assume an installation with existing transfer pumps and pipe lines. The second example will treat the same mixing problems when using propeller agitators.

The induction of surrounding fluid into the turbulent jet will be considered to extend across the tank to 75 per cent of the tank diameter. All fluid which has thus entered the jet will be considered completely mixed, and such mixing as takes place in the recirculatory process will be neglected. Questions of jet location and direction are admittedly important, but are not included in the analyses, which assume jets discharging perpendicularly from the tank wall and directed along a tank diameter.

As a typical example, consider a 100-ft-diam petroleum storage tank containing gasoline of 2.7×10^{-5} sq ft per sec kinematic viscosity. A low specific speed (810) centrifugal transfer pump is connected to the tank by 2100 equivalent feet of 12-in. suction line, and the same length of 10-in. discharge line. The transfer-pump characteristics are given in Fig. 4. The friction factor in the Weisbach equation

$$h_L = f\frac{L}{D}\frac{V^2}{2g}$$

for the transfer lines may be taken as 0.02 for a flow range of from 200 to 1200 gpm. Considering the equivalent length of transfer line and a nozzle (diameter of D_o ft) at the discharge, the pipe-line characteristic is

$$\Delta h = f\frac{L_1}{D_1}\frac{V_1^2}{2g} + f\frac{L_2}{D_2}\frac{V_2^2}{2g} + \frac{V_o^2}{2g} \qquad [11]$$

which may be rewritten using the continuity expression, $Q_o' = (D^2/4)\,V$, as

$$\Delta h = \frac{16Q_o'^2}{2g}\left[\frac{fL_1}{D_1^5} + \frac{fL_2}{D_2^5} + \frac{1}{D_o^4}\right] \qquad [12]$$

For the given example, substitution of numerical values results in

$$\Delta h = \frac{Q_o^2}{7.96 \times 10^6}\left[146 + \frac{1}{D_o^4}\right] \qquad [13]$$

for Q_o expressed in gpm.

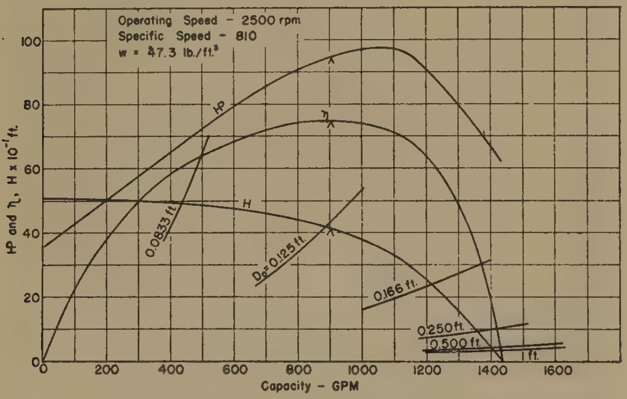

Fig. 4 Application Example of Transfer-Pump Performance Curves With Head Characteristics Plotted Versus Flow Rate, Q_o gpm

(Pump operating speed 2500 rpm, specific speed 810, pumping gasoline of specific weight, w = 47.3 pcf, through 2100 ft of 12-in. suction line and 2100 ft of 10-in. discharge line.)

The system characteristics, Equation [13], for several jet-nozzle diameters are plotted on the pump-performance curve, Fig. 4. The intersection of the system and pump characteristic curves provides the discharge rate, Q_o gpm, from which the hydraulic power (kinetic-energy rate) in the jet at the nozzle discharge may be calculated

$$P_o = \frac{Q_o^3 \times 10^{-6}}{41{,}600\,D_o^4}\,\text{hp} \qquad [14]$$

For a 100-ft-diam tank, the estimated effective mixing distance is 75 ft. Data from Fig. 3 provide the quantity $Q_s/P_o^{1/3}$, from which the induced flow, Q_s gpm, may be calculated, using the hydraulic power P_o, from the solution of Equation [14]. The performance parameter Q_s/P_{in}, is the result of the final calculation.

In this manner the curves of performance parameters, Q_s/P_{in}, versus jet-nozzle diameter P_o, for various mixing distances x, were calculated for Fig. 5. Comparison of the typical jet-characteristic curves of Fig. 3 reveals the large influence of the p and pipe line on the system performance. In Fig. 5 the cri importance of choosing the correct jet diameter is apparent. the jet alone, the ideal arrangement is to use large jet diame and flow rates. For such operation, the high-head low-spec speed transfer pump is unsatisfactory, as is illustrated by low efficiency in the desired operating range. In addition, desirable large flow rates result in large head losses with the pipe lines.

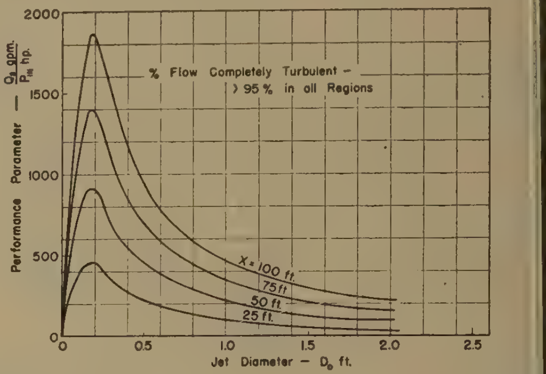

Fig. 5 Induced Flow, Q_s gpm, per Hp Input to Pump, P_{in} Versus Jet Diameter for Varied Free-Jet Distances

(Plotted for gasoline, w = 47.3 pcf, and pumping system of 2100 ft of 1 suction line, 2100 ft of 10-in. discharge line, and transfer pump of spe speed 810.)

From Fig. 5 it may be observed that an optimum perfo ance of 1400 gpm per hp at x = 75 ft is obtained for a jet diame of about $^1/_6$ ft. From Fig. 4 the corresponding power input the pump is 89 hp.

For a comparative evaluation of this over-all performa assume the 89-hp expenditure were available as hydraulic po at the jet discharge.

From Fig. 3 an ideal induced flow rate may be calculated follows:

For D_o = 0.166 ft and x = .75 ft

$$\left(\frac{Q_s}{P_o^{1/3}}\right) = 32{,}600$$

Since

$$P_o = 89 \text{ hp}$$

$$Q_s = 32{,}600 \times (89)^{1/3} = 146{,}000 \text{ gpm}$$

The performance parameter is

$$\frac{146{,}000}{89} = 1630 \text{ gpm per hp}$$

Another basis of comparison would be to assume the hydra power of 89 hp available at the jet but to employ the optim jet diameter of 4.38 ft, as shown in Fig. 3, for a 75-ft mixing d tance. Calculations similar to the foregoing establish the th retically best performance parameter for this arrangement 3610 gpm per hp.

Investigations indicate that mixing may be improved by us high-specific-speed pumps. These pumps would allow effici use of larger jet nozzles. Installation of a single central hi specific-speed pump to replace the transfer pumps is a possibil which could be considered in an economic analysis.

A second method of mixing is by the use of shrouded or u shrouded propellers mounted within the tank. The same type analysis can be used to evaluate the essential characteristics of t process. The rotation of the discharge jet may be neglected. has been shown that a large-diameter jet is desirable, and t

TABLE 1 RESULTS OF PERFORMANCE CALCULATIONS FOR VARIOUS MIXING METHODS

	Mixing equipment	Performance parameter, gpm/hp	Relative performance
1	Optimum mixing ($D_o = 4.38$ ft)	3610	1.00
2	Propeller—22 in. diam, 60 per cent efficient	2810	0.78
3	Jet only—$D_o = {}^1/_6$ ft	1630	0.45
4	Transfer pump and lines, $D_o = {}^1/_6$ ft	1400	0.39

propeller produces such a jet with a power loss due only to the driving system and propeller inefficiency.

A 22-in-diam unshrouded propeller, operating at 60 per cent over-all efficiency (including motor losses) and in the same tank, has been selected as an example. From Fig. 3, with $D_o = 22/12$ ft, $x = 75$ ft, and for the hydraulic power of 0.6×89 hp, the performance parameter for the propeller mixer is 2810 gpm per hp. A comparison of performance parameters indicates the propeller mixing to be twice as efficient as the arrangement of transfer lines and pump.

The summary results of the calculations for the optimum performance of the several mixing methods as applied to the example installation are given in Table 1.

The previous analysis did not attempt to specify a total time required to complete the mixing process. This time is dependent upon the degree of uniformity desired throughout the tank. For instance, it may be possible to disseminate additives sufficiently in a short time to allow diffusion to complete the mixing process without power expenditure. Quite apart from such considerations, considerable data are required before an accurate prediction of the concentration-time gradient at various points in the tank can be made. Owing to the complicated circulation flow pattern, the fluid in the center portions of the tank will enter and leave the jet region several times during the period in which the fluid near the tank wall follows the contour of the tank and returns to the jet region. As a consequence, several multiples of the entire tank volume must pass through the jet mixing before adequate uniformity will be obtained.

The total time required for an equivalent tank volume to pass through the jet may be calculated from the performance parameter. With this magnitude as a reference, the sparse data, given by Bissell (6), for a propeller-mixing process indicate that at least 10 equivalent tank-volume turnovers are required for adequate mixing of gasoline constituents in large storage tanks.

Considering again the typical problem using transfer pump and pipe lines, the time required for 10 equivalent tank-volume turnovers of the 3,200,000-gal tank volume is

$$\frac{3{,}200{,}000 \times 10}{89 \times 1400} = 257 \text{ min} = 4 \text{ hr } 17 \text{ min}$$

while for the propeller installation using the same power, the time requirement is reduced to 128 min or 2 hr 8 min.

Without adequate transient-concentration data taken under controlled conditions, the calculation of mixing times is principally comparative. Alternative systems may be compared, however, and the basis for an economic comparison has been established.

CONCLUSIONS

The existing theoretical and experimental data for a free turbulent jet are applied to the problem of jet mixing of fluids in large tanks. The results expressed in terms of a performance parameter are restricted to mixing similar fluids of low viscosity, but include the effect of jet-nozzle diameters, flow rates, and effective mixing distances. The calculated performance parameters for different types of auxiliary equipment indicate the superiority of propeller mixers over the other types of jet-mixing installations considered.

ACKNOWLEDGMENT

The authors are indebted to Mr. Paul L. Armstrong and Mr. J. S. Gallagher of Los Angeles for suggesting the problem, and to the Standard Oil Company of California for a grant in aid which made the investigation possible.

BIBLIOGRAPHY

1 "Isothermal and Nonisothermal Air-Jet Investigations," by V. Cleeves and L. M. K. Boelter, *Chemical Engineering Progress*, vol. 43, March, 1947, pp. 123–134.

2 "Investigation of Flow in an Axially Symmetrical Heated Jet of Air," by S. Corrsin, NACA Wartime Report ACR No. 3L23, W-94, December, 1943.

3 "Investigations of the Turbulent Mixing Regions Formed by Jets," by A. M. Kuethe, Trans. ASME, vol. 57, 1935, pp. 87–95.

4 "Momentum Transfer Theory for a Jet," by W. Tollmien, Trans. NACA TM 1085, Washington, D. C., 1945 (ZAMM, vol. 6, 1926, pp. 468–478).

5 "Elementary Mechanics of Fluids," by H. Rouse, John Wiley & Sons, Inc., New York, N. Y., 1946, p. 172.

6 "The Role of Blending in the Production of Aviation Motor Fuel," by E. S. Bissell, *Refiner and Natural Gasoline Manufacturer*, vol. 21, January, 1942, pp. 59–65.

A Remote-Indicating Pressure Gage for Aircraft

By R. G. JEWELL,[1] LYNN, MASS.

The indication of aircraft-engine oil and fuel pressures resents numerous problems. A brief study of existing ages shows that the two most serious problems are low emperature and engine vibration. A new gage has been eveloped to overcome these difficulties. The gage utilizes second-harmonic remote-indicating system which is nique in that only one lead wire and ground return are equired between indicator and transmitter.

INTRODUCTION

THE measurement of oil and fuel pressure on aircraft engines has been accomplished by gages which can be classified into two broad groups, namely, direct-reading and electrically emote-indicating.

The direct-reading gages are used in two ways. One way is to onnect the gage to the oil or fuel line through a capillary tube. While this method is simple, it has the disadvantages of difficult stallation on multiengine airplanes, of possible loss of indicaon at low temperatures due to the oil congealing in the capillaries, nd of a fire hazard if accidental leaks occur.

In order to overcome some of these difficulties, another method f using direct-reading gages has been developed. This ethod uses a diaphragm in the oil and fuel capillaries near the ngine to separate the oil and fuel from a special liquid which lls the remainder of the capillaries between the separating diahragms and the instruments. This transmitting liquid does not ongeal at low temperatures and does not present a fire hazard. Therefore it overcomes two of the difficulties encountered with he first method. However, two other difficulties arise. During stallation, and also when changing an engine, the air must be led from the capillaries connecting the separating diaphragms the indicators, an operation which takes an appreciable amount f time. The other difficulty is that any appreciable leakage in he capillaries or connections between the separating diaphragms nd the indicators causes erroneous indications which may be ore dangerous than no indication.

The remote-indicating systems, consisting of a transmitter ear the engine, connected electrically to an indicator on the strument panel, overcome most of the difficulties of directeading gages. However, up to the present time, the transmitters ould not be mounted directly on the engine because the severe ngine vibration caused bearing failures in the transmitter. ocating it at a point near the engine where vibration is not so evere requires at least a short length of capillary. Although his can be in an area which is kept heated after the engine is in peration, failure of indication may occur when starting the ngine in cold weather. Engines have been ruined under these onditions when lack of indication was attributed to frozen oil in he capillary but was actually caused by dangerously low oil ressure.

A real need therefore exists for a remote-indicating gage having a transmitter mounted directly on the engine. Such a transmitter must be capable of withstanding vibration accelerations up to at least 100 g. The ideal transmitter to withstand severe vibration is one which has neither bearings, gears, linkages, nor make-and-break contacts, and which uses a minimum number of connecting leads. The remote-indicating circuits previously available have all used either rotary motions requiring bearings and gears or linear motions, involving close clearances or make-and-break contacts.

Early in the development of the transmitter for direct engine mounting, it became evident that a short linear motion should be used and that this should act directly on the electrical system to eliminate all bearings and linkages. Furthermore, the electrical system should have only one lead wire connecting the transmitter to the indicator so that a good solid connection to a terminal stud could be used. Failure of this one lead due to grounding or breakage should not cause a false indication but should cause the indicator pointer to move to an off-scale position.

A remote-indicating pressure system meeting these requirements has been developed and tests have proved that the desired advantages have been obtained. This system makes use of a bellows-operated transmitter which utilizes the so-called second-harmonic principle[2] to transmit a signal to a ratio-type indicator on the instrument panel. This principle requires a source of alternating-current power for its operation and the present equipment is designed for 400-cycle power supplies.

In describing this system, the recently introduced method[3] for analyzing measurement equipment is useful in gaining a clear understanding of its fundamental functions. As shown in Fig. 1,

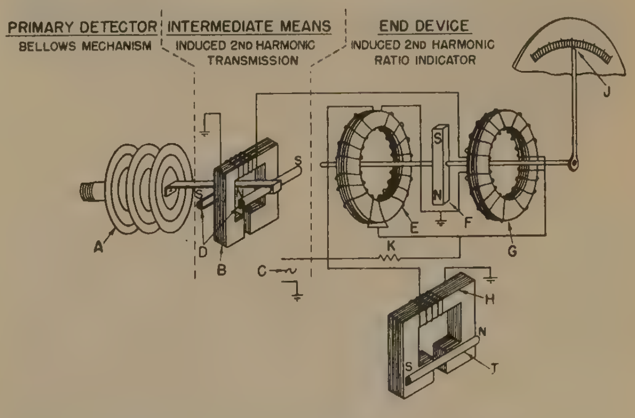

FIG. 1 FUNCTIONAL ANALYSIS DIAGRAM OF REMOTE-INDICATING SYSTEM

A Bellows
B, H Saturable reactors—generators
E, G Saturable reactors—receivers
C Power source
J Pointer and scale
K Resistor
D, I, F Permanent magnets

---

[1] Aeronautical Instrument Development Section, General Elecic Company.

Contributed by the Industrial Instruments and Regulators Divion and presented at the Semi-Annual Meeting, Milwaukee, Wis., ay 30–June 5, 1948, of THE AMERICAN SOCIETY OF MECHANICAL NGINEERS.

NOTE: Statements and opinions advanced in papers are to be nderstood as individual expressions of their authors and not those the Society. Paper No. 48—SA-12.

[2] "Magnesyn Remote Indication," by R. S. Childs, *Electrical Engineering*, vol. 63, 1944, pp. 679–682.

[3] "Functional Analysis of Measurement," by I. F. Kinnard, *Electrical Engineering*, vol. 66, 1947, pp. 11–15.

it is divided into three functional groupings, namely, the primary detector, the intermediate means, and the end device.

Primary Detector

The primary detector is a bellows which was developed specifically for this gage. The spring rate of the bellows is such that it requires no control spring, and the deflection with rated pressure applied is approximately $^1/_{16}$ in. Life tests made by cycling the bellows from zero to rated pressure and to zero show that several million cycles are necessary to show any evidence of failure.

The oil-pressure bellows is designed to operate with the pressure applied to the outside so that as the pressure is increased the bellows plates come closer together. The clearance between plates is controlled so that at a little over full-scale pressure, the plates contact each other. Overpressure has no further effect on the deflection and stops are not necessary. This is important on the oil-pressure bellows, since a thrust of 600 lb would have to be taken by an overload stop and such a stop would add considerably to the weight and size of the transmitter.

The fuel-pressure bellows on overpressure test exerts a thrust of only 25 lb so that a conventional stop can be used and this allows the pressure to be applied to the inside of the bellows.

Intermediate Means

The intermediate means as shown in Fig. 1 consists of a saturable reactor B, two movable permanent magnets D, and a power source C.

The two movable permanent magnets are positioned with respect to the saturable reactor in response to the deflection of the primary detector. The unidirectional flux from the permanent magnets is superimposed on the alternating flux in the saturable reactor core and produces a second-harmonic component in the current which is utilized by the end device to give a unidirectional flux. This unidirectional flux in the end device exerts torque on the magnet attached to the indicator shaft. The manner in which this unidirectional flux is produced is best understood by a study of the simplified system shown in Fig. 2.

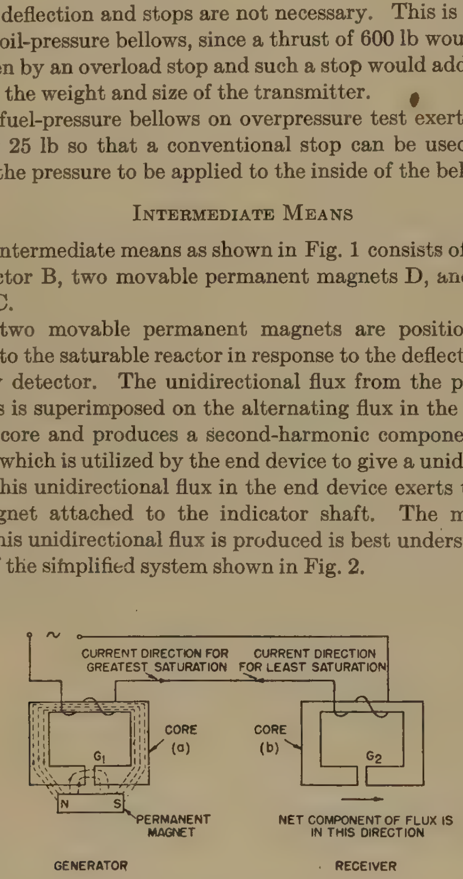
~
CURRENT DIRECTION FOR GREATEST SATURATION
CURRENT DIRECTION FOR LEAST SATURATION
CORE (a)
CORE (b)
G1
G2
N
S
PERMANENT MAGNET
NET COMPONENT OF FLUX IS IN THIS DIRECTION
GENERATOR
RECEIVER

Fig. 2 Simplified Second-Harmonic System

The cores (*a*) and (*b*) in Fig. 2 are identical cores of ferromagnetic material. It is desirable that these cores have high permeability so that they will saturate at a low value of mmf. With no permanent magnet near core (*a*) the alternating-current voltage is adjusted so that the current which flows is sufficient to saturate the core inside the winding during that part of the cycle when peak current flows. Since both cores (*a*) and (*b*) are similar and have similar windings, they both saturate similarly. That part of the core which is not inside the winding has several times the cross section of that section which is inside and therefore does not saturate. The flux must cross the air gaps (g_1) and (g_2) and therefore a field extends out into the space surrounding each gap. If the voltage impressed on the terminals is symmetrical about the zero axis then the flux crossing the gap is symmetrical about the zero axis and there is no unidirectio component of flux.

With a permanent magnet near core (*a*), as shown in Fig. unidirectional flux from the magnet links the core as indicate The air gap (g_1) prevents all of the permanent-magnet flux fro being shunted by the bottom leg of the core and therefore fl from the magnet also goes through that part of the core which surrounded by the winding. During the half-cycle when th alternating current is in the direction indicated for greate saturation, the permanent-magnet flux is added to the alte nating-current flux in the top of the core and causes it to satura much earlier in the cycle than before the permanent-magnet flu was added. During the other half-cycle, the alternating-curre flux and magnet flux through the winding are opposed, and satu ration is either prevented or reduced to a smaller part of the cycl It is true that the two fluxes add in the lower part of the core du ing the second half of the cycle, but the cross section of this part the core is made large enough so that saturation never occurs.

The saturation at the top of core (*a*) causes the peak curre to increase above normal. This current flows through the co on core (*b*) and causes the top of this core to saturate for nearl the same length of time as in core (*a*). During the second hal cycle, the peak current is less, which either prevents saturatio altogether or reduces the saturation to a smaller part of the cycle If a direct-current ammeter is placed in series with the lin supplying power to this system, it is found that no reading is ob tained, which means that although the peak value varies, th average value (or the area) of the positive and negative halve of the current cycle are equal. However, because of the saturatio of the core during the positive half of the current cycle and no during the negative half, the average value of the flux (or are under the curve) during the negative half will be more tha during the positive half. This is shown in Fig. 3.

The result is a net component of flux in the direction shown o core (*b*) in Fig. 2. Increasing the permanent-magnet flux in cor (*a*) increases the net flux in the direction shown on core (*b*) Reversing the magnet flux in core (*a*) will reverse the direction o the net flux in core (*b*). Thus flux rectification is obtained b using a nonlinear magnetic circuit, whereas current rectificatio could be obtained in the same system by using a nonlinear resistor in series with the line. If the resistance decreases with a increase in current as most nonlinear resistors do, the direction o the flux obtained in core (*b*) by this means would be opposite t that obtained by the flux rectification just described.

The principle of flux rectification described is sometimes called the second harmonic principle because the current which flows has in it a large component of a frequency that is twice that of the

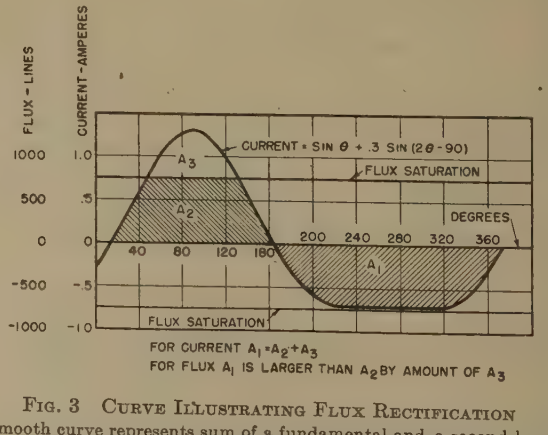

Fig. 3 Curve Illustrating Flux Rectification

(The smooth curve represents sum of a fundamental and a second-harmonic current. Curve enclosing cross-hatched area represents flux which this current produces in a core which saturates at 750 lines.)

wer supply. For simplicity, the saturable reactor which causes e second-harmonic component of current will be called a enerator" and the saturable reactor which makes use of the cond-harmonic component of current will be called a "reiver."

End Device

The end device, as shown in Fig. 1, consists of two receivers, E d G, a permanent magnet F, a pointer and scale J, and a generor H.

The receivers used in the end device are somewhat different om that shown in Fig. 2. The cores of the receivers used in the d device must be round, continuous, and centered with respect the shaft which carries the permanent magnet so that the rces on the permanent magnet will be balanced and not cause torque on the shaft as the magnet and shaft are rotated. One anch of the end device is shown in Fig. 4. With no magnet adcent to the generator core, the two windings on the receiver re must produce the same magnetomotive force per unit angle. therwise, the magnet centered in the receiver core will proice a second-harmonic component of current of greatest magtude in the winding having the greatest magnetomotive force d this in turn will produce an unwanted torque on the maget. The purpose of the balancing winding shown in Fig. 4 to get a constant value of magnetomotive force per degree of gle around the core.

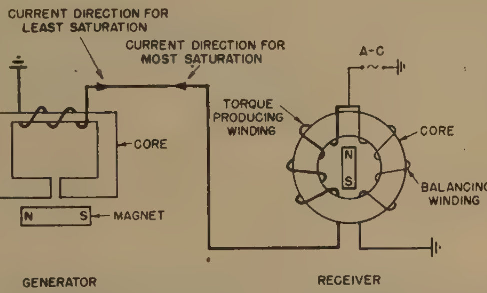

G. 4 One Branch of Electrical Circuit Showing Type of Receiver Used in Indicator

The torque-producing winding of the receiver is connected in ries with the generator winding. The operation is then similar that in Fig. 2. The permanent magnet of the generator proces a higher value of saturation in both cores for one direction current, as indicated by the arrows in Fig. 4. The average alue of flux for this direction of current flow will then be less than e average value of flux for the next half-cycle when the direcon of current and flux is reversed. The indicator magnet will lign itself with the highest average value of flux as shown. The rque produced will be proportional to the value of permanentagnet flux in the generator core and also to the sine of the angle etween the indicator magnet and its position of equilibrium own in Fig. 4. If the generator magnet is reversed, the maxium saturation occurs on the opposite half-cycle, and the indiator magnet will rotate 180 deg.

Two sets of the receivers of Fig. 4 are used in the end device, he two receivers are mounted with the coils of one receiver tated 90 deg with respect to the coils of the other receiver.

One generator H in Fig. 1, similar to the intermediate means, mounted in the indicator case and has a permanent magnet, which is adjustable manually for calibration purposes, but therwise is fixed. This produces a net component of flux in the eceiver E of constant magnitude, except for variations in supply oltage and frequency; hence the name "fixed-vector generator" as been applied to it.

The other receiver G which is connected to the intermediate means produces a unidirectional flux of a magnitude and direction depending upon the position of the permanent magnets D. This flux is at right angles to the flux produced by receiver E, and combines vectorially to give a resultant along which the magnet F, aligns itself. The pointer J is therefore positioned according to the position of the magnets D. Inasmuch as the position of magnets D is determined by the pressure applied to the primary detector, the scale is calibrated in terms of pressure units.

Transmitter

The primary detector A, in Fig. 1, and the saturable reactor B, and magnets D, are assembled into one case and termed a transmitter. The external appearance of the transmitter is shown in Fig. 5. One end of the magnet support is fastened to the bellows as shown in Fig. 1, and the other end is supported on a G-shaped spring which allows motion in the direction of bellows deflection but prevents other motion. Guide bearings are not required and close clearances are not necessary. Only one external connection lead is required. The design therefore satisfies the requirements for direct engine mounting.

The transmitters of the same pressure rating must be interchangeable with each other and therefore require adjustments to take care of the variation in bellows lengths and spring rates. For a given deflection of the bellows, the change in output of the transmitter is increased by decreasing the distance between the two permanent magnets. The output at zero pressure is set by moving the generator core with respect to the two magnets.

Direct engine mounting requires the transmitter to operate at temperatures as low as —55 C and as high as 125 C. The strength of the permanent magnets decreases as the temperature is increased. Compensation for this change is obtained by inserting a temperature-sensitive magnetic alloy in the air gap of the generator core. This shunts a portion of the permanent-magnet flux from the winding. Less flux is shunted at the higher temperatures, thus compensating for the temperature effect on the permanent magnets. The amount of compensation is controlled by the portion of the air gap which is filled with the temperature-sensitive magnetic alloy.

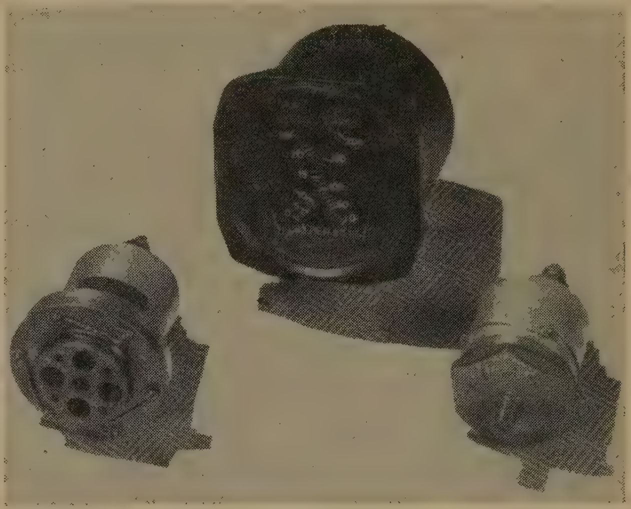

Fig. 5 Indicator and Transmitters
(Differential fuel-pressure transmitter is at left and oil-pressure transmitter is at right.)

Indicator

All of the basic elements of the end device plus the terminals for the power supply are mounted in one case and compose the indicator. Two indicators mounted in one case are shown in Fig. 5.

As with the transmitters, the indicators must also be interchangeable with each other. The scale length is adjusted by positioning manually the permanent magnet on the fixed-vector generator located in the indicator case. As the center of the magnet is moved away from the air gap in the core, less permanent-magnet flux links the winding and the fixed vector becomes shorter, thus causing the resultant vector to swing through a larger angle for the same change in transmitter output. The indicator is set on zero by rotating the whole assembly with respect to the scale.

Temperature compensation of the indicator is obtained in the same manner as in the transmitter. It is applied only to the fixed-vector generator since the strength of the magnet on the pointer shaft does not influence the indication.

The indicator pointer is caused to move off scale when power is removed from the terminals. This is accomplished by a specially designed stationary permanent magnet which reacts with the pointer-shaft magnet to give a constant torque in the down-scale direction.

Failure of the connecting wire between transmitter and indicator causes the indicator pointer to move off scale. If this wire breaks, the magnetomotive force around one receiver core is so greatly unbalanced that the torque on the indicator magnet causes the pointer to move off-scale. If the wire becomes grounded, the magnetomotive force is again unbalanced because of the increased current in one receiver coil and the pointer is moved to an off-scale position. In order to limit the current when the connecting wire is grounded, a resistor is placed in series with the power supply as shown in Fig. 1.

TABLE 1 PERFORMANCE DATA ON DEVELOPMENT-SAMPLE PRESSURE GAGE

Total power consumption, volt-amperes	3.3
Scale angle, deg	100
Indicator torque (90-deg torque), gmm	0.41
Moving element weight, g	0.76
Torque-to-weight ratio	0.54
Response time (zero to full scale rest), sec	1.0
Accuracy (per cent of full scale deviation from standard calibration curves)	
Transmitter	± 2
Indicator	± 3
Voltage error (maximum in per cent of full scale taken with frequency held at 400 cycles)	
26 to 22 volts	2.5
26 to 30 volts	3.0
Frequency error (maximum in per cent of full scale taken with voltage held at 26 volts)	
400 to 370 cycles	1.0
400 to 430 cycles	1.0
Ambient temperature errors on indicator (maximum error in per cent of full scale)	
+25 C to +75 C	1.3
+25 C to —50 C	5.0
Ambient-temperature errors on transmitter (maximum error in per cent of full scale)	
+25 C to +125 C	3.3
+25 C to — 50 C	6.0

PERFORMANCE

The performance data on the sample is shown in Table 1. The effect of direct-current potential drops in the airplane must also be considered in any discussion on performance. Tests s that 1 per cent error is caused by 0.05-volt direct-current poten in the ground circuit between the transmitter and indicator. error is proportional to the direct-current voltage, and if drop is greater than about 0.2 volt it is advisable to unground system in order to eliminate this source of error.

CONCLUSIONS

The remote-indicating pressure gage described meets the quirements for mounting the transmitter directly on the gine. The size and weight of the transmitter and indicator h been kept to a minimum, and the over-all installed weight is duced by the use of a single connecting lead between the tra mitter and the indicator.

The $^1/_8$-in-pipe connection shown in Fig. 5 on the oil-press transmitter, by which the transmitter is mounted on the engi is to be changed to a $1^1/_{16}$-in. 12 straight thread to agree w proposed changes on the engine oil-pressure transmitter mou ing pad.

The 400-cycle power supply required is standard equipment many of the large airplanes now in use. On airplanes not alrea equipped, the 400-cycle power can be obtained from a sm inverter.

Discussion

F. F. UEHLING.[4] The writer is disappointed that the princip involved in the author's remote indicator does not lend itself to higher degree of accuracy. Furthermore, it is apparent that whe the system is in balance, the indicating member as represented b the permanent magnet will have zero torque and will requi some form of servomechanism if the receiving end is to do an work.

However, the writer is greatly interested in the principle in volved and hopes that further refinements will result in bo greater accuracy and higher torque.

AUTHOR'S CLOSURE

Mr. Uehling's discussion on accuracy and torque require some comment.

The accuracy limits specified in Table 1 are largely due to th requirement that any indicator can be used with any transmitter. The over-all accuracy obtainable from a matched se (i.e., an indicator calibrated with a particular transmitter) is much better than Table 1 indicates. If the voltage, frequency and ambient temperature are held within a few per cent of the nominal values, the indication error of a matched set would be less than 1 per cent of full scale.

Although the torque of the indicator is too low to operate external mechanisms, it is sufficient to give an indication with no apparent frictional error.

---

[4] Consulting Engineer, Passaic, N. J. Mem. ASME.

Motion Analysis of Several Intermittent Variable-Speed Mechanisms

eaturing Zero or Near-Zero Acceleration and Deceleration Conditions at Start and at End of Motion of Output Shaft

By G. J. TALBOURDET,[1] BEVERLY, MASS.

The purpose of this paper is to present a description and alysis of several intermittent variable-speed devices which former difficulties have been overcome. These anges have proved valuable in the design of turret-lexing mechanisms and in many other applications.

NOMENCLATURE

The following nomenclature is used in the paper:

= angular displacement of uniformly rotating member
= angular velocity of uniformly rotating member, radians per sec
= pitch radius of output sun pinion, in.
= pitch radius of internal sun gear, in.
= pitch radius of planet pinion, in.
= distance between centers of sun and planet pinions
= radius of eccentricity, in.
= pitch radius of cage gear
= pitch line velocity of output sun pinion, in.
= pitch line velocity of internal sun gear, in.
= linear velocity of center of planet pinions, in.
= angular displacement of cage or arm
= angular velocity of cage, radians per sec
= angular acceleration of cage, radians per sec^2
= angular velocity of internal gear, radians per sec
= angular displacement of output sun pinion
= angular velocity of output sun pinion, radians per sec
= angular acceleration of output sun pinion, radians per sec^2
= number of teeth in driving gear
= number of teeth in driven external gear
= number of teeth in internal sun gear
= number of teeth in output sun pinion
= gear ratio between driving and mating external gear $= \dfrac{N_B}{N_D}$
= gear ratio between internal sun gear and output sun pinion $= \dfrac{N_{s2}}{N_{s1}}$
= linear displacement of rack, in.
= linear velocity of rack, in. per sec
= linear acceleration of rack, in. per sec^2

INTRODUCTION

In the field of automatic machinery, many interesting intermittent variable-speed mechanisms have been conceived and successfully applied to impart a definite and controlled variable speed to a rotary member. However, most of these ingenious devices are satisfactory only when the speed of operation is relatively low and the inertia of the driven parts is proportionally small.

In many instances such devices could be successfully used at relatively high speeds and with appreciable inertia of the driven member, provided that the forces acting on the driven members are gradually applied during the period of acceleration. Also, that the energy stored in the driven parts during that period is gradually taken away during the deceleration period, so that no residual energy is left in the driven body when it comes to rest. Then, to obtain these desirable features, the motion of the driven rotary member should meet the following requirements:

1 Negligible acceleration at the start.
2 Gradual change in acceleration.
3 Smooth change from acceleration to deceleration.
4 Gradual change in deceleration.
5 Negligible deceleration as the rotating body comes to rest.

It is evident that these requirements can be met only if, at any instant, the motion of the input shaft is known, whatever its characteristics. This paper, however, will confine itself to the case in which the input shaft has a uniform angular velocity throughout its cycle. It will also assume that deflections of parts, gear-teeth backlash, and bearing clearances are sufficiently small as to have a negligible effect on the motion of the output shaft. Furthermore, it shall assume that mass-to-stiffness ratios throughout the system are such as to preclude the existence of resonant torsional vibrations in the range of the desired operating speeds.

Design must therefore consider all the foregoing factors; otherwise, the motion of the output shaft will not follow that given in the subsequent analyses.

With these conditions in mind, we can then readily vizualize a flow of energy from the driving to the driven rotating member during the acceleration period and vice versa during the period of deceleration. It requires of course a reservoir of energy in the driving member, which is most easily obtained by the use of a suitable flywheel on the input shaft.

The purpose of this paper is to present therefore the description and the analysis of several intermittent variable-speed devices in which the features mentioned have been incorporated and proved of real value in the design of turret-indexing mechanisms and in many other applications.

In general, these devices, Fig. 1, are the results of the combination of planetary-gear systems, quadric cranks, links and cams, in which one of the members of the planetary-gear system is driven at a uniform angular velocity, while another is given a

---

[1] Mechanical Engineer, Research Division, United Shoe Machinery rporation.

Contributed by the Machine Design Division and presented at the mi-Annual Meeting, Milwaukee, Wis., May 30–June 5, 1948, of IE AMERICAN SOCIETY OF MECHANICAL ENGINEERS.

NOTE: Statements and opinions advanced in papers are to be derstood as individual expressions of their authors and not those the Society. Paper No. 48—SA-18.

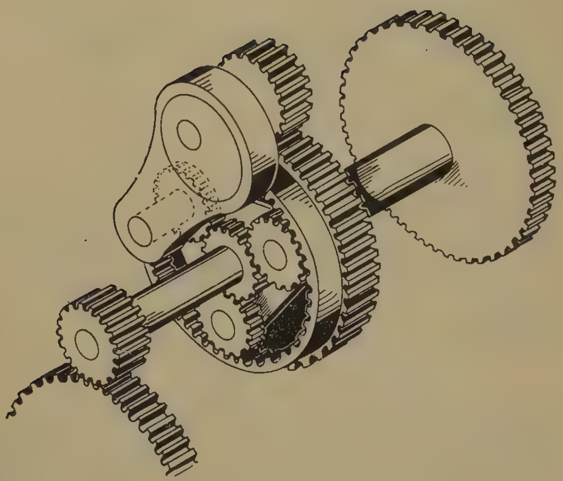

INTERNAL PLANETARY GEAR SYSTEM WITH QUADRIC CRANK CONTROL MECHANISM

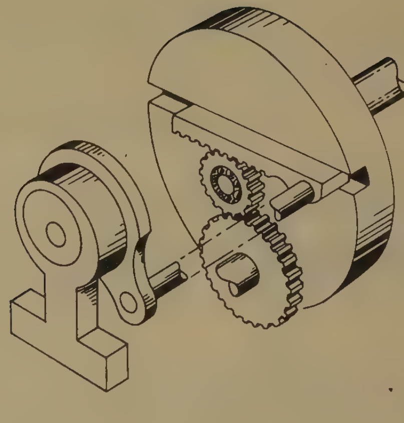

FIXED ECCENTRIC AND SLIDING RACK CONTROL MECHANISM

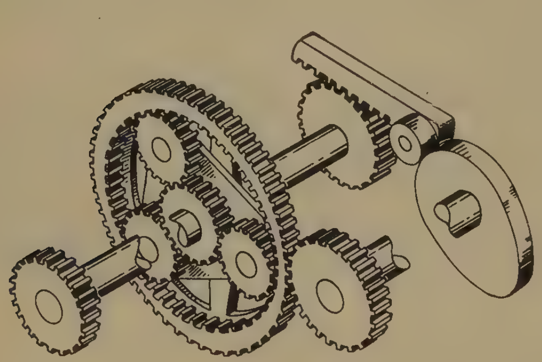

INTERNAL PLANETARY GEAR SYSTEM WITH RACK OR SEGMENTS AND CAM CONTROL MECHANISM

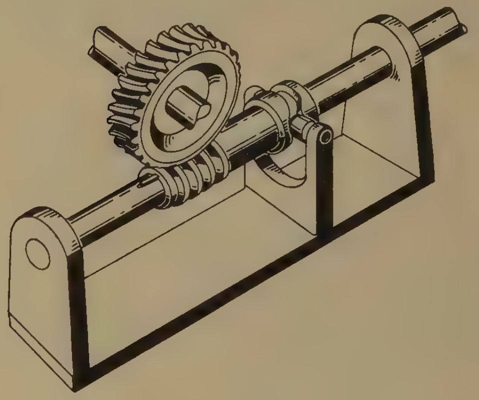

SCREW AND GEAR WITH CAM CONTROL MECHANISM

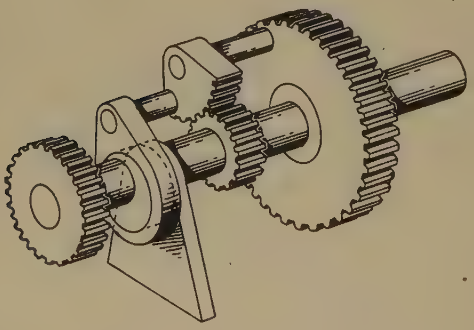

SIMPLE EXTERNAL PLANETARY SYSTEM AND FIXED ECCENTRIC CONTROL MECHANISM

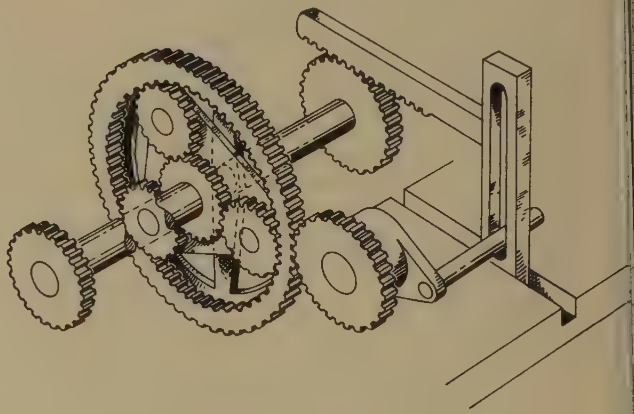

INTERNAL PLANETARY GEAR SYSTEM WITH RACK AND SCOTCH YOKE CONTROL MECHANISM

Fig. 1—Typical Gear Systems

controlled oscillatory motion, thus imparting to the driven member a definite and variable angular motion. It is also possible to obtain an appreciable dwell of the output shaft when the oscillatory member of the planetary-gear system is actuated by a cam. Furthermore, by the use of such a cam, the output shaft can not only be given a dwell period but also it can be made to reverse its direction of rotation. It all depends on the characteristics of the motion of the oscillatory member of the planetary-gear system.

Basic Principles Demonstrated

To bring out the basic principles used in the analysis, we shall consider the planetary-gear system shown in Fig. 2 in which the internal sun gear S_2 is driven at uniform speed, cage A carrying planet pinion P is given a variable motion, and sun pinion S_1 is the driven output member.

Then, using the velocity vectors and instant center methods of attack, we can vizualize readily that the output of sun pinion S_1 remains stationary, only when the instant center I is at the pitch point C of the sun gear S_1 and planet pinion P.

Then from Fig. 3, when $\omega_{s1} = 0$

$$V_A = \frac{V_{s2}}{2} \qquad [1]$$

$$\omega_A = \frac{\omega_{s2} R_{s2}}{2R_A} \qquad [2]$$

For conditions $V_A > V_{s2}/2$, the sun pinion rotates in the direction of the internal sun gear S_2, because the instant center I lies on the center line OO_p and between pitch point C and center O.

From the geometry of Fig. 4 we have

$$V_{s1} = 2V_A - V_{s2} \qquad [3]$$

$$\omega_{s1} = \frac{2\omega_A R_A - \omega_{s2} R_{s2}}{R_{s1}} \qquad [4]$$

For condition $V_A < V_{s2}/2$, instant center I lies on the center line OO_p between O_p and pitch point C. In this case, S_1 rotates in the opposite direction to the internal sun gear S_2. Then from Fig. 5

$$V_{s1} = 2V_A - V_{s2} \qquad [5]$$

$$\omega_{s1} = \frac{2\omega_A R_A - \omega_{s2} R_{s2}}{R_{s1}} \qquad [6]$$

For condition V_A in the opposite direction to V_{s2}, Fig. 6, instant center I lies between O_p and pitch point C_1. Then the sun pinion S_1 will rotate in the opposite direction to the internal sun gear S_2, and

$$V_{s1} = 2V_A - V_{s2}$$

$$\omega_{s1} = \frac{2\,\omega_A R_A - \omega_{s2} R_{s2}}{R_{s1}}$$

when $\omega_A = O_1$ instant center I lies on O_p and

$$\omega_{s1} = \frac{V_{s2} R_{s2}}{R_{s1}}$$

Thus by changing the angular velocity of cage A, while the internal sun gear S_2 rotates at a uniform angular speed, sun pinion S_1 can be made to remain at rest or to rotate at a definite angular velocity in either direction.

When the cage is given a simple harmonic motion, we have a special case in which the conditions of zero acceleration at the start of the motion of the driven sun pinion and zero deceleration at the end of its motion are fulfilled, provided, as explained before, the moving bodies are rigid.

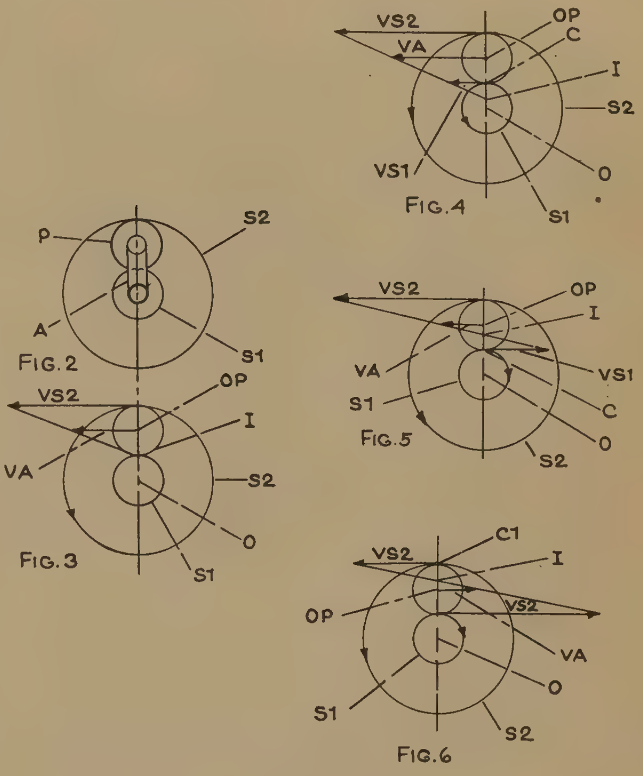

Figs. 2 to 6

A consideration of the foregoing conditions and of the relationships between the members of a planetary-gear system led to the design of the following devices, the description and analysis of which will be given:

Internal planetary-gear system with rack and Scotch-yoke control mechanism.

Fixed-eccentric and sliding-rack control mechanism.

Simple external planetary system and fixed-eccentric control mechanism.

Internal planetary-gear system with rack or segment and cam control mechanism.

Screw and gear with cam control mechanism.

Internal Planetary-Gear System With Rack and Scotch-Yoke Control Mechanism

Description of Mechanism. As shown in Fig. 7, the mechanism consists of a drive shaft A, gear B, and crank C. Gear B meshes with gear D integral with internal gear S_2 of a planetary-gear unit, while crank C is part of a Scotch-yoke mechanism to which rack E is attached. Rack E in turn actuates gear F fastened to cage G carrying planet pinions P free to rotate on pins H mounted on cage G. Pinions P are in mesh with both internal sun pinion S_2 and output sun pinion S_1. Thus we have a simple planetary system in which the internal gear is the driving member rotating at uniform velocity, while the center of the planet pinions moves in a simple harmonic motion.

Analysis of the Motion. From the geometrical conditions of Figs. 8, 9, and 10, we have the following:

(*a*) Motion of rack

$$S_R = -R_0 \sin\theta$$
$$V_R = -\omega R_0 \cos\theta$$
$$a_R = \omega^2 R_0 \sin\theta$$

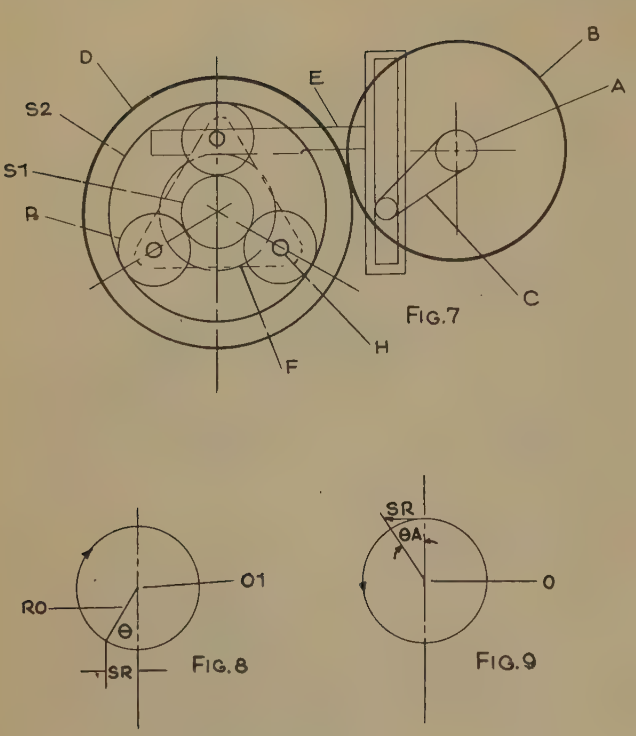

FIGS. 7, 8, AND 9

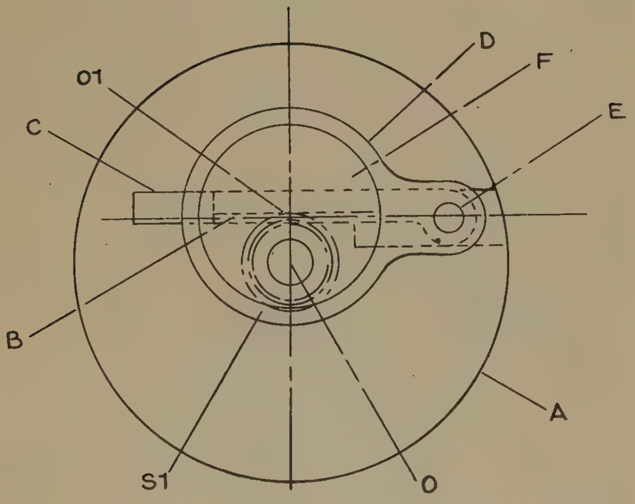

FIG. 10

(*b*) Motion of cage

$$\theta_A = \frac{-R_0 \sin \theta}{R_F}$$

$$\omega_A = \frac{-\omega R_0 \cos \theta}{R_F}$$

$$\alpha_A = \frac{\omega^2 R_0 \sin \theta}{R_F}$$

(*c*) Motion of output sun pinion

Since sun gear S_1 rotates in the opposite direction to sun gear S_2, we have from Fig. 5 and Equations [5] and [6]

$$V_{s1} = 2\,V_A - V_{s2}$$

$$\omega_{s1} = \frac{2\omega_A R_A - \omega_{s2} R_{s2}}{R_{s1}}$$

or as a function of ω and gear ratios m_1 and m_2

$$\omega_{s1} = \frac{m_1 m_2 R_{s1}\omega - 2R_0\omega \cos\theta \dfrac{R_A}{R_F}}{R_{s1}}$$

$$= \omega\left[m_1 m_2 - \frac{(m_2+1) R_0 \cos\theta}{R_F}\right] \quad \ldots\ldots\ldots [7$$

where

$$\omega_{s2} = -m_1\omega,\ R_{s2} = m_2 R_{s1},\ R_A = \frac{R_{s1}\,(m_2+1)}{2}$$

Since $\theta = \omega t$

$$\alpha_{s1} = \frac{d\omega_{s1}}{d_t} = (m_2+1)\frac{R_0}{R_F}\sin\theta \quad \ldots\ldots\ldots [8]$$

$$\theta_{s1} = \int \omega_{s1} d_t = \omega \int \left(m_1 m_2 - \frac{(m_2+1) R_0 \cos\theta}{R_F}\right) d_t$$

$$\theta_{s1} = m_1 m_2 \omega t - \frac{(m_2+1) R_0 \sin \omega t}{R_F} + c = m_1 m_2 \theta - \frac{(m_2+1) R_0 \sin\theta}{R_F} + c$$

When

$$\theta = 0,\ t = 0,\ \sin\theta = 0,\ \therefore c = 0$$

and

$$\theta_{s1} = m_1 m_2 \theta - \frac{(m_2+1) R_0 \sin\theta}{R_F} \quad \ldots\ldots\ldots [9]$$

From Equation [7] the value of R_0 is determined from the condition $\omega_{s1} = 0$. When $\theta = 0$, then

$$0 = m_1 m_2 - (m_2+1)\frac{R_0}{R_F}$$

and

$$R_0 = \frac{m_1 m_2}{m_2+1} R_F$$

Replacing R_0 by its value, we have the following:

Equations of motion of rack

$$S_R = -\frac{m_1 m_2}{m_2+1} R_F \sin\theta$$

$$V_R = -\frac{m_1 m_2}{m_2+1} R_F\,\omega \cos\theta$$

$$a_R = \frac{m_1 m_2}{m_2+1} R_F \omega^2 \sin\theta$$

Equations of motion of cage

$$\theta_A = -\frac{m_1 m_2}{m_2+1} \sin\theta$$

$$\omega_A = -\frac{m_1 m_2}{m_2+1} \omega \cos\theta$$

$$\alpha_A = \frac{m_1 m_2}{m_2+1} \omega^2 \sin\theta$$

Equations of motion of output sun pinion

$$\theta_{s1} = m_1m_2\,(\theta - \sin\theta)$$
$$\omega_{s1} = m_1m_2\omega\,(1 - \cos\theta)$$
$$\alpha_{s1} = m_1m_2\omega^2 \sin\theta$$

These are the equations of the planetary system and Scotch-oke mechanism previously described. The equation of the ac-eleration of the output pinion indicates that the acceleration urve is a sine wave which fulfills the conditions of the zero ac-eleration at the start and zero deceleration at the end of the notion of the output shaft. This is illustrated in Fig. 11 where the angular displacement, velocity, and acceleration of the output shaft have been plotted as a function of the angular displacement of a drive shaft rotating uniformly at the rate of 1 radian per sec, and for values of m_1m_2 varying from $^1/_2$ to 6.

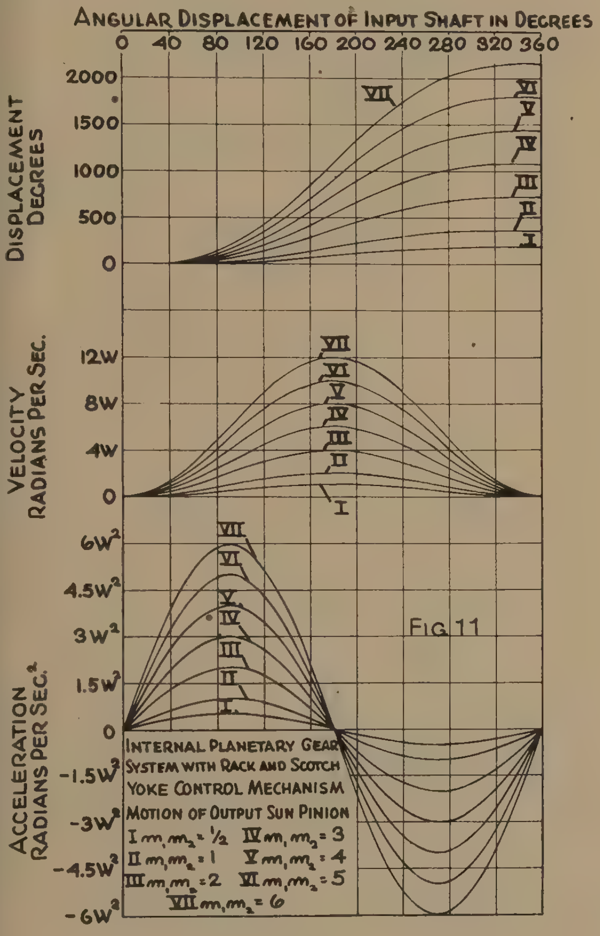

FIG. 11

For reasons of design, construction, and compactness, as well as to eliminate the sliding actions inherent to a Scotch-yoke mechanism, it is preferable, in many instances, to replace the Scotch-yoke and rack mechanism by a quadric crank. In so doing, however, the motion of the cage deviates from simple harmonic, due to the effect of the angularity of the connecting link. This deviation in the motion of the cage results in a departure from the sine-wave acceleration and from the symmetry of the motion of the output shaft.

In some applications this deviation may be objectionable, but, in general, the value of the acceleration and deceleration at the start and at the end of the motion of the output shaft is sufficiently small to be of no importance in practice.

When the Scotch-yoke and rack mechanism is replaced by a quadric crank, the analysis of the motion of the cage and of the output shaft is more complex. The equations of the motion of the driven member of a four-bar linkage, which are also those of the oscillating cage, must be introduced in the analysis. These have been published,[2] and can be readily applied. However, the radius of the crank must be determined accurately so that the maximum angular velocity of the driven link or cage will be made equal to $(m_1m_2\omega)/(m_2 + 1)$.

To determine this radius, we know that it should be less than $(m_1m_2R_{s1})/2$ and therefore must use values somewhat smaller, and calculate the angular velocity of the cage until we obtain a crank radius which imparts to the cage a maximum angular velocity equal to $(m_1m_2\omega)/(m_2 + 1)$. This angular velocity should in no case be greater, otherwise the output shaft will reverse its motion, and in practice it is advisable to decrease the crank radius by a few thousandths of an inch. While this procedure may appear cumbersome, the required crank radius can be determined accurately and rapidly with calculating machines. Then, knowing the radius of the crank, the equations of motion of the cage are combined with the motion of the internal sun gear of the planetary system to determine the motion of the output sun pinion.

FIXED ECCENTRIC AND SLIDING-RACK CONTROL MECHANISM

Description of Mechanism. As shown in Fig. 10, the mechanism consists of rack B moving in slot C cut in disk or flywheel A, and also in mesh with pinion S_1 attached to the output shaft.

Motion of rack B is controlled positively by strap or connecting link D fastened to B by means of pin E. Strap D is also free to turn around a dead crank or stationary shaft F, fixed in the frame and off center with flywheel A.

Thus we have a flywheel rotating at uniform speed which, through pin E, constrains strap D to turn around stationary shaft F, and to cause rack B not only to slide back and forth in slot C but also to roll on pinion S_1. Then, under the combined motions of rack B, a variable-speed motion is imparted to the output pinion S_1.

To obtain a condition of zero velocity and zero acceleration at the start and at the end of the cycle of the output pinion, distance OO_1 between the center of the flywheel and the center of the stationary shaft must be equal to the pitch radius of the output pinion.

Analysis of Motion. When R = length of connecting link, in., and all other symbols are the same as before, we have from the geometrical conditions of Fig. 12

$$S_R = R + R_{s1} \sin\theta - \sqrt{R^2 - R_{s1}^2\,(1 - \cos\theta)^2}$$

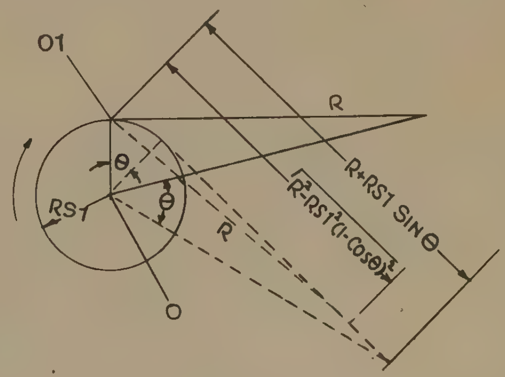

FIG. 12

---

[2] "Simplifying Graphical Solution of Linkages," by H. A. Bolz, *Machine Design*, vol. 14, 1942, pp. 68–70.

then

$$V_{sR} = \frac{d_{sR}}{d_t} = R_{s1}\,\omega\left[\cos\theta + \frac{\sin\theta\,(1-\cos\theta)}{\sqrt{\frac{R^2}{R_{s1}^{\,2}} - (1-\cos\theta)^2}}\right]$$

and

$$a_{sR} = \frac{d^2S_R}{d_t^{\,2}} = R_{s1}\omega^2\left\{-\sin\theta + \frac{1}{\sqrt{\frac{R^2}{R_{s1}^{\,2}} - 1\,(1-\cos\theta)^2}}\right.$$

$$\left.\left[\sin^2\theta + \cos\theta\,(1-\cos\theta) + \frac{\sin^2\theta\,(1-\cos\theta)^2}{\frac{R^2}{R_{s1}^{\,2}} - (1-\cos\theta^2)}\right]\right\}$$

Equations of motion of output pinion

$$\theta_{s1} = \theta - \frac{S_R}{R_{s1}}$$

$$\omega_{s1} = \omega - \frac{V_{sR}}{R_{s1}}$$

$$\alpha_{s1} = -\frac{a_{sR}}{R_{s1}}$$

These equations indicate that for values

$$\theta = 0,\ \theta = 2\pi,\ \omega_{s1} = 0,\ \text{and}\ \alpha_{s1} = 0$$

which fulfills the conditions of zero acceleration at the start and zero deceleration at the end of the motion of the output pinion. This is illustrated in Fig. 13 where for values $R_{s1} = 1$ in. and $R = 6$ in., the angular displacement, velocity, and acceleration of the output pinion have been plotted as a function of the angular displacement of a flywheel rotating uniformly at the rate of 1 radian per sec and counterclockwise to compare it with the output motion of the next device. Here, the curves of the motion of the output pinion are not symmetrical.

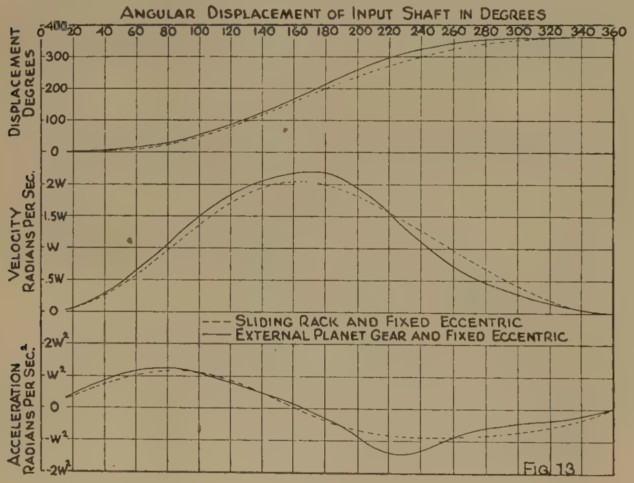

Fig. 13

Simple External Planetary System and Fixed-Eccentric Control Mechanism

The mechanism is a sequence of the sliding-rack and fixed-eccentric device previously described. Here, the rack is replaced by an oscillating external gear segment to eliminate the sliding action of the rack.

Description of Mechanism. As shown in Fig. 14, it consists of an external gear segment B whose center is free to oscillate on p C attached to disk or flywheel A; B is also in mesh with pinio S_1 fastened to the output shaft. Through pin E, the motion gear segment B is controlled positively by a strap or link D, whic is free to turn around a dead crank or stationary shaft F fixed i the frame and off-center with that of flywheel A.

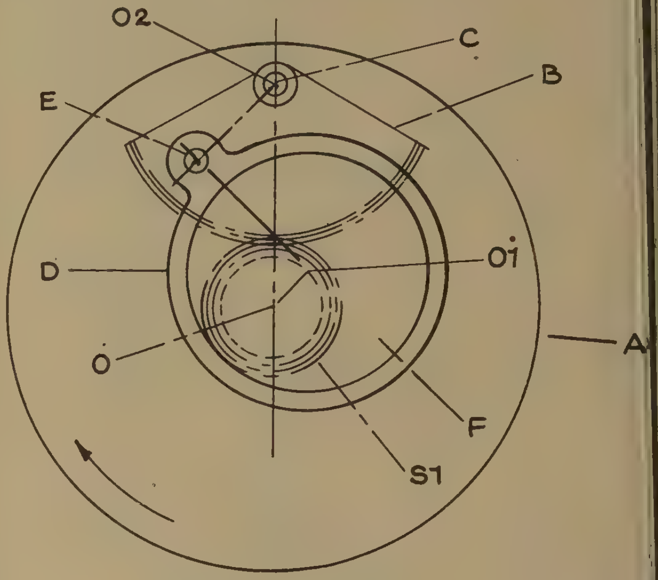

Fig. 14

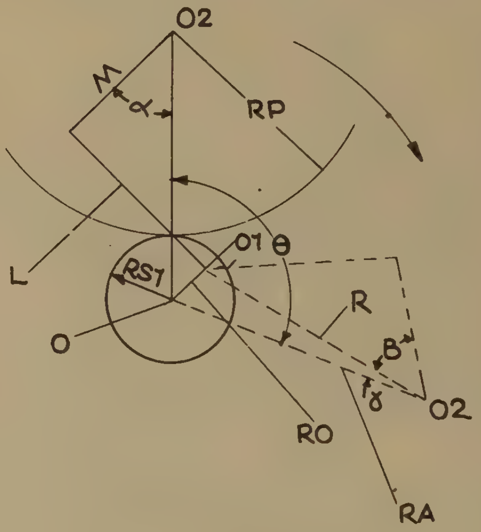

Fig. 15

Thus we have a flywheel rotating at uniform speed which, through pin E, constrains link D to rotate around stationary shaft F and to cause gear segment B to oscillate about center O_2 of pin C and also to roll on pinion S_1. Under the combined oscillating and rolling motions of gear B, a variable motion is imparted to output pinion S_1.

Fig. 14 shows the mechanism at its starting position when link D is normal to center line OO_1 and to the line joining pins C and E. At that position, link D passes through the common pitch point of gear B and pinion S_1

Analysis of Motion:

When

M = center distance between pins C and E, in.

L = length of connecting link, in.
R = distance $O1/n$ O_2, in.
α = angle between M and center line O O_2, deg
θ_p = angular displacement of planet-gear segment around center O_2, deg
ω_p = angular velocity, radians per sec
α_p = angular acceleration, radians per sec² and all other symbols are the same as before

We have from the geometrical conditions of Fig. 15

$$\gamma = \tan^{-1} \frac{R_0 \sin (\theta - \alpha)}{R_A - R_0 \cos (\theta - \alpha)}$$

$$\beta = \cos^{-1} \frac{M_2^2 + R^2 - L^2}{2MR}$$

vhere

$$R_A = R_{s1} + R'_p, \text{ and } R = \sqrt{R_A^2 + R_0^2 - 2R_A R_0 \cos (\theta - \alpha)}$$

Letting

$$\begin{aligned} \phi &= \theta - \alpha \\ \phi_p &= \beta + \gamma - \alpha \\ K &= M^2 + R_A^2 + R_0^2 - L^2 \\ B &= R_A^2 + R_0^2 - 2R_A R_0 \cos \phi \\ D &= K - 2R_A R_0 \cos \phi \end{aligned}$$

we have

$$\gamma = \tan^{-1} \frac{R_0 \sin \phi}{R_A - R_0 \cos \phi}$$

$$\beta = \cos^{-1} \frac{D}{2M \sqrt{B}}$$

and

$$\theta_p = \tan^{-1} \frac{R_0 \sin \phi}{R_A - R_0 \cos \phi} + \cos^{-1} \frac{D}{2M \sqrt{B}} - \alpha$$

$$\omega_p = \frac{d\theta_p}{d_t} = R_0 \omega \left[\frac{R_A \cos \phi - R_0}{B} - \frac{R_A \sin \phi \left(2 - \frac{D}{B}\right)}{\sqrt{4M^2 B - D^2}} \right]$$

$$\begin{aligned} \alpha_p = \frac{d^2\theta_p}{d_t^2} = - R_0 R_A \omega^2 \Bigg\{ & \frac{1}{\sqrt{4M^2 B - D^2}} \Bigg[\frac{2R_A R_0 \sin^2 \phi}{B} \\ & \left(\frac{D}{B} - 1\right) + \left(2 - \frac{D}{B}\right) \left[\cos \phi - \frac{2R_A R_0 \sin^2 \phi \, (2M^2 - D)}{4M^2 B - D^2} \right] \Bigg] \\ & + \frac{\sin \phi}{B} \left[\frac{2R_0 (R_A \cos \phi - R_0)}{B} + 1 \right] \Bigg\} \end{aligned}$$

Equations of motion of output pinion

$$\theta_{s1} = \theta - \frac{R_p}{R_{s1}} \theta_p$$

$$\omega_{s1} = \omega - \frac{R_p}{R_{s1}} \omega_p$$

$$\alpha_{s1} = - \frac{R_0}{R_{s1}} \alpha_p$$

The conditions of zero acceleration at the start and zero deceleration at the end of the motion of the output pinion are obtained when

$$\begin{aligned} \alpha &= 45 \text{ deg} \\ R_0 &= R_{s1} \cos 45 \text{ deg} = 0.7071\, R_{s1} \\ M &= R_p \cos 45 \text{ deg} = 0.7071\, R_p \\ L &= M + R_0 = 0.7071\, (R_{s1} + R_p) = 0.7071\, R_A \end{aligned}$$

To compare the motion of the output pinion with that of the preceding device, the angular displacement, velocity, and acceleration have been plotted in Fig. 13 for values R_{s1} = 1 in., and R_p = 3 in. Here, again, the curves are not symmetrical and deviate more from the curves shown in Fig. 11 than those obtained by the sliding-rack and fixed-eccentric mechanism.

In many applications, this deviation is more than offset by the elimination of the sliding action present with the rack and fixed eccentric-controlled mechanism.

While the foregoing device uses an external gear segment, the same results can be obtained with an internal gear segment.

Internal Planetary-Gear System With Rack or Segment and Cam Control Mechanism

Description of Mechanism. As shown in Fig. 16, this mechanism is similar to the internal planetary-gear system with rack and Scotch-yoke mechanism (see Fig. 1), except that the Scotch yoke is replaced by a cam and a radial cam follower.

It consists of a drive shaft A, gear B, and cam C. Gear B meshes with gear D integral with internal gear S_2 of a planetary-gear unit, while cam C, through its radial follower I, actuates rack E in mesh with gear F fastened to cage G, carrying planet pinions P free to rotate on pins H mounted on G. Planet pinions P also engage with internal sun gear S_2 and output sun pinion S_1.

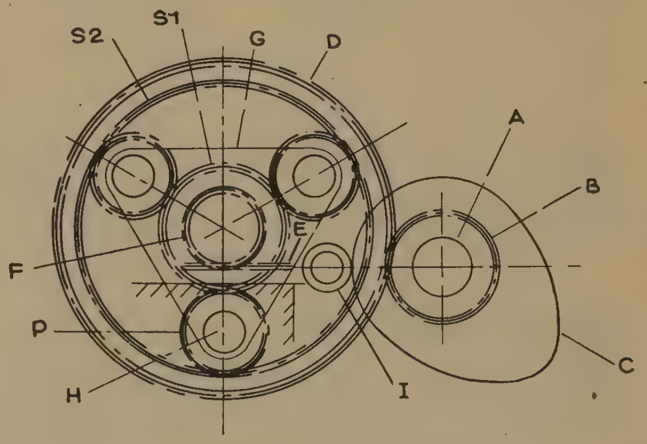

Fig. 16

Here, again, we have a simple internal planetary system in which the internal gear S_2 is the driving member rotating at a uniform velocity, while the motion of the center of the planet pinion is controlled by that of a cam follower.

Thus by varying the characteristics of the motion of the cam follower, the motion of the output sun pinion can be made to meet some specific conditions, such as, to remain at rest during a given angular displacement of the driving member, then to rotate a definite amount during the remaining part of the cycle of the driving member while fulfilling the zero-acceleration conditions at the start and the end of its motion. While many other conditions can be obtained, such as the reversal of the motion of the output sun pinion, the following analysis will consider only the first conditions mentioned; that is, a definite rest period followed by a rotation of the output pinion during the remaining part of the cam cycle.

Analysis of the Motion. When θ_1 = angular displacement of cam during rest period of output sun pinion, θ_2 = angular displacement of cam during motion of output sun pinion, and K =

ratio between a complete cam cycle and its angular displacement required to rotate sun gear S_1 a desired amount, and all the other symbols as before, we shall then determine the equations of motion of rack and cage when output pinion is stationary. From Equation [2]

$$\omega_{s1} = 0, \quad \text{when } \omega_A = \frac{\omega_{s2} R_{s2}}{2R_A}$$

since

$$\omega_{s2} = -m_1\omega, \; R_{s2} = m_2 R_{s1}$$

and

$$R_A = \frac{R_{s1}(m_2 + 1)}{2}$$

then

$$\omega_A = -\frac{m_1 m_2 \omega}{m_2 + 1}$$

This equation indicates that the output sun pinion remains stationary as long as the angular velocity of the cage carrying the planet pinion is uniform and a function of gear ratios m_1 and m_2. We have

$$\theta_A = -\frac{m_1 m_2}{m_2 + 1} \int_0^t \omega dt = -\frac{m_1 m_2}{m_2 + 1} \omega t$$

Since

$$\omega t = \theta$$

then

$$\theta_A = -\frac{m_1 m_2}{m_2 + 1} \theta$$

Where θ varies from 0 to θ_1

$$\theta_{A\,\max} = -\frac{m_1 m_2 \, \theta_1}{m_2 + 1}$$

Linear displacement of rack and radial cam follower

$$S_R = -R_F\theta_A = -\frac{m_1 m_2 \, R_F \theta}{m_2 + 1}$$

$$S_{R\,\max} = -\frac{m_1 m_2 \, R_F \theta_1}{m_2 + 1}$$

Linear velocity

$$V_R = -\frac{m_1 m_2 \, R_F \omega}{m_2 + 1}$$

In the analysis of the internal planetary system and Scotch-yoke device, we have shown that the angular-acceleration curve of the output sun pinion is a sine function and its angular velocity is $m_1 m_2 \omega \, (1 - \cos \theta)$, where θ varies from 0 to 2π.

In this case, θ varies from 0 to θ_2, where the value of θ_2 is 2π or less than 2π. When

$$\theta_2 = 2\pi, \qquad \theta_1 = 0, \qquad \therefore K = \frac{2\pi}{2\pi} = 1$$

and the equations of motion of the output sun pinion and of the cage are similar to those given for the internal planetary system and Scotch-yoke mechanism.

However, when $\theta_2 < 2\pi$, that is, when $\theta_1 > 0$

$$K = \frac{2\pi}{\theta_2}$$

and

$$\omega_{s1} = m_1 m_2 K\omega \, (1 - \cos K\theta)$$

then

$$\theta_{s1} = m_1 m_2 K\omega \int (1 - \cos K\omega t) \, dt = m_1 m_2 K\left(\omega t - \frac{\sin K\omega t}{K}\right) +$$

when

$$t = 0, \qquad \theta_{s1} = 0, \qquad \therefore c = 0$$

and

$$\theta_{s1} = m_1 m_2 \, (K\theta - \sin K\theta)$$

$$\alpha_{s1} = \frac{d}{dt} \omega_{s1} = m_1 m_2 K^2 \omega^2 \sin K\theta$$

From the geometrical conditions of Fig. 5 and from Equatio [6] we have

$$\omega_A = \frac{\omega_{s1} R_{s1} + \omega_{s2} R_{s2}}{2R_A}$$

Since $\omega_2 = -m_1\omega$

$$R_{s2} = m_2 R_{s1} \text{ and } R_A = R_{s1}\left(\frac{m_2 + 1}{2}\right)$$

Then

$$\omega_A = \frac{\omega_{s1} - m_1 m_2 \omega}{m_2 + 1}$$

but

$$\omega_{s1} = m_1 m_2 K\omega \, (1 - \cos K\theta)$$

and

$$\omega_A = \frac{m_1 m_2 \omega}{m_2 + 1} [K\,(1 - \cos K\theta) - 1]$$

then

$$\theta_A = \int \omega_A \, dt = \frac{m_1 m_2 \omega}{m_2 + 1} \int [K(1 - \cos K\theta) - 1] \, dt$$

$$\theta_A = \frac{m_1 m_2 \omega}{m_2 + 1}\left[K\left(t - \frac{\sin K\omega t}{K\omega}\right) - t\right] + c$$

$$\theta_A = \frac{m_1 m_2}{m_2 + 1} [K\omega t - \sin K\omega t - \omega t] + c$$

when

$$t = 0, \; \theta_A = 0, \; \therefore c = 0$$

and

$$\theta_A = \frac{m_1 m_2}{m_2 + 1} [\theta\,(K - 1) - \sin K\theta]$$

It should be noted that values of θ_A for any value of θ are obtained directly up to $\theta = \theta_2/2$. Then for $\theta_2/2$ to θ_2, use twice the value of θ_A when $\theta = \theta_2/2$ minus value of θ_A for $\theta = \theta_2/2$ to $\theta = 0$

$$\alpha_A = \frac{d\omega_A}{dt} = \frac{m_1 m_2 K^2}{m_2 + 1} \omega^2 \sin K\theta$$

The linear motions of the rack, hence of the radial cam follower, are readily obtained by introducing in the equations of motion of the cage, the radius R_F of gear F.

Equations of motion of rack and radial cam follower

$$S_R = R_F\theta_A$$
$$V_R = R_F\omega_A$$
$$a_R = R_F\alpha_A$$

Equations of motion of cage

$$\theta_A = \frac{m_1 m_2}{m_2 + 1} [\theta(K - 1) - \sin K\theta]$$

$$\omega_A = \frac{m_1 m_2}{m_2 + 1}\,\omega[K(1 - \cos K\theta) - 1]$$

$$\alpha_A = \frac{m_1 m_2}{m_2 + 1}\,K^2\omega^2 \sin K\theta$$

Equations of motion of output sun pinion

$$\theta_{s1} = m_1 m_2\,(K\theta - \sin K\theta)$$

$$\omega_{s1} = m_1 m_2\,K\omega\,(1 - \cos K\theta)$$

$$\alpha_{s1} = m_1 m_2 K^2\omega^2 \sin K\theta$$

For stationary conditions of output sun pinion

$$\theta_A = \frac{-m_1 m_2 \theta}{m_2 + 1}$$

$$\omega_A = \frac{-m_1 m_2}{m_2 + 1}\,\omega$$

$$\alpha_A = 0$$

$$S_R = -R_F\theta_A = \frac{-m_1 m_2}{m_2 + 1}\,R_F\theta$$

$$S_{R\,\max} = \frac{-m_1 m_2}{m_2 + 1}\,R_F\theta_1$$

$$V_R = -R_F\omega_A = \frac{-m_1 m_2}{m_2 + 1}\,R_F\omega$$

$$a_R = 0$$

Since S_R is the displacement of the radial cam follower, the radius vector of the cam can be readily obtained for any value of θ from 0 to θ_1 during the rest period, and for any value of θ from 0 to θ_a during the rotation of the output sun pinion.

So far we have assumed the motion of the cage to be controlled by a rack and a radial cam. The same results also can be obtained by replacing the sliding rack by a segmental gear and the radial follower by a swinging cam follower. When

R_f = pitch radius of gear segment, in.
θ_f = angular displacement of segmental gear and swinging cam follower
ω_f = angular velocity
α_f = angular acceleration

then

$$\theta_f = \frac{R_F}{R_f}\,\theta_A$$

$$\omega_f = \frac{R_F}{R_f}\,\omega_A$$

$$\alpha_f = \frac{R_F}{R_f}\,\alpha_A$$

To determine the radius vector and its co-ordinates required for the manufacture of the cam leader, we will let

R = radius vector, in.
C = center distance between cam and swinging cam follower = OO_2, in.
M = length of follower arm, in.
α = angle between OO_2 and extreme outward position of cam follower M, deg
ϵo = angle between OO_2 and radius vector when cam follower is at its extreme outward position, deg
ϵ = any angle between OO_2 and radius vector, deg
$\delta = \epsilon - \epsilon o$
$R \sin \delta$ = horizontal co-ordinate, in.
$R \cos \delta$ = vertical co-ordinate, in.

From the geometrical condition shown in Fig. 17 we have

$$R = \sqrt{M^2 + C^2 - 2CM \cos(\alpha - \theta_f)}$$

$$R_{\max} = \sqrt{M^2 + C^2 - 2CM \cos \alpha}$$

$$\cos \epsilon = \frac{R^2 + C^2 - M^2}{2RC}$$

From these equations the radius vector and its co-ordinates can be calculated.

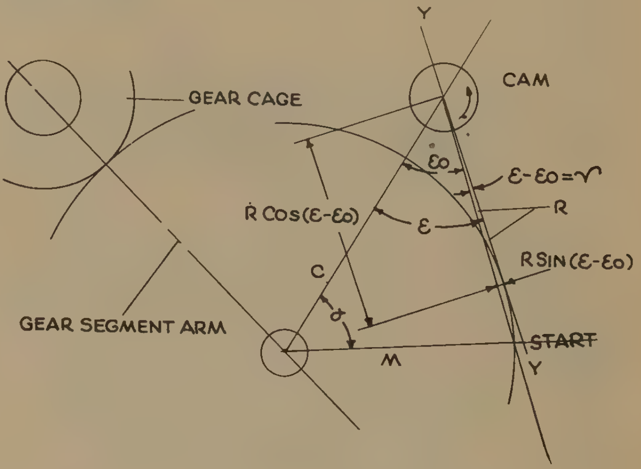

FIG. 17

To illustrate the motions of the cage and of the output sun pinion under conditions of no dwell, 90-deg dwell, 180-deg dwell, and 270-deg dwell of the output pinion, the angular displacements, velocities, and accelerations of cage and output sun pinion have been plotted, respectively, in Figs. 18 and 19, assuming gear ratios $m_1 = {}^1/_4$ and $m_2 = 2$.

SCREW AND GEAR WITH CAM CONTROL MECHANISM

Description of Mechanism. As shown in Fig. 20, the mechanism consists of screw B and cam C, free to slide on input shaft A. The sliding motion of screw B and cam C is controlled by the action of cam C against a roll D fixed in the frame of the machine. Screw B is also integral to cam B and engages with output gear S_1.

Thus we have a screw subjected to two positive motions; a uniform angular rotation, and a variable axial translation. The combined motion of rotation and translation of the screw determines the characteristics of the motion of the output gear.

As with the mechanism previously described, the motion of the output gear can be made to meet some specific conditions, but, again, the analysis will only consider a definite rest period followed by a rotation of the output gear during the remaining part of the cam cycle.

Analysis of the Motion:

When

θ_1 = angular displacement of screw and cam during rest period of output gear
θ_2 = angular displacement of screw and cam during motion of output gear
K = ratio between one complete revolution of cam and angular displacement required to rotate output gear desired amount
L = lead of screw, in.
R = pitch radius of output gear, in.
m = ratio between number of starts in screw and number of teeth in gear

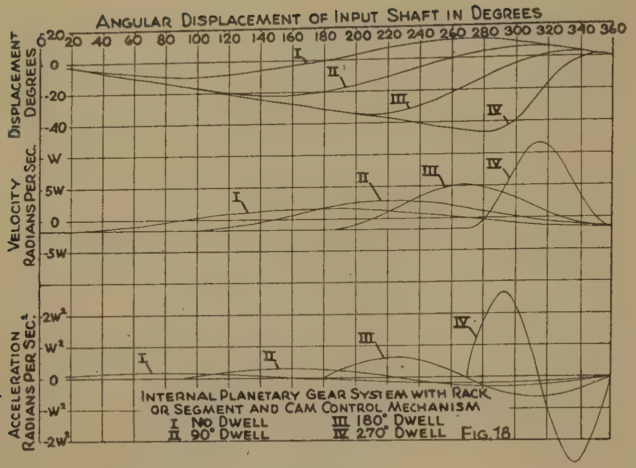

Fig. 18

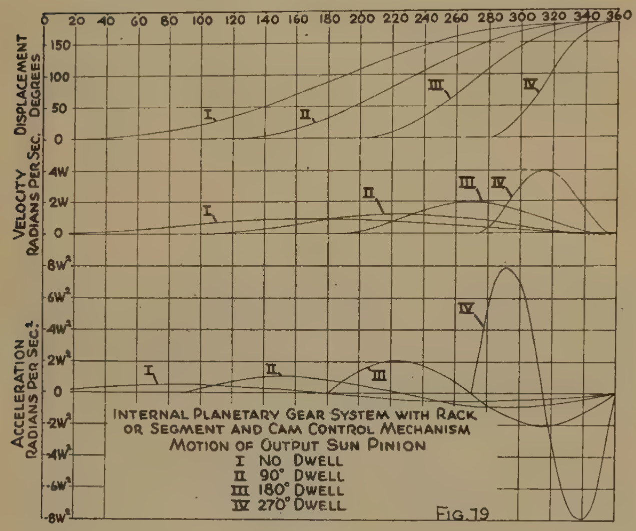

Fig. 19

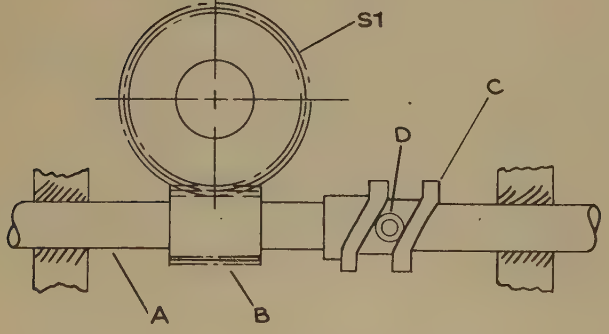

Fig. 20

V = uniform axial velocity of screw thread, ips

S_a = axial displacement of screw and cam, in.

V_a = axial velocity of screw and cam, ips

a = axial acceleration of screw and cam, ips

S_0 = total axial displacement of screw and cam during rest period of output gear, in., and all the other symbols as before

We shall determine the equations of axial motion of screw and cam when the output gear is stationary, i.e., when $\omega_{s1} =$ Assuming clockwise rotation of screw and a left-hand helix

$$V_{s1} = V + V_a$$

Since

$$\omega_{s1} = 0, \; V_{s1} = 0$$

and

$$V_a = -V$$

but

$$V = \frac{L\omega}{2\pi}$$

$$\therefore V_a = -\frac{L\omega}{2\pi}$$

This equation indicates that the output gear remains stationary a long as the axial velocity of the screw is equal and in opposit direction to that of the screw thread.

Then

$$S_a = V_a dt = -\frac{L\omega}{2\pi}\,dt = -\frac{L\omega t}{2\pi} + C$$

when

$$t = 0, \quad S_a = 0, \quad \therefore C = 0$$

and

$$S_a = -\frac{L\theta}{2\pi}$$

when

$$\theta = \theta_1, \quad S_a = S_0$$

$$\therefore S_0 = -\frac{L\theta_1}{2\pi}$$

Then during the rest period of output gear

$$S_a = -\frac{L\theta}{2\pi}, \quad S_0 = -\frac{L\theta_1}{2\pi}, \quad \text{and } V_a = -\frac{L\omega}{2\pi}$$

We shall now assume that during the rotation of the output gear its angular acceleration is a sine function and its angular velocity is $mK\omega\,(1 - \cos K\theta)$; that is, the equations of motion of the output gear are similar to those given in the analysis of the internal planetary-gear system with rack and cam control mechanism. Then

$$\theta_{s1} = m(K\theta - \sin K\theta)$$
$$\omega_{s1} = mK\omega\,(1 - \cos K\theta)$$
$$\alpha_{s1} = mK^2\omega^2 \sin K\theta$$

where θ varies from 0 to θ_2 and $K = 2\pi/\theta_2$.

To determine the equations of axial motion of screw and cam, we have from Fig. 21

$$V_{s1} = V + V_A$$

or

$$mRK\omega\,(1 - \cos K\theta) = \frac{L\omega}{2\pi} + V_A$$

$$\therefore V_A = mRK\omega\,(1 - \cos K\theta) - \frac{L\omega}{2\pi}$$

and

$$S_a = \left(mRK\omega\,(1 - \cos K\omega t) - \frac{L\omega}{2\pi}\right) dt$$

$$= mRK\omega\left(t - \frac{\sin K\omega t}{K\omega}\right) - \frac{L\omega t}{2\pi} + C$$

$$S_a = mR\,(K\omega t - \sin K\omega t) - \frac{L\omega t}{2\pi} + C$$

$$= mR\,(K\theta - \sin K\theta) - \frac{L\theta}{2\pi} + C$$

en

$$\theta = 0,\ S_a = S_0 \qquad \therefore C = S_0$$

n

$$S_a = mR\,(K\theta - \sin K\theta) - \frac{L\theta}{2\pi} + S_0$$

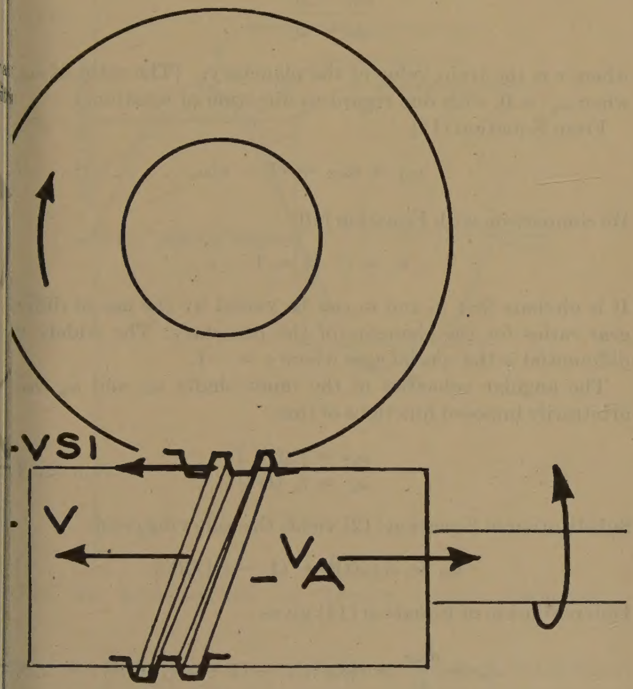

Fig. 21

ce

$$S_0 = -\frac{L\theta_1}{2\pi}$$

en

$$S_a = mR\,(K\theta - \sin K\theta) - \frac{L}{2\pi}\,(\theta + \theta_1)$$

It should be noted that values of S_a for any value of θ are ob-
ned directly up to $\theta = \theta_2/2$. Then for $\theta_2/2$ to θ_2, use twice the
lue of S_a when $\theta = \theta_2/2$ minus value of S_a for $\theta = \theta_2/2$ to $\theta = 0$

$$a = \frac{dV_a}{dt} = mRK^2\omega^2 \sin K\theta$$

Equations of axial motion of screw and cam:

1 During dwell period

$$S_a = -\frac{L\theta}{2\pi}, \quad S_0 = -\frac{L\theta_1}{2\pi}, \quad V_a = -\frac{L\omega}{2\pi}, \quad a = 0$$

iere θ varies from 0 to θ_1.

2 During motion of output gear

$$S_a = mR\,(K\theta - \sin K\theta) - \frac{L}{2\pi}\,(\theta + \theta_1)$$

$$V_a = mRK\omega\,(1 - \cos K\theta) - \frac{L\omega}{2\pi}$$

$$a = mRK^2\omega^2 \sin K\theta$$

where θ varies from 0 to θ_2 and $K = 360/\theta_2$

Equations of motion of output gear

$$\theta_{s1} = m\,(K\theta - \sin K\theta)$$

$$\omega_{s1} = mK\omega\,(1 - \cos K\theta)$$

$$\alpha_{s1} = mK^2\omega^2 \sin K\theta$$

The values required for the manufacture of the cylindrical cam are readily obtained from those of the axial displacement S_a of the screw and cam. To illustrate, the axial motion of screw and cam under conditions of no dwell, 90-deg dwell, 180-deg dwell, and 270-deg dwell of the output gear, the axial displacement, velocity, and acceleration of the screw and cam have been plotted in Fig. 22, assuming gear ratio $m = m_1m_2 = 1/2$. This ratio is used in the calculations for the results plotted in Figs. 17 and 18. In this case, the motions of the output gear are the same as those of the output sun pinion plotted in Fig. 19. A comparison of Figs. 18 and 22 also shows the characteristics of the angular motion of the cage and the axial motion of the screw to be similar, i.e., the motion of the cam follower actuating the cage is the same as that of the cam actuating the screw. This type of mechanism is especially adapted for relatively high reduction ratio, but, here again, the sliding action of the screw is not as favorable as the oscillating motion of the cage of the preceding device.

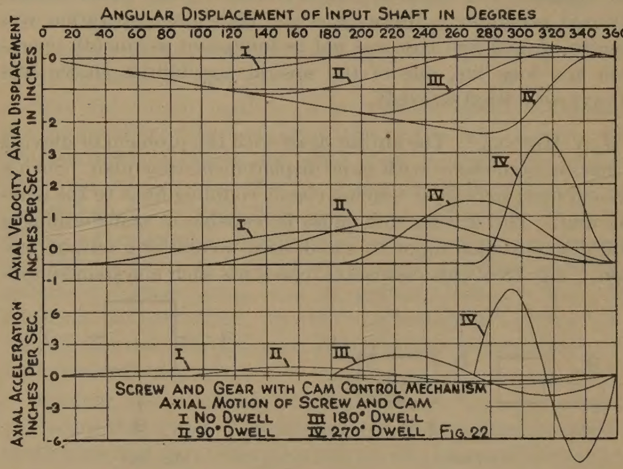

Fig. 22

Conclusion

The description and analysis of devices with conditions of zero acceleration at the start of the output member and zero deceleration at the end of its motion have been the primary objective of this paper. Many deviations from these conditions can be obtained. Specific requirements and conditions influence the choice of the device for a given application.

Discussion

J. F. Downie Smith.[3] Since the writer was connected with the United Shoe Machinery Corporation, Research Division, for 7 years, until 15 months ago, and it was during his stay there that a large part of the development work on this mechanism took place, he is reasonably familiar with the various possible combinations, where they were used, and with what success.

---

[3] Iowa State College, Ames, Iowa. Fellow ASME.

When the design was first proposed by Messrs. L. James, L. Topham, and other designers at that corporation, a careful engineering analysis was considered necessary, and this analysis has been largely done by the author.

In case the reader might be tempted to slight the thoughts involved in this paper, because of the extensive mathematics, it is suggested that he study the motions and charts carefully. It is the writer's firm conviction that the movements will become extremely important wherever indexing at high speeds is desired.

Many such designs were incorporated into equipment built for the armed services during the war, with almost uncanny results. For obvious reasons further details will be omitted.

Wherever such a device was introduced the indexing problem became easier, and, generally, higher speed of machine operation was permissible. Several such indexing and variable-speed mechanisms have been built into production machines, with satisfying results.

For some types of machines, the mechanisms proposed might be considered too complicated and costly to be justified, and an analysis of the various factors involved sometimes indicated to the designers and engineers that a simpler scheme could be substituted profitably. However, where high-speed operation was concerned, and first cost was not as important as smooth operation and long life, one of the several possibilities shown was always considered seriously.

J. A. Hrones.[4] The author deals with the problem of moving a mass in accordance with some displacement-time plan. Such a system must invariably employ elastic coupling links to the driving unit. The driving unit must be capable of transforming a uniform rotational input to the desired nonuniform output motion. Fig. 23 of this discussion represents such a system simplified to its basic elements. The nomenclature for Fig. 23 is as follows

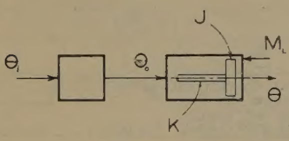

Fig. 23

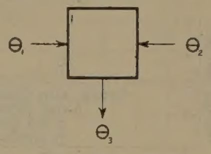

Fig. 24

Fig. 23 Block Diagram of Over-All System

Fig. 24 Block Representation of Planetary Gear Transducer Unit

$\dot{\theta}_i$ = uniform input velocity
θ_0 = displacement of output shaft of transducer
θ = displacement of inertia J
J = moment of inertia of driven mass
K = rotational stiffness of system coupling J to output shaft of transducer
M_L = load torque applied to J

The driving unit (transducer) must be so designed that it gives a satisfactory motion of the inertia J. A recent paper by the discusser[5] considered the performance of such a system where the transducer was a cam. Analysis of such a system for various displacement-time contours of the cam showed that significant reductions in peak forces can be realized if sudden changes in $(d^2\theta_0)/(dt^2)$ are avoided. The author has cleverly employed the planetary-gear system as an adder to produce a relatively complex motion from several simple input motions. The use planetary-gear system as an adding device is of such gre portance as to merit additional discussion. A planeta system may be represented by the box shown in Fig. 24 with. In this θ_1 and θ_2 represent arbitrary angular displac time motions, θ_0 represents the output angular displaceme duced by the two input motions θ_1 and θ_2. It can be show the following relationship exist between the three motions

$$\theta_0 = k_1\theta_1 + k_2\theta_2 \ldots\ldots\ldots\ldots$$

Using the author's nomenclature let $\dot{\theta}_0 = \omega_{s1}$, $\dot{\theta}_1 = \omega_{s2}$, $\dot{\theta}_2$ Then

$$\frac{\omega_{s1} - \omega_a}{\omega_{s2} - \omega_a} = e \ldots\ldots\ldots\ldots$$

where e is the train value of the planetary. (The ratio of when $\omega_a = 0$, with due regard to direction of rotation.)

From Equation [11]

$$\omega_{s1} = e\omega_{s2} + (1 - e)\omega_a \ldots\ldots\ldots\ldots$$

By comparison with Equation [10]

$$k_1 = e; \; k_2 = 1 - e$$

It is obvious that k_1 and k_2 can be varied by the use of diff gear ratios for the elements of the planetary. The widely differential is the special case where $e = -1$.

The angular velocities of the input shafts ω_{s2} and ω_a ca arbitrarily imposed functions of time

$$\left.\begin{aligned} \omega_{s2} &= f_{s2}(t) \\ \omega_a &= f_a\,(t) \end{aligned}\right\} \ldots\ldots\ldots\ldots$$

Substitution in Equation [12] yields the following result

$$\omega_{s1} = e[f_{s2}(t)] + (1 - e)[f_a(t)] \ldots\ldots\ldots\ldots$$

Differentiation of Equation [14] gives

$$\alpha_{s1} = \frac{d\omega_{s1}}{dt} = e[f_{s2}'(t)] + (1 - e)[(f_a'(t)] \ldots\ldots$$

In the first mechanism

$$[f_{s2}(t)] = M_1\omega$$

and

$$[f_a(t)] = -\frac{R_0\omega}{R_F}\cos\theta_i$$

By the use of various types of drives, a large number of co binations of $f_{s2}(t)$ and $f_a(t)$ can be obtained, resulting in a w variety of possible output motions.

The author's discussion of a number of practical methods producing several types of input motions with an analysis of t output motion resulting should prove of great value to designe

Maurice Knott.[6] We use several intermittent motion mech nisms on our machine tools. They all give satisfactory servic The most difficult intermittent motion is on our automatic scre machines, where Geneva mechanisms are used to index the tu rets. Typical of conditions is one six-station turret having t inertia of a 10-in. disk, 1 in. wide, which is indexed $^1/_6$ revoluti in $^1/_6$ sec.

Because we have no present difficulties we are principally inte ested in understanding this paper for possible future use. T point we would like discussed is why the acceleration of the drive member should meet the requirements outlined as follows:

---

[4] Professor of Mechanical Engineering, Massachusetts Institute of Technology, Cambridge, Mass. Mem. ASME.

[5] "An Analysis of the Dynamic Forces in a Cam-Driven System," by J. A. Hrones, Trans. ASME, vol. 70, 1948, pp. 473-482.

[6] Machine Design Engineer, Brown & Sharpe Manufacturi Company, Providence, R. I. Jun. ASME.

1 Negligible acceleration at the start.
2 Gradual change in acceleration.
3 Smooth change from acceleration to deceleration.
4 Gradual change in deceleration.
5 Negligible deceleration as the rotating body comes to rest.

Fig. 25 herewith, in addition to the acceleration curve for the neva mechanism mentioned and a typical curve from the per, shows a constant acceleration - constant deceleration rve. If we had a difficult intermittent motion, due to speed or rtia, this acceleration curve would be our first choice if it were ssible to attain it. What point are we missing which makes foregoing requirements a better solution?

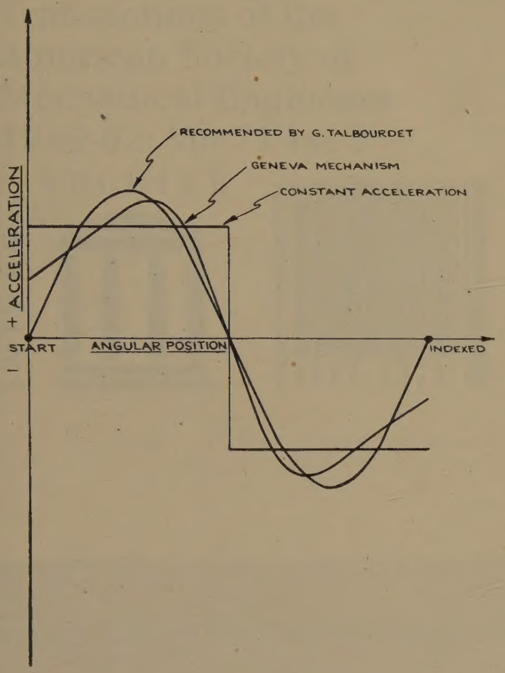

Fig. 25 Acceleration of Turret During Indexing

The moments of inertia, the amount of the angular motion, d the time for the indexing of some of the turrets the author has rked on would be an interesting addition to the paper.

Author's Closure

As stated by Dr. Smith in his discussion of the paper, mechams featuring zero or near-zero acceleration conditions at the rt and at the end of the motion of the output shaft have been signed, built, and found to give satisfying results in several plications.

Although the mathematical analyses of the motions may appear be somewhat extensive, the final equations are relatively sim- and easily applied to determine the forces acting on the rious members, thus obtaining the information required for od design.

In designing these mechanisms special attention must be given the rigidity of the moving parts, in order to avoid detrimental flections and resonant torsional vibrations in the range of the deed operating speeds. The input member also must have a fficient reservoir of energy to control the motion of the output mber at any time.

Prof. J. A. Hrones' discussion and comments are a welcome dition to the paper. The basic elements of a simple system are ll illustrated in Fig. 23 of the discussion. His presentation of the planetary-gear system shown in Fig. 24, together with the analysis of the relationship between the two input motions and the output motion, give a clear idea of the variety of output motions which can be obtained through the combinations of planetary-gear systems, quadric cranks, links, and cams.

A question may be raised regarding the accuracy of manufacture of the cam contour required to obtain a stationary condition or no motion of the output member during a definite motion of the driving shaft. This accuracy is within the limits of manufacture, as proved in several mechanisms where no motion of the output member could be detected during the expected dwell period.

The discussion presented by Mr. Knott is somewhat typical of the school of thought which assumes that the most and only important consideration in the characteristics of a motion is to keep the peak acceleration and deceleration imparted to the output member at a minimum, that is, to consider only the constant acceleration-constant deceleration characteristics which result in the smallest possible acceleration and deceleration values.

No attempt is made to evaluate the effects of the rate of change in acceleration upon the peak forces exerted on the output member, although it should be evident that with constant acceleration-constant deceleration conditions, the peak forces are influenced by the action of a suddenly applied load at the very start of the motion, then of a sudden reversal of the load when maximum velocity is reached, and of a sudden removal of the load when the member comes to rest.

Since the output motions of intermittent-speed mechanisms are comparable to those imparted by cams to cam followers with dwell conditions before and after their motions, the analysis presented by Professor Hrones brings out some extremely interesting and important findings upon the effects of the rate of change in acceleration of cam followers. For example, the main argument of those in favor of the constant acceleration and deceleration characteristics, or of the gravity motion, is that with harmonic characteristics, the resulting maximum acceleration is 1.24 greater than gravity, and, with cycloidal characteristics, it is 1.57 greater than gravity.

However, as indicated by Professor Hrones, the peak forces do not follow that trend. On the contrary, in assuming the product of the mass and the acceleration of a gravity-motion follower to be 1, the peak forces exerted on the follower are not 1 but 1 × 3 or 3, while those on the harmonic-motion follower are 1.24 × 2 or 2.48, and on the cycloidal-motion follower 1.57 × 1.06 or only 1.66 for equal lifts and angles of action. Furthermore, the vibratory forces at the end of the cycloidal motion are only a fraction of those imparted by the gravity motion.

In intermittent-speed mechanisms, especially, smoothness of operation is highly desirable and cannot be obtained when the output member is subjected to sudden application, sudden reversal, and sudden removal of forces which occur when the characteristics of the motion are of the constant acceleration-constant deceleration type. Excessive peak forces with reversal conditions can only result in shocks, wear on the moving parts, and detrimental torsional vibrations when the output member comes to rest.

For these reasons a Geneva motion which approaches harmonic characteristics is without doubt preferable to that of a gravity motion but is not nearly as satisfactory as that obtained with the cycloidal motion.

To conclude, it might be of interest to mention an experience with a spring-loaded follower which could not operate satisfactorily at 1100 rpm; excessive noise of operation and overthrow when imparted a gravity motion, but ran smoothly at the same speed when the deceleration of the follower had sine-wave characteristics. At 960 rpm the gravity-motion follower was still too noisy to be satisfactory in service, although its deceleration was less than that of the cycloidal-motion follower at 1100 rpm. High-speed movies of these motions showed striking differences in the smoothness of operation of the driven member.

It is positive indication that the rate of change in acceleration and not the maximum acceleration only should be conside when designing cam-driven systems and intermittent-sp mechanisms.

The author wishes to thank the discussers of this paper have brought up many pertinent and interesting points.